MECHANICAL SIGNALING IN PLANTS: FROM PERCEPTION TO CONSEQUENCES FOR GROWTH AND MORPHOGENESIS (THIGMOMORPHOGENESIS) AND ECOLOGICAL SIGNIFICANCE

EDITED BY: Catherine Coutand, Stephen J. Mitchell, Sara Puijalon and Gabrielle Monshausen

PUBLISHED IN: Frontiers in Plant Science

frontiers Research Topics

ISSN 1664-8714
ISBN 978-2-88945-074-9
DOI 10.3389/978-2-88945-074-9

About Frontiers

Frontiers is more than just an open-access publisher of scholarly articles: it is a pioneering approach to the world of academia, radically improving the way scholarly research is managed. The grand vision of Frontiers is a world where all people have an equal opportunity to seek, share and generate knowledge. Frontiers provides immediate and permanent online open access to all its publications, but this alone is not enough to realize our grand goals.

Frontiers Journal Series

The Frontiers Journal Series is a multi-tier and interdisciplinary set of open-access, online journals, promising a paradigm shift from the current review, selection and dissemination processes in academic publishing. All Frontiers journals are driven by researchers for researchers; therefore, they constitute a service to the scholarly community. At the same time, the Frontiers Journal Series operates on a revolutionary invention, the tiered publishing system, initially addressing specific communities of scholars, and gradually climbing up to broader public understanding, thus serving the interests of the lay society, too.

Dedication to Quality

Each Frontiers article is a landmark of the highest quality, thanks to genuinely collaborative interactions between authors and review editors, who include some of the world's best academicians. Research must be certified by peers before entering a stream of knowledge that may eventually reach the public - and shape society; therefore, Frontiers only applies the most rigorous and unbiased reviews.
Frontiers revolutionizes research publishing by freely delivering the most outstanding research, evaluated with no bias from both the academic and social point of view.
By applying the most advanced information technologies, Frontiers is catapulting scholarly publishing into a new generation.

What are Frontiers Research Topics?

Frontiers Research Topics are very popular trademarks of the Frontiers Journals Series: they are collections of at least ten articles, all centered on a particular subject. With their unique mix of varied contributions from Original Research to Review Articles, Frontiers Research Topics unify the most influential researchers, the latest key findings and historical advances in a hot research area! Find out more on how to host your own Frontiers Research Topic or contribute to one as an author by contacting the Frontiers Editorial Office: **researchtopics@frontiersin.org**

MECHANICAL SIGNALING IN PLANTS: FROM PERCEPTION TO CONSEQUENCES FOR GROWTH AND MORPHOGENESIS (THIGMOMORPHOGENESIS) AND ECOLOGICAL SIGNIFICANCE

Topic Editors:
Catherine Coutand, Institut National de la Recherche Agronomique (INRA), France
Stephen J. Mitchell, University of British Columbia, Canada
Sara Puijalon, University of Lyon, France
Gabrielle Monshausen, PennState University, USA

Pine growing under prevailing wind.
Reprint with courtesy of Catherine Lenne
(umr PIAF, Clermont-Ferrand, France)

During the 1970s, renewed interest in plant mechanical signaling led to the discovery that plants subjected to mechanical stimulation develop shorter and thicker axes than undisturbed plants, a syndrome called thigmomorphogenesis. Currently, mechanosensing is being intensively studied because of its involvement in many physiological processes in plants and particularly in the control of plant morphogenesis.

From an ecological point of view, the shaping of plant architecture has to be precisely organized in space to ensure light capture as well as mechanical stability. In natural environments terrestrial plants are subjected to mechanical stimulation mainly due to wind, but also due to precipitation, while aquatic and marine plants are subjected to current and wave energy. Plants acclimate to mechanically challenging environments by sensing mechanical stimulations and modifying their growth in length and diameter and their tissue properties to reduce potential for buckling or breakage. From a morphogenetic point of view, both external and internal mechanical cues play an important role in the control of cell division and meristem development likely by modulating microtubule orientation.

How mechanical stimulations are being sensed by plants is an area of intense research. Different types of mechanosensors have been discovered or proposed, including ion channels gated by membrane tension (stretch activation) and plasma membrane receptor-like kinases that monitor the

cell wall deformations. Electrophysiologists have measured the conductances of some stretch-activated channels and have showed that SAC of different structures can exhibit different conductances. The role of these differences in conductance has not yet been established.

Once a mechanical stimulus has been perceived, it must be converted into a biological signal that can lead to variations of plant phenotype. Calcium has been shown to function as an early second messenger, tightly linked with changes in cytosolic and apoplastic pH. Transcriptional analyses of the effect of mechanical stimulation have revealed a considerable number of differentially expressed genes, some of which appear to be specific to mechanical signal transduction. These genes can thus serve as markers of mechanosensing, for example, in studies attempting to define signalling threshold, or variations of mechanosensitivity (accommodation). Quantitative biomechanical studies have lead to a model of mechanoperception which links mechanical state and plant responses, and provides an integrative tool to study the regulation of mechanosensing. This model includes parameters (sensitivity and threshold) that can be estimated experimentally. It has also been shown that plants are desensitized when exposed to multiple mechanical signals as a function of their mechanical history. Finally, mechanosensing is also involved in osmoregulation or cell expansion. The links between these different processes involving mechanical signalling need further investigation.

This frontier research topic provides an overview of the different aspects of mechanical signaling in plants, spanning perception, effects on plant growth and morphogenesis, and broad ecological significance.

Citation: Coutand, C., Mitchell, S. J., Puijalon, S., Monshausen, G., eds. (2017). Mechanical Signaling in Plants: From Perception to Consequences for Growth and Morphogenesis (Thigmomorphogenesis) and Ecological Significance. Lausanne: Frontiers Media. doi: 10.3389/978-2-88945-074-9

Table of Contents

Thigmomorphogenesis: Ecological significance and link with others plant functions

frontiers in Plant Science

EDITORIAL
published: 06 October 2016
doi: 10.3389/fpls.2016.01441

Editorial: Mechanical Signaling in Plants: From Perception to Consequences for Growth and Morphogenesis (Thigmomorphogenesis) and Ecological Significance

Catherine Coutand[1,2]* *and Stephen J. Mitchell*[3]

[1] Institut Nationale de la Recherche Agronomique, UMR 547 PIAF, Clermont-Ferrand, France, [2] Clermont Université, Université Blaise Pascal, UMR 547 PIAF, Clermont-Ferrand, France, [3] Faculty of Forestry, Department of Forest and Conservation Sciences, University of British Columbia, Vancouver, BC, Canada

Keywords: thigmomorphogenesis, acclimation to mechanical stress, model of mechanoperception, stretch activated channels, aquatic organisms, mechanosensing in plants

The Editorial on the Research Topic

Mechanical Signaling in Plants: From Perception to Consequences for Growth and Morphogenesis (Thigmomorphogenesis) and Ecological Significance

OPEN ACCESS

Edited and reviewed by:
Andreas P. M. Weber, University of Düsseldorf, Germany

***Correspondence:**
Catherine Coutand
catherine.coutand@inra.fr

Specialty section:
This article was submitted to Plant Physiology, a section of the journal Frontiers in Plant Science

Received: *06 July 2016*
Accepted: *09 September 2016*
Published: *06 October 2016*

Citation:
Coutand C and Mitchell SJ (2016) Editorial: Mechanical Signaling in Plants: From Perception to Consequences for Growth and Morphogenesis (Thigmomorphogenesis) and Ecological Significance. Front. Plant Sci. 7:1441. doi: 10.3389/fpls.2016.01441

Plant morphogenesis and its regulation have fascinated researchers for more than two centuries. Among determinants of morphogenesis mechanical signals appear as an important cue. The fact that plants respond to mechanical stimuli was reported by Darwin in the 1850's. As described by Iida in this research topic, mechanical stimuli were used in traditional agriculture practices like *mugifumi*. In the past 40 years, the study of mechanical signaling in plants has regained interest because of its implication in fundamental processes of organo- and morphogenesis and their potential as an innovative means of controlling plant growth. The focus of this research topic is the quantification of mechanical signals and of their effects on plant growth, the ecological significance of mechanoperception and thigmomorphogenesis, and the potential use of mechanical stimuli in agriculture practices. The papers in this research topic summarize the current state of knowledge, present new experimental results, identify areas where further investigation is warranted, and propose investigative protocols.

Mechanical signals can come from internal forces due to turgor pressure or externally from the environment. In natural conditions, aerial portions of plants experience mechanical stimuli due to wind, snow and rain, while aquatic plants experience water flow, waves or tides. Plants perceive, transduce respond physiologically to mechanical signals, collectively referred to as thigmomorphogenesis. Thigmomorphogenesis has been described in herbaceous as well as woody plant species. In growing shoots and roots, the first response observed after a mechanical signal is perceived is a transitory growth cessation followed by a progressive recovery of elongation rate and an increase of radial growth rate. When repeated mechanical signals are applied, the classical thigmomorphogenetic growth response of aerial plants is a reduced elongation of axes and, for plants which exhibit an active cambial growth, an increase of growth in girth. Thigmomorphogenesis in aquatic plants has been less well examined.

This research topic includes two articles on mechanosensing in aquatic plants. Schoenlynck et al. examine the response of the aquatic plant *Egeria densa* to hydrodynamic stress and describe

the variations of biogenic silicate, cellulose and lignin content and resulting plant mechanical strength. Tesson and Charrier review the role of mechanical signals in brown algae morphogenesis and discuss the advantages of atomic force microscopy to quantify the mechanical signals and the resulting modifications of composition and strength of algal filaments.

For the past 20 years, progress has been made in understanding the mechanosensing signal perception from two points of view: (i) by identifying the sensors; and, (ii) by quantifying the mechanical signals and linking them to responses. In this research topic Peyronnet et al. focus on the role of mechanosensitive protein channels. Moulia et al. review the quantification of mechanical signals perceived by plants and explain how the S3m model of mechanoperception quantifies the link between perception and responses. They illustrate this approach with two examples, the thigmomorphogenetic syndrome of plant shoots bending, and the mechanosensitive control of shoot apical meristem morphogenesis.

The transduction phase refers to the cascade of events within the plants tissues that lead to responses. In Arabidopsis, the expression of more than a thousand genes is modified after signal perception. Among these mechanosensing actors, some are also triggered by heat, salinity and drought. Other actors are far more specific to mechanical stimuli, including touch-genes or the zinc-finger transcription factor PtaZFP2 cloned in poplar. In their review paper, Leblanc-Fournier et al. note that the expression of PTaZFP2 is related to the number and intensity of strain signals, making it an interesting marker in mechanosensing studies. It also appears as a key factor in plant acclimation to recurrent mechanical signals. Also in this research topic, Cazzonelli et al. describe the role of the chromatin modifying enzyme SDG8, which appears as a key enzyme in the mechanosensing process in Arabidopsis by enabling the expression of many touch responsive genes.

From an ecological point of view, thigmomorphogenesis can be seen as a strategy for better resisting wind or water flow, as discussed in the article by Schoenlynck et al.

Stems of aerial plants, especially those of trees which can grow very tall, must combine mechanical stability and hydraulic conductivity. These two functions have been often seen as antagonistic, implying necessarily that trade-offs are made. There is actually no means to predict the way a tree will acclimate or will optimize the different functions of its wood by modifying the wood structure. In this research topic Badel et al. review acclimation of wood xylem anatomy, and its resulting mechanical and hydraulic functions to recurrent mechanical strains generally engendered by wind with a special focus on the construction costs and possible trade-off.

The research topic concludes with an article by Lopez et al. that explores the link between perception of mechanical signals and perception of gravity, and proposes new protocols for differentiating gravity-specific signal transduction and responses.

AUTHOR CONTRIBUTIONS

All authors listed, have made substantial, direct and intellectual contribution to the work, and approved it for publication.

ACKNOWLEDGMENTS

We are grateful to all the contributors to this research topic.

Conflict of Interest Statement: The authors declare that the research was conducted in the absence of any commercial or financial relationships that could be construed as a potential conflict of interest.

frontiers in
PLANT SCIENCE

OPINION ARTICLE
published: 12 September 2014
doi: 10.3389/fpls.2014.00453

Mugifumi, a beneficial farm work of adding mechanical stress by treading to wheat and barley seedlings

Hidetoshi Iida*

Department of Biology, Tokyo Gakugei University, Koganei-shi, Tokyo, Japan
**Correspondence: iida@u-gakugei.ac.jp*

Edited by:
Catherine Coutand, Institut Nationale de la Recherche Agronomique, France

Reviewed by:
Naomi Nakayama, University of Edinburgh, UK

Keywords: mechanical stress, mechanosensing, treading, trampling, stamping, wheat, barley, crop yield

Plant scientists are now aware that mechanical stresses, such as touching, bending and treading, affect the growth and development of trees and grasses, including crops (Jaffe, 1973; Mitchell and Myers, 1995; Telewski, 2006). However, Japanese farmers have known for centuries of the efficacy of applying a mechanical stress—treading, trampling, or stamping—to the seedlings of autumn-sown wheat and barley, and call this process "mugifumi" [mugifúmi] in Japanese. According to a comprehensive, narrative guidebook written in the 17th century, Japanese farmers enthusiastically treaded seedlings in winter because they empirically knew that treading prevented spindly growth, strengthened the roots to grow and spread, shortened plant height, increased tillers and ear length, and eventually gave a good yield (Anonymous, 1680's). Japanese researchers at agricultural experiment stations have described the methodology of treading and many quantitative data on its remarkable effects over the last several decades. However, the information on this practice in English has remained scarce, since it had been targeted to local farmers and written in Japanese only. I here attempted to provide an insight into the significance of treading and advocate the importance of further studies with cutting-edge technology to promote a better understanding of the molecular mechanisms underlying mechanosensing and mechanotransduction in crop plants.

WHAT IS MUGIFUMI?

Mugifumi is the combination of mugi and fumi. Mugi is the general term for wheat and barley and fumi means treading. Therefore, mugifumi is the act of treading wheat and barley plants, especially their seedlings. In relatively small fields, farmers, their families, and sometimes neighbors tread the seedlings using their feet (**Figure 1A**), while farmers use an agricultural tractor equipped with a treading roller to tread seedlings in large fields (**Figure 1B**). Mugifumi is also called "touatsu" [touátsu], which is the combination of tou (treading) and atsu (pressure). Mugifumi is more familiarly used than touatsu.

Mugifumi is known to significantly affect wheat and barley plants. Treated plants have less spindly growth and lodgings, more tillers, longer spikes, and higher yields than untreated plants if farmers perform mugifumi properly.

The timing and number of times mugifumi is performed are important to obtain good results. Special care is needed when performing mugifumi because the growth of wheat and barley varies from year to year and from region to region. This variation depends on wheat and barley varieties and is influenced by yearly and weekly climate changes. If farmers miss the right time and perform mugifumi an incorrect number of times, they may damage the seedlings and have a reduced grain yield. The appropriate weight for mugifumi corresponds to the body weight per seedling.

Wheat and barley seeds are generally sown in the period between November and early December in Japan. Treading is typically started early in January when the seedlings have three leaves, is then performed several times almost every 10 days, and is stopped before internodes start to grow. The number of times treading is performed varies depending on the growth conditions. To avoid letting the soil become too firm, it is important to tread seedlings when the soil is dry. Another beneficial effect of treading is that it permits roots that have risen from the soil due to the growth of frost columns to be settled.

HOW EFFECTIVE IS MUGIFUMI?

Although many studies have been written in Japanese on the effects of mugifumi on the growth of wheat and barley plants and the yield of gains, to the best of my knowledge, none have been written in English. Of those written in Japanese and available online, a small section of the most comprehensive article written on mugifumi by Ohtani (1950) has been described herein. This article covered a wide range of effects of mugifumi on wheat and barley, including those on developmental, morphological, and physiological traits. I focused on some developmental traits of treaded wheat plants, including grain yields.

Supplementary Table 1 shows the effects of treading on the development of wheat seedlings. In this experiment, the seeds of wheat were sown in a field in the middle of November; seedlings were treaded with feet 32, 62, 73, and 84 days after sowing; and the effects of treading were examined 101 days after sowing. Treading clearly resulted in favorable effects on seedling development from an agricultural viewpoint. Regarding the shoot, the numbers of stems and leaves as well as the wet weight were increased by treading by 74, 10, and 50%, respectively. The length and number of roots were also increased by 4 and 7%,

FIGURE 1 | Scene of mugifumi. (A) Are they dancing in the wheat fields? No, they are not. Farmers and their neighboring children tread wheat seedlings (in Fujisawa, Kanagawa Pref., Japan). Courtesy of the Chiikimiryoku, a nonprofit organization. **(B)** Large-scale treading. Farmers use an agricultural tractor equipped with a specifically designed treading roller to tread wheat seedlings (in Kamishihoro, Hokkaido, Japan). Courtesy of Mr. Haruo Hoshino.

respectively. These findings indicate that treading induces tillering and stimulates the roots to grow and spread. These quantitative findings substantiate the accuracy of the narrative guidebook for farmers described over 300 years ago (Anonymous, 1680's).

Supplementary Table 2 shows the effects of wheat treading on grain yields. In this experiment, seeds were sown on seedbeds near the end of October and the seedlings were transplanted to fields 42 days after sowing. Treading was performed twice on seedlings with feet 151 and 156 days after sowing. This treading led to good yields: the number of spikes per plant, weight of whole plant, and grain weight per plant were increased by 18, 41, and 54%, respectively.

PERSPECTIVE

These two examples demonstrate that mechanical stress, such as treading, modifies the development and growth of wheat, resulting in higher numbers of stems, leaves, roots, and spikes, all of which increase grain yields. Although data was not shown here, a previous study reported that wounds caused by treading facilitated the evaporation of water and thus increased the osmolality of cells, thereby conferring cold resistance on the treaded seedlings (Ohtani, 1950). The effects of treading were also investigated extensively using botanical, biochemical, and physical approaches more than 60 years ago (Ohtani, 1950). However, further studies are warranted to investigate the effects of treading wheat and barley plants with modern technologies not only from agricultural viewpoints, but also from the aspect of basic science.

Beneficial effects of mechanical stress are not limited to wheat and barley. There are many studies on the effect of mechanical stress on vegetable plants (for review, see Latimer, 1991). For example, rubbed soybean plants exhibited reduction in stem elongation and frost resistance (Jaffe and Biro, 1979). Mechanically rubbed stems of common bean were hardened because of an increase in flexibility and acquired resistance to bending-caused breaking (Jaffe et al., 1984). Wind-induced mechanical stress increased resistance to an arthropod herbivore and a fungal pathogen in common bean (Cipollini, 1997).

Effects of mechanical stress on trees have also been studied extensively (for review, see Coutand, 2010). For instance, mechanical bending of the stem increased biomass allocation toward the root in wild cherry tree seedlings, avoiding the formation of poor root systems and the reduction of diameter growth of the trunk seen in mechanically untreated seedlings (Coutand et al., 2008). Mechanical stress given to the upper part of the order 1 axis of young rose plants resulted in a reduction in axis length and an increase in the number of branching, leading to the compactness of the bush, a favorable horticultural trait (Morel et al., 2012). Thus, it is possible that chemical plant growth regulators or chemical plant growth retardants, which are frequently used in horticulture, can be replaced by an appropriate mechanical stress, that is an environment-friendly treatment. As is the case for mugifumi, however, careful application of mechanical stress is needed in consideration of degree of forces applied, the stage of plant growth, soil conditions, weather, and so on. It is worthwhile to note that those favorable effects of mechanical stress on vegetable plants and trees are similarly seen on wheat and barely as described above.

As for mugifumi, the following future studies would be of interest: treading-induced early signaling, gene expression, changes in the cytoskeleton and cell wall, hormone synthesis and transport, and changes in metabolism. These researches should provide a novel insight into mechanosensing and mechanotransduction in plants, especially in monocots. Such lines of study have recently been conducted using a model dicot, *Arabidopsis thaliana*. For example, by whole genome microarray analysis, mechanical wounding

of leaf tissues was shown to induce a number of rapid wound response genes that overlaps with those induced by a wide range of biotic and abiotic environmental stresses (Walley et al., 2007). Repetitive touching enhanced resistance to fungus (*Botrytis cinerea*) infection and cabbage looper (*Trichoplusia ni*) infestation in a defense phytohormone jasmonate-dependent manner (Chehab et al., 2012). Gentle mechanical sweeping of leaf surfaces induced a rapid increase in cytosolic Ca^{2+} concentration and a release of reactive oxygen species, and then enhanced resistance to *B. cinerea* in a jasmonate-independent manner (Benikhlef et al., 2013). Technically and conceptually similar studies on mugifumi-treated wheat and barley should offer a clue to increase the yield of grain and alleviate the shortage of the food worldwide without using a large amount of fertilizers, production and use of which increase environmental burdens.

ACKNOWLEDGMENTS

I thank Ms. Minori Tanaka of the Chiikimiryoku and Mr. Haruo Hoshino for allowing me to use the photographs and Ms. Yumiko Higashi for her secretarial assistance. This work was supported by Grants-in-Aid for Scientific Research on Priority Area No. 21026009 (to Hidetoshi Iida), No. 23120509 (to Hidetoshi Iida) and No. 25120708 (to Hidetoshi Iida) from the Ministry of Education, Culture, Sports, Science and Technology of Japan, and a Grant-in-Aid for Scientific Research B No. 26291026 (to Hidetoshi Iida) from the Japan Society for the Promotion of Science.

SUPPLEMENTARY MATERIAL

The Supplementary Material for this article can be found online at: http://www.frontiersin.org/journal/10.3389/fpls.2014.00453/full

REFERENCES

Anonymous, (1680's). *Hyakusho-denki (Guidebook for Farmers)*. Vol. 1–15 (in Japanese). Annotated by T. Furushima (1977), Tokyo: Iwanami Shoten Publ.

Benikhlef, L., L'Haridon, F., Abou-Mansour, E., Serrano, M., Binda, M., Costa, A., et al. (2013). Perception of soft mechanical stress in Arabidopsis leaves activates disease resistance. *BMC Plant Biol.* 13:133. doi: 10.1186/1471-2229-13-133

Chehab, E. W., Yao, C., Henderson, Z., Kim, S., and Braam, J. (2012). *Arabidopsis* touch-induced morphogenesis is jasmonate mediated and protects against peasts. *Curr. Biol.* 22, 701–706. doi: 10.1016/j.cub.2012.02.061

Cipollini, D. F. Jr. (1997). Wind-induced mechanical stimulation increases pest resistance in common bean. *Oecologia* 111, 84–90. doi: 10.1007/s004420050211

Coutand, C. (2010). Mechanosensing and thigmomorphogenesis, a physiological and biochemical point of view. *Plant Sci.* 179, 168–182. doi: 10.1016/j.plantsci.2010.05.001

Coutand, C., Dupraz, C., Jaouen, G., Ploquin, S., and Adam, B. (2008). Mechanical stimuli regulate the allocation of biomass in trees: demonstration with young *Prumus avium* trees. *Ann. Bot.* 101, 1421–1432. doi: 10.1093/aob/mcn054

Jaffe, M. (1973). Thigmomorphogenesis: the response of plant growth and development to mechanical stimulation. *Planta* 114, 143–157. doi: 10.1007/BF00387472

Jaffe, M. J., and Biro, R. (1979). "Thigmomorphogenesis: the effect of mechanical perturbation on the growth of plants, with special reference to anatomical changes, the role of ethylene, and interaction with other environmental stresses," in *Stress Physiology in Crop Plants*, eds H. Mussell and R. C. Staples (New York, NY: John Wiley and Sons), 25–59.

Jaffe, M. J., Telewski, F. W., and Cooke, P. W. (1984). Thigmomorphogenesis: on the mechanical properties of mechanically perturbed bean plants. *Physiol. Plant.* 62, 73–78. doi: 10.1111/j.1399-3054.1984.tb05925.x

Latimer, J. G. (1991). Mechanical conditioning for control of growth and quality of vegetable transplants. *Hortscience* 26, 1456–1461.

Mitchell, C. A., and Myers, P. N. (1995). Mechanical stress regulation of plant growth and development. *Hortic. Rev.* (*Am. Soc. Hortic. Sci.*) 17, 1–42.

Morel, P., Crespel, L., Galopin, G., and Moulia, B. (2012). Effect of mechanical stimulation on the growth and branching of garden rose. *Sci. Hort.* 135, 59–64. doi: 10.1016/j.scienta.2011.12.007

Ohtani, Y. (1950). Studies on the stamping of wheat and barley. *Bul. Natl. Agr. Exp. Stn. Jpn.* 67, 1–76.

Telewski, F. W. (2006). A united hypothesis of mechanoperception in plants. *Am. J. Bot.* 93, 1466–1476. doi: 10.3732/ajb.93.10.1466

Walley, J. W., Coughlan, S., Hudson, M. E., Covington, M. F., Kaspi, R., Banu, G., et al. (2007). Mechanical stress induces biotic and abiotic stress response via a novel *cis*-element. *PLoS Genet.* 3:e172. doi: 10.1371/journal.pgen.0030172

Conflict of Interest Statement: The author declares that the research was conducted in the absence of any commercial or financial relationships that could be construed as a potential conflict of interest.

Received: 14 July 2014; paper pending published: 18 August 2014; accepted: 21 August 2014; published online: 12 September 2014.

Citation: Iida H (2014) Mugifumi, a beneficial farm work of adding mechanical stress by treading to wheat and barley seedlings. Front. Plant Sci. ***5****:453. doi: 10.3389/fpls.2014.00453*

This article was submitted to Plant Physiology, a section of the journal Frontiers in Plant Science.

frontiers in
PLANT SCIENCE

ORIGINAL RESEARCH ARTICLE
published: 05 February 2015
doi: 10.3389/fpls.2015.00043

Thigmomorphogenetic responses of an aquatic macrophyte to hydrodynamic stress

Jonas Schoelynck[1]*, Sara Puijalon[2], Patrick Meire[1] and Eric Struyf[1]

[1] *Ecosystem Management Research Group, Department of Biology, University of Antwerp, Wilrijk, Belgium*
[2] *UMR CNRS 5023 Laboratoire d'Ecologie des Hydrosystèmes Naturels et Anthropisés, Université Lyon 1, Villeurbanne, France*

Edited by:
Stephen J. Mitchell, University of British Columbia, Canada

Reviewed by:
Rui Shi, North Carolina State University, USA
Klaus Harter, University of Tuebingen, Germany

****Correspondence:***
Jonas Schoelynck, Ecosystem Management Research Group, Department of Biology, University of Antwerp, Universiteitsplein 1, 2610 Wilrijk, Belgium
e-mail: jonas.schoelynck@uantwerpen.be

The response of aquatic plants to abiotic factors is a crucial study topic, because the diversity of aquatic vegetation is strongly related to specific adaptations to a variety of environments. This biodiversity ensures resilience of aquatic communities to new and changing ecological conditions. In running water, hydrodynamic disturbance is one of the key factors in this context. While plant adaptations to resource stress (nutrients, light...) are well documented, adaptations to mechanical stress, particularly flow, are largely unknown. The submerged species *Egeria densa* was used in an experiment to detect whether the presence or absence of hydrodynamic stress causes plant thigmomorphogenetic responses (i) in terms of plant biogenic silica (BSi), cellulose and lignin concentrations, and (ii) in terms of plant strength. Plant silica concentrations, as well as lignin concentrations were significantly higher in presence of hydrodynamic stress. These physiological changes are accompanied by some significant changes in stem biomechanical traits: stem resistance to tensile forces (breaking force and breaking strength) and stiffness were higher for plants exposed to hydrodynamic stress. We conclude that the response of this aquatic plant species to mechanical stress is likely the explaining factor for a higher capacity to tolerate stress through the production of mechanically hardened shoots.

Keywords: silica, lignin, cellulose, *Egeria densa*, tensile strength, bending strength, Young's modulus

INTRODUCTION

Aquatic plants can be exposed to important external mechanical forces resulting from pressure exerted by water movement, particularly in flowing ecosystems such as rivers and streams (Puijalon et al., 2011; Puijalon and Bornette, 2013). The consequences for the plants depend on the magnitude of these hydrodynamic forces and on the plants' capacity to resist to the effect of these forces (Schutten et al., 2005; Puijalon et al., 2011). Shoot breakage occurs when the forces encountered by plants exceed their capacity to resist breakage (i.e., breaking force; Vogel, 2003; Schutten et al., 2005). Plants' ability to tolerate water movement without suffering mechanical damage relies either on minimizing the hydrodynamic forces or maximizing its resistance to breakage. When growing under permanent flow conditions, aquatic plants may present important thigmomorphogenetic responses (i.e., developmental responses to external mechanical stimulation; Braam, 2005; Telewski, 2006), which can increase the plant capacity to tolerate hydrodynamic forces. These thigmomorphogenetic responses involve many morphological traits (e.g., reduced plant mass and height, reduced leaf sizes, higher biomass allocation to below-ground organs; Doyle, 2001; Strand and Weisner, 2001), sometimes resulting in extremely modified morphologies such as dwarfed individuals (Puijalon and Bornette, 2013). Studies have demonstrated that these thigmomorphogenetic responses have an adaptive value, reducing the hydrodynamic forces encountered by aquatic plants (Puijalon et al., 2005, 2008), but consequences of these responses for resistance to breakage have rarely been assessed. The resistance to breakage of a plant stem depends on its cross-sectional area and its material strength (Denny, 1988; Niklas, 1992; Vogel, 2003), linked to the proportion of strengthening tissues (Ennos, 1997; Read and Stokes, 2006; Telewski, 2006). Both stem cross-sectional area and proportion of strengthening tissues may be affected by thigmomorphogenetic responses (Bociag et al., 2009), but the actual consequences for aquatic plant resistance to breakage still needs to be investigated.

The strengthening tissue in plants consists mainly of cellulose, which is the majority of plant cell wall material. In the intercellular space, lignin can be incorporated to provide additional rigidity and compressive strength to cell walls. It also renders the cell wall hydrophobic and impermeable to water (Turner et al., 2001). Cellulose is a relatively pure compound of glucose units (i.e., polysaccharides). Lignin, however, does not have a unique chemical formula, but is a complex molecule composed of repeating phenylpropane units composed of an aromatic ring with three carbon side-chains. The phenolic groups vary between plants, further confounding the definition of lignin (Palm and Rowland, 1997). Fundamental physiological research on how these components give strength to plants is mainly restricted to (parts of) terrestrial vegetation. During tree growth, for example, cellulose microfibrils give cell walls tensile strength (Sjostrom,

1993), and lignin encasing the cellulose microfibrils imparts rigidity to cell walls (Hu et al., 1999; Genet et al., 2005). For non-woody species, Carpita et al. (2001) state that it is likely that 15% of the *Arabidopsis* genome is dedicated to cell wall biogenesis and modification, which allows the cell to resist the gravitational forces and/or tensile forces associated with the transpirational pull on a column of water. Turner et al. (2001) showed that mutation of *Arabidopsis*, rendering it incapable of secondary cell wall synthesis, causes the cells to collapse. Additionally, cell wall analysis in barley mutants revealed that the maximum bending stress correlated significantly with the cellulose content but not with lignin. Generally, according to Kaufman et al. (1999), the use of lignin diminishes flexibility. The pathways for cellulose and lignin biosynthesis must thus be regulated in a highly coordinated manner, to achieve the proper deposition of these polymers during secondary wall formation. How this co-ordination is achieved remains largely unclear (Turner et al., 2001).

Apart from strength provided by lignin and cellulose, biogenic silica (BSi) can also provide support to the shoot (Kaufman et al., 1999) by giving structural rigidity to the cell wall (Green et al., 1975) at a 10- to 20-fold lower cost (Raven, 1983). Silica is an energetically cheap stiffening material, promoting upright stature and resistance to lodging (flattening by wind or rain). A first relation between silica, cellulose and lignin for aquatic vegetation was shown by Schoelynck et al. (2010). These authors found interspecific relations between silica and cellulose and antagonistic relations between silica and lignin. Relations could be positive or negative, depending on the growth form of the species (submerged versus emerged). Later, Schoelynck et al. (2012) showed that these relations could hold up intraspecifically in the stems of a single submerged aquatic species (*Nuphar lutea* L.): more silica is associated with less cellulose and with more lignin. This study also demonstrated that, in absence of hydrodynamic stress, Si in the biomass of *Egeria densa* Planch. was positively logarithmically related to increasing ambient Si concentrations, until apparent saturation is reached, beyond which biomass Si concentration stabilized. Next it was demonstrated that exposure to hydrodynamic stress could induce higher Si concentrations in stem and leaf tissue of *E. densa* and *Limnophila heterophylla* (Roxb.) Benth. under experimental conditions and in the tissue of *N. lutea* under natural conditions. The authors however, demonstrated neither the direct effect of hydrodynamic stress on cellulose and lignin production nor the consequences of the changes in silica, cellulose and lignin induced by hydrodynamic stress on the plants' resistance to this stress (i.e., the plants' strength).

In this study, we experimentally tested whether Si is involved in plant thigmomorphogenetic adaptations to mechanical perturbation, resulting in higher mechanical resistance. It is hypothesized that in case of mechanical perturbation, the plants take up Si, resulting in higher mechanical resistance due to the association of Si with cellulose and lignin.

MATERIALS AND METHODS

EXPERIMENTAL SETUP

Two aquaria (110 L) were filled with tap water (nutrient concentration: 3.65 ± 0.25 mg L^{-1} NO_3^- and 0.15 ± 0.04 mg L^{-1} PO_4^{3-}; pH: 8.4). Dissolved silicon concentration was set at 5.0 ± 0.4 mg Si L^{-1} by adding silicic acid (SiO_2*xH_2O; Merck, Darmstadt, Germany, DAB certificated). This concentration is on the lower end of what is commonly found in lowland rivers and streams (Struyf et al., 2010). Silica concentrations were carefully monitored by analysis on an ICP-OES spectrometer (iCAP 6000 series, Thermo Scientific, Cambridge, UK) to maintain equal concentrations in both aquaria, with SiO_2 added when necessary. Nutrient availability was regularly monitored by analysis on a colorimetric segmented flow analyzer (SAN^{++}, Skalar, Breda, Netherlands) but did not change significantly during the course of the experiment. In the first aquarium, hydrodynamic stress was created by installing a rotor (Turbelle Stream, Tunze, Penzberg, Germany) in the top one-third of the water column. This rotor created a highly turbulent flow regime with a top speed of 0.5 ± 0.1 m s^{-1} around the plants. This pushed the plants mainly in the downstream direction, but because of the turbulence, they were moving constantly (as in a natural situation). The water was also aerated with a regular air stone. In the second aquarium, the water was almost static as a regular air stone created only little water movement, minimizing boundary layers around the shoots. In each aquarium, 100 mature shoots of the submerged macrophyte *Egeria densa* Planch. (non-commelinoid monocots) were added in 10 groups of 10 individuals each. An extra control group of 10 shoots was kept apart to determine original stem morphological traits (length, diameter and fresh mass) before the experiment. The plants were bought at a plant nursery shop where they were grown in tap water under optimal conditions. The experiment ran for 21 days in a climate chamber at a constant temperature (20°C) and a day–night regime of 14 h light (PAR: 50 μmol m^{-2} s^{-1}).

MEASUREMENTS OF BIOMECHANICAL TRAITS

All plants were entirely defoliated immediately after the experiment. 30 stems were randomly picked per aquarium (three per group), and total length, diameter, and fresh mass of the stems was determined. The diameter was measured with a digital caliper (±0.01 mm) at three different points along the 5 cm basal stem part and averaged per sample. The differences between these data and that of 10 original control stems give an indication of the growth and performance of the plants over the course of the experiment (21 days). Next, the biomechanical properties of this subset of stems from the experiment were measured through (i) bending and (ii) tensile tests using a universal testing machine (Instron 5942, Canton, MA, USA).

Bending tests

As three-point bending tests could not be performed due to the too high flexibility of the plant stems, the samples were tested as cantilever beams using a one-fixed end bending test (Hamann and Puijalon, 2013). The basal stem samples (5 cm long) were clamped horizontally at their basal end while a force was applied at their midpoint by lowering a probe at a constant rate of 10 mm min^{-1}. We calculated the following biomechanical traits related to bending:

– The bending Young's modulus (E in Pa) quantifies the material stiffness and is calculated as the slope of the stress-strain curve in the elastic deformation region.

– The second moment of area (I in m^4) quantifies the distribution of material around the axis of bending, accounting for the effect of the cross-sectional geometry of a structure on its bending stress. As stem cross section was circular, I was calculated as $I = (\pi r^4)/4$, where r is the radius of stem cross section (Niklas, 1992).
– The flexural stiffness (EI in N m^2) quantifies the stiffness of the stem fragment, i.e., the extent to which the segment resists deformation in response to an applied force, and was calculated by multiplying E and I.

Tensile tests

The stem fragments (approximately 8 cm long) were clamped into the jaws of the testing machine and a constant extension rate of 5 mm min^{-1} was applied to the upper jaw until they broke. We calculated the following biomechanical traits at the sample breaking point:

– The breaking force (in N) is defined as the maximum force that the sample can bear without suffering mechanical failure.
– The tensile strength (in N m^{-2}) is calculated as the breaking force per cross-sectional area and quantifies the maximum force that the sample can bear corrected by its cross-sectional area.
– The tensile Young's modulus (E in Pa) is defined as the slope of a sample's stress–strain curve in the elastic deformation region and quantifies the segment stiffness, i.e., the extent to which the segment resists deformation in response to an applied force.

The diameter of all the stem fragments was measured using a digital caliper (±0.02 mm) at three different points along the sample.

CHEMICAL ANALYSES

After the strength measurements, the subset of basal stem parts was rejoined with their respective upper parts and all entire 200 shoots were dried at 70°C for 48 h. Stems and leaves were kept separated, but individuals were grouped together per original set of ten shoot, resulting in 40 samples (10 leaf samples and 10 stem samples from the aquarium with hydrodynamic stress and similar for the aquarium without stress). This was needed to obtain sufficient dry matter to perform all chemical analyses. Samples were grounded and homogenized with a mill. BSi was then extracted from 25 mg of dry plant material by incubation in a 0.1 M Na_2CO_3 mixture at 80°C during 5 h (DeMaster, 1981). The extracted and dissolved silica was analyzed on a colorimetric segmented flow analyser (SAN^{++}, Skalar, Breda, The Netherlands). The extraction in 0.1 M Na_2CO_3 at 80° has been well established and tested: it is capable of fully dissolving the BSi from plant phytoliths at the solid–solution ratios and extraction time we applied (Saccone et al., 2007). For lignin analysis, basically two major techniques are often used: "Klason lignin" determination for forestry products (Effland, 1977) and "ADF-lignin" for assessing animal forage quality (Van Soest, 1963). The latter is often referred to as more precise and more reproducible (Ryan et al., 1990; Rowland and Roberts, 1994). Moreover, the Van Soest (1963) method also enables to determine α-cellulose separately from hemicellulose, in contrast to the Effland (1977) method. We used the Van Soest (1963) method to analyze the plant samples for α-cellulose and ADF-lignin. In short, between 0.5 and 1 g of dry plant material was treated with cetyl-trimethylammonium-bromide to dissolve and remove proteins. The remaining material was treated with a 72% sulphuric acid. After weighing and drying (105°C), the α-cellulose content is calculated by subtracting the mass before and after the sulphuric acid treatment and dividing this value by the initial material mass. In a third step the remaining material was ignited at 550°C: the ADF lignin content was then calculated by subtracting the mass before and after ignition and dividing it by the initial material mass. We will further refer to ADF-lignin and α-cellulose as lignin and cellulose.

STATISTICS

Per aquarium, the 30 biomechanical traits analyses on stems and 20 chemical analyses on stems and leaves were averaged and a standard deviation was calculated. We used a Shapiro–Wilk normality test and a Bartlett test of homogeneity of variances on all datasets. Depending whether the assumptions were met or not, we used a t-test test or Kruskal–Wallis chi-squared test respectively.

RESULTS

All plants survived both treatments and performed well (**Table 1**). There was no significant difference in the length of the mature shoots between the two treatments ($t_{204} = 0.73$, $p = 0.46$, t-test) and between the control and treatment plants ($t_{56} = -1.13$, $p = 0.26$, t-test control × stress and $t_{70} = -1.62$, $p = 0.11$, t-test control × no stress). This implies no length growth (growth rate = 0 cm day^{-1}). The experimental stems did increase significantly in diameter as compared to the controls ($t_{13} = -8.29$, $p < 0.001$, t-test control × stress and $t_{19} = -9.67$, $p < 0.001$, t-test control × no stress), but did not differ significantly between the two treatments ($t_{38} = -3.38$, $p > 0.05$, t-test). This implies a diameter increase of 0.05 mm day^{-1}. The experimental stems did also increase significantly in fresh mass as compared to the controls ($t_{90} = -5.87$, $p < 0.001$, t-test control × stress and $t_{94} = -8.75$, $p < 0.001$, t-test control × no stress), but did not differ significantly between the two treatments ($t_{13} = -8.29$, $p > 0.05$, t-test). This implies a mass increase of 50 mg day^{-1}.

CHEMICAL TRAITS

Silica concentration was always higher in leaves than in stems. Individuals that were exposed to hydrodynamic stress had significantly higher Si concentrations in both leaves and stems, as compared to individuals not exposed to stress (**Figure 1A**;

Table 1 | Stem morphological traits (length, diameter, and fresh mass).

	Control	No stress	Stress
Length (cm)	23.6 ± 4.0^a	25.0 ± 5.4^a	24.5 ± 4.2^a
Diameter (mm)	1.05 ± 0.23^a	1.94 ± 0.27^b	1.72 ± 0.16^b
Fresh mass (g)	2.06 ± 0.59^a	3.31 ± 1.04^b	2.90 ± 0.97^b

Characters in superscript reflect the significant differences between treatments (control, no stress, stress) for each morphological trait, $p < 0.05$.

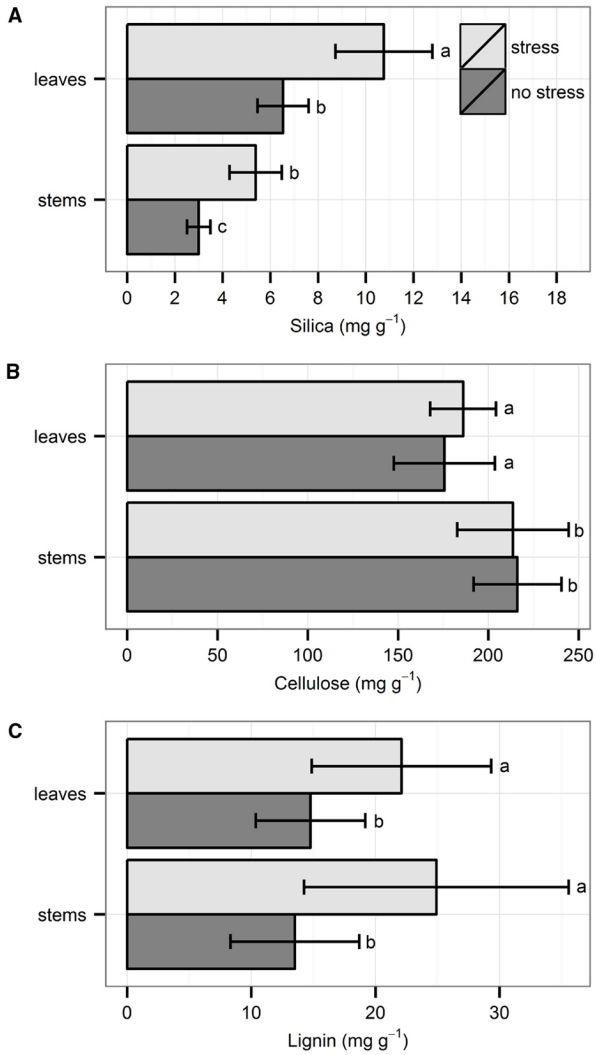

FIGURE 1 | Chemical properties of the leaves and shoots: (A) silica, (B) cellulose, and (C) lignin. Data are averages with standard deviation ($n = 10$). Character symbols reflect the significant differences between treatments (stress, no stress) for each plant organ (leaves, stems) and between each plant organ; $p < 0.05$.

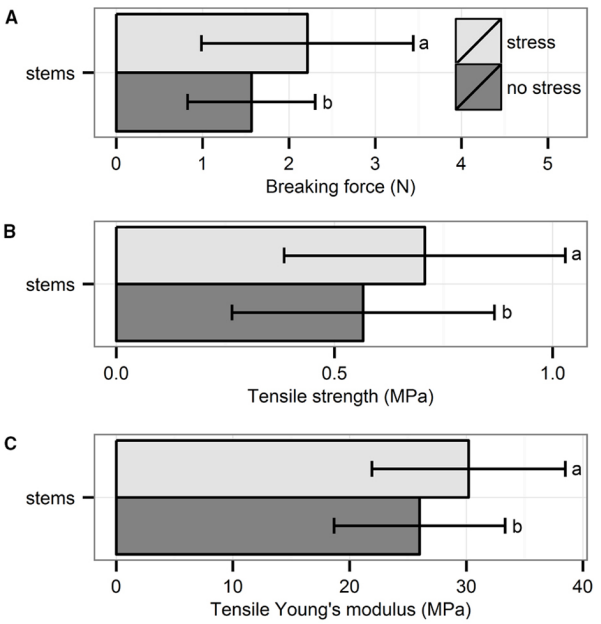

FIGURE 2 | Biomechanical properties of the stems measured through tensile test: (A) breaking force, (B) tensile strength, and (C) tensile Young's modulus. Data are averages with standard deviation ($n = 30$). Character symbols reflect the significant differences between treatments (stress, no stress); $p < 0.05$.

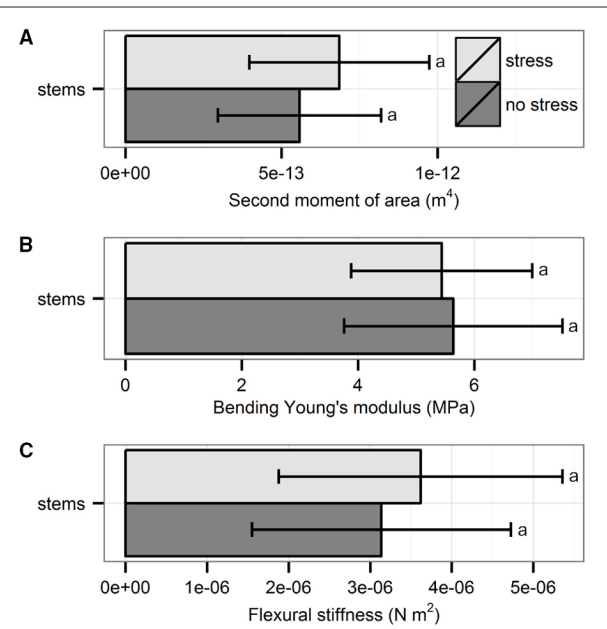

FIGURE 3 | Biomechanical properties of the stems measured through bending tests: (A) second moment of area, (B) bending Young's modulus, and (C) flexural stiffness. Data are averages with standard deviation ($n = 30$). No significant differences were found; $p > 0.05$.

$\chi^2_1 = 13.72$, $p < 0.001$, Kruskal–Wallis test). Cellulose concentration was always higher in stems than in leaves, but there was no significant difference between the two treatments (**Figure 1B**; $t_{18} = 0.20$, $p = 0.84$, t-test). There was no difference in lignin concentration between stems and leaves, but the concentration was always significantly higher under stressful conditions in both organs (**Figure 1C**; $\chi^2_1 = 8.17$, $p < 0.01$, Kruskal–Wallis test).

BIOMECHANICAL TRAITS

The three biomechanical traits measured through tensile tests were significantly higher for plants exposed to hydrodynamic stress (**Figure 2**): breaking force ($\chi^2_1 = 4.76$, $p = 0.03$, Kruskal–Wallis test), tensile strength ($\chi^2_1 = 4.26$, $p = 0.04$, Kruskal–Wallis test) and tensile Young's modulus ($\chi^2_1 = 4.28$, $p = 0.04$, Kruskal–Wallis test).

The three biomechanical traits measured through bending tests did not differ significantly between plants from the two treatments (**Figure 3**): second moment of area ($t_{56} = 1.76$, $p = 0.08$,

t-test), Young's modulus ($t_{54} = -0.44$, $p = 0.66$, t-test) and flexural stiffness ($\chi^2_1 = 1.07$, $p = 0.30$, Kruskal–Wallis test)

DISCUSSION

In accordance with our hypothesis, the results demonstrate that some biomechanical traits of *Egeria densa* were significantly affected by mechanical stimulation: exposure to hydrodynamic stress led to higher resistance to tensile forces (higher breaking force and tensile strength) and higher stiffness in tension, but did not modify the biomechanical traits in bending. Due to their high flexibility, the shoots of submerged aquatic plants exposed to flow generally align in the flow direction, and are consequently mostly subjected to tensile forces induced by hydrodynamic forces (Usherwood et al., 1997; Schutten and Davy, 2000; Puijalon et al., 2011). A high breaking force and tensile strength represents thus an important adaptation to flowing waters, reducing the risk for the plants to suffer mechanical failure of their shoots (Usherwood et al., 1997; Puijalon et al., 2011; Miler et al., 2012). The thigmomorphogenetic response to hydrodynamic stress observed in the present study may thus have an important adaptive value in increasing the capacity of the plants to tolerate the stress encountered through the production of a mechanically hardened phenotype. The response time is also rather fast as the experiment lasted for only 21 days. The present study demonstrates that the aquatic plants can adapt relatively quick to longer periods of hydrodynamic stress (order of weeks) not only through the production of a phenotype reducing the hydrodynamic forces (Puijalon et al., 2005, 2008), but also through the production of phenotypes increasing the mechanical resistance (i.e., higher resistance to breakage). Adaptation to mechanical stress through production of morphologies mechanically more resistant has been demonstrated for a long time on terrestrial plant species exposed to wind (e.g., Jaffe et al., 1984; Telewski and Jaffe, 1986), on marine algae exposed to waves (e.g., Biedka et al., 1987; Anderson et al., 2006), but not on aquatic plants (Bociag et al., 2009).

This research also confirms the earlier relation between lignin and biogenic Si deposition observed in submerged macrophytes (Schoelynck et al., 2010), and the observed silica uptake by macrophytes in response to hydrodynamical stress (Schoelynck et al., 2012). Emerging research links lignification and biogenic Si metabolism (Ghasemi et al., 2013; Zhang et al., 2013). It has been suggested that lignin can act as a precursor for biogenic Si deposition (Zhang et al., 2013), but the actual physiological mechanisms are currently not known. Although research is also still limited, more evidence points towards silica deposition being closely related to cellulose biosynthesis too. It was found that silica is present in beech leaves as precipitates in the walls of the epidermal and parenchymatous cells, either in the middle lamellae or in the cells against the walls or in the cell intersections (Watteau and Villemin, 2001). In this case, BSi and cellulose, hemicellulose and pectic substances are closely associated (Watteau and Villemin, 2001). Later, Shobbar et al. (2008) found that plants have evolved a broad protective mechanism linking the health and growth of the secondary cell wall with resistance to abiotic and biotic stresses, and abscisic acid (ABA) is the mediator of the mechanism. In times of stress, ABA induces transcripts that encode for cellulose synthase and, at the same time, these transcripts appear in so-called silica cells. These silica containing cells are equally important for leaf strength as is the cell wall. In a recent paper, Fraysse et al. (2010) support the hypothesis of the existence of individual molecules H_4SiO_4 or small polymers (silica gel, $SiO_2 \cdot nH_2O$) dispersed in the organic matrix of the cell wall.

The inclusion of Si uptake as a plant functional trait is important to assess links between plant physiology, plant distribution and plant tolerance to environmental changes, but also to understand the role of vegetation on nutrient fluxes through the watershed (Schoelynck et al., 2014b). There is a growing line of evidence that Si uptake in wetland and aquatic macrophytes has important implications for other biogeochemical cycles. In a recent study, Si content of aquatic macrophytes increased decomposition rate of the litter, even under low quality conditions with a low C/N ratio (Schaller and Struyf, 2013). Interestingly, when shredders were present, Si had an adverse impact on the decomposition rate. Si uptake in aquatic macrophytes has further also been linked to concentrations of both macro- and micronutrients (Schaller et al., 2012; Schaller and Struyf, 2013), with, e.g., CNP ratios altered by Si deposition and reduced uptake of metals. If plants thus adapt to alterations in hydrological conditions, e.g., induced by more frequent occurrence of peak floods after drainage basin build-up or due to increased occurrence of storm rains, this could alter their impact on other biogeochemical cycles. Aquatic macrophytes are known to create biogeochemical hotspots in their growth patches compared to adjacent non-vegetated areas, with increased organic matter storage and nutrient cycling observed in the patches (Sand-Jensen, 1998; Cotton et al., 2006; Kleeberg et al., 2010; Schoelynck et al., 2014a). Interestingly, the engineering capacity of macrophyte patches to trap and store organic matter is itself to a great extent determined by the rigidity of the stems (Gurnell, 2014).

CONCLUSION

We conclude that the presence of hydrodynamic stress triggers the uptake of silica in *Egeria densa*, which is linked to changes in the lignin concentration. These responses to mechanical stress are likely the explaining factor for a higher capacity to tolerate this stress through the production of mechanically hardened shoots. These thigmomorphogenetic responses can help to improve the survival chances of the species.

ACKNOWLEDGMENTS

We would like to thank Ruby Neervoort and Marie-Rose Viricel for helping with the experiments. This research was executed with the financial support of the Tournesol framework 2013 and 2014: The role of biogenic silica in macrophyte resistance to hydrodynamic stress (project n° T2013.23 and n° 28897QG), and also partly of FWO Flanders for the Scientific Research Network (WOG) "the functioning of river ecosystems through plant-flow-soil interactions" (W0.027.11N).

REFERENCES

Anderson, K., Close, L., Dewreede, R. E., Lynch, B. J., Ormond, C., and Walker, M. (2006). Biomechanical properties and holdfast morphology of coenocytic algae (Halimedales, Chlorophyta) in Bocas del Toro, Panama. *J. Exp. Mar. Biol. Ecol.* 328, 155–167. doi: 10.1016/j.jembe.2005.07.005

Biedka, R. F., Gosline, J. M., and Dewreede, R. E. (1987). Biomechanical analysis of wave-induced mortality in the marine alga Pterygophora californica. *Mar. Ecol. Prog. Ser.* 36, 163–170. doi: 10.3354/meps036163

Bociag, K., Galka, A., Lazarewicz, T., and Szmeja, J. (2009). Mechanical strength of stems in aquatic macrophytes. *Acta Soc. Bot. Pol.* 78, 181–187. doi: 10.5586/asbp.2009.022

Braam, J. (2005). In touch: plant responses to mechanical stimuli. *New Phytol.* 165, 373–389. doi: 10.1111/j.1469-8137.2004.01263.x

Carpita, N., Tierney, M., and Campbell, M. (2001). Molecular biology of the plant cell wall: searching for the genes that define structure, architecture and dynamics. *Plant Mol. Biol.* 47, 1–5. doi: 10.1023/A:1010603527077

Cotton, J. A., Wharton, G., Bass, J. A. B., Heppell, C. M., and Wotton, R. S. (2006). The effects of seasonal changes to in-stream vegetation cover on patterns of flow and accumulation of sediment. *Geomorphology* 77, 320–334. doi: 10.1016/j.geomorph.2006.01.010

DeMaster, D. J. (1981). The supply and accumulation of silica in the marine-environment. *Geochim. Cosmochim. Acta* 45, 1715–1732. doi: 10.1016/0016-7037(81)90006-5

Denny, M. (1988). *Biology and the Mechanics of the Wave-Swept Environment*. Princeton, NJ: Princeton University Press.

Doyle, R. D. (2001). Effects of waves on the early growth of *Vallisneria americana*. *Freshw. Biol.* 46, 389–397. doi: 10.1046/j.1365-2427.2001.00668.x

Effland, M. J. (1977). Modified procedure to determine insoluble lignin in wood and pulp. *Tappi* 60, 143–144.

Ennos, A. R. (1997). Wind as an ecological factor. *Trends Ecol. Evol.* 12, 108–111. doi: 10.1016/s0169-5347(96)10066-5

Fraysse, F., Pokrovsky, O. S., and Meunier, J. D. (2010). Experimental study of terrestrial plant litter interaction with aqueous solutions. *Geochim. Cosmochim. Acta* 74, 70–84. doi: 10.1016/j.gca.2009.09.002

Genet, M., Stokes, A., Salin, F., Mickovski, S. B., Fourcaud, T., Dumail, J. F., et al. (2005). The influence of cellulose content on tensile strength in tree roots. *Plant Soil* 278, 1–9. doi: 10.1007/s11104-005-8768-6

Ghasemi, E., Ghorbani, G. R., Khorvash, M., Emami, M. R., and Karimi, K. (2013). Chemical composition, cell wall features and degradability of stem, leaf blade and sheath in untreated and alkali-treated rice straw. *Animal* 7, 1106–1112. doi: 10.1017/s1751731113000256

Green, N. E., Hadwiger, L. A., and Graham, S. O. (1975). Phenylalanine ammonia-lyase, tyrosine ammonia-lyase, and lignin in weat inoculated with *Erysiphe graminis* f-sp Tritici. *Phytopathology* 65, 1071–1074. doi: 10.1094/Phyto-65-1071

Gurnell, A. M. (2014). Plants as river system engineers. *Earth Surf. Proc. Landforms* 39, 4–25. doi: 10.1002/esp.3397

Hamann, E., and Puijalon, S. (2013). Biomechanical responses of aquatic plants to aerial conditions. *Ann. Bot.* 112, 1869–1878. doi: 10.1093/aob/mct221

Hu, W. J., Harding, S. A., Lung, J., Popko, J. L., Ralph, J., Stokke, D. D., et al. (1999). Repression of lignin biosynthesis promotes cellulose accumulation and growth in transgenic trees. *Nat. Biotechnol.* 17, 808–812. doi: 10.1038/11758

Jaffe, M. J., Telewski, F. W., and Cooke, P. W. (1984). Thigmomorphogenesis—on the mechanical properties of mechanically perturbed bean plants. *Physiol. Plant.* 62, 73–78. doi: 10.1111/j.1399-3054.1984.tb05925.x

Kaufman, P. B., Cseke, L. J., Warber, S., Duke, J. A., and Brielman, H. L. (1999). *Natural Products from Plants*. Boca Raton, FL: CRC Press LCC.

Kleeberg, A., Kohler, J., Sukhodolova, T., and Sukhodolov, A. (2010). Effects of aquatic macrophytes on organic matter deposition, resuspension and phosphorus entrainment in a lowland river. *Freshw. Biol.* 55, 326–345. doi: 10.1111/j.1365-2427.2009.02277.x

Miler, O., Albayrak, I., Nikora, V., and O'hare, M. (2012). Biomechanical properties of aquatic plants and their effects on plant-flow interactions in streams and rivers. *Aquatic Sci.* 74, 31–44. doi: 10.1007/s00027-011-0188-5

Niklas, K. J. (1992). *Plant Biomechanics: An Engineering Approach to Plant form and Function*. Chicago, IL: University of Chicago Press.

Palm, C. A., and Rowland, A. P. (1997). "Chemical characterization of plant quality for decomposition," in *Driven by Nature: Plant Litter Quality and Decomposition*, eds G. Cadish and K. E. Giller. (Wallingford: CAB International), 379–392.

Puijalon, S., and Bornette, G. (2013). "Ecohydraulics: an integrated approach," in *Multi-Scale Macrophyte Responses to Hydrodynamic Stress and Disturbances: Adaptive Strategies and Biodiversity Patterns*, eds I. Maddock, A. Harby, P. Kemp, and P. Wood. (Chichester: John Wiley & Sons, Ltd.), 462.

Puijalon, S., Bornette, G., and Sagnes, P. (2005). Adaptations to increasing hydraulic stress: morphology, hydrodynamics and fitness of two higher aquatic plant species. *J. Exp. Bot.* 56, 777–786. doi: 10.1093/jxb/eri063

Puijalon, S., Bouma, T. J., Douady, C. J., Van Groenendael, J., Anten, N. P. R., Martel, E., et al. (2011). Plant resistance to mechanical stress: evidence of an avoidance-tolerance trade-off. *New Phytol.* 191, 1141–1149. doi: 10.1111/j.1469-8137.2011.03763.x

Puijalon, S., Lena, J. P., Riviere, N., Champagne, J. Y., Rostan, J. C., and Bornette, G. (2008). Phenotypic plasticity in response to mechanical stress: hydrodynamic performance and fitness of four aquatic plant species. *New Phytol.* 177, 907–917. doi: 10.1111/j.1469-8137.2007.02314.x

Raven, J. A. (1983). The transport and function of silicon in plants. *Biol. Rev. Camb. Philos. Soc.* 58, 179–207. doi: 10.1111/j.1469-185X.1983.tb00385.x

Read, J., and Stokes, A. (2006). Plant biomechanics in an ecological context. *Am. J. Bot.* 93, 1546–1565. doi: 10.3732/ajb.93.10.1546

Rowland, A. P., and Roberts, J. D. (1994). Lignin and cellulose fractionation in decomposition studies using acid-detergent fiber methods. *Commun. Soil Sci. Plant Anal.* 25, 269–277. doi: 10.1080/00103629409369035

Ryan, M. G., Melillo, J. M., and Ricca, A. (1990). A comparison of methods for determining proximate carbon fractions of forest litter. *Can. J. For. Res.* 20, 166–171. doi: 10.1139/x90-023

Saccone, L., Conley, D. J., Koning, E., Sauer, D., Sommer, M., Kaczorek, D., et al. (2007). Assessing the extraction and quantification of amorphous silica in soils of forest and grassland ecosystems. *Eur. J. Soil Sci.* 58, 1446–1459. doi: 10.1111/j.1365-2389.2007.00949.x

Sand-Jensen, K. (1998). Influence of submerged macrophytes on sediment composition and near-bed flow in lowland streams. *Freshw. Biol.* 39, 663–679. doi: 10.1046/j.1365-2427.1998.00316.x

Schaller, J., Brackhage, C., Gessner, M. O., Baüker, E., and Dudel, E. G. (2012). Silicon supply modifies C:N:P stoichiometry and growth of *Phragmites* australis. *Plant Biol.* 14, 392–396. doi: 10.1111/j.1438-8677.2011.00537.x

Schaller, J., and Struyf, E. (2013). Silicon controls microbial decay and nutrient release of grass litter during aquatic decomposition. *Hydrobiologia* 709, 201–212. doi: 10.1007/s10750-013-1449-1

Schoelynck, J., Bal, K., Backx, H., Okruszko, T., Meire, P., and Struyf, S. (2010). Silica uptake in aquatic and wetland macrophytes: a strategic choice between silica, lignin and cellulose? *New Phytol.* 186, 385–391. doi: 10.1111/j.1469-8137.2009.03176.x

Schoelynck, J., Bal, K., Puijalon, S., Meire, P., and Struyf, E. (2012). Hydrodynamically mediated macrophyte Si dynamics. *Plant Biol.* 14, 997–1005. doi: 10.1111/j.1438-8677.2012.00583.x

Schoelynck, J., Bal, K., Verschoren, V., Penning, E., Struyf, E., Bouma, T., et al. (2014a). Different morphology of *Nuphar lutea* in two contrasting aquatic environments and its effect on ecosystem engineering. *Earth Surf. Proc. Landforms* 39, 2100–2108. doi: 10.1002/esp.3607

Schoelynck, J., Müller, F., Vandevenne, F., Bal, K., Barao, L., Smis, A., et al. (2014b). Silicon-vegetation interaction in multiple ecosystems: a review. *J. Veg. Sci.* 25, 301–313. doi: 10.1111/jvs.12055

Schutten, J., Dainty, J., and Davy, A. J. (2005). Root anchorage and its significance for submerged plants in shallow lakes. *J. Ecol.* 93, 556–571. doi: 10.1111/j.1365-2745.2005.00980.x

Schutten, J., and Davy, A. J. (2000). Predicting the hydraulic forces on submerged macrophytes from current velocity, biomass and morphology. *Oecologia* 123, 445–452. doi: 10.1007/s004420000348

Shobbar, Z. S., Oane, R., Gamuyao, R., De Palma, J., Malboobi, M. A., Karimzadeh, G., et al. (2008). Abscisic acid regulates gene expression in cortical fiber cells and silica cells of rice shoots. *New Phytol.* 178, 68–79. doi: 10.1111/j.1469-8137.2007.02365.x

Sjostrom, E. (1993). *Wood Chemistry Fundamentals and Applications*. San Diego: Academic Press Inc.

Strand, J. A., and Weisner, S. E. B. (2001). Morphological plastic responses to water depth and wave exposure in an aquatic plant (*Myriophyllum spicatum*). *J. Ecol.* 89, 166–175. doi: 10.1046/j.1365-2745.2001.00530.x

Struyf, E., Smis, A., Van Damme, S., Garnier, J., Govers, G., Van Wesemael, B., et al. (2010). Historical land use change has lowered terrestrial silica mobilization. *Nat. Commun.* 1:129. doi: 10.1038/ncomms1128

Telewski, F. W. (2006). A unified hypothesis of mechanoperception in plants. *Am. J. Bot.* 93, 1466–1476. doi: 10.3732/ajb.93.10.1466

Telewski, F. W., and Jaffe, M. J. (1986). Thigmomorphogenesis—field and laboratory studies of *Abies fraseri* in response to wind or mechanical perturbation. *Physiol. Plant.* 66, 211–218. doi: 10.1111/j.1399-3054.1986.tb02411.x

Turner, S. R., Taylor, N., and Jones, L. (2001). Mutations of the secondary cell wall. *Plant Mol. Biol.* 47, 209–219. doi: 10.1023/A:1010695818416

Usherwood, J. R., Ennos, A. R., and Ball, D. J. (1997). Mechanical and anatomical adaptations in terrestrial and aquatic buttercups to their respective environments. *J. Exp. Bot.* 48, 1469–1475. doi: 10.1093/jxb/48.7.1469

Van Soest, P. J. (1963). Use of detergents in analysis of fibrous feeds.II. a rapid method for determination of fiber and lignin. *J. Assoc. Off. Agric. Chem.* 46, 829–835.

Vogel, S. (2003). *Comparative Biomechanics: Life's Physical World*. New Jersey: Princeton University Press.

Watteau, F., and Villemin, G. (2001). Ultrastructural study of the biogeochemical cycle of silicon in the soil and litter of a temperate forest. *Eur. J. Soil Sci.* 52, 385–396. doi: 10.1046/j.1365-2389.2001.00391.x

Zhang, C. C., Wang, L. J., Zhang, W. X., and Zhang, F. S. (2013). Do lignification and silicification of the cell wall precede silicon deposition in the silica cell of the rice (*Oryza sativa* L.) leaf epidermis? *Plant Soil* 372, 137–149. doi: 10.1007/s11104-013-1723-z

Conflict of Interest Statement: The authors declare that the research was conducted in the absence of any commercial or financial relationships that could be construed as a potential conflict of interest.

Received: 12 September 2014; accepted: 15 January 2015; published online: 05 February 2015.

*Citation: Schoelynck J, Puijalon S, Meire P and Struyf E (2015) Thigmomorphogenetic responses of an aquatic macrophyte to hydrodynamic stress. Front. Plant Sci. **6**:43. doi: 10.3389/fpls.2015.00043*

This article was submitted to Plant Physiology, a section of the journal Frontiers in Plant Science.

frontiers in
PLANT SCIENCE

PERSPECTIVE ARTICLE
published: 17 September 2014
doi: 10.3389/fpls.2014.00471

Brown algal morphogenesis: atomic force microscopy as a tool to study the role of mechanical forces

Benoit Tesson*[1] *and* ***Bénédicte Charrier*[2,3]***

[1] *Marine Biology Research Division, Scripps Institution of Oceanography, University of California San Diego, La Jolla, CA, USA*
[2] *Centre National de la Recherche Scientifique-Unités Mixtes de Recherche 8227 Integrative Biology of Marine Models, Station Biologique de Roscoff, Roscoff, France*
[3] *Sorbonne Universités, Université Pierre-et-Marie-Curie, Unités Mixtes de Recherche 8227 Integrative Biology of Marine Models, Roscoff, France*

Edited by:
Sara Puijalon, Université Lyon 1, France

Reviewed by:
Naomi Nakayama, University of Edinburgh, UK
Nabil I. Elsheery, Tanta University, Egypt

****Correspondence:***
Benoit Tesson, Marine Biology Research Division, Scripps Institution of Oceanography, University of California San Diego, 9500 Gilman Dr., La Jolla, CA 92093-0202, USA
e-mail: tessonben@gmail.com;
Bénédicte Charrier, CNRS, UMR 8227 Integrative Biology of Marine Models, Station Biologique de Roscoff, CS 90074, F-29688 Roscoff cedex, France
e-mail: benedicte.charrier@sb-roscoff.fr

Over the last few years, a growing interest has been directed toward the use of macroalgae as a source of energy, food and molecules for the cosmetic and pharmaceutical industries. Besides this, macroalgal development remains poorly understood compared to other multicellular organisms. Brown algae (Phaeophyceae) form a monophyletic lineage of usually large multicellular algae which evolved independently from land plants. In their environment, they are subjected to strong mechanical forces (current, waves, and tide), in response to which they modify rapidly and reversibly their morphology. Because of their specific cellular features (cell wall composition, cytoskeleton organization), deciphering how they cope with these forces might help discover new control mechanisms of cell wall softening and cellulose synthesis. Despite the current scarcity in knowledge on brown algal cell wall dynamics and protein composition, we will illustrate, in the light of methods adapted to *Ectocarpus siliculosus*, to what extent atomic force microscopy can contribute to advance this field of investigation.

Keywords: brown algae, *Ectocarpus siliculosus*, morphogenesis, cell wall, mechanical forces, AFM

In addition to cell differentiation, the morphogenesis of multicellular organisms depends both on growth rates and growth directions. As there are now several evidences indicating that mechanical forces are important factors of cell growth and polarity (Braam, 2005; Hamant, 2013), researchers recently started to combine genetic information with biophysical measurements.

In plant organisms, two kinds of mechanical stimuli may influence growth rates and directions. Environmental stimuli like wind, current or rock, were known for a long time to influence plant growth. More recently, several evidences suggested that internal mechanical forces as well, generated by the growth itself, could be considered as morphogenetic factors, which control the spatial organization of the organism like biochemical gradients do (Monshausen and Gilroy, 2009; Hamant and Traas, 2010).

How external or internal mechanical forces impact on cell growth in land plants will likely be covered in this special issue by colleagues. We will present herein how external mechanical factors also contribute to morphogenetic changes in brown algae and we will introduce the method of investigation that we are currently deploying to identify the biophysical and molecular factors at play in this process.

Abbreviations: AFM, Atomic Force Microscopy; MF, Microfilament; MT, Microtubule.

IMPACT OF MECHANICAL FORCES IN BROWN ALGAL MORPHOGENESIS: THEMES AND VARIATIONS COMPARED TO LAND PLANTS

Brown algae form a monophyletic group of multicellular organisms, which is phylogenetically divergent from the other groups of macroalgae (red and green) and other multicellular organisms like land plants and metazoans. They also differ from land plants in many ways, and particularly by their habitat and morphologies. They are dominant in the highly variable coastal environment and display very diverse body architectures, from microscopic species to giant kelp of up to 50 m long. Brown algae and land plants live in different environments, each presenting distinct physical constraints. In particular, gravity is less perceived in seawater which is denser than air and provides support to organisms allowing more flexible bodies.

IMPACT OF EXTERNAL FORCES

In the ocean, mechanical forces such as currents and tides control both shape and size of macroalgae. Their flexible bodies are particularly suitable to adapt to such changing environments. In particular, macroalgae are capable to rapidly change their morphologies in a reversible way in response to environmental changes. This is actually a key factor for their survival and propagation in the ocean (Koehl, 1984; Dudgeon and Johnson,

1992; Blanchette, 1997). This ability might be attributable to their low body complexity with only a few cells types, in addition to a high responsiveness to external stimuli (Charrier et al., 2012). Adaptation is achieved by a phenomenon called flexible reconfiguration which allows the organisms to reduce drag. Flexible reconfiguration involves shape change and size reduction (Boller and Carrington, 2006; Martone et al., 2012).

On rocky shores water velocity induced by waves ranges from 2 to 25 $m.s^{-1}$ with acceleration exceeding 400 $m.s^{-2}$ (Friedland and Denny, 1995). These speeds could seem rather low compared to the wind but it is without accounting for the density which is about 1000 times higher for water compared to air. Force resulting from a 2 $m.s^{-1}$ current would correspond to a 208 $km.h^{-1}$ wind (Denny and Gaylord, 2002). These particularly turbulent conditions require macroalgae to be flexible and to adapt by changing their morphology if they are to survive. An intrinsic adaptation of algae to mechanical forces is their simple body architecture allowing a very large diversity of shapes and their flexible body. This flexibility is due to material constituting algal cell wall which is characterized by a low stiffness and a high extensibility. Stiffness of algal material is in the range of 1–100 MPa, i.e., about 1000 times softer compared to land plants (Denny and Gaylord, 2002). Adaptation of macroalgae to wave swept environments usually involves narrow, thick, and flat blades while the counterpart in sheltered habitats display wide, thin, and undulated blades. Undulation has been shown to result from differential growth in the center and at the periphery of the blades. Higher longitudinal growth at the periphery than in the center of the blade produces ruffles on the edges due to elastic buckling (Koehl et al., 2008). Undulated, wide blades found in low flow regime increase drag and light interception while the inverse is observed for flat and narrow blades from wave exposed sites (Koehl et al., 2008). Buoyancy is also affected by mechanical stress. Within the same species, and in protected areas, algae develop a specific cell type called "pneumatocysts" increasing buoyancy, while in exposed areas, pneumatocysts are either very small or absent (Stewart, 2006). These morphological variations are due to the plasticity of macroalgae and not only to genetic traits, as algae are able to rapidly change their morphology in response to flow regime changes (Fowler-Walker et al., 2006).

POTENTIAL INTERNAL MECHANICAL FORCES INVOLVED IN CELL GROWTH AND CELLULAR RESPONSES

Tip-growing brown algae, such as *Sphacelaria* (Order Sphacelariales) and *Ectocarpus* (Ectocarpales) are particularly suitable models to study the role of mechanical forces on cell growth rate and direction. As in the other tip-growing cells, the cylindrical shape of the apical cells results in a stress in the circumferential direction twice as large as in the axial direction (Castle, 1937). Cell wall of tip-growing cells of *Sphacelaria rigidula* consists of four layers: (i) an external thin amorphous layer, (ii) a layer consisting of fibrillar materials embedded in an amorphous matrix, (iii) a layer made of transversally oriented cellulose fibers and (iv) a layer of longitudinally oriented cellulose fibers (Karyophyllis et al., 2000). The external amorphous layer likely consists of amorphous alginates mainly, while the more internal layers are enriched in cellulose. Interestingly, the cell wall was found to be thinner at the tip, consisting only of the first two layers, likely making the wall softer in this region. Moreover, transversal orientation of cellulose fibers at the flank provides resistance to deformation in this direction. To promote tip growth, cells need to modulate the mechanical properties of their cell wall. Two mechanisms are possible: 1- softening of the cell wall at the tip and/or 2- anisotropic organization of the cellulose fibers to resist transversal deformation and favor tip elongation (Mirabet et al., 2011).

Softening of the cell wall at the tip

In pollen tube, tip-growth is mediated by secretion of methyl-esterified pectin at the tip and gradual stiffening is achieved by de-esterification of pectin and calcium mediated cross-linking of the carboxyl groups (Rounds and Bezanilla, 2013). No pectin was reported to be present in brown algal cell walls. However, other compounds could fulfill the same role. Brown algal cell wall is composed principally of alginates, sulfated fucans and of a relatively low amount of cellulose (Kloareg and Quatrano, 1988). Alginates are polymers of mannuronic and guluronic acids in various amounts. Interestingly, their properties depends on the relative amount of manuronnans and guluronans, as stiffness increases with increasing guluronan content, the latter forming binding sites for calcium ions, thereby inducing gelation (Draget and Taylor, 2011). Secretion of alginates composed of manuronans at the tip and subsequent epimerization of mannuronans into guluronans by the mannuronan C5 epimerase (MC5E) (Michel et al., 2010) would lead to a softer wall at the tip compared to shank. In addition, recent chemical analyses of brown algal cell walls (Order Fucales) showed that alginates were linked to most phenolic compounds present in the cell wall (Deniaud-Bouët et al., 2014). The progressive linkage of apical newly-deposited alginates to phenolic compounds mediated by the activity of extracellular haloperoxidases could increase stiffness in the flanks of the cell during tip-growth. Noteworthily, fucose-containing sulfated polysaccharides (FCSP) were also shown to be tightly linked to cellulose and cell wall proteins, but these would be more involved in the regulation of water retention at the cell surface than to cell wall mechanical resistance (Deniaud-Bouët et al., 2014).

Actin-mediated cellulose orientation

At the cellular level, localization of actin microfilaments (MF) and microtubules (MT) as well as the use of cytoskeleton inhibitors on the brown algae *Sphacelaria rigidula* revealed major differences with land plants and some similarities with diatoms, which are the closest relative to brown algae (Katsaros et al., 2006). Indeed, like in diatoms and animal cells, cytokinesis requires the formation of an actin plate, and, in contrast with land plants, cellulose microfibril deposition seems to be under the control of actin MF and not of MT (Katsaros et al., 2006; De Martino et al., 2009). Localization of actin MFs in *Sphacelaria* apical cells showed that they are oriented in the longitudinal direction except at the base of the apex, where actin is organized as a ring in the transverse section, and at the tip of the apex itself, where MFs are randomly oriented. Orientation of MFs corresponds to the orientation of the cellulose fibers in the inner layer of the cell wall. Furthermore,

treatment with cytochalasin D, an inhibitor of actin polymerization induced tip growth arrest and altered orientation of newly deposited cellulose fibrils (Karyophyllis et al., 2000; Katsaros et al., 2003).

Altogether, both local biochemical modifications of amorphous cell wall materials and actin-mediated cellulose microfibril orientation could control cell wall stiffness and promote the anisotropic growth of tip-growing cells in brown algae.

MEASURING MECHANICAL FORCES EXPERIENCED BY BROWN ALGAL CELLS

AVAILABLE TECHNICAL TOOLS AND APPLICATION TO PLANT CELLS

Several tools allowing the measurement of cell mechanical properties have been developed including single cell compression, ball tonometry, microindentation, Cellular Force Microscopy (CFM), Nanoscale Dynamic Mechanical Analysis (NanoDMA), and Atomic Force Microscopy (AFM). One of the differences between these tools is the size of the probe which is an important parameter for the study of microorganisms. Ball sizes in the ball tonometry method range from 300 to 5000 μm and microindentation and CFM probes are 2–11 μm. NanoDMA and AFM have a wider range of probes from 10 nm (pyramidal tip) to several microns (spherical probes). For more advanced reviews see Milani et al. (2013) and Routier-Kierzkowska and Smith (2013).

Recently, properties of land plant cell walls were monitored using AFM (Milani et al., 2011; Fernandes et al., 2012) and changes in mechanical properties were correlated with growth and activity of cell wall enzymes (Milani et al., 2011; Peaucelle et al., 2011).

Cell wall is not homogeneous. Depending on the size of the probes, of the indentation depth, and of the turgor pressure, the contribution of underlying materials might influence the measured stiffness. On the one hand, by dividing force indention curves into segments, Roduit et al. (2009) developed "AFM tomography" and used it to differentiate layers with distinct mechanical properties within the cell wall of *Arabidopsis* cell suspension (Radotić et al., 2012).

On the other hand, nanoindentation and CFM combined with finite element modeling were recently used to measure turgor pressure in plant cells, and allowed to complement data obtained using pressure probes or the plasmolysis limit method. Indentations were realized at various depths and in different conditions of turgor pressure to isolate cell wall properties *per se* from turgor pressure (Forouzesh et al., 2013; Vogler et al., 2013).

Simple indentation shows the instantaneous elastic behavior. However, the cell wall is a more complex material with viscoelastic properties, meaning that deformation is time dependent. Elastic behavior is associated with the stretching of bonds while viscosity is associated with the diffusion of molecules in amorphous polymers. Various methods can be used to determine viscoelastic properties including Dynamic Mechanical Analysis (DMA), stress relaxation, and creep. Determination of viscoelastic properties of plant cell walls revealed distinct properties in mutants, ecotypes, and at different maturity stages (Hayot et al., 2012; Forouzesh et al., 2013).

AFM TO STUDY MECHANICAL FORCES IN THE BROWN ALGA ECTOCARPUS

In order to start studying the role of physical forces in brown algal cell growth and morphogenesis, we are currently investigating the mechanical properties of the tip-growing filamentous

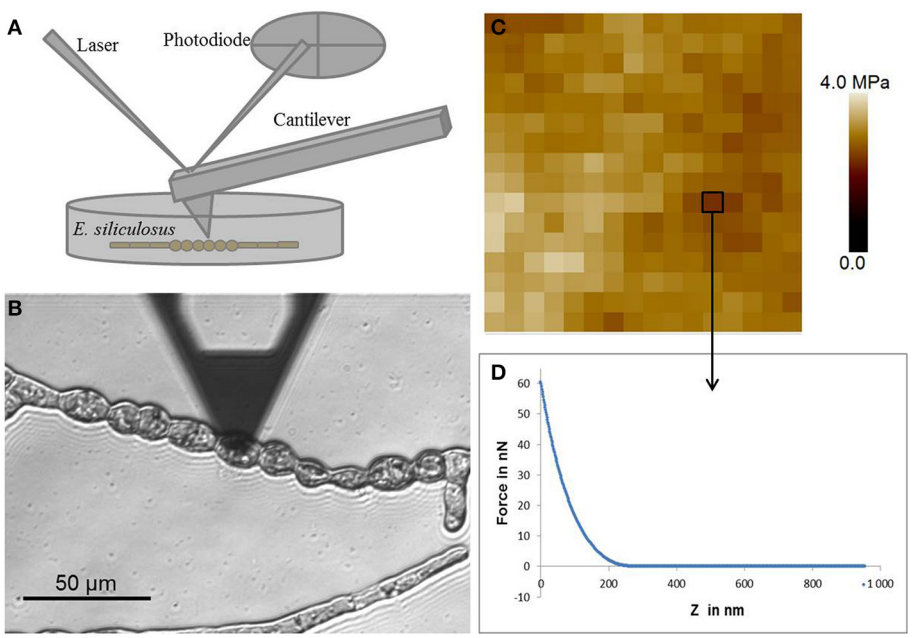

FIGURE 1 | Atomic force microscopy. (A) Schematic representation of the AFM setting. **(B)** Optical micrograph of the AFM cantilever located at the surface of a round cell of *E. siliculosus* filament. **(C)** Example of force curve, x axis represents the z motion of the cantilever and y axis represents the force applied at the surface of the cell. **(D)** Elasticity map of a 1 μm^2 area consisting of an array of 16 by 16 force curves.

alga *Ectocarpus siliculosus*. Given the size of *Ectocarpus* cells, nanoindentation tools such as AFM are better suited.

AFM principle and applications

AFM is a surface scanning technique. Originally it was mainly used to image the surface of samples but it evolved into a versatile tool with a wide range of applications (Muller and Dufrene, 2011). Principle is based on the scanning of a surface with a probe consisting in a tip located at the end of a cantilever (**Figure 1A**). Compared to the other techniques, AFM displays the advantage of allowing surface imaging with a very high resolution in native (hydrated) conditions. Tip sizes can vary from a few nanometers to few tens of nanometers and bead sizes from 100 nm to 20 µm. The coupling to an inverted microscope allows highly resolutive localization and observation of the sample prior to analysis with the AFM, which is a prerequisite for the study of microorganisms. In order to measure cell mechanical properties, force deformation curves are acquired by pushing on the cell surface. From this curve, elastic modulus (E) is determined by fitting the curve using mechanical models for elastic materials. The most well-known is the Hertz model which was developed for spherical indenters implying that the deformation depth is much smaller than the indenter radius (Hertz, 1882). The Hertz model was modified by Sneddon to be adapted to conical indenters implying that the indentation depth is greater than the tip radius of the indenter (Sneddon, 1965). Viscoelastic properties can be determined using AFM by performing relaxation or creep tests. Resulting curves are then fitted with a model consisting in various arrangements of springs and dash pots representing elastic and viscous behavior respectively.

Two main limitations are inherent to the use of AFM: (i) the sample should adhere to a substrate and (ii) be accessible to the tip. Hence, in plants, AFM was particularly adapted to study the cell wall of the moss *Physcomitrella* filaments (Wyatt et al., 2008), the angiosperm pollen tubes (Wu et al., 2008) and hypocotyls (Marga et al., 2005). In addition, as AFM can be carried out in liquid medium, it is particularly suitable for algae, and was used in diatoms, both at the surface of live cells (Francius et al., 2008) and from extracted cell walls (Tesson and Hildebrand, 2010a,b, 2013).

Application of AFM to Ectocarpus filaments

Ectocarpus is a filamentous brown algae growing attached to a substrate (a Petri dish in laboratory conditions) which makes cells easily accessible to experimentation. However, at late stages (2–3 weeks after spore germination), secondary filaments grow in the "z" direction, which makes the primary filaments less accessible (**Figure 2A**). For this reason AFM analysis in *Ectocarpus* was so far only carried out at early stages when the body was two-dimensional (**Figures 1B**, **2B**). *E. siliculosus* differentiates two cell

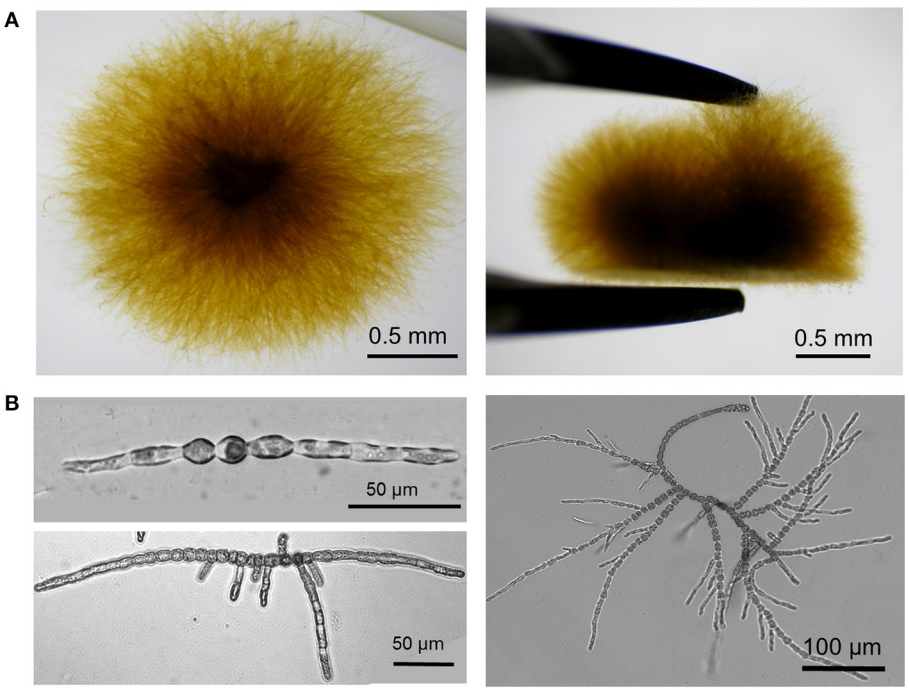

FIGURE 2 | Developmental pattern of *E. siliculosus*. (A) Top (left) and side (right) views of an *Ectocarpus* sporophyte grown in laboratory condition for 1 month in sea water. For the side view, the algal body was taken off from the bottom of the Petri dish with pliers. **(B)** *Ectocarpus* sporophyte is formed of branched uniseriate filaments. In the early stages, the sporophyte differentiates only two cell types: round cells localized in the center of the filament and elongated cells at the apices. Initially, mito-spores attach to the substrate and divide by successive uniaxial mitoses to form the young sporophyte filament (top left). Young sporophytes grow apically by both elongation and division of the apical elongated cells, which eventually differentiate into round cells. Branching takes place by emergence of secondary filaments preferentially on round cells in the center of the filament (Le Bail et al., 2008) (bottom left). Re-iteration of this process on each newly formed filament gives rise to a highly branched organism (bottom right and Panel **A**).

types, which are differentially located along the filament (Le Bail et al., 2008), we used an AFM coupled to an inverted microscope (Bioscope catalyst, Bruker) to precisely localize the AFM tip over the filament.

In details, *E. siliculosus* samples were prepared from spore release in small Petri dishes (60 mm diameter, fitting on the microscope stage) in the presence of 10 mL sea water (for detailed description, see Le Bail and Charrier, 2013). Filaments adhered and grew to the bottom of the Petri dish until the stage of interest was reached. Force indentation curves were acquired using ScanAsyst fluid cantilevers (Bruker) with a spring constant of approximately 1.5 N/m. Cantilever was calibrated by measuring deflexion sensitivity and spring constant. The deflexion sensitivity was determined by recording a force curve on a hard surface in seawater. The spring constant was then measured using the thermal tune method in air, which consists in the determination of the resonance frequency of the cantilever. A maximum load of 60 nN was used leading to deformations between 100 and 300 nm (depending on cells) which was below cell wall thickness (approximately 400 nm) (**Figure 1C**). Cartographies of elasticity were obtained by fitting the curves with the Sneddon model (**Figure 1D**). So far, measurements on several filaments from different Petri dishes allowed to obtain reproducible and consistent data on different *Ectocarpus* cell types (Tesson and Charrier, in prep), showing the suitability of this technique to this alga. Further experiments will be necessary to obtain a full description of the mechanical landscape in *Ectocarpus* filament.

PERSPECTIVES

Characterization of the mechanical properties of cells along the filament will allow to determine the role of mechanical constraints in cell growth and differentiation. This information will be then correlated with biochemical and genetic data. Beside the description of the physical properties of the brown algal cell wall using AFM as a technical tool, the molecular factors involved in the mechanosensitive pathways should be investigated (**Figure 3**). By looking at sequence similarities between the genome of *E. siliculosus* (Cock et al., 2010) with land plants, bacteria, and

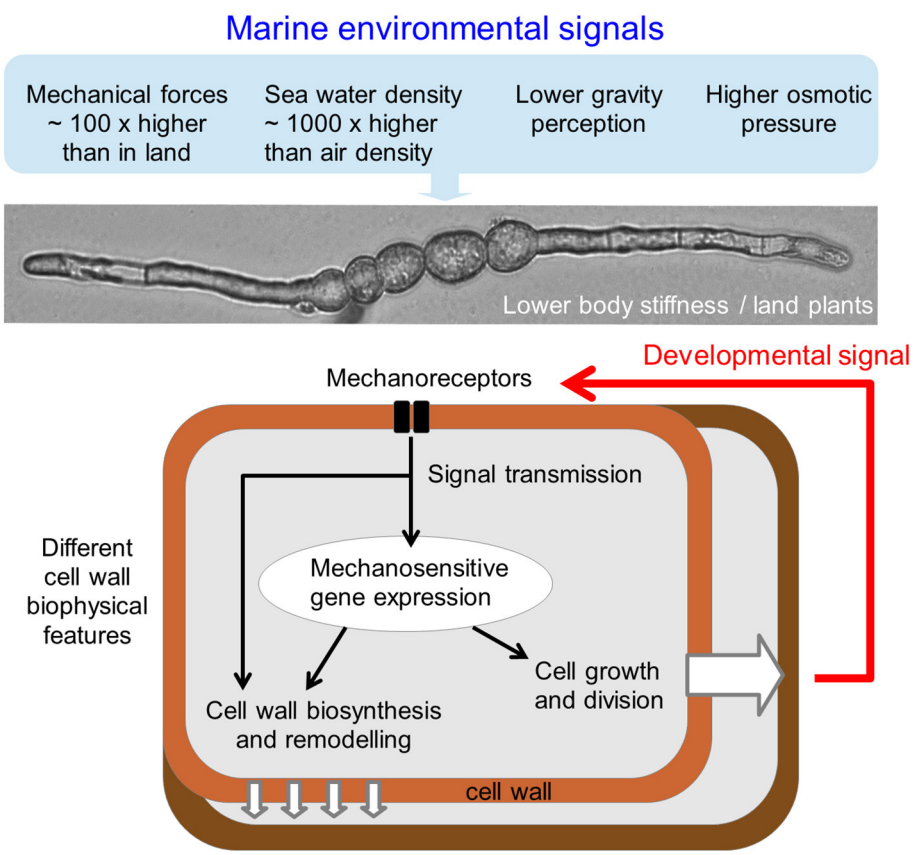

FIGURE 3 | Schematic representation of cell responses to mechanical signals. The specific environmental and cellular features of marine brown algae likely make molecular responses to mechanical signals different from land plants. In addition to the higher external osmotic pressures, mechanical forces and density and to the lower gravity perception, brown algal cell wall composition, structure, and physical properties differ from land plants. Nevertheless, similarly to land plants, primary molecular factors involved in perception and response to mechanical signals likely include transmembrane mechanoreceptors and signaling pathway factors. Resulting activation of the nuclear (mitosis and gene expression) and cell wall (biosynthesis and remodeling) machineries will allow relevant physiological and mechanical adjustment to the external mechanical constraints. Modification of the spatial and biophysical extracellular conditions due to the growth within the algal thallus will also likely generate mechanical signals perceived by similar or distinct mechanosensors.

animal proteins, putative genes involved in mechanosensing were identified (Charrier et al., 2012). These candidate genes include transmembrane receptor-like kinase (RLK), mechanosensitive channels (MscS), and transmembrane proteins showing similarities with alpha integrins. Alpha integrins are usually found only in metazoans. Additionally, in a study of auxin signaling in *E. siliculosus*, the gene *EsGRP1* was shown to be over-expressed in the presence of exogenous auxin and differentially expressed in morphogenetic mutants. Interestingly, this protein contains extensin-like domains with RGD motifs and glycine-rich regions (Le Bail et al., 2010). Extensins are plant cell wall proteins involved in cell wall formation (Lamport et al., 2011), and a glycine-rich protein (AtGRP3) was shown to bind and regulate the wall associated kinase WAK1 (Park et al., 2001). RGD motifs are known to be involved in interaction with integrins (Takada et al., 2007), and despite the absence of true integrin homologs, the RGD peptide was shown to interfere with several developmental events in plants (Jaffe et al., 2002).

However, these are only candidates based on sequence similarities, and mechanosensors specific for brown algae will be identified more likely by functional studies. A bank of morphogenetic mutants grown in standard conditions was generated in *Ectocarpus* (Le Bail and Charrier, 2013). Several mutants, for which altered physical properties of the cell wall could easily account for their phenotypes, include those displaying irregular cell contours or cell bursting. The identification of the mutated genes responsible for these phenotypes together with the detailed study of the cell wall structure and of its mechanical properties by AFM will allow to establish for the first time a functional link between genes and the overall composition and organization of the cell wall in brown algae and its function in cell shape. In parallel to studying morphological mutants growing in standard conditions, mutants subjected to mechanical stress should be investigated. Morphological responses of *Ectocarpus* to artificial sea currents mimicked by rotational shear stresses generated by an orbital shaker (Yun et al., 2002; Dardik et al., 2005; Sumpio et al., 2005) should be screened in order to select for mechanically hypo- or hyper-sensitive mutants. Whether these mechanosensors share similarities with land plant or even metazoan counterparts, or are specific to brown algae, will then be determined.

REFERENCES

Blanchette, C. A. (1997). Size and survival of intertidal plants in response to wave action: a case study with *Fucus gardneri*. *Ecology* 78, 1563–1578. doi: 10.1890/0012-9658(1997)078[1563:SASOIP]2.0.CO;2

Boller, M. L., and Carrington, E. (2006). The hydrodynamic effects of shape and size change during reconfiguration of a flexible macroalga. *J. Exp. Biol.* 209, 1894–1903. doi: 10.1242/jeb.02225

Braam, J. (2005). In touch: plant responses to mechanical stimuli. *New Phytol.* 165, 373–389. doi: 10.1111/j.1469-8137.2004.01263.x

Castle, E. S. (1937). Membrane tension and orientation of structure in the plant cell wall. *J. Cell. Comp. Physiol.* 10, 113–121. doi: 10.1002/jcp.1030100110

Charrier, B., Le Bail, A., and De Reviers, B. (2012). Plant Proteus: brown algal morphological plasticity and underlying developmental mechanisms. *Trends Plant Sci.* 17, 468–477. doi: 10.1016/j.tplants.2012.03.003

Cock, J. M., Sterck, L., Rouze, P., Scornet, D., Allen, A. E., Amoutzias, G., et al. (2010). The *Ectocarpus genome* and the independent evolution of multicellularity in brown algae. *Nature* 465, 617–621. doi: 10.1038/nature09016

Dardik, A., Chen, L., Frattini, J., Asada, H., Aziz, F., Kudo, F. A., et al. (2005). Differential effects of orbital and laminar shear stress on endothelial cells. *J. Vasc. Surg.* 41, 869–880. doi: 10.1016/j.jvs.2005.01.020

De Martino, A., Amato, A., and Bowler, C. (2009). Mitosis in diatoms: rediscovering an old model for cell division. *Bioessays* 31, 874–884. doi: 10.1002/bies.200900007

Deniaud-Bouët, E., Kervarec, N., Michel, G., Tonon, T., Kloareg, B., and Hervé, C. (2014). Chemical and enzymatic fractionation of cell walls from Fucales: insights into the structure of the extracellular matrix of brown algae. *Ann. Bot.* doi: 10.1093/aob/mcu096. [Epub ahead of print].

Denny, M., and Gaylord, B. (2002). The mechanics of wave-swept algae. *J. Exp. Biol.* 205, 1355–1362.

Draget, K. I., and Taylor, C. (2011). Chemical, physical and biological properties of alginates and their biomedical implications. *Food Hydrocoll.* 25, 251–256. doi: 10.1016/j.foodhyd.2009.10.007

Dudgeon, S. R., and Johnson, A. S. (1992). Thick vs thin - thallus morphology and tissue mechanics influence differential drag and dislodgment of 2 codominant seaweeds. *J. Exp. Mar. Biol. Ecol.* 165, 23–43. doi: 10.1016/0022-0981(92)90287-K

Fernandes, A. N., Chen, X. Y., Scotchford, C. A., Walker, J., Wells, D. M., Roberts, C. J., et al. (2012). Mechanical properties of epidermal cells of whole living roots of *Arabidopsis thaliana*: an atomic force microscopy study. *Phys. Rev. E Stat. Nonlin. Soft Matter Phys.* 85, 1–8. doi: 10.1103/PhysRevE.85.021916

Forouzesh, E., Goel, A., Mackenzie, S. A., and Turner, J. A. (2013). *In vivo* extraction of Arabidopsis cell turgor pressure using nanoindentation in conjunction with finite element modeling. *Plant J.* 73, 509–520. doi: 10.1111/tpj.12042

Fowler-Walker, M., Wernberg, T., and Connell, S. (2006). Differences in kelp morphology between wave sheltered and exposed localities: morphologically plastic or fixed traits? *Mar. Biol.* 148, 755–767. doi: 10.1007/s00227-005-0125-z

Francius, G., Tesson, B., Dague, E., Martin-Jezequel, V., and Dufrene, Y. F. (2008). Nanostructure and nanomechanics of live *Phaeodactylum tricornutum* morphotypes. *Environ. Microbiol.* 10, 1344–1356. doi: 10.1111/j.1462-2920.2007.01551.x

Friedland, M. T., and Denny, M. W. (1995). Surviving hydrodynamic forces in a wave-swept environment: consequences of morphology in the feather boa kelp, *Egregia menziesii* (Turner). *J. Exp. Mar. Biol. Ecol.* 190, 109–133. doi: 10.1016/0022-0981(95)00038-S

Hamant, O. (2013). Widespread mechanosensing controls the structure behind the architecture in plants. *Curr. Opin. Plant Biol.* 16, 654–660. doi: 10.1016/j.pbi.2013.06.006

Hamant, O., and Traas, J. (2010). The mechanics behind plant development. *New Phytol.* 185, 369–385. doi: 10.1111/j.1469-8137.2009.03100.x

Hayot, C. M., Forouzesh, E., Goel, A., Avramova, Z., and Turner, J. A. (2012). Viscoelastic properties of cell walls of single living plant cells determined by dynamic nanoindentation. *J. Exp. Bot.* 63, 2525–2540. doi: 10.1093/jxb/err428

Hertz, H. (1882). Ueber die Berührung fester elastischer Körper. *J. Reine Angew. Math.* 92, 156–171.

Jaffe, M. J., Leopold, A. C., and Staples, R. C. (2002). Thigmo responses in plants and fungi. *Am. J. Bot.* 89, 375–382. doi: 10.3732/ajb.89.3.375

Karyophyllis, D., Katsaros, C., and Galatis, B. (2000). F-actin involvement in apical cell morphogenesis of *Sphacelaria rigidula* (Phaeophyceae): mutual alignment between cortical actin filaments and cellulose microfibrils. *Eur. J. Phycol.* 35, 195. doi: 10.1080/09670260010001735791

Katsaros, C., Karyophyllis, D., and Galatis, B. (2003). F-actin cytoskeleton and cell wall morphogenesis in brown algae. *Cell Biol. Int.* 27, 209–210. doi: 10.1016/S1065-6995(02)00312-8

Katsaros, C., Karyophyllis, D., and Galatis, B. (2006). Cytoskeleton and morphogenesis in brown algae. *Ann. Bot.* 97, 679–693. doi: 10.1093/aob/mcl023

Kloareg, B., and Quatrano, R. (1988). Structure of the cell walls of marine algae and ecophysiological functions of the matrix polysaccharides. *Oceanogr. Mar. Biol. Ann. Rev.* 26, 259–315.

Koehl, M. A. R. (1984). How do benthic organisms withstand moving water. *Am. Zool.* 24, 57–70.

Koehl, M. A. R., Silk, W. K., Liang, H., and Mahadevan, L. (2008). How kelp produce blade shapes suited to different flow regimes: a new wrinkle. *Integr. Comp. Biol.* 48, 834–851. doi: 10.1093/icb/icn069

Lamport, D. T., Kieliszewski, M. J., Chen, Y., and Cannon, M. C. (2011). Role of the extensin superfamily in primary cell wall architecture. *Plant Physiol.* 156, 11–19. doi: 10.1104/pp.110.169011

Le Bail, A., Billoud, B., Kowalczyk, N., Kowalczyk, M., Gicquel, M., Le Panse, S., et al. (2010). Auxin metabolism and function in the multicellular brown alga *Ectocarpus siliculosus*. *Plant Physiol.* 153, 128–144. doi: 10.1104/pp.109.149708

Le Bail, A., Billoud, B., Maisonneuve, C., Peters, A. F., Cock, J. M., and Charrier, B. (2008). Early development pattern of the brown alga *Ectocarpus siliculosus* (Ectocarpales, phaeophyceae) sporophyte. *J. Phycol.* 44, 1269–1281. doi: 10.1111/j.1529-8817.2008.00582.x

Le Bail, A., and Charrier, B. (2013). "Culture methods and mutant generation in the filamentous brown algae *Ectocarpus siliculosus*," in *Plant Organogenesis*, ed I. De Smet (New York, NY: Humana Press). doi: 10.1007/978-1-62703-221-6_22

Marga, F., Grandbois, M., Cosgrove, D. J., and Baskin, T. I. (2005). Cell wall extension results in the coordinate separation of parallel microfibrils: evidence from scanning electron microscopy and atomic force microscopy. *Plant J.* 43, 181–190. doi: 10.1111/j.1365-313X.2005.02447.x

Martone, P. T., Kost, L., and Boller, M. (2012). Drag reduction in wave-swept macroalgae: alternative strategies and new predictions. *Am. J. Bot.* 99, 806–815. doi: 10.3732/ajb.1100541

Michel, G., Tonon, T., Scornet, D., Cock, J. M., and Kloareg, B. (2010). The cell wall polysaccharide metabolism of the brown alga *Ectocarpus siliculosus*. Insights into the evolution of extracellular matrix polysaccharides in Eukaryotes. *New Phytol.* 188, 82–97. doi: 10.1111/j.1469-8137.2010.03374.x

Milani, P., Braybrook, S. A., and Boudaoud, A. (2013). Shrinking the hammer: micromechanical approaches to morphogenesis. *J. Exp. Bot.* 64, 4651–4662. doi: 10.1093/jxb/ert169

Milani, P., Gholamirad, M., Traas, J., Arneodo, A., Boudaoud, A., Argoul, F., et al. (2011). *In vivo* analysis of local wall stiffness at the shoot apical meristem in Arabidopsis using atomic force microscopy. *Plant J.* 67, 1116–1123. doi: 10.1111/j.1365-313X.2011.04649.x

Mirabet, V., Das, P., Boudaoud, A., and Hamant, O. (2011). The role of mechanical forces in plant morphogenesis. *Annu. Rev. Plant Biol.* 62, 365–385. doi: 10.1146/annurev-arplant-042110-103852

Monshausen, G. B., and Gilroy, S. (2009). Feeling green: mechanosensing in plants. *Trends Cell Biol.* 19, 228–235. doi: 10.1016/j.tcb.2009.02.005

Muller, D. J., and Dufrene, Y. F. (2011). Atomic force microscopy: a nanoscopic window on the cell surface. *Trends Cell Biol.* 21, 461–469. doi: 10.1016/j.tcb.2011.04.008

Park, A. R., Cho, S. K., Yun, U. J., Jin, M. Y., Lee, S. H., Sachetto-Martins, G., et al. (2001). Interaction of the Arabidopsis receptor protein kinase Wak1 with a glycine-rich protein, AtGRP-3. *J. Biol. Chem.* 276, 26688–26693. doi: 10.1074/jbc.M101283200

Peaucelle, A., Braybrook, S. A., Le Guillou, L., Bron, E., Kuhlemeier, C., and Hofte, H. (2011). Pectin-induced changes in cell wall mechanics underlie organ initiation in Arabidopsis. *Curr. Biol.* 21, 1720–1726. doi: 10.1016/j.cub.2011.08.057

Radotić, K., Roduit, C., Simonović, J., Hornitschek, P., Fankhauser, C., Mutavdžić, D., et al. (2012). Atomic force microscopy stiffness tomography on living *Arabidopsis thaliana* cells reveals the mechanical properties of surface and deep cell-wall layers during growth. *Biophys. J.* 103, 386–394. doi: 10.1016/j.bpj.2012.06.046

Roduit, C., Sekatski, S., Dietler, G., Catsicas, S., Lafont, F., and Kasas, S. (2009). Stiffness tomography by atomic force microscopy. *Biophys. J.* 97, 674. doi: 10.1016/j.bpj.2009.05.010

Rounds, C. M., and Bezanilla, M. (2013). Growth mechanisms in tip-growing plant cells. *Annu. Rev. Plant Biol.* 64, 243–265. doi: 10.1146/annurev-arplant-050312-120150

Routier-Kierzkowska, A.-L., and Smith, R. S. (2013). Measuring the mechanics of morphogenesis. *Curr. Opin. Plant Biol.* 16, 25–32. doi: 10.1016/j.pbi.2012.11.002

Sneddon, I. N. (1965). The relation between load and penetration in the axisymmetric boussinesq problem for a punch of arbitrary profile. *Int. J. Eng. Sci.* 3, 47–57. doi: 10.1016/0020-7225(65)90019-4

Stewart, H. (2006). Morphological variation and phenotypic plasticity of buoyancy in the macroalga *Turbinaria ornata* across a barrier reef. *Mar. Biol.* 149, 721–730. doi: 10.1007/s00227-005-0186-z

Sumpio, B. E., Yun, S., Cordova, A. C., Haga, M., Zhang, J., Koh, Y., et al. (2005). MAPKs (ERK1/2, p38) and AKT can be phosphorylated by shear stress independently of platelet endothelial cell adhesion molecule-1 (CD31) in vascular endothelial cells. *J. Biol. Chem.* 280, 11185–11191. doi: 10.1074/jbc.M414631200

Takada, Y., Ye, X., and Simon, S. (2007). The integrins. *Genome Biol.* 8, 215. doi: 10.1186/gb-2007-8-5-215

Tesson, B., and Hildebrand, M. (2010a). Dynamics of silica cell wall morphogenesis in the diatom *Cyclotella cryptica*: substructure formation and the role of microfilaments. *J. Struct. Biol.* 169, 62–74. doi: 10.1016/j.jsb.2009.08.013

Tesson, B., and Hildebrand, M. (2010b). Extensive and intimate association of the cytoskeleton with forming silica in diatoms: control over patterning on the meso- and micro-scale. *PLoS ONE* 5:e14300. doi: 10.1371/journal.pone.0014300

Tesson, B., and Hildebrand, M. (2013). Characterization and localization of insoluble organic matrices associated with diatom cell walls: insight into their roles during cell wall formation. *PLoS ONE* 8:e61675. doi: 10.1371/journal.pone.0061675

Vogler, H., Draeger, C., Weber, A., Felekis, D., Eichenberger, C., Routier-Kierzkowska, A.-L., et al. (2013). The pollen tube: a soft shell with a hard core. *Plant J.* 73, 617–627. doi: 10.1111/tpj.12061

Wu, J.-Z., Lin, Y., Zhang, X.-L., Pang, D.-W., and Zhao, J. (2008). IAA stimulates pollen tube growth and mediates the modification of its wall composition and structure in *Torenia fournieri*. *J. Exp. Bot.* 59, 2529–2543. doi: 10.1093/jxb/ern119

Wyatt, H. D. M., Ashton, N. W., and Dahms, T. E. S. (2008). Cell wall architecture of *Physcomitrella patens* is revealed by atomic force microscopy. *Botany* 86, 385–397. doi: 10.1139/B08-003

Yun, S., Dardik, A., Haga, M., Yamashita, A., Yamaguchi, S., Koh, Y., et al. (2002). Transcription factor Sp1 phosphorylation induced by shear stress inhibits membrane type 1-matrix metalloproteinase expression in endothelium. *J. Biol. Chem.* 277, 34808–34814. doi: 10.1074/jbc.M205417200

Conflict of Interest Statement: The authors declare that the research was conducted in the absence of any commercial or financial relationships that could be construed as a potential conflict of interest.

Received: 14 June 2014; accepted: 28 August 2014; published online: 17 September 2014.

*Citation: Tesson B and Charrier B (2014) Brown algal morphogenesis: atomic force microscopy as a tool to study the role of mechanical forces. Front. Plant Sci. **5**:471. doi: 10.3389/fpls.2014.00471*

This article was submitted to Plant Physiology, a section of the journal Frontiers in Plant Science.

frontiers in
PLANT SCIENCE

REVIEW ARTICLE
published: 21 October 2014
doi: 10.3389/fpls.2014.00558

Mechanosensitive channels: feeling tension in a world under pressure

Rémi Peyronnet[1], Daniel Tran[2], Tiffanie Girault[2] and Jean-Marie Frachisse[2]*

[1] National Heart and Lung Institute, Imperial College London, London, UK
[2] Institut des Sciences du Végétal – Centre National de la Recherche Scientifique, Saclay Plant Sciences, Gif-sur-Yvette, France

Edited by:
Gabriele B. Monshausen, Pennsylvania State University, USA

Reviewed by:
Hidetoshi Iida, Tokyo Gakugei University, Japan
Boris Martinac, Victor Chang Cardiac Research Institute, Australia

***Correspondence:**
Jean-Marie Frachisse, Institut des Sciences du Végétal – Centre National de la Recherche Scientifique, Saclay Plant Sciences, Bat 22-23A, Avenue de la Terrasse, 91198 Gif-sur-Yvette, France
e-mail: jean-marie.frachisse@isv.cnrs-gif.fr

Plants, like other organisms, are facing multiple mechanical constraints generated both in their tissues and by the surrounding environments. They need to sense and adapt to these forces throughout their lifetimes. To do so, different mechanisms devoted to force transduction have emerged. Here we focus on fascinating proteins: the mechanosensitive (MS) channels. Mechanosensing in plants has been described for centuries but the molecular identification of MS channels occurred only recently. This review is aimed at plant biologists and plant biomechanists who want to be introduced to MS channel identity, how they work and what they might do *in planta*? In this review, electrophysiological properties, regulations, and functions of well-characterized MS channels belonging to bacteria and animals are compared with those of plants. Common and specific properties are discussed. We deduce which tools and concepts from animal and bacterial fields could be helpful for improving our understanding of plant mechanotransduction. MS channels embedded in their plasma membrane are sandwiched between the cell wall and the cytoskeleton. The consequences of this peculiar situation are analyzed and discussed. We also stress how important it is to probe mechanical forces at cellular and subcellular levels *in planta* in order to reveal the intimate relationship linking the membrane with MS channel activity. Finally we will propose new tracks to help to reveal their physiological functions at tissue and plant levels.

Keywords: stretch-activated channels, mechanotransduction, mechanobiology, cytoskeleton, plant, MSL, MscS, membrane tension

INTRODUCTION

All organisms, from bacteria to mammals and plants, experience mechanical forces. These forces are ubiquitous and very diverse coming from both the internal and the external environment. One of the most common external sources of stimulation sensed by both plants and animals is touch (pressure, shear stress). Like animals, plants are sensitive to gravity which guides their growth with respect to the gravity vector. Cells also generate their own intracellular forces as is obvious during cell division, cell elongation, or adjustment after osmotic challenge. While animals have to deal with circulating liquids (blood and urinary) and gases (lungs) as well as contractile elements (muscles), plant cells with their high turgor pressure represent very peculiar and interesting living systems from a mechanical point of view.

Over the last few years, it has become apparent that the ability of cells to sense and adapt to these forces is crucial for a wide range of biological processes. After two decades, during which the vast majority of studies were devoted to the dissection of gene regulatory pathways, mechanics is now being progressively integrated into the network, both as output (the impact of genes on cell mechanics) and input (the impact of mechanical signals on gene activity; **Figure 1**). Emerging techniques and tools now enable the measurement and manipulation of mechanical forces *in vitro* and progressively *in vivo*. This has led to an ongoing renaissance in studying mechanics.

Cells not only survive mechanical stimulation but also use it as a driving force to design their own architecture and to serve biological functions. This explains why cells and organisms have established mechanosensors. Three groups of proteins can fulfill this function: linkage proteins, structural elements, and MS ion channels.

Amongst the most well-known linkage proteins are integrins. These proteins are embedded in the plasma membrane and allow a mechanical coupling between the extra cellular matrix and the actin cytoskeleton. They are well described in the animal field and integrin-like proteins are reported in plants. NDR1 (Non-race-specific Disease Resistance1) for example is suggested to play a role in plasma membrane-cell wall adhesion and is required during plant-pathogen interaction (Knepper et al., 2011). In plants, serine-threonine protein kinases associated with the cell wall are good candidates to transduce mechanical forces. Among them are WAKs and THESEUS receptor-like kinase (RLKs; Monshausen and Gilroy, 2009) and other members of the large family of membrane-localized RLKs (Monshausen and Haswell, 2013). The cytoskeleton can be involved in several steps during mechanotransduction processes as demonstrated extensively in the animal field. It can directly transmit mechanical forces across the cell (Hayakawa et al., 2012) and also greatly control membrane tension (Gauthier et al., 2012) and organization (Jaqaman and Grinstein, 2012).

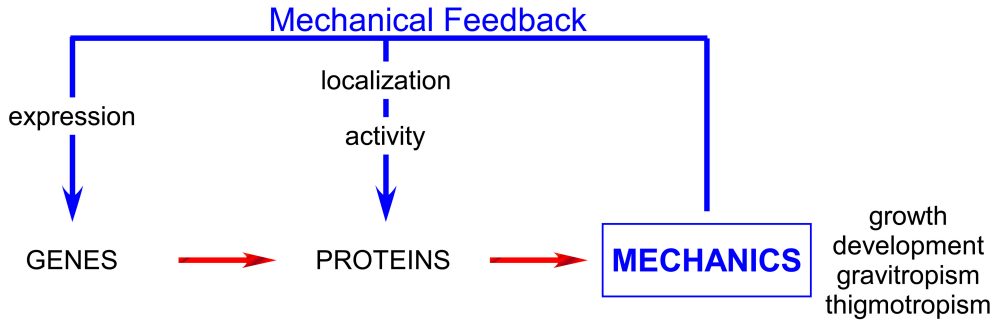

FIGURE 1 | Mechanical feedback affects the whole plant physiology acting on both gene and proteins and plays major role especially in development, growth and tropisms.

In this review we will focus on the most well-known mechanosensors: the MS channels.

MS CHANNELS: A COMMON FEATURE OF LIVING ORGANISMS FROM BACTERIA TO MAMMALS

Mechanosensitive channels are fascinating proteins, being able to serve both as sensors and effectors. Embedded in membranes, they convert mechanical stimuli such as in-plane membrane tension and curvature into electrical or biochemical signals, leading to regulation of a wide repertoire of cellular processes allowing adaptive response. Directly gated by the mechanical stimulus, MS channels convert (within milliseconds) a mechanical force into electrical trans-membrane potential variation. Therefore MS channels are (with phototransduction) the most rapid transducers known to date in biological systems.

Mechanosensitive channels were discovered in embryonic chick skeletal myocytes by Guharay and Sachs (1984) using the patch-clamp technique (Hamill et al., 1981). Then, in 1987 the first recordings were obtained on bacteria (Martinac et al., 1987) and were followed one year later by the first recordings on plants (Falke et al., 1988). It was at this time that the hunt for molecular candidates began. The first MS channel to be cloned was the MscL (MS channel Large conductance) from *Escherichia coli* in 1994 (Sukharev et al., 1994b) and a second important step was the cloning of the first mammalian MS channel in 1998 (Patel et al., 1998). Since then, deciphering organism genomes has provided several protein candidates for mechanosensing. Numerous other MS channels have been identified but it is only recently (20 years after the first recording of a plant MS channel) that MS channels belonging to two different families were identified in plants (Nakagawa et al., 2007; Haswell et al., 2008). Mid1-Complementing Activity (MCA) exhibiting 10% identity to yeast Mid1 (Nakagawa et al., 2007) and correlated to Ca^{2+} influx for MCA1 together with MSL (MscS-Like), homologs of the weakly selective bacterial stretch-activated MscS channels, have opened a new field of investigation.

The combination of genomics, molecular, and electrophysiological approaches is starting to provide exciting information on the role of MS channels from mechanical perception to organism behavior.

In this review, rather than listing channel candidates characterized within several organisms, we will present some emblematic channels in bacterial and plant systems. We chose to present only well-electrophysiologically characterized channels whose membrane stretching represents a major regulation factor. Exhaustive overviews of the different MS channels characterized can be found notably in (Arnadottir and Chalfie, 2010; Martinac, 2011; Nilius and Honore, 2012; Kurusu et al., 2013; Monshausen and Haswell, 2013; Wilson et al., 2013).

MscL AND MscS: THE BACTERIAL SAFETY-VALVES

Mechanical senses originated in unicellular organisms. In evolution, the first to appear was osmosensing, which allows a cell to maintain membrane integrity when confronted with varying aqueous environments. In fact, the most extensively characterized MS channels are the MscL (MS channel Large conductance) and MscS (Small conductance; Sukharev et al., 1994a; Levina et al., 1999) which were discovered 25 years ago in bacteria *E. coli* (Martinac et al., 1987) then cloned in 1994 and 1999 (Sukharev et al., 1994b; Levina et al., 1999) and crystallized in 1998 and 2002 (Chang et al., 1998; Bass et al., 2002). Both have very large conductances, or pore sizes, relative to eukaryotic channels, which are usually on the order of a few 10s of picosiemens; MscL, at about three nanosiemens, meaning a flux of 3 billion ions per second (at a membrane potential of 150 mV) is the largest gated channel, while MscS conductance is about one nanosiemens (**Table 1**). These two channels reflect distinct families of proteins. The MscS family, found in several species belonging to bacteria, archaea, algae, fungi, and plants, is quite diverse and a single organism may encode multiple members in its genome. For example, the genome of the model plant *Arabidopsis* encodes for 10 MscS-like (Haswell and Meyerowitz, 2006). The MscL channel is highly conserved, with only a single copy of the gene found in fungal and bacterial organisms. Unlike most of channels, Msc S and L have a lack of ionic specificity and are permeable to any charged molecule smaller than 1,000 molecular weight including proline, potassium glutamate, trehalose, and ATP (Hamill and Martinac, 2001). In respect to small ions, MscL is non-selective for both anions and cations (Martinac et al., 2008), whereas MscS exhibits a slight preference for chloride over potassium with a permeability ratio $PCl:PK$ in the range of 1.5–3

Table 1 | Characteristics and functions of the four MS channels, MscL, MscS, TREK-1, and Piezo involved in mechanosensation in bacteria and mammals.

Channel	MscL	MscS	TREK-1	Piezo
Cloned from (organism)	*E. coli*	*E. coli*	Mouse	Mouse
Homologs in other organisms	Bacteria, archeabacteria, fungi	Bacteria, algae, fungi, archaebacteria, plant	Mammals	Mammals, plant, protozoa, invertebrates
Conductance	∼3000 pS [a, b]	∼ 1000 pS [a, b]	∼50 pS [c]	∼25–70 pS [d, n, k]
Selectivity	not-selective [b, e]	weak: $Cl^- > K^+ >$ metabolites [b, e]	K^+ [c]	cation non-selective [d][f]
Activation	$T_{1/2}$: ∼12 mN.m^{-1} [g]	$T_{1/2}$: ∼6 mN.m^{-1} [h]	$P_{1/2}$: –20 to –60 mm Hg [c, i, j]	$P_{1/2}$: -25 to -48 mm Hg [d, k, l]
Inactivation	No	Yes (spheroplast) [a, m]	Yes, τ ∼46 ms [c]	Yes, τ ∼ 45 ms [n]
Activation factors	Membrane tension Membrane curvature [o]	Membrane tension Membrane curvature [p]	Membrane tension, Membrane curvature [q] heat, acdic pH, depol., …..	unknown
Functions	"Emergency release valve"	"Non-emergency release valve" Internal crowding sensor	Pain perception, ischemia, vasodilatation…	Red blood cell volume touch and pain perception …

a: Perozo and Rees (2003), b: Sukharev et al. (1997), c: Honore et al. (2006), d: Coste et al. (2010):, e: Martinac et al. (2008), f: Bae et al. (2013), g: Sukharev (1999), h: Sukharev (2002), i: Patel et al. (1998), j: Bang et al. (2000), k: Bae et al. (2011), l: Peyronnet et al. (2012), m: Sotomayor et al. (2007), n: Gottlieb et al. (2012), o: Mukherjee et al. (2014), p: Vasquez et al. (2008), q: Maingret et al. (2000).

(Martinac et al., 2008). Each Msc (S or L) in *E. coli* exhibits a unique threshold tension for activation of ∼6.0 and ∼12.0 mN/m respectively, (Sukharev et al., 1999; Sukharev, 2002; Nomura et al., 2012). Biophysical approaches on MscS and MscL as well as studies performed on purified MscL, show that the protein alone reconstituted into liposomes retained mechanosensitivity, indicating that both channels directly sense membrane tension developed in the lipid bilayer alone (Sukharev et al., 2001; Perozo et al., 2002).

Bacteria are well documented for their ability to survive and grow in conditions of changing osmolarity. When they face a sudden hypoosmotic shock (which may take place, for instance, in gastrointestinal bacteria exposed to food processing, marine bacteria suddenly exposed to fresh water or soil bacteria trapped in rain water), a rapid influx of water will occur. Consequently, the mechanical membrane tension will rapidly rise. This should not exceed around 15 mN.m^{-1} (Evans and Ludwig, 2000; Boer et al., 2011). Above this level the rupture of the membrane will produce lysis of the cell. In order to avoid this situation, excessive membrane tension should be rapidly relieved. Based on experiments performed on knock-out (KO) bacteria, it was proposed by Levina et al. (Levina et al., 1999) that MscS and MscL represent two efficient "valves" acting synergistically allowing osmolyte efflux after swelling. MscS is the non-emergency "valve" while MscL represents the ultimate "valve" before membrane rupture.

Combining electrophysiological analyses of *Ec*MscS mutants with modeling, Rowe et al. (2014) provided an exciting new perspective on MscS function. The authors addressed the question of macromolecular crowding (Ellis, 2001), which reduces the intracellular volume of solvent available for other molecules, upon MscS functioning. They show that besides its role as an efflux valve, MscS is also one of the sensors of internal crowding of large-molecular-weight compounds. They argue for a function of MscS in turgid walled-cells on the maintenance of their volume, shape, and mechanical strength by avoiding excessive draining. Considering the thinness of the cytosol compartment (2–10% of the plant cell volume), which is probably highly crowded, this provides an interesting new function to look for in the MscS-like channels of plant plasma membranes.

TREK-1: A POLYMODAL CHANNEL

Mechanosensitive channels can be modulated by numerous stimuli other than mechanical ones and TREK channels which are well described in mammals constitute a good example. TREK means TWIK-related potassium channel, TWIK standing for "Tandem of two-pore K^+ domains in a weak inwardly rectifying K^+." In mammals, TREK belongs to the two-pore domain potassium channel (K_{2p}) family and, as a potassium channel, is responsible for cell repolarization, thus controlling both the resting and the dynamic electrical activity of cells. TREK-1, TREK-2, and TRAAK are the only members being mechanogated and TRAAK is the only eukaryotic MS channel for which crystal structures have been determined (Brohawn et al., 2012, 2013), with the bacterial MscS and MscL being the only other MS channels crystallized so far. TREK-1 together with TRAAK, as bacterial MS channels, retain their mechanosensitivity when reconstituted into

liposomes (Brohawn et al., 2014) indicating that they are sensitive to stretch without the need for a second messenger or any form of tethering from the cytoskeleton or the extracellular matrix. This common behavior of MscL, MscS, TREK-1, TRAAK shows that the force from lipid (FFL) principle, first proposed for *E. coli* MS channels of spheroplast by Martinac et al. (1987), can be generalized to structurally unrelated eukaryotic channels. The FFL is a fundamental physicochemical principle based on the fact that the self-assembled bilayer necessitates inherent forces that are large and anisotropic. Then, proteins embedded in the bilayer are subjected to these push and pull forces. The principle of FFL and its relevance to MS channels in biophysical and physiological contexts was recently illustrated by Teng et al. (2014).

Several structure function studies also provided crucial information for a better understanding of the gating of these channels and together these approaches contribute to make TREK, one of the most studied MS channels with the bacterial MscS and MscL. Apart from the bilayer itself, TREK-1 activity is regulated by a plethora of stimuli (**Table 1**). Its activity is up-modulated by heat, intracellular acidosis, depolarization, volatile anesthetics and down-modulated by extracellular activation of PKA and PKC phosphorylation pathways. In addition, stimulation of Gq-coupled receptors, including metabotropic mGluR1, and mGluR5 receptors, inhibits TREK-1 activity (see Dedman et al., 2009; Noel et al., 2011 for review). More directly related to mechanical stimulation, TREK-1 is modulated by heat, lipids (lysophospholipids and polyunsaturated fatty acids) and also by the cytoskeleton acting as a tonic repressor (Lauritzen et al., 2005; Peyronnet et al., 2012). Aside from these regulations, TREK channels are characterized by the existence of several variants produced by alternative splicing and alternative translation initiation also contributing to the diversity of TREK functions. To date, no TREK analog has been found in sequenced plant genomes.

In mammals (humans/mice) TREK-1 has a wide tissue distribution and with its complex gating regulation is involved in diverse biological processes. It plays a central role in ischaemic and epileptic neuroprotection, vasodilatation, depression (Heurteaux et al., 2006), general anesthesia (Heurteaux et al., 2004) and pain perception (Alloui et al., 2006).

PIEZO: A LARGE CHANNEL WITH A ROLE IN MECHANOPERCEPTION

Piezo protein (from the Greek "pίesi" meaning pressure) discovered by Coste et al. (2010) was shown to be an essential component of a cationic non-selective MS channel from mouse neuroblastoma cells (**Table 1**). The protein is approximately 2500 amino acids long with 24–36 predicted trans-membrane domains showing no homology to other already known MS or voltage sensitive channels. In the membrane, Piezo1 proteins are found to be organized in a gigantic homotetrameric structure but the experiment did not show that the pore-forming unit was a tetramer.

Coste et al. also cloned a homologous gene called Piezo2 from mouse dorsal root ganglion cells with similar electrophysiological properties. After expression, purification, and reconstitution in artificial lipid bilayers, Piezo1 was shown to be the pore-forming subunit (Coste et al., 2012). Piezo1 mutations were associated with autosomal dominant hemolytic anemia (Zarychanski et al., 2012). Patapoutian's group also demonstrated that Piezo2 is expressed in a mechanoreceptor complex in mouse skin and is required for gentle touch perception (Woo et al., 2014). In the same way, Piezo proteins in *Drosophila* larvae have been shown to be crucial for responses to noxious mechanical stimuli (Coste et al., 2012).

Piezos are fascinating proteins (see Gottlieb and Sachs, 2012; Nilius and Honore, 2012 for reviews) and it is still unclear why these proteins are so big. It is tempting to hypothesize that the large number of transmembrane domains along with the proteins' large size could constitute an effective sensor for membrane curvature. In any case, this unusual structure for a mechanotransducer is likely to suggest other functions. Piezo, an evolutionarily conserved protein, presents a single homolog in the genome of the model plant *Arabidopsis*, providing an interesting new candidate for plant mechanosensors.

ACCESSING MS ACTIVITY AT CELLULAR LEVEL

PATCH-CLAMP COMBINED WITH HIGH SPEED PRESSURE-CLAMP REVEALS INTIMATE PROPERTIES OF MECHANOSENSITIVE CHANNELS

Patch clamp is a powerful technique that allows the recording of channel activity with a high resolution in terms of time (ms) as well as ion flux (pA). **Figure 2A** is a summary of the different configurations that can be achieved in patch clamp. The use of whole cell configuration allows the recording of channel population activity present on a membrane while the other possible patch configurations select a small number of channels at the tip of the pipette, enabling resolution of single channel activity. These latter configurations are reached through a cell attached configuration that maintains intracellular integrity, thus complying with the transduction pathways, or through an excised patch allowing a better characterization through which the ionic environment on both sides of the membrane is fully controlled. Excised patch configurations also allow us to test the role of the cytoskeleton. It has been shown that cytoskeleton elements are strongly destabilized in this configuration in comparison with cell attached mode (Lauritzen et al., 2005; Peyronnet et al., 2012). Only excised and cell attached patches allow application of a large range of pressures and therefore, the highlighting of the relationship between open probability and membrane tension of a single channel. The development of the pressure clamp system in the nineties (McBride and Hamill, 1992; Hurwitz and Segal, 2001) has become a key tool for applying fast pressure steps to membrane patches (**Figure 2B**). The ability to measure channel relaxations following step changes in positive/negative pressure in combination with patch clamp techniques has launched many studies on the analysis of the time, voltage and pressure dependence of the opening and closing of MS channels from different organisms, exemplified in **Figure 2B** with the *Arabidopsis* mechanosensitve MSL10 channel. Thus the relationship between open probability/pressure fits a sigmoid curve called a Boltzmann function, indicating the threshold and maximum (saturation) tension values of the channel. The slope of the sigmoid depicts the strength of the channel dependence toward membrane tension. The most artificial, but best controlled situation, is encountered when the

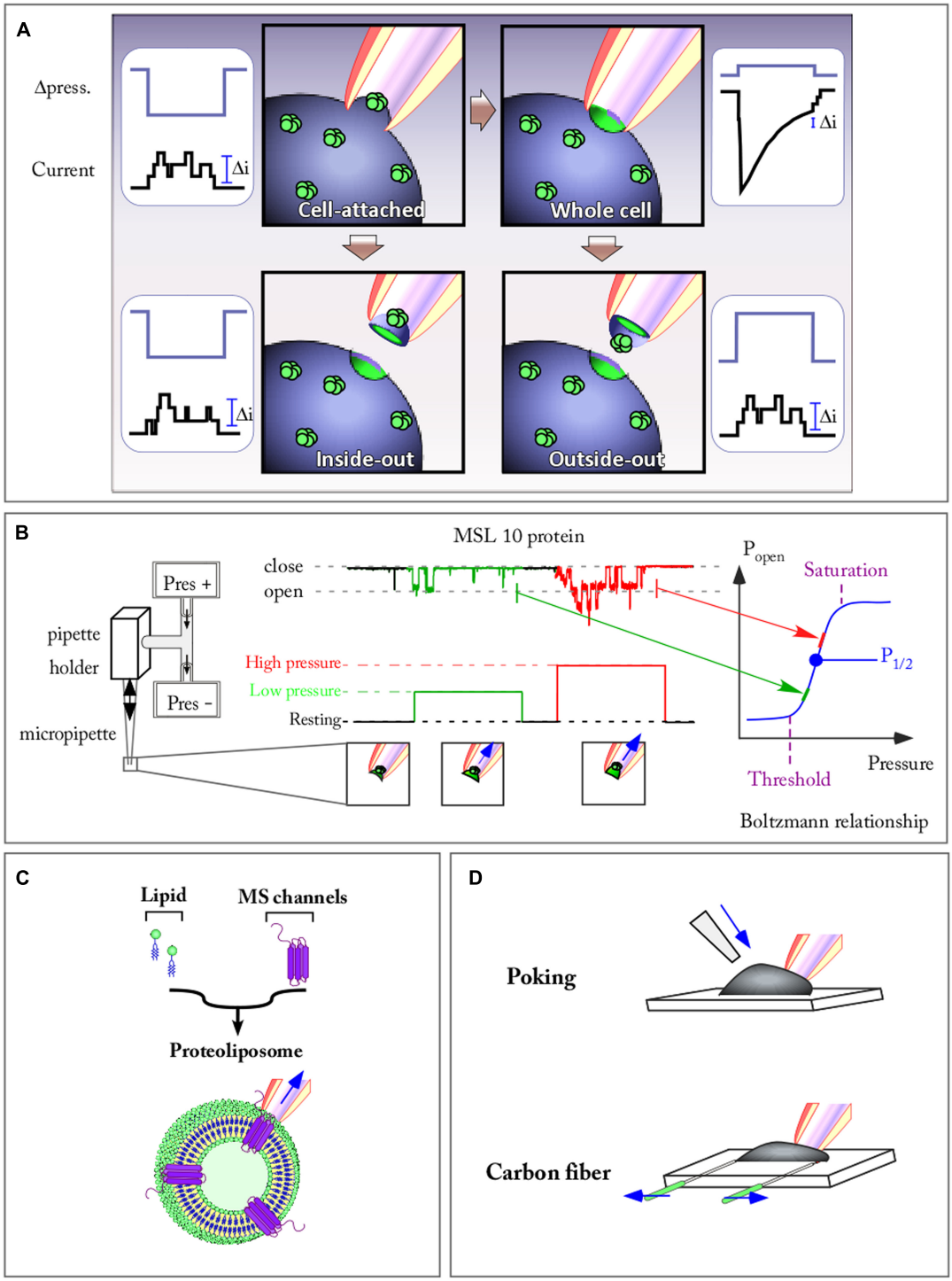

FIGURE 2 | Patch clamp combined with fast speed pressure stimulation allows to study kinetic properties of mechanosensitive (MS) channels. **(A)** The four patch clamp configuration allowing to record either single channel current (Cell attached, Inside-out, and Outside-out) or a population channel current (Whole cell) are represented. Channels are stimulated by applying a pulse of pressure against the membrane. **(B)** Recording of the *Arabidopsis* MSL10 channel activity in outside-out configuration. The activity of the channel is elicited by pulses of increasing pressure. The open probability (P_{open})-pressure relationship of the channel fit a Boltzmann function on which are mentioned: the activation threshold, the half pressure activation ($P_{1/2}$), the pressure of maximum activation. **(C)** MS channel reconstituted in a spherical proteoliposome. **(D)** Poking and carbon fiber techniques allow to apply membrane stretch while recording the cell (arrows show forces applied to the system).

MS channel is reconstituted in an artificial membrane bilayer of a spherical shaped proteoliposome (**Figure 2C**). Here, not only is the ionic environment well controlled, but the lipid composition of the membrane is also mastered. The absence of cytoskeleton elements is also a strong advantage allowing direct access to membrane mechanical properties without the cytoskeleton interfering with either the channel or the membrane itself. In these different configurations, applying a positive or negative pressure will allow delivery of controlled tension to the membrane if curvature of the patch is measured (Suchyna et al., 2004). Following this, single MS channels can be characterized with a very good time resolution (milliseconds) either in native or artificial membranes.

Careful and detailed analysis of physical phenomena that are generated on the patch of membrane sealed at the pipette tip have led authors to underline the limit of the patch-pressure clamp technique. Although the pressure in the pipette can be controlled precisely, its conversion into local tension, the parameter that activates MS channels, is not straightforward. In his paper, Sachs (2010) discusses the different components involved in the generation of local mechanical stress: far-field tension, phase separation, the cytoskeleton, and the adhesion energy between the membrane and the patch pipette. The pressure-clamp technique is currently one of the easiest ways to mechanically activate and record single channels, but various methods of mechanical stimulation have been developed to stimulate and record channels at the whole cell level.

OTHER TECHNIQUES TO ACTIVATE MS CHANNELS

The advantages and limitations of these techniques are a matter of active discussion (Kamkin and Kiseleva, 2008). In **Figure 2D** two of these techniques are illustrated. The poking technique is commonly used to apply mechanical stimulation to single cells. While recording in whole cell configuration, the stimulation is generally achieved using a fire-polished glass pipette (tip diameter 3–5 μm). Controlled downward movements of this probe press the cell against its support, thus activating MS channels. This technique notably led to the discovery of Piezo channels (Coste et al., 2010).

The carbon fiber technique allows a controlled axial stretch of the cell and was first developed on cardiomyocytes (Le Guennec et al., 1990). Carbon fibers are attached to the cell membrane *via* electrostatic forces (the same forces that seal the patch-clamp pipette to the membrane). Carbon fiber bending is converted into forces generated by the cell (such as in response to an osmotic shock) while a microelectrode records the current flowing through MS channels (**Figure 2D**). Instead of using carbon fiber, it is also possible to use glass capillaries coated with glue. These capillaries are attached to a force transducer allowing a direct recording of the force generated by the cell while stretching. These techniques are also used to test mechanical properties of tissues such as stiffness. Regarding the poking technique, the amplitude of the downward movement compared to the cell diameter might, in some experiments, produce excessive deformation. This prompts a use of this technique with stimuli generating cell strain physiologically relevant. Until now these techniques have exclusively been developed on animal cells. Their adaptation to plant cells is of major interest in order to develop our knowledge of plant MS channels.

Both in-plane membrane tension and membrane curvature have been shown to activate MS channels. This can be achieved by asymmetric incorporation of cone-shaped amphipaths (Martinac et al., 1990). These molecules, able to insert selectively in one membrane leaflet (Sheetz and Singer, 1974), create positive or negative curvature. The activation by amphipaths differs from in-plane membrane tension because it implies local membrane curvature as the activation factor (**Table 1**; Yoo and Cui, 2009). MscL and MscS are activated, even in the absence of applied pressure, when cone-shaped lysophosphatidylcholine is inserted into the membrane (Vasquez et al., 2008; Mukherjee et al., 2014). This activation property is also shared by the eukaryotic channel. TREK-1 for example, is opened by crenators, while it is closed by cup-formers. (Patel et al., 1998; Maingret et al., 2000).

MS CHANNELS ARE FAST TRANSDUCERS OF MEMBRANE TENSION CHANGES

The ability to precisely control mechanical stimulation with the fast pressure clamp system has provided valuable kinetics information on the activation, inactivation, and deactivation of MS channels from different organisms. The MscS, acting as a tension-driven osmolyte release valve in bacteria, exhibits rapid activation in the 10 ms time range (Boer et al., 2011). In response to sustained and moderate stimulus *Ec*MscS exhibits complex desensitization kinetics that is composite of both channel adaptation that is likely linked to membrane mechanics and inactivation of the channel (Belyy et al., 2010; Boer et al., 2011; Kamaraju et al., 2011; Cox et al., 2014). In **Figure 3A**, the current decay of the MscS population is represented in the case of a sub-saturating tension applied to the membrane. In such conditions, the fraction of decrease due to inactivation is dominant over the fraction due to adaptation. However, using a specific pressure protocol (not presented in **Figure 3**), combining prolonged conditioning steps interspersed with short saturating pulses (Akitake et al., 2007; Kamaraju et al., 2011) allowed for distinction between these two interrelated processes and led Rowe et al. to show that inactivation is increased in the presence of crowding agents (Rowe et al., 2014). The potential physiological relevance proposed as a result of this channel adaptation and this inactivation crowded dependent is to link sensitivity to both membrane tension and crowding pressure in order to limit the dissipation of the vital gradient and to maintain cell strength and turgor during hypoosmotic shock.

Several eukaryotic MS channels also exhibit complex kinetics, with TREK and Piezo being well-known examples. They both activate in a very short period of time, in the range of a few milliseconds, and then inactivate under sustained membrane tension (**Figure 3B**). TREK desensitization was reported as weakly or not at all dependent on the cytoskeleton and the voltage in mammalian cells (Honore et al., 2006) and this was recently confirmed in artificial lipid bilayers where TREK and TRAAK were still inactivated (Brohawn et al., 2014). Piezo1 inactivation is abolished when Zn^{2+} instead of Mg^{2+} is perfused on the intracellular face and no other regulators have been described until now (Gottlieb et al., 2012). Mechanisms modulating desensitization of MS

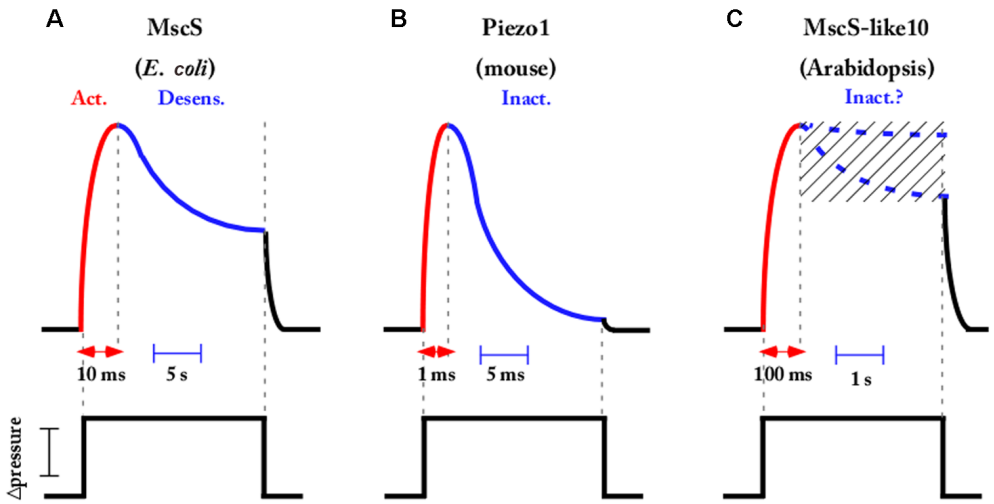

FIGURE 3 | Most MS channels exhibit fast activation followed by a slower inactivation or desensitization kinetics in response to pressure stimulation. Schematic representations showing that activation inactivation and desensitization kinetics occurred in the time range of ms to s depending on the channel **(A)** *Escherichia coli* MscS [inspired from Boer et al. (2011)], **(B)** Piezo mouse channels [inspired from Coste et al. (2012)], and **(C)** *Arabidopsis* MscS-like 10 channel [inspired from Maksaev and Haswell (2012)]. For MscS-like 10, the presence or absence of inactivation not being definitively settled, the two possibilities are mentioned. Channels are elicited by a step of sub-saturating pressure applied to the membrane.

channels are far from being fully understood and deserve further study as they constitute a major characteristic of ion channel activity.

From a functional perspective, inactivation can have different roles. One role of inactivation could be to protect the cell against nonspecific responses. Indeed, inactivation guarantees that if the channel should open it cannot stay open for a long period of time. Inactivation also means that channels become desensitized to the stimulation, so if the stimulation occurs at a high frequency, the first stimulus will activate channels but not the following stimuli, and in this case the channel can act as a frequency filter.

Concerning MS channels in plants, very little electrophysiological data has been available to date. The recent discovery of anion permeable MscS-like and cation permeable MCA channels in *Arabidopsis* has not yet given the authors the opportunity to deliver a complete kinetics characterization. However, a recent electrophysiological study of AtMscS-like10 expressed in *Xenopus* oocytes (Maksaev and Haswell, 2012) indicates slow opening and closing kinetics of the channel in response to sharp steps of tension applied to the membrane. Unlike *Ec*MscS, but like many other prokaryotic MscS-like channels (MscSP, MscCG, MscK) (Nakayama et al., 2013; Petrov et al., 2013), no inactivation of the plant homologous under sustained tension was detected (for a review see Cox et al., 2014). The authors of the present paper also found activation and deactivation kinetics, in the 0.1 s range, when overexpressing AtMscS-like10 in a homologous system (**Figure 3C**). The existence or not of an inactivation process of the plant MscS-like10 channel is still under investigation and might depend on the expression system used (*Xenopus* oocyte/plant protoplast). Such an inactivation process would mean accommodation of the cell under a sustained mechanical stimulation as occurred in *E. coli* for its MscS counterpart. Further exploration is needed in plants in order to obtain a complete picture of plant MS channel function.

PLANT MS CHANNELS

PLANT CELLS PROVIDE A PECULIAR "MECHANICAL ENVIRONMENT" FOR MS CHANNELS

Plant and animal cells have developed their own intracellular and extracellular matrices which differ in organization and structural composition. Plant cells exhibit very stiff pecto-cellulosic walls, notably because of the presence of cellulose microfibrils which has stiffness comparable to that of steel. Conversely, animals have wall-less cells in which the mechanical properties of the membrane are heavily dependent on the cytoskeleton network. In plants, microtubules form a dense cortical network and actin creates a slight internal network while in animal cells the situation is inverted. In the latter, cell mechanics are highly relayed to an actin contractile cytoskeleton and membrane whereas in plants, the presence of a stiff extracellular matrix is designed to moderate the contribution of the cytoskeleton. In animals, there is increasing evidence of a significant role for actin as a relay in MS channel activation (Lauritzen et al., 2005; Peyronnet et al., 2012). In plants, only one study performed on MS guard cell channels (combining electrophysiology and pharmacology) indicates channel activation when actin filaments are disrupted and channel inhibition with stabilization of actin (Zhang et al., 2007). Microtubules which represent the major mechanical component of the plant cytoskeleton (Nick, 2013) have not yet been investigated for their role in MS channel activation.

Looking deeper into the structure of the plant wall-membrane-cytoskeleton continuum, it is worth considering the contact points connecting these compartments. For the membrane-cytoskeleton, this is exemplified by a plethora of microtubule-associated proteins identified by the recently sequenced genomes of model plants

(Gardiner, 2013). Cytoplasmic linker associated protein (CLASP) represents one example of these recently identified anchorage proteins although the intimate mechanism still needs to be investigated (Brandizzi and Wasteneys, 2013). The abnormal root cell swelling and increased microtubule ordering of *clasp-1* mutants (Ambrose et al., 2007) stresses the importance of this linkage-protein in cell shaping and suggests a role in force cortex sensing. Another indication of the link between cell wall and microtubule networks is the parallel patterning of cellulose microfibrils with microtubules (Szymanski and Cosgrove, 2009). Furthermore, live cell imaging experiments in hypocotyl provide evidence that the cortical cytoskeleton guides the movement of cellulose synthase complexes (Paredez et al., 2006; Chan et al., 2011). The physical and biophysical significances of these tight contacts in terms of stress information is well discussed by Szymanski and Cosgrove (2009) and Cosgrove and Jarvis (2012) but little investigated by the scientific community. In addition to the contribution of their structural elements, the mechanical properties of cells largely depend on osmotic pressure commonly in the range of 2,300–6,800 mm Hg (0.3–0.9 MPa) in growing cells (Cosgrove, 1993) and estimated at up to 75,000–375,000 mm Hg (10–50 MPa) for wall tensile stresses. To bring these values into context and help realize how peculiar the mechanical environment is in plants, we have illustrated some pressures recorded in plant cells with regard to some milestones and pressures used in electrophysiology to activate MS channels. As tension rather than pressure activates MS channels, we have also illustrated tensions even if very little data has been available in the literature until now (**Figure 4**).

While turgor pressure is uniform and isotropic within the cell, wall stresses are not generally uniform, but depend on cell geometry, cell wall thickness, and wall mechanical properties. In the case of a growing cell (often encountered in plants) physical properties are dynamic, with wall extensibility varying within minutes or even seconds (Wolf et al., 2012).

All the points mentioned require integration into a biophysical vision of the plant cell. Combining molecular physics and modeling approaches will lead to drawing a map of forces within the cell, allowing crucial questions to be answered such as; what is the mechanical contribution of the cell wall? Does it absorb most of the tension applied to the cell or does the plasma membrane beneath behave as the element under tension? Are the linkage points hot spots for stress? Then, MS channels characterized by the patch clamp technique (in simplified environments: bilayer, proteoliposome, protoplast) could be mapped with the cellular strain distribution in order to understand where and when they are physiologically relevant.

PROBING MECHANICAL FORCES IN PLANT. A GREAT JOB TO DO IN THE NEAR FUTURE!

A crucial step in understanding the role of mechanosensors is to know where and when mechanical forces occur within cells and tissues and to be able to quantify them. Membrane curvature as well as membrane and cytoskeleton tension, which are essential MS channel modulators, have been poorly described until now. The main reason is that until recently, there were no techniques to study these forces *in vivo*. Fortunately, today this important area controlling many biological processes is regaining a lot of interest due to the emergence of new tools.

It has become better and better established that the cytoskeleton is a powerful regulator of membrane tension, shape and organization in animal cells (Ofer et al., 2011; Saravanan et al., 2013; Al-Rekabi et al., 2014). In plant cells, for which its role is less established, probing its mechanical state will be very helpful to better understand its effect on MS channels. Fluorescent probes based on the Förster resonance energy transfer (FRET) technique were recently engineered to sense tension variations within the cytoskeleton (Meng and Sachs, 2011; Guo et al., 2013) with single piconewton sensitivity (Grashoff et al., 2010). Adaptation of these sensors to plant cells represents an exciting challenge and will allow mechanical forces within the plant body to be mapped.

To complete this "strain mapping" *in planta*, the use of fluorescent probes sensitive to curvature (asymmetry in lipid packing) will enable the drawing of the membrane micro curvature map, another important MS channel regulator. Genetically encoded fluorescent probes already exist in animals like the BAR domain proteins (Bin1-Amphiphysin-Rvs167; Peter et al., 2004; Ren et al., 2006) which have homolog in plants (Zhuang and Jiang, 2014) and α-Synuclein (Pranke et al., 2011). Interestingly, these curvature sensors have been shown to be efficient in different organisms (Pranke et al., 2011), making the translation to plants realistic.

Promising probes for sensing changes in the membrane mechanical state are MS channels themselves. Very recently, Wang et al. (Wang et al., 2014) revealed MscL's conformational changes using single molecule FRET. Using engineered MS channels with a FRET sensor and a known activation threshold allowed direct probing of mechanical changes. Other techniques with non-genetic probes are also being developed. For example, based on oil droplet deformations, Campás et al. (2014) describe mechanical forces within living embryonic tissues. Deformable microchips also exist to monitor tissue deformations (Kim et al., 2012). Bioimaging approaches combining the use of such tension/curvature probes with the subcellular localization of pre-labeled (with fluorescent protein) MS channels will allow the correlation of tension distribution with the presence of the channel. Such probes would help further understanding of whether MS channels are preferentially localized in the area of a curved membrane, close to cytoskeleton structures, or areas of membrane under tension, leading to the elucidation of the regulation and the role of MS channels *in vivo*.

GENETIC APPROACH

Several genetic strategies exist to highlight the roles of MS channels at the whole organism level. KO mutants have been extensively used to reveal MS channel functions. Bacterial Msc S and L channels (Levina et al., 1999), mammalian TREK-1 (Alloui et al., 2006; Heurteaux et al., 2006), and Piezos (Kim et al., 2012; Woo et al., 2014) are some successful examples illustrating this strategy. For plant MS channels the KO mutant approach is only in its infancy. Referring to TREK and TRAAK MS channels candidates mentioned in the first section of this review, no homologs of these

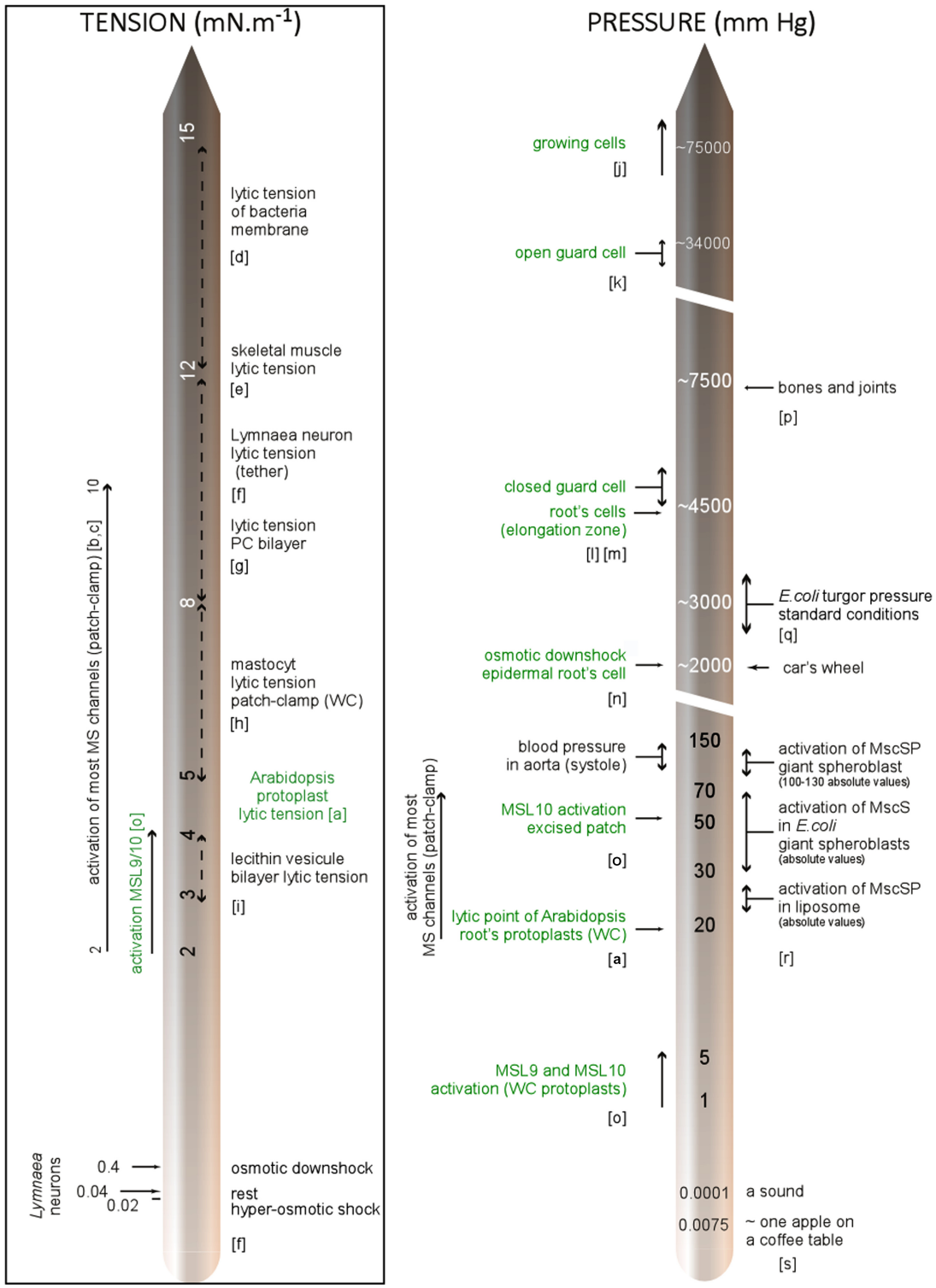

FIGURE 4 | Membrane tension and pressure within cells: milestones and experimental data. References; a: Wolfe et al. (1985), b: Gustin et al. (1988), c: Sachs and Morris (1998), d: Boer et al. (2011), e: Nichol and Hutter (1996), f: Dai et al. (1998), g: Evans and Ludwig (2000), h: Solsona et al. (1998), i: Kwok and Evans (1981), j: Meckel et al. (2004), k: Cosgrove (1996), l: Franks et al. (2001), m: Pritchard et al. (1990), n: Shabala and Lew (2002), o: Haswell et al. (2008), p: Sukharev and Sachs (2012), q: (Wood, 1999), r: Petrov et al. (2013), s: Morris and Homann (2001). In green: characteristics related to plant, WC, whole-cell configuration; PC, phosphatidylcholine.

mammalian proteins were found in currently sequenced plant genomes. By contrast, Piezo, an evolutionarily conserved protein, is expressed in invertebrates, plants, and protozoa. In plants, Piezo has only one homolog making this putative plant mechanosensor even more interesting, which urges experimenters to apply the KO strategy for this gene. In the same way, considering the prokaryotic MscS channels, homolog are present in plants but not in mammals. AtMSL 2 and 3, the closest *Arabidopsis* member of *E. coli*, were shown by Haswell and Meyerowitz (2006) and Wilson et al. (2011) to be involved in chloroplast shaping and Z-ring elaboration. Although AtMSL9 and AtMSL10 were proved to be channels activated by membrane stretching in *Arabidopsis* (Haswell et al., 2008; Peyronnet et al., 2008; Maksaev and Haswell, 2012) the KO strategy applied to these genes and related AtMSL4, AtMSL5, AtMSL6 members did not reveal phenotypes. A complementary approach to develop in this situation is the generation of gain of function (GOF) mutants. Indeed, MS channels must be closed in resting conditions in order to avoid unsuitable elicitation and unnecessary ion gradient dissipation. Hence, finding the "window of activation" is mandatory in order to obtain a phenotype. The use of conditional GOF, either in channels constitutively open or with a lowered activation threshold, can considerably enlarge this window and help reveal functions. This strategy was applied notably for Piezo2 and might be insightful for MSL in plants.

COUPLING CHANNEL ACTIVATION TO SECONDARY MESSENGERS?

The immediacy of the MS channel activation and the earliness of cellular ion fluxes and ROS variations (Monshausen et al., 2009; Coutand, 2010) in response to membrane stretching raises the question of the nature of the coupling between the channel and secondary messengers. Two types of situations might be considered. First, the simplest is due to the high capacity of the MS channel to efflux ions. As a consequence, an activation of the channel will lead to a loss of osmolyte occurring in a few minutes. This situation will lead to rapid protection of the cell against damage from hypoosmotic shock, as it does in *E. coli* upon activation of MscS and MscL channels. In the latter case, no immediate coupling with a second messenger is required since the predominant effect is a massive efflux of ions passively moving down the electrochemical gradient. Secondly, in less severe situations, the way in which the coupling occurs between MS channel activation and early Ca, pH, and ROS variation is still unknown. In response to either mechanical curvature of the plant root (Monshausen and Gilroy, 2009) or the oscillatory cell wall deformation occurring during hypocotyl cell elongation (Wolf et al., 2012), the earliest response is a rise in cytosolic calcium. In their attempt to connect plasma membrane stretching with Ca^{2+} influx, authors almost always, speculate about the intervention of a MS Ca channel. Until now, the only proposed MS channel suspected to be Ca permeable has been MCA1, which generates cation currents upon membrane stretching when expressed in *Xenopus* oocytes (Furuichi et al., 2012). Then, calcium influx would be amplified by a Ca-induced Ca-released mechanism requiring intracellular calcium stores. Another way to effectively link MS channels with Ca variation would be through an electrical coupling. Indeed, voltage dependent channels selective for calcium have been described on the plasma membrane (Miedema et al., 2008). These channels are activated by plasma membrane depolarization. Now, let us consider a membrane in which a MS AtMSL10 channel and a calcium voltage dependent channel coexist. Stretching this membrane will activate the AtMSL10 anion permeable channel (Haswell et al., 2008; Maksaev and Haswell, 2012) which will bring the membrane potential toward an equilibrium potential for anions (Cl^- and NO_3^-), meaning a large depolarization. In turn, a Ca voltage dependent channel will be activated by electrocoupling (Action Potential is an example of electrocoupling between Na^+ and K^+ channels in animals) producing an inward Ca current. In order to check this scenario it is of major interest to compare, in the near future, the Ca signature of mechanically stimulated wild type versus KO plants for MS genes such as MSL, MCA, or Piezo.

THE PECULIAR STATUS OF TONOPLAST MS CHANNELS

Over the past 20 years, distinct MS channel activities have been characterized using the patch clamp method (for review see Haswell, 2007). The majority of them were described on the plasma membrane which was easily amenable to the patch clamp technique. The few studies performed on mechanogated channels on plant tonoplast did not allow for molecular identification. However, it is in 2003, in yeast (Zhou et al., 2003), that the first vacuolar membrane MS channel belonging to the TRP family was characterized. Channels of the TRP superfamily are associated with sensations of force, temperature, and chemicals in animals. These channels are formed of tetramer subunits selective for small cations. To date, no homologous has been found in plant (Kung et al., 2010; Eijkelkamp et al., 2013). The yeast TRP1, like other TRP, is polymodal, responding to voltage, membrane stretch force, and cytosolic Ca^{2+} concentration. In plant, only three studies (Alexandre and Lassalles, 1991; Badot et al., 1992; Maathuis, 2011) report the presence of mechanogated channels in the tonoplast membrane. The most meticulous characterization concerns a beetroot (*Beta vulgaris)* MS non-selective channel activated by hydrostatic and osmotic pressure but inhibited by the MS channel blocker gadolinium (Alexandre and Lassalles, 1991). It was recently shown by Maathuis (2011) that vacuolar channels from the two pores K^+ family (TPKs) from the three species *Arabidopsis*, rice, and barley were stretch sensitive. The dependence of these channels on membrane stretching and osmotic gradients led the author to propose a role for intracellular osmosensors for TPKs contributing to K^+-released induced by hypo-osmotic shock. Considering the large size of the vacuole (the largest cell compartment being up to 90% of the cell volume) and the presence of MS activities in its membrane, it remains crucial to further study tonoplast mechanosensitivity. It is noteworthy that the physical forces applied to this membrane and its links with the cytoskeleton should be rather distinct to those of the plasma membrane. In conclusion, the molecular identification of tonoplast MS channels and the understanding of the role of the vacuole in mechanoperception are part of the next exciting challenges.

OUTLOOK

Despite many structural and mechanical differences, MS channels were conserved in plant and animal cells with similar

characteristics. Considering the great difference in their life style, animal channels are presumably devoted to different functions to those of their plant counterparts. Therefore, it is of interest to predict in which function plant MS channels might be involved in order to design experimental conditions to reveal their role. If the ancestral role of the bacterial MscS channel is conserved, some MS channels might be involved in osmoregulation. Thus, looking at the kinetics of either cell swelling (root hair cell) or root ionic flux under different osmotic conditions will give an indication of this function. The root network also has to face obstacles and adapt to the hardness of the substrate during its anchorage role. Considering that MSLs are well expressed in root tissues (Haswell et al., 2008; Peyronnet et al., 2008), it is of interest to develop experimental devices in order to thoroughly study the root growth in relation to MS channel activity. Movement, although less spectacular than in animals, is ubiquitous in plants. It might be rapid, such as the closure of the Venus fly trap or leaflets of *Mimosa pudica,* or slow as occurs in flowers and leaves during nastic movements. All plants are also able to sense both gravity and their own shape in order to grow straight. In animals this property is called proprioception (Bastien et al., 2013). All of these reorientation movements involve osmotic pressure as well as cell curvature and are likely to require MS channels. Designing screens based on imaging to capture movement would help in deciphering the MS channel role in plants.

ACKNOWLEDGMENTS

This work is supported by the grant ANR-09-BLAN-0245-03 from the Agence Nationale de la Recherche (ANR, project SENZO) and the grant ANR-11-BSV7-010-02 from the Agence Nationale de la Recherche (ANR, project CAROLS). We apologize to all authors whose work could not be cited due to space constraints.

REFERENCES

Akitake, B., Anishkin, A., Liu, N., and Sukharev, S. (2007). Straightening and sequential buckling of the pore-lining helices define the gating cycle of MscS. *Nat. Struct. Mol. Biol.* 14, 1141–1149. doi: 10.1038/nsmb1341

Alexandre, J., and Lassalles, J. P. (1991). Hydrostatic and osmotic pressure activated channel in plant vacuole. *Biophys. J.* 60, 1326–1336. doi: 10.1016/S0006-3495(91)82170-1

Al-Rekabi, Z., Haase, K., and Pelling, A. E. (2014). Microtubules mediate changes in membrane cortical elasticity during contractile activation. *Exp. Cell Res.* 322, 21–29. doi: 10.1016/j.yexcr.2013.12.027

Alloui, A., Zimmermann, K., Mamet, J., Duprat, F., Noel, J., Chemin, J., et al. (2006). TREK-1, a K^+ channel involved in polymodal pain perception. *EMBO J.* 25, 2368–2376. doi: 10.1038/sj.emboj.7601116

Ambrose, J. C., Shoji, T., Kotzer, A. M., Pighin, J. A., and Wasteneys, G. O. (2007). The *Arabidopsis* CLASP gene encodes a microtubule-associated protein involved in cell expansion and division. *Plant Cell* 19, 2763–2775. doi: 10.1105/tpc.107.053777

Arnadottir, J., and Chalfie, M. (2010). Eukaryotic mechanosensitive channels. *Annu. Rev. Biophys.* 39, 111–137. doi: 10.1146/annurev.biophys.37.032807.125836

Badot, P. M., Ding, J. P., and Pickard, B. G. (1992). Mechanically activated ion channels occur in vacuoles of onion bulb scale parenchyma. *C. R. Acad. Sci. Gen.* 315, 437–443.

Bae, C., Gottlieb, P. A., and Sachs, F. (2013). Human PIEZO1: removing inactivation. *Biophys. J.* 105, 880–886. doi: 10.1016/j.bpj.2013.07.019

Bae, C., Sachs, F., and Gottlieb, P. A. (2011). The mechanosensitive ion channel piezo1 is inhibited by the peptide GsMTx4. *Biochemistry* 50, 6295–6300. doi: 10.1021/bi200770q

Bang, H., Kim, Y., and Kim, D. (2000). TREK-2, a new member of the mechanosensitive tandem-pore K1 channel family. *J. Biol. Chem.* 275, 17412–17419. doi: 10.1074/jbc.M000445200

Bass, R. B., Strop, P., Barclay, M., and Rees, D. C. (2002). Crystal structure of *Escherichia coli* MscS, a voltage-modulated and mechanosensitive channel. *Science* 298, 1582–1587. doi: 10.1126/science.1077945

Bastien, R., Bohr, T., Moulia, B., and Douady, S. (2013). Unifying model of shoot gravitropism reveals proprioception as a central feature of posture control in plants. *Proc. Natl. Acad. Sci. U.S.A.* 110, 755–760. doi: 10.1073/pnas.1214301109

Belyy, V., Kamaraju, K., Akitake, B., Anishkin, A., and Sukharev, S. (2010). Adaptive behavior of bacterial mechanosensitive channels is coupled to membrane mechanics. *J. Gen. Physiol.* 135, 641–652. doi: 10.1085/jgp.200910371

Boer, M., Anishkin, A., and Sukharev, S. (2011). Adaptive MscS gating in the osmotic permeability response in *E. coli*: the question of time. *Biochemistry* 50, 4087–4096. doi: 10.1021/bi1019435

Brandizzi, F., and Wasteneys, G. O. (2013). Cytoskeleton-dependent endomembrane organization in plant cells: an emerging role for microtubules. *Plant J.* 75, 339–349. doi: 10.1111/tpj.12227

Brohawn, S. G., Campbell, E. B., and Mackinnon, R. (2013). Domain-swapped chain connectivity and gated membrane access in a Fab-mediated crystal of the human TRAAK K^+ channel. *Proc. Natl. Acad. Sci. U.S.A.* 110, 2129–2134. doi: 10.1073/pnas.1218950110

Brohawn, S. G., Del Marmol, J., and Mackinnon, R. (2012). Crystal structure of the human K_{2P} TRAAK, a lipid- and mechano-sensitive K^+ ion channel. *Science* 335, 436–441. doi: 10.1126/science.1213808

Brohawn, S. G., Su, Z., and Mackinnon, R. (2014). Mechanosensitivity is mediated directly by the lipid membrane in TRAAK and TREK1 K^+ channels. *Proc. Natl. Acad. Sci. U.S.A.* 111, 3614–3619. doi: 10.1073/pnas.1320768111

Campás, O., Mammoto, T., Hasso, S., Sperling, R. A., O'connell, D., Bischof, A. G., et al. (2014). Quantifying cell-generated mechanical forces within living embryonic tissues. *Nat. Methods* 11, 183–189. doi: 10.1038/nmeth.2761

Chan, J., Eder, M., Crowell, E. F., Hampson, J., Calder, G., and Lloyd, C. (2011). Microtubules and CESA tracks at the inner epidermal wall align independently of those on the outer wall of light-grown *Arabidopsis* hypocotyls. *J. Cell Sci.* 124, 1088–1094. doi: 10.1242/jcs.086702

Chang, G., Spencer, R. H., Lee, A. T., Barclay, M. T., and Rees, D. C. (1998). Structure of the MscL homolog from *Mycobacterium tuberculosis*: a gated mechanosensitive ion channel. *Science* 282, 2220–2226. doi: 10.1126/science.282.5397.2220

Cosgrove, D. J. (1993). Water uptake by growing cells: an assessment of the controlling roles of wall relaxation, solute uptake, and hydraulic conductance. *Int. J. Plant Sci.* 154, 10–21. doi: 10.1086/297087

Cosgrove, D. J. (1996). Plant cell enlargement and the action of expansins. *Bioessays* 18, 533–540. doi: 10.1002/bies.950180704

Cosgrove, D. J., and Jarvis, M. C. (2012). Comparative structure and biomechanics of plant primary and secondary cell walls. *Front. Plant Sci.* 3:204. doi: 10.3389/fpls.2012.00204

Coste, B., Mathur, J., Schmidt, M., Earley, T. J., Ranade, S., Petrus, M. J., et al. (2010). Piezo1 and Piezo2 are essential components of distinct mechanically activated cation channels. *Science* 330, 55–60. doi: 10.1126/science.1193270

Coste, B., Xiao, B., Santos, J. S., Syeda, R., Grandl, J., Spencer, K. S., et al. (2012). Piezo proteins are pore-forming subunits of mechanically activated channels. *Nature* 483, 176–181. doi: 10.1038/nature10812

Coutand, C. (2010). Mechanosensing and thigmomorphogenesis, a physiological and biomechanical point of view. *Plant Sci.* 179, 168–182. doi: 10.1016/j.plantsci.2010.05.001

Cox, C. D., Nakayama, Y., Nomura, T., and Martinac, B. (2014). The evolutionary 'tinkering' of MscS-like channels: generation of structural and functional diversity. *Pflugers Arch.* doi: 10.1007/s00424-014-1522-2

Dai, J., Sheetz, M. P., Wan, X., and Morris, C. E. (1998). Membrane tension in swelling and shrinking molluscan neurons. *J. Neurosci.* 18, 6681–6692.

Dedman, A., Sharif-Naeini, R., Folgering, J. H., Duprat, F., Patel, A., and Honore, E. (2009). The mechano-gated K(2P) channel TREK-1. *Eur. Biophys. J.* 38, 293–303. doi: 10.1007/s00249-008-0318-8

Eijkelkamp, N., Quick, K., and Wood, J. N. (2013). Transient receptor potential channels and mechanosensation. *Annu. Rev. Neurosci.* 36, 519–546. doi: 10.1146/annurev-neuro-062012-170412

Ellis, R. J. (2001). Macromolecular crowding: obvious but underappreciated. *Trends Biochem. Sci.* 26, 597–604. doi: 10.1016/S0968-0004(01)01938-7

Evans, E., and Ludwig, F. (2000). Dynamic strengths of molecular anchoring and material cohesion in fluid biomembranes. *J. Phys. Condens. Matter* 12:A315. doi: 10.1088/0953-8984/12/8A/341

Falke, L. C., Edwards, K. L., Pickard, B. G., and Misler, S. (1988). A stretch-activated anion channel in tobacco protoplasts. *FEBS Lett.* 237, 141–144. doi: 10.1016/0014-5793(88)80188-1

Franks, P. J., Buckley, T. N., Shope, J. C., and Mott, K. A. (2001). Guard cell volume and pressure measured concurrently by confocal microscopy and the cell pressure probe. *Plant Physiol.* 125, 1577–1584. doi: 10.1104/pp.125.4.1577

Furuichi, T., Iida, H., Sokabe, M., and Tatsumi, H. (2012). Expression of *Arabidopsis* MCA1 enhanced mechanosensitive channel activity in the *Xenopus laevis* oocyte plasma membrane. *Plant Signal. Behav.* 7, 1022–1026. doi: 10.4161/psb.20783

Gardiner, J. (2013). The evolution and diversification of plant microtubule-associated proteins. *Plant J.* 75, 219–229. doi: 10.1111/tpj.12189

Gauthier, N. C., Masters, T. A., and Sheetz, M. P. (2012). Mechanical feedback between membrane tension and dynamics. *Trends Cell Biol.* 22, 527–535. doi: 10.1016/j.tcb.2012.07.005

Gottlieb, P. A., Bae, C., and Sachs, F. (2012). Gating the mechanical channel Piezo1. A comparison between whole-cell and patch recording. *Channels* 6, 282–289. doi: 10.4161/Chan.21064

Gottlieb, P. A., and Sachs, F. (2012). Piezo1: properties of a cation selective mechanical channel. *Channels* 6, 214–219. doi: 10.4161/chan.21050

Grashoff, C., Hoffman, B. D., Brenner, M. D., Zhou, R., Parsons, M., Yang, M. T., et al. (2010). Measuring mechanical tension across vinculin reveals regulation of focal adhesion dynamics. *Nature* 466, 263–266. doi: 10.1038/nature09198

Guharay, F., and Sachs, F. (1984). Stretch-activated single ion channel currents in tissue-cultured embryonic chick skeletal muscle. *J. Physiol.* 352, 685–701.

Guo, J., Sachs, F., and Meng, F. (2013). Fluorescence-based force/tension sensors: a novel tool to visualize mechanical forces in structural proteins in live cells. *Antioxid. Redox Signal.* 20, 986–999. doi: 10.1089/ars.2013.5708

Gustin, M. C., Zhou, X. L., Martinac, B., and Kung, C. (1988). A mechanosensitive ion channel in the yeast plasma membrane. *Science* 242, 762–765. doi: 10.1126/science.2460920

Hamill, O. P., and Martinac, B. (2001). Molecular basis of mechanotransduction in living cells. *Physiol. Rev.* 81, 685–740.

Hamill, O. P., Marty, A., Neher, E., Sakmann, B., and Sigworth, F. J. (1981). Improved patch-clamp techniques for high-resolution current recording from cells and cell-free membrane patches. *Pflugers Arch.* 391, 85–100. doi: 10.1007/BF00656997

Haswell, E. S. (2007). "MscS-like proteins in plants,"in *Mechanosensitive Ion Channels, Part A*, ed. O. P. Hamill (San Diego, CA: Elsevier and Academic Press), 329–359. doi: 10.1016/S1063-5823(06)58013-5

Haswell, E. S., and Meyerowitz, E. M. (2006). MscS-like proteins control plastid size and shape in *Arabidopsis thaliana*. *Curr. Biol.* 16, 1–11. doi: 10.1016/j.cub.2005.11.044

Haswell, E. S., Peyronnet, R., Barbier-Brygoo, H., Meyerowitz, E. M., and Frachisse, J. M. (2008). Two MscS homologs provide mechanosensitive channel activities in the *Arabidopsis* root. *Curr. Biol.* 18, 730–734. doi: 10.1016/j.cub.2008.04.039

Hayakawa, K., Tatsumi, H., and Sokabe, M. (2012). Mechano-sensing by actin filaments and focal adhesion proteins. *Commun. Integr. Biol.* 5, 572–577. doi: 10.4161/cib.21891

Heurteaux, C., Guy, N., Laigle, C., Blondeau, N., Duprat, F., Mazzuca, M., et al. (2004). TREK-1, a K^+ channel involved in neuroprotection and general anesthesia. *EMBO J.* 23, 2684–2695. doi: 10.1038/sj.emboj.7600234

Heurteaux, C., Lucas, G., Guy, N., El Yacoubi, M., Thummler, S., Peng, X. D., et al. (2006). Deletion of the background potassium channel TREK-1 results in a depression-resistant phenotype. *Nat. Neurosci.* 9, 1134–1141. doi: 10.1038/nn1749

Honore, E., Patel, A. J., Chemin, J., Suchyna, T., and Sachs, F. (2006). Desensitization of mechano-gated K_{2P} channels. *Proc. Natl. Acad. Sci. U.S.A.* 103, 6859–6864. doi: 10.1073/pnas.0600463103

Hurwitz, C. G., and Segal, A. S. (2001). Application of pressure steps to mechanosensitive channels in membrane patches: a simple, economical, and fast system. *Pflugers Arch.* 442, 150–156. doi: 10.1007/s004240100541

Jaqaman, K., and Grinstein, S. (2012). Regulation from within: the cytoskeleton in transmembrane signaling. *Trends Cell Biol.* 22, 515–526. doi: 10.1016/j.tcb.2012.07.006

Kamaraju, K., Belyy, V., Rowe, I., Anishkin, A., and Sukharev, S. (2011). The pathway and spatial scale for MscS inactivation. *J. Gen. Physiol.* 138, 49–57. doi: 10.1085/jgp.201110606

Kamkin, A., and Kiseleva, I. (2008). "Mechanically gated channels and mechanosensitive channels," in *Mechanosensitivity in Cells and Tissues*: *Mechanosensitive Ion Channels*, eds A. Kamkin and I. Kiseleva, (Berlin: Springer), xiii–xviii. doi: 10.1007/978-1-4020-6426-5

Kim, S. E., Coste, B., Chadha, A., Cook, B., and Patapoutian, A. (2012). The role of *Drosophila* Piezo in mechanical nociception. *Nature* 483, 209–212. doi: 10.1038/nature10801

Knepper, C., Savory, E. A., and Day, B. (2011). *Arabidopsis* NDR1 is an integrin-like protein with a role in fluid loss and plasma membrane-cell wall adhesion. *Plant Physiol.* 156, 286–300. doi: 10.1104/pp.110.169656

Kung, C., Martinac, B., and Sukharev, S. (2010). Mechanosensitive channels in microbes. *Annu. Rev. Microbiol.* 64, 313–329. doi: 10.1146/annurev.micro.112408.134106

Kurusu, T., Kuchitsu, K., Nakano, M., Nakayama, Y., and Iida, H. (2013). Plant mechanosensing and Ca^{2+} transport. *Trends Plant Sci.* 18, 227–233. doi: 10.1016/j.tplants.2012.12.002

Kwok, R., and Evans, E. (1981). Thermoelasticity of large lecithin bilayer vesicles. *Biophys. J.* 35, 637–652. doi: 10.1016/S0006-3495(81)84817-5

Lauritzen, I., Chemin, J., Honore, E., Jodar, M., Guy, N., Lazdunski, M., et al. (2005). Cross-talk between the mechano-gated K_{2P} channel TREK-1 and the actin cytoskeleton. *EMBO Rep.* 6, 642–648. doi: 10.1038/sj.embor.7400449

Le Guennec, J. Y., Peineau, N., Argibay, J. A., Mongo, K. G., and Garnier, D. (1990). A new method of attachment of isolated mammalian ventricular myocytes for tension recording: length dependence of passive and active tension. *J. Mol. Cell Cardiol.* 22, 1083–1093. doi: 10.1016/0022-2828(90)90072-A

Levina, N., Totemeyer, S., Stokes, N. R., Louis, P., Jones, M. A., and Booth, I. R. (1999). Protection of *Escherichia coli* cells against extreme turgor by activation of MscS and MscL mechanosensitive channels: identification of genes required for MscS activity. *EMBO J.* 18, 1730–1737. doi: 10.1093/emboj/18.7.1730

Maathuis, F. J. (2011). Vacuolar two-pore K^+ channels act as vacuolar osmosensors. *New Phytol.* 191, 84–91. doi: 10.1111/j.1469-8137.2011.03664.x

Maingret, F., Patel, A. J., Lesage, F., Lazdunski, M., and Honore, E. (2000). Lysophospholipids open the two-pore domain mechano-gated K^+ channels TREK-1 and TRAAK. *J. Biol. Chem.* 275, 10128–10133. doi: 10.1074/jbc.275.14.10128

Maksaev, G., and Haswell, E. S. (2012). MscS-Like10 is a stretch-activated ion channel from *Arabidopsis thaliana* with a preference for anions. *Proc. Natl. Acad. Sci. U.S.A.* 109, 19015–19020. doi: 10.1073/pnas.1213931109

Martinac, B. (2011). Bacterial mechanosensitive channels as a paradigm for mechanosensory transduction. *Cell Physiol. Biochem.* 28, 1051–1060. doi: 10.1159/000335842

Martinac, B., Adler, J., and Kung, C. (1990). Mechanosensitive ion channels of *E. coli* activated by amphipaths. *Nature* 348, 261–263. doi: 10.1038/348261a0

Martinac, B., Buechner, M., Delcour, A. H., Adler, J., and Kung, C. (1987). Pressure-sensitive ion channel in *Escherichia coli*. *Proc. Natl. Acad. Sci. U.S.A.* 84, 2297–2301. doi: 10.1073/pnas.84.8.2297

Martinac, B., Saimi, Y., and Kung, C. (2008). Ion channels in microbes. *Physiol. Rev.* 88, 1449–1490. doi: 10.1152/physrev.00005.2008

McBride, D. W. Jr., and Hamill, O. P. (1992). Pressure-clamp: a method for rapid step perturbation of mechanosensitive channels. *Pflugers Arch.* 421, 606–612. doi: 10.1007/BF00375058

Meckel, T., Hurst, A. C., Thiel, G., and Homann, U. (2004). Endocytosis against high turgor: intact guard cells of Vicia faba constitutively endocytose fluorescently labelled plasma membrane and GFP-tagged K-channel KAT1. *Plant J.* 39, 182–193. doi: 10.1111/j.1365-313X.2004.02119.x

Meng, F., and Sachs, F. (2011). Visualizing dynamic cytoplasmic forces with a compliance-matched FRET sensor. *J. Cell Sci.* 124, 261–269. doi: 10.1242/jcs.071928

Miedema, H., Demidchik, V., Very, A. A., Bothwell, J. H., Brownlee, C., and Davies, J. M. (2008). Two voltage-dependent calcium channels co-exist in the apical plasma membrane of *Arabidopsis thaliana* root hairs. *New Phytol.* 179, 378–385. doi: 10.1111/j.1469-8137.2008.02465.x

Monshausen, G. B., Bibikova, T. N., Weisenseel, M. H., and Gilroy, S. (2009). Ca^{2+} regulates reactive oxygen species production and pH during mechanosensing in *Arabidopsis* roots. *Plant Cell* 21, 2341–2356. doi: 10.1105/tpc.109.068395

Monshausen, G. B., and Gilroy, S. (2009). Feeling green: mechanosensing in plants. *Trends Cell Biol.* 19, 228–235. doi: 10.1016/j.tcb.2009.02.005

Monshausen, G. B., and Haswell, E. S. (2013). A force of nature: molecular mechanisms of mechanoperception in plants. *J. Exp. Bot.* 64, 4663–4680. doi: 10.1093/jxb/ert204

Morris, C. E., and Homann, U. (2001). Cell surface area regulation and membrane tension. *J. Membr. Biol.* 179, 79–102. doi: 10.1007/s002320010040

Mukherjee, N., Jose, M. D., Birkner, J. P., Walko, M., Ingolfsson, H. I., Dimitrova, A., et al. (2014). The activation mode of the mechanosensitive ion channel, MscL, by lysophosphatidylcholine differs from tension-induced gating. *FASEB J.* 28, 4292–4302. doi: 10.1096/fj.14–251579

Nakagawa, Y., Katagiri, T., Shinozaki, K., Qi, Z., Tatsumi, H., Furuichi, T., et al. (2007). *Arabidopsis* plasma membrane protein crucial for Ca^{2+} influx and touch sensing in roots. *Proc. Natl. Acad. Sci. U.S.A.* 104, 3639–3644. doi: 10.1073/pnas.0607703104

Nakayama, Y., Yoshimura, K., and Iida, H. (2013). Electrophysiological characterization of the mechanosensitive channel MscCG in *Corynebacterium glutamicum*. *Biophys. J.* 105, 1366–1375. doi: 10.1016/j.bpj.2013.06.054

Nichol, J. A., and Hutter, O. F. (1996). Tensile strength and dilatational elasticity of giant sarcolemmal vesicles shed from rabbit muscle. *J. Physiol.* 493(Pt 1), 187–198.

Nick, P. (2013). Microtubules, signalling and abiotic stress. *Plant J.* 75, 309–323. doi: 10.1111/tpj.12102

Nilius, B., and Honore, E. (2012). Sensing pressure with ion channels. *Trends Neurosci.* 35, 477–486. doi: 10.1016/j.tins.2012.04.002

Noel, J., Sandoz, G., and Lesage, F. (2011). Molecular regulations governing TREK and TRAAK channel functions. *Channels* 5, 402–409. doi: 10.4161/chan.5.5.16469

Nomura, T., Cranfield, C. G., Deplazes, E., Owen, D. M., Macmillan, A., Battle, A. R., et al. (2012). Differential effects of lipids and lyso-lipids on the mechanosensitivity of the mechanosensitive channels MscL and MscS. *Proc. Natl. Acad. Sci. U.S.A.* 109, 8770–8775. doi: 10.1073/pnas.1200051109

Ofer, N., Mogilner, A., and Keren, K. (2011). Actin disassembly clock determines shape and speed of lamellipodial fragments. *Proc. Natl. Acad. Sci. U.S.A.* 108, 20394–20399. doi: 10.1073/pnas.1105333108

Paredez, A. R., Somerville, C. R., and Ehrhardt, D. W. (2006). Visualization of cellulose synthase demonstrates functional association with microtubules. *Science* 312, 1491–1495. doi: 10.1126/science.1126551

Patel, A. J., Honore, E., Maingret, F., Lesage, F., Fink, M., Duprat, F., et al. (1998). A mammalian two pore domain mechano-gated S-like K^+ channel. *EMBO J.* 17, 4283–4290. doi: 10.1093/emboj/17.15.4283

Perozo, E., Kloda, A., Cortes, D. M., and Martinac, B. (2002). Physical principles underlying the transduction of bilayer deformation forces during mechanosensitive channel gating. *Nat. Struct. Biol.* 9, 696–703. doi: 10.1038/nsb827

Perozo, E., and Rees, D. C. (2003). Structure and mechanism in prokaryotic mechanosensitive channels. *Curr. Opin. Struct. Biol.* 13, 432–442. doi: 10.1016/S0959-440X(03)00106-4

Peter, B. J., Kent, H. M., Mills, I. G., Vallis, Y., Butler, P. J., Evans, P. R., et al. (2004). BAR domains as sensors of membrane curvature: the amphiphysin BAR structure. *Science* 303, 495–499. doi: 10.1126/science.1092586

Petrov, E., Palanivelu, D., Constantine, M., Rohde, P. R., Cox, C. D., Nomura, T., et al. (2013). Patch-clamp characterization of the MscS-like mechanosensitive channel from Silicibacter pomeroyi. *Biophys. J.* 104, 1426–1434. doi: 10.1016/j.bpj.2013.01.055

Peyronnet R., Haswell, E. S., Barbier-Brygoo H., and Frachisse, J. M. (2008). AtMSL9 and AtMSL10: Sensors of plasma membrane tension in *Arabidopsis* roots. *Plant Signal. Behav.* 3, 726–729. doi: 10.4161/psb.3.9.6487

Peyronnet, R., Sharif-Naeini, R., Folgering, J. H., Arhatte, M., Jodar, M., El Boustany, C., et al. (2012). Mechanoprotection by polycystins against apoptosis is mediated through the opening of stretch-activated K_{2P} channels. *Cell Rep.* 1, 241–250. doi: 10.1016/j.celrep.2012.01.006

Pranke, I. M., Morello, V., Bigay, J., Gibson, K., Verbavatz, J. M., Antonny, B., et al. (2011). alpha-Synuclein and ALPS motifs are membrane curvature sensors whose contrasting chemistry mediates selective vesicle binding. *J. Cell Biol.* 194, 89–103. doi: 10.1083/jcb.201011118

Pritchard, J., Barlow, P. W., Adam, J. S., and Tomos, A. D. (1990). Biophysics of the inhibition of the growth of maize roots by lowered temperature. *Plant Physiol.* 93, 222–230. doi: 10.1104/pp.93.1.222

Ren, G., Vajjhala, P., Lee, J. S., Winsor, B., and Munn, A. L. (2006). The BAR domain proteins: molding membranes in fission, fusion, and phagy. *Microbiol. Mol. Biol. Rev.* 70, 37–120. doi: 10.1128/MMBR.70.1.37-120.2006

Rowe, I., Anishkin, A., Kamaraju, K., Yoshimura, K., and Sukharev, S. (2014). The cytoplasmic cage domain of the mechanosensitive channel MscS is a sensor of macromolecular crowding. *J. Gen. Physiol.* 143, 543–557. doi: 10.1085/jgp.201311114

Sachs, F. (2010). Stretch-activated ion channels: what are they? *Physiology (Bethesda)* 25, 50–56. doi: 10.1152/physiol.00042.2009

Sachs, F., and Morris, C. E. (1998). Mechanosensitive ion channels in nonspecialized cells. *Rev. Physiol. Biochem. Pharmacol.* 132, 1–77. doi: 10.1007/BFb0004985

Saravanan, S., Meghana, C., and Narasimha, M. (2013). Local, cell-nonautonomous feedback regulation of myosin dynamics patterns transitions in cell behavior: a role for tension and geometry? *Mol. Biol. Cell* 24, 2350–2361. doi: 10.1091/mbc.E12-12–0868

Shabala, S. N., and Lew, R. R. (2002). Turgor regulation in osmotically stressed *Arabidopsis* epidermal root cells. Direct support for the role of inorganic ion uptake as revealed by concurrent flux and cell turgor measurements. *Plant Physiol.* 129, 290–299. doi: 10.1104/pp.020005

Sheetz, M. P., and Singer, S. J. (1974). Biological membranes as bilayer couples. A molecular mechanism of drug-erythrocyte interactions. *Proc. Natl. Acad. Sci. U.S.A.* 71, 4457–4461. doi: 10.1073/pnas.71.11.4457

Solsona, C., Innocenti, B., and Fernandez, J. M. (1998). Regulation of exocytotic fusion by cell inflation. *Biophys. J.* 74, 1061–1073. doi: 10.1016/S0006-3495(98)74030-5

Sotomayor, M., Vasquez, V., Perozo, E., and Schulten, K. (2007). Ion conduction through MscS as determined by electrophysiology and simulation. *Biophys. J.* 92, 886–902. doi: 10.1529/biophysj.106.095232

Suchyna, T. M., Tape, S. E., Koeppe, R. E. II, Andersen, O. S., Sachs, F., and Gottlieb, P. A. (2004). Bilayer-dependent inhibition of mechanosensitive channels by neuroactive peptide enantiomers. *Nature* 430, 235–240. doi: 10.1038/nature02743

Sukharev, S. (1999). Mechanosensitive channels in bacteria as membrane tension reporters. *FASEB J.* 13 (Suppl.), S55–S61.

Sukharev, S. (2002). Purification of the small mechanosensitive channel of *Escherichia coli* (MscS): the subunit structure, conduction, and gating characteristics in liposomes. *Biophys. J.* 83, 290–298. doi: 10.1016/S0006-3495(02)75169-2

Sukharev, S., Betanzos, M., Chiang, C. S., and Guy, H. R. (2001). The gating mechanism of the large mechanosensitive channel MscL. *Nature* 409, 720–724. doi: 10.1038/35055559

Sukharev, S., and Sachs, F. (2012). Molecular force transduction by ion channels: diversity and unifying principles. *J. Cell Sci.* 125, 3075–3083. doi: 10.1242/jcs.092353

Sukharev, S. I., Blount, P., Martinac, B., Blattner, F. R., and Kung, C. (1994a). A large-conductance mechanosensitive channel in *E. coli* encoded by mscL alone. *Nature* 368, 265–268. doi: 10.1038/368265a0

Sukharev, S. I., Martinac, B., Blount, P., and Kung, C. (1994b). Functional reconstitution as an assay for biochemical isolation of channel proteins: application to the molecular identification of a bacterial mechanosensitive channel. *Methods* 6, 51–59. doi: 10.1006/meth.1994.1007

Sukharev, S. I., Blount, P., Martinac, B., and Kung, C. (1997). Mechanosensitive channels of *Escherichia coli*: the MscL gene, protein, and activities. *Annu. Rev. Physiol.* 59, 633–657. doi: 10.1146/annurev.physiol.59.1.633

Sukharev, S. I., Sigurdson, W. J., Kung, C., and Sachs, F. (1999). Energetic and spatial parameters for gating of the bacterial large conductance mechanosensitive channel, MscL. *J. Gen. Physiol.* 113, 525–540. doi: 10.1085/jgp.113.4.525

Szymanski, D. B., and Cosgrove, D. J. (2009). Dynamic coordination of cytoskeletal and cell wall systems during plant cell morphogenesis. *Curr. Biol.* 19, R800–R811. doi: 10.1016/j.cub.2009.07.056

Teng, J., Loukin, S., Anishkin, A., and Kung, C. (2014). The force-from-lipid (FFL) principle of mechanosensitivity, at large and in elements. *Pflugers Arch.* doi: 10.1007/s00424-014-1530-2 [Epub ahead of Print].

Vasquez, V., Sotomayor, M., Cordero-Morales, J., Schulten, K., and Perozo, E. (2008). A structural mechanism for MscS gating in lipid bilayers. *Science* 321, 1210–1214. doi: 10.1126/science.1159674

Wang, Y., Liu, Y., Deberg, H. A., Nomura, T., Hoffman, M. T., Rohde, P. R., et al. (2014). Single molecule FRET reveals pore size and opening mechanism of a mechano-sensitive ion channel. *Elife* 3:e01834. doi: 10.7554/eLife.01834

Wilson, M. E., Jensen, G. S., and Haswell, E. S. (2011). Two mechanosensitive channel homologs influence division ring placement in *Arabidopsis* chloroplasts. *Plant Cell* 23, 2939–2949. doi: 10.1105/tpc.111.088112

Wilson, M. E., Maksaev, G., and Haswell, E. S. (2013). MscS-like mechanosensitive channels in plants and microbes. *Biochemistry* 52, 5708–5722. doi: 10.1021/bi400804z

Wolf, S., Hematy, K., and Hofte, H. (2012). Growth control and cell wall signaling in plants. *Annu. Rev. Plant Biol.* 63, 381–407. doi: 10.1146/annurev-arplant-042811–105449

Wolfe, J., Dowgert, M. F., and Steponkus, P. L. (1985). Dynamics of membrane exchange of the plasma membrane and the lysis of isolated protoplasts during rapid expansion in area. *J. Membr. Biol.* 86, 127–138. doi: 10.1007/BF01870779

Woo, S. H., Ranade, S., Weyer, A. D., Dubin, A. E., Baba, Y., Qiu, Z., et al. (2014). Piezo2 is required for Merkel-cell mechanotransduction. *Nature* 509, 622–626. doi: 10.1038/nature13251

Wood, J. M. (1999). Osmosensing by bacteria: signals and membrane-based sensors. *Microbiol. Mol. Biol. Rev.* 63, 230–262.

Yoo, J., and Cui, Q. (2009). Curvature generation and pressure profile modulation in membrane by lysolipids: insights from coarse-grained simulations. *Biophys. J.* 97, 2267–2276. doi: 10.1016/j.bpj.2009.07.051

Zarychanski, R., Schulz, V. P., Houston, B. L., Maksimova, Y., Houston, D. S., Smith, B., et al. (2012). Mutations in the mechanotransduction protein PIEZO1 are associated with hereditary xerocytosis. *Blood* 120, 1908–1915. doi: 10.1182/blood-2012-04-422253

Zhang, W., Fan, L. M., and Wu, W. H. (2007). Osmo-sensitive and stretch-activated calcium-permeable channels in Vicia faba guard cells are regulated by actin dynamics. *Plant Physiol.* 143, 1140–1151. doi: 10.1104/pp.106.091405

Zhou, X. L., Batiza, A. F., Loukin, S. H., Palmer, C. P., Kung, C., and Saimi, Y. (2003). The transient receptor potential channel on the yeast vacuole is mechanosensitive. *Proc. Natl. Acad. Sci. U.S.A.* 100, 7105–7110. doi: 10.1073/pnas.1230540100

Zhuang, X., and Jiang, L. (2014). Autophagosome biogenesis in plants: roles of SH3P2. *Autophagy* 10, 704–705. doi: 10.4161/auto.28060

Conflict of Interest Statement: The authors declare that the research was conducted in the absence of any commercial or financial relationships that could be construed as a potential conflict of interest.

Received: 01 July 2014; accepted: 29 September 2014; published online: 21 October 2014

Citation: Peyronnet R, Tran D, Girault T and Frachisse J-M (2014) Mechanosensitive channels: feeling tension in a world under pressure. Front. Plant Sci. ***5****:558. doi: 10.3389/fpls.2014.00558*

This article was submitted to Plant Physiology, a section of the journal Frontiers in Plant Science.

frontiers in
PLANT SCIENCE

REVIEW ARTICLE
published: 23 February 2015
doi: 10.3389/fpls.2015.00052

Mechanosensitive control of plant growth: bearing the load, sensing, transducing, and responding

Bruno Moulia [1,2]*†, ***Catherine Coutand*** [1,2†] ***and Jean-Louis Julien*** [1,2]

[1] NRA, UMR 547 PIAF, Clermont-Ferrand, France
[2] Clermont Université, Université Blaise Pascal, UMR 547 PIAF, Clermont-Ferrand, France

Edited by:
Burkhard Schulz, Purdue University, USA

Reviewed by:
Wei-Hua Tang, Chinese Academy of Sciences, China
Nabil I. Elsheery, Tanta University, Egypt

***Correspondence:**
Bruno Moulia, UMR, PIAF Integrative Physics and Physiology of Trees, Institut National de la Recherche Agronomique, 5 chemin de Beaulieu, F-63039 Clermont-Ferrand, France
e-mail: bruno.moulia@clermont.inra.fr

† *These authors have contributed equally to this work.*

As land plants grow and develop, they encounter complex mechanical challenges, especially from winds and turgor pressure. Mechanosensitive control over growth and morphogenesis is an adaptive trait, reducing the risks of breakage or explosion. This control has been mostly studied through experiments with artificial mechanical loads, often focusing on cellular or molecular mechanotransduction pathway. However, some important aspects of mechanosensing are often neglected. (i) What are the mechanical characteristics of different loads and how are loads distributed within different organs? (ii) What is the relevant mechanical stimulus in the cell? Is it stress, strain, or energy? (iii) How do mechanosensing cells signal to meristematic cells? Without answers to these questions we cannot make progress analyzing the mechanobiological effects of plant size, plant shape, tissue distribution and stiffness, or the magnitude of stimuli. This situation is rapidly changing however, as systems mechanobiology is being developed, using specific biomechanical and/or mechanobiological models. These models are instrumental in comparing loads and responses between experiments and make it possible to quantitatively test biological hypotheses describing the mechanotransduction networks. This review is designed for a general plant science audience and aims to help biologists master the models they need for mechanobiological studies. Analysis and modeling is broken down into four steps looking at how the structure bears the load, how the distributed load is sensed, how the mechanical signal is transduced, and then how the plant responds through growth. Throughout, two examples of adaptive responses are used to illustrate this approach: the thigmorphogenetic syndrome of plant shoots bending and the mechanosensitive control of shoot apical meristem (SAM) morphogenesis. Overall this should provide a generic understanding of systems mechanobiology at work.

Keywords: mechanobiology, biomechanics, thigmomorphogenesis, wind, turgor pressure, curvature, mechanotransduction, stress

INTRODUCTION

Land plants continuously encounter mechanical challenges from without and within. External mechanical loads are imposed by the wind, rain, neighboring plants or solid substrates. The external bending loads imposed by winds induce a syndrome of mechanosensitive growth responses in the aerial stems of plants known as thigmomorphogenesis. The activity of their meristems is modulated to stunt vertical growth and stimulate an increase in girth, thereby making the plant more wind-resistant (see Telewski, 2006; Coutand, 2010; Monshausen and Haswell, 2013 for reviews). Internal loads may be imposed by the plant's own weight, inertial forces and the large hydrostatic turgor pressure in cells. Even meristems, although protected from many external mechanical loads by young leaves in the shoot apical bud or by the bark in the lateral cambium, are under considerable direct mechanical stress due to the inner turgor pressure and the mechanical barriers imposed by neighboring organs or tissues (e.g., Couturier et al., 2012; Baskin and Jensen, 2013). Therefore, precise mechanosensitive control of the magnitude and direction of growth is required so that the size, shape, and edges of the growing organs and tissues are produced in a regular and stable way (Hamant, 2013). It follows that acclimation responses of growth and morphogenesis have been naturally selected to reduce the risk of breakage or explosion of plant parts during growth and development.

These two adaptive responses, stem thigmomorphogenesis and meristem growth, ultimately rely on mechanosensing of the internal mechanical state of the living cells of the plant as a cue for the regulation of growth and morphogenesis (Coutand, 2010; Moulia et al., 2011; Hamant, 2013; Monshausen and Haswell, 2013). Mechanosensing occurs at the cell level, yet mechanical stimulation involves loads that act on the whole organ, either at its boundaries (e.g., for wind-drag) or across its full volume (e.g., weight, inertial forces or turgor pressure). Therefore, changes in the mechanical state of tissues and cells that trigger cell mechanosensing depend on the load, on the mechanical structure of the organ, and on the mechanosensitive structure.

The mechanosensitive structure is defined as the location and amount of mechanosensitive tissues involved in a response. Some mechanosensed modulations of growth and morphogenesis are triggered through long-distance internal signaling so the connection between the mechanosensitive structure and the responding structure also needs to be borne in mind (Coutand, 2010; Moulia et al., 2011).

Analyzing and modeling the biology of mechanosensing and of mechanosensitive growth responses thus involves three phases (Moulia et al., 2011). (i) Biomechanical analysis reveals how mechanical loads are distributed over the constitutive plant tissues and cells. (ii) The local mechanosensitive pathways are analyzed in the sensing cells. (iii) Mechanobiological integration combines the models describing how the plant's local mechanosensing relates to global growth responses. Other comprehensive reviews have focused on the local analysis of the mechanosensitive pathway or on the global responses of growth and morphogenesis (e.g., Braam, 2005; Telewski, 2006; Coutand, 2010; Monshausen and Haswell, 2013 to cite just a few). Our purpose instead is to review the integrative aspects, tracing them down the scale from the effect of the load on the plant to the effects on tissue elements and cells, and then up the scale from mechanosensitive gene expression to the growth and morphogenetic responses of the organ. Two mechanosensitive growth responses have been particularly extensively studied in the last two decades: thigmomorphogenesis of stems responding to external bending loads, and growth and morphogenesis of the shoot apical meristem (SAM). In particular, we aim to illustrate how integrative models combining structural mechanics with mechanosensory biology have been instrumental in understanding how mechanical loads are distributed within the plant, defining the heterogeneous stress and strain fields. We explain how the models become key experimental tools to qualitatively and quantitatively assess hypotheses about sensory mechanisms (e.g., does sensing occur through stretch-activated channels or wall-associated transmembrane proteins? Is strain sensed or is stress sensed or both?) or the influence of organ geometry and tissue distribution on the magnitude of mechanosensitive responses. This review is designed for a general biologist audience and aims to help biologists master the mechanical models they need for mechanobiological studies. There is no need for an advanced background in mechanics, mathematics or modeling as the crucial equations are introduced both verbally and graphically. The list of the models and of their acronyms can be found in **Table 1**.

Table 1 | List of models with their acronyms and references.

Acronym of the model	Full name	References
CBmS	Composite beam model of the Stem (in flexion)	Moulia and Fournier, 1997; Gibson et al., 1988; Coutand and Moulia, 2000
PVm	Pressurized vessel model of the SAM	Hamant et al., 2008; Traas and Hamant, 2009
FEm	Finite elements model of two patches of the L1 + L2 tissues	Hamant et al., 2008
2D SFm	Two-dimensional cellular stress feedback model	Hamant et al., 2008
S^3m	Sum of strain-sensing model	Coutand and Moulia, 2000; Coutand et al., 2009; Moulia et al., 2011
SAM SFm	Integrative SAM stress feedback model ()	Hamant et al., 2008
GSFm	Growth-strain feedback model	see replies to Hamant et al., 2008 by Schopfer and Meyerowitz in Science e-letters

MECHANICAL CHARACTERISTICS OF LOADS AND THEIR HETEROGENEOUS DISTRIBUTION WITHIN THE PLANT

Some central concepts are introduced briefly here that are essential when taking a mechanical view of plant structure. More complete primers in plant mechanics, including lists of definitions, are available (Boudaoud, 2010; Moulia et al., 2011; Moulia, 2013).

CRUCIAL MECHANICAL CONCEPTS

Mechanical loads may involve the action of localized forces (e.g., intermittent contact with a neighboring stone or organ) or distributed loads (e.g., external drag by wind flow, self-weight or the internal turgor pressure of the living cells). Some loads are static or quasi-static (their rate of change is slow), whereas others are dynamic so inertial forces due to the acceleration of mass need to be considered (e.g., wind-induced oscillations) (Rodriguez et al., 2008; Pivato et al., 2014).

Under the action of internal and/or external load(s) a solid body such as a plant organ can be globally displaced. This displacement involves a translation of the center of mass of the body and the body might rotate around the center of mass, described in terms of velocity. In addition, parts of the body may be displaced relative to one another, resulting in a change of shape, called deformation. These deformations are measured locally by strains, written as ε. Strains may be linear or shear (angular) and are measured in relative units (i.e., strains are dimensionless). Straining stretches bonds and causes slide/shear of internal elements, thereby allowing internal reaction forces to build up. In this way the mechanical load is distributed through the material with the storage of elastic strain energy across the deformed body until an internal and external mechanical equilibrium is achieved, i.e., all the forces and moments acting on the body are balanced. The density of the resulting internal forces, i.e., the internal forces per unit of area, is called stress, written as σ and measured in Pascal (Pa) which is equivalent to $N.m^{-2}$. Strains and stresses can be very heterogeneous across the body. Deformation is characterized by the strain and stress fields, i.e., the amount of strain and stress at every location of the body at a given time. The

strain and stress fields in a given load situation therefore, measure the mechanical state of a body like a cell, an organ or a plant.

The amount of stress produced by straining is linked to the rheological properties of the material. Rheology can be modeled in a so-called constitutive equation. If the stress increases linearly with increasing strain and linearly reverts during unloading, the material behaves as a linear elastic material. The slope of the stress-strain curve is called the Young's modulus, such that a stiff, rigid material has a high Young's modulus. Over a certain threshold, some materials may yield plastically (irreversibly). From this point, in pure plastic materials, stress does not increase further with strain, but in visco-plastic materials it varies depending on the strain rate. The growing cell wall has a visco-plastic rheology (called the Bingham flow model, see Dumais, 2013 for more details). Finally, when internal forces overcome the strength of the material, fracture occurs.

POSING THE PROBLEM: EXPERIMENTAL SETUPS

Thigmomorphogenetic experiments are generally conducted in the lab by subjecting single plant stems to static bending. Typically a stem is bent by moving the top of the stem laterally while the base is anchored immobile in the soil (Telewski and Pruyn, 1998). Alternatively, the stem is first clamped in a vertical position with the roots bathed in a liquid medium, then the basal part of the stem is displaced (**Figure 1**). The latter setup decouples the effects of stem bending from tilting the apical growth zone (Coutand et al., 2000). Dynamic loading can also be imposed by vibrating the plant, for example (Der Loughian et al., 2014).

For most SAM experiments, the meristem is cut from the stem and the surrounding young leaves are removed (**Figure 2**). The isolated SAM is then cultured on a growth medium. Three types of mechanical perturbations have been used on excised SAM. The osmotic potential of the bathing solution can be changed to transiently manipulate the inner turgor pressure of the cells (Peaucelle et al., 2011). External loads, such as lateral compression of the whole meristem, can be applied mechanically (Hamant et al., 2008). Alternatively, outer cells can be ablated to create holes, thereby modifying the mechanical structure and state of the SAM (Hamant et al., 2008). To our knowledge, the mechanical states of intact SAM have not been studied so far.

In both experimental systems, the next step is to estimate the amount and spatial distribution of the changes in mechanical state (stress and strains). This can be done as (i) the external mechanical load and the mechanical structure of the organ are known, and (ii) the changes imposed by the experimenter or by the environmental conditions are measured. However, to estimate changes that occur at very different scales, we need to consider how a change in a unit of the cell wall or tissue affects the whole organ (and vice versa). For this, a mechanical model needs to be developed, using a scientific method originating from mechanical engineering called integrative structural mechanics (ISM) modeling. More complete coverage of ISM modeling can be found in Moulia et al. (2011).

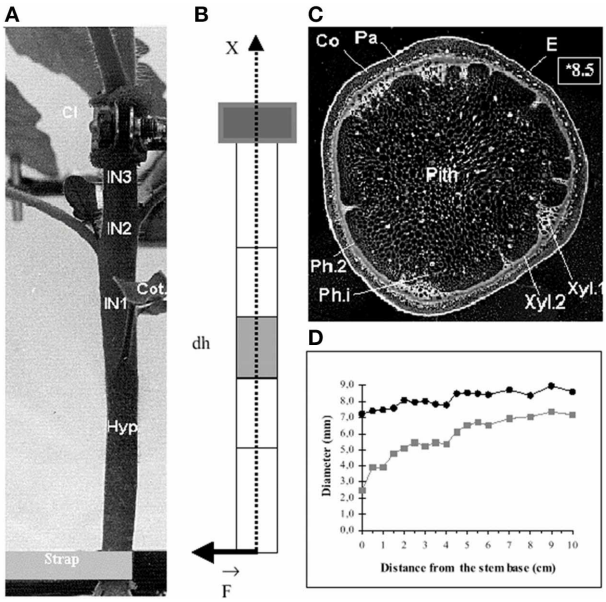

FIGURE 1 | Morphological and anatomical structure of a stem submitted to an external bending load from Coutand and Moulia (2000), Journal of Experimental Botany, by permission of the Society for Experimental Biology. (A) Side view of the basal part of the stem base before the application of bending. The stem is grown in hydroponics, and clamped below the primary growth zone, so that bending does not affect its position (Cl, metal clamp; IN 1–3, internodes; Hyp, hypocotyl; Cot, cotyledons. **(B)** Idealized geometrical scheme **(A)** as a cantilever beam. **(C)** Negative photograph of a cross-section (note the quasi-circular shape and the concentric layers of tissues (E, epidermis; Co, collenchyma; Pa, parenchyma; Ph.2, metaphloem; Ca, cambium; Xyl.2, metaxylem; Xyl.1, protoxylem; Ph.i, internal phloem). **(D)** Changes in the external diameter (•) and of the diameter of the pith (■) along the basal part of the stem.

INTEGRATIVE MODELS IN MECHANICS

The general structure of an ISM model is shown in **Figure 3**, using schematic graphical conventions that will be used throughout this review. The major aspects of the models can be understood independently of the detailed model equations. First, the constitutive materials of the structure, the elementary "bricks" or units, are defined and the rheological properties of these elements specified. Do they behave elastic or do they undergo viscoplastic deformations? Are they isotropic, displaying the same properties in all directions? If they are anisotropic, in which direction is the anisotropy? (Coutand and Moulia, 2000; Hamant et al., 2008; Baskin and Jensen, 2013). It is very important to know the shape of these elements at rest (without a load) and whether the shape is dependent on other physical variables such as temperature, water status or time (e.g., Moulia, 2000; Hamant et al., 2008). The size of these elements is not prescribed as the mechanical structure of plants is multiscale and the scale at which to work is mostly a matter of informed choice (Boudaoud, 2010; Niklas and Spatz, 2012; Gibson, 2013). Next, the structure is defined by specifying how the elements are assembled (topology) and displayed geometrically. Note that to model heterogeneous organs, several materials may need to be considered (e.g., Moulia and Fournier, 1997; Coutand and Moulia, 2000; Routier-Kierzkowska et al.,

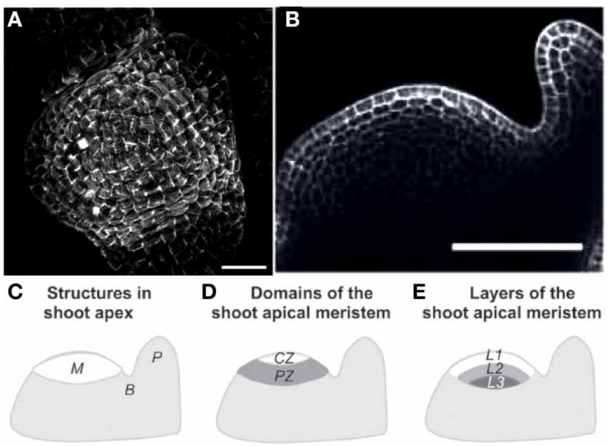

FIGURE 2 | Structure of the shoot apical meristem (SAM). (A) View of an *Arabidopsis thaliana* SAM from above Hamant et al. (2008), reprinted with permission from AAAS. **(B)** Side view of a tomato SAM (Robinson et al., 2013). **(C–E)** Generalized schematic representations of a typical dome-shaped shoot apex bearing a cylindrical young primordium. **(C)** Major structures. M, shoot apical meristem; P, organ primordium; B, boundary between the meristem and the primordium. **(D)** Morphological domains of the SAM. CZ, central zone, PZ, peripheral zone where new organs are generated. **(E)** Internal organization of the SAM. L1, presumed epidermis, L1 and L2, tunica layers, L3, corpus from Robinson et al. (2013), Journal of Experimental Botany, by permission of the Society for Experimental Biology.

2012). Finally, the mechanical loading applied to the structure is defined, as well as including any boundary conditions, which are displacement or force constraints at the boundaries of the structure.

With these three steps the model is now fully defined. When input values are known like the load applied or the structural change (e.g., making a hole in the structure), the state of the structure in the loaded state can be computed because mechanical laws specify(i) the conditions for equilibrium (static or dynamic), and (ii) the compatibility of strains between adjacent material elements or boundaries. Depending on the structure's geometry, some simplifying hypotheses can be used for calculations, e.g., beam or shell theories. In some cases the problem can even be solved analytically (e.g., Hamant et al., 2008). Mostly, however, numerical methods are required for computations. The outputs of such models can be multiple: knowledge of strain and stress fields, the velocity of the top of a plant, or bending rigidity, etc.

Plants are open systems. If cells grow or differentiate the amount and/or rheology of constitutive materials may change (e.g., cell wall maturation) and will need to be accounted for in a model. This has important implications in formulating the mechanical problems that are specific to biomechanical models (Moulia and Fournier, 2009). For example, for the tree gravitropic reaction, the problem can be solved by using beam theory hypotheses but requires an incremental formulation of the problem (e.g., Fournier et al., 1994; Fourcaud et al., 2008; Coutand et al., 2011) to take into account the growth and shrinkage of the cell wall rest-length during wood maturation (Coutand et al., 2011; Pot et al., 2014).

LOAD DISTRIBUTION FROM THE PLANT TO MECHANOSENSITIVE CELLS

Two examples of analyzing load distribution from the scale of the whole plant down to the scale of mechanosensitive cells will be presented.

COMPOSITE BEAM MODEL OF THE STEM SUBJECTED TO BENDING

The dicot stem is composed of several tissues of very variable stiffness, e.g., epidermis, parenchyma, sclerenchyma, and wood. Growth activity is concentrated in (i) the primary growth zone just below the SAM and (ii) the cambial zone, a thin shell of 1–20 layers of meristematic cells near the lateral surface of the stem, just beneath the bark. The primary growth zone is responsible for longitudinal growth, and the cambial zone for most radial expansion.

As the stem is generally a slender structure (the diameter:length ratio is less than 1/20) (see **Figure 1**) and its constitutive tissues are in transverse layers, the mechanical analysis can be simplified using the theory of heterogeneous composite beams or rods (Gibson et al., 1988; Moulia and Fournier, 1997), reframed in a mechanobiological context (Coutand and Moulia, 2000), and called the the Composite Beam model of the Stem (CBmS) in the following.

This mechanical modeling is detailed step by step in **Figure 4**. Only longitudinal strains and stresses will be considered, noted by the subscript LL, as transverse shearing can be neglected when analyzing slender structures, which exhibit pure bending. The material element in the CBmS is a small volume of tissue. Two types of tissues, broadly organized into three concentric rings, were defined. Tissues such as parenchyma or phloem were treated as compliant materials, and tissues like wood as stiff materials. These elements are assumed to behave in the linear elastic range as has been confirmed experimentally (Coutand et al., 2000). These tissue elements are then assembled into infinitesimal slices of dS thickness according to the known anatomy of the stems. Finally, the stem can be viewed as a pile of infinitesimal slices, glued one next to another along an imaginary line inside the stem, called the neutral line.

During bending experiments one end of the stem is fixed and one end is free to move. The stem therefore, operates mechanically as a cantilever subjected to a local force $\vec{F}$ transverse to the stem. The action of $\vec{F}$ depends on the amount of the force F and on the lever arm L, i.e., the distance from the application point of the force to a given slice. This mechanical amplification effect can be modeled using a quantity called the bending moment $\widehat{M}$, the magnitude of which is M = F.L (Equation 1).

A central property of beam bending is that each cross section remains flat and orthogonal to the neutral line all along the deformed beam. A change in $\widehat{M}$ will thus induce a relative rotation (through an angle $d\theta$) of two successive stem slice cross-sections. The effect of the rotation is an increment of length dl on the tensed side and a decrement of dl on the compressed side. The ratio $C = \frac{d\theta}{dS}$ (Equation 2) is called the curvature. It measures the spatial density (rate) of bending rotation and $\varepsilon_{LL} = \frac{dl}{dS}$ (Equation 3) measures the longitudinal strain. The strain at any point located at a distance y from the cross-section center can

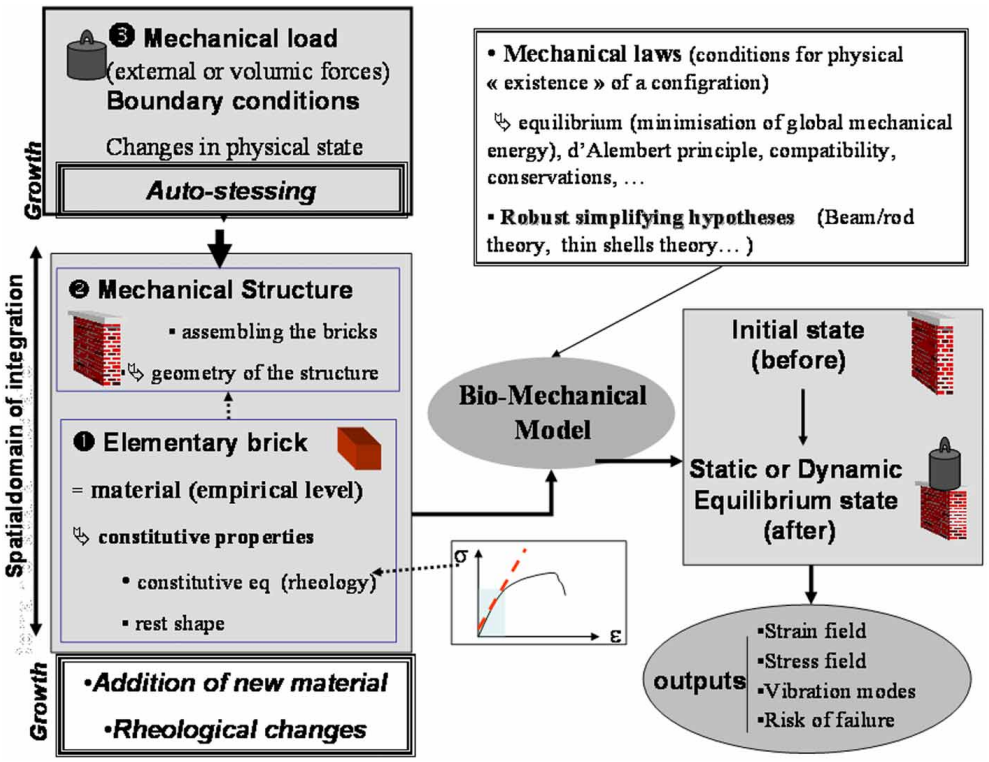

FIGURE 3 | Structure of an integrative structural mechanics (ISM) model from Moulia et al. (2011), by permission of Springer-Verlag Berlin Heidelberg. The structure of an ISM model for use in plant biomechanics. ISM models consider (at least) two scales in the system: a scale of phenomenological empiricism called the material scale, and a scale of mechanistic spatial integration, the mechanical structure. The internal and boundary loads (inputs) result in a change in mechanical state that can be calculated using mechanical principles and robust simplifying theories. ISM models can produce various outputs characterizing mechanical state or dynamics, such as strain (ε) and stress (σ) fields, vibration modes, or rupture risk factors.

be computed as the product of the change in curvature and the distance y to the central line of the stem, $\varepsilon_{LL,y} = y \cdot (C - C_0)$ (Equation 4), where C_0 is the initial stem curvature before the load (if the initial configuration of the stem is straight). The value of the longitudinal strain thus varies with the position along the beam, being maximal at the beam periphery ($y = R$) along a radius aligned with $\vec{F}$.

Straining allows internal reaction forces to build up to balance the effect of the external load. For elastic constitutive materials, the stress is calculated as the strain multiplied by the appropriate Young's modulus: $\sigma_{LL,x,y,i} = \varepsilon_{LL,x,y} E_{LL,i}$ (Equation 5) where $E_{LL,i}$ is the longitudinal elastic modulus of the ith material and x, y are the spatial coordinates within the cross section.

The amount and distribution of stresses and strains can then be calculated so that they balance out $\widehat{M}$ (as detailed in supplemental data). This yields $\varepsilon_{LL} = y\,(C - C_0) = My/\left(E_{soft} I_1 + E_{stiff} I_2 + E_{soft} I_3\right)$ and $\sigma_{LL} = E_i \varepsilon_{LL}$, (Equation 6). E_i is the Young's modulus of the ith tissue slice. I_j measures the effect of all the internal lever arms of the resisting stresses in a given tissue and works out as $I_i = \pi \frac{R^4_{Out,i} - R^4_{in,i}}{4}$ where $R_{out,i}$ and $R_{in,i}$ are the outer and inner radii of the jth annulus of tissue. These formula specify the consequences of loading (F), stem geometry and anatomy (L, I_j), and material stiffness (E_i) on the stress and strain fields. Note that if strains increase linearly from the center to the periphery, stress may be distributed non-continuously. Another striking property of beam bending apparent in the previous equation is that changes in cross-sectional geometry have much more effect on stresses and strains than changes in material stiffness. For example, for a given load F, doubling the elastic stiffness of all the tissues halves the longitudinal strain without changing longitudinal stress. Doubling the stem radius however (keeping the same proportion of concentric tissues) reduces both strains and stresses at the stem periphery 8-fold. This is another example of mechanical amplification by lever arms. We will see that this has profound consequences on the mechanical stability and the mechanosensitivity of a given stem. Finally, stresses and strains are highly anisotropic, with their principal component lying longitudinally along the length of the stem.

Shell model of the SAM under internal pressure load

The SAM, a group of continuously growing and dividing cells, is a dome-shaped structure (**Figure 2**) composed of two outer layers, named L1 (the outer epidermis) and L2, and an inner bulk of cells named L3. Future definite lateral organs, like leaves, sepals, or petals, are initiated as primordia, bulges at the periphery (see reviews by Kwiatkowska, 2008; Burian et al., 2013; Robinson

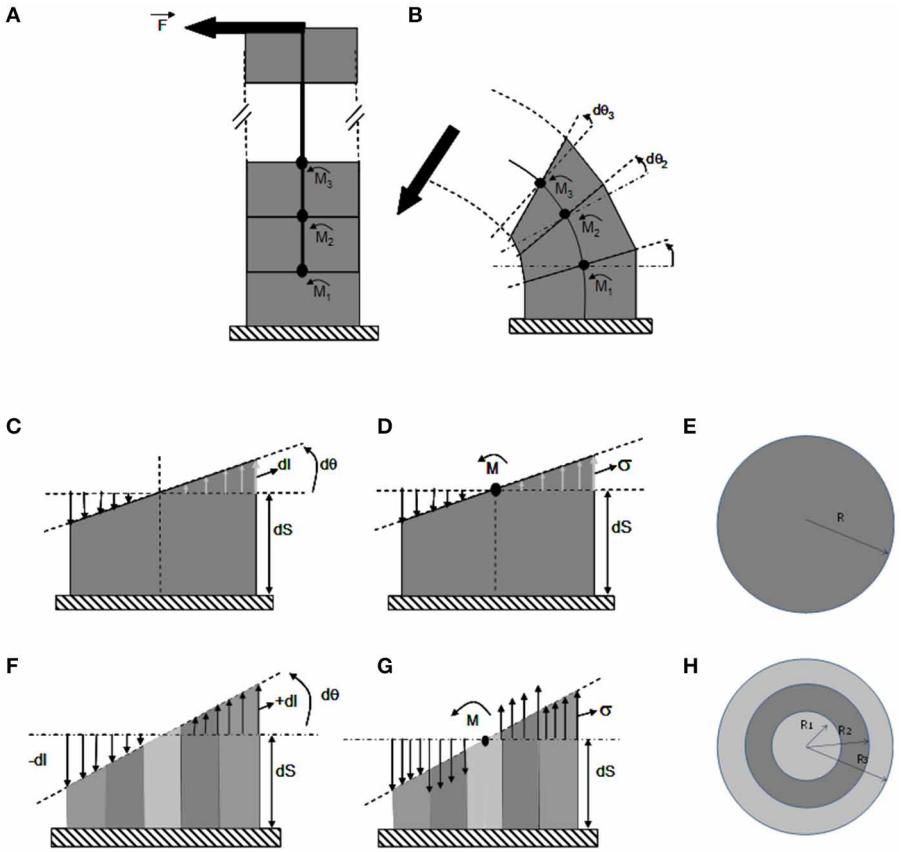

FIGURE 4 | The ISM beam model of pure bending of a stem. ISM model used to analyze stem bending experiments, using the theory of composite heterogeneous beams in a cantilever setting. **(A)** Unloaded beam. The beam is composed of a pile of (virtual) slices of infinitesimal thickness delimited by (virtual) successive cross-sections, along a central line. **(B)** Loaded beam. Under bending moment $\widehat{M}(\zeta)$, the beam curves. Each cross-section rotates by a small angle $d\theta(\zeta)$, with ζ being the position along the stem and x, y the coordinates within the current cross-section of the stem. **(C–E)** Detailed side **(C,D)** and top **(E)** views of a bent slice in a homogeneous stem. **(F–H)** Detailed side **(F,G)** and top **(H)** views of a bent slice in a heterogeneous stem made of one stiff (dark gray) and two compliant (light gray) concentric annuli of tissues. **(C,F)** Strain distribution across the cross-section. Note that the cross-section remains flat during the bending and only rotates respective to the previous cross-section at the bottom of the slice by an angle $d\theta$, irrespective of the anatomy of the stem. The spatial rate of change in angle of the successive cross-sections is the stem curvature $C = \frac{d\theta}{dS}$. Accordingly, the stem is elongated on the convex side by $dl(x, y) > 0$ and shortened on the concave side by $dl_{(x,y)} < 0$, with no change on the central (neutral) line. The longitudinal strain $\varepsilon_{LL} = \frac{dl}{dS}$ is thus maximal at the periphery on the sides of the slice that face downwards and away from the orientation of the bending force. The heterogeneous anatomy of the stem has no effect on the relative distribution of strain across the cross-section, which remains linear and is given by $\varepsilon_{LL,y} = y \cdot (C - C_0)$. Straining allows for internal reaction forces, which density is measured by stresses, to build up balancing the effect of the external load. Therefore, the amount of change in stem curvature (and hence the global amount of straining) only depends on the amount of external bending moment and on the overall bending stiffness of the stem. **(E,F)** Stress distribution in the cross-section. For elastic constituents, the stress is equal to the strain multiplied by the Young's modulus: $\sigma_{LL,x,y,i} = \varepsilon_{LL,x,y} E_{LL,i}$ where $E_{LL,i}$ is the longitudinal elastic modulus of material i. In homogeneous stems stresses parallel strains. However, on a stem with a heterogeneous anatomy **(F)** the stresses also depend on the local stiffness of the tissue and they de-correlated with strains across the cross-section (with maximal stresses possibly occurring inside the stem).

et al., 2013). Between the primordium and the apical dome, a saddle-shaped boundary forms which later becomes a sharp crease that separates the growing primordium from the SAM. The thin-walled fully turgid cells in the SAM are under considerable mechanical load from turgor pressure and cell-to-cell mechanical interactions known as "tissue tensions."

The mechanical analysis of the meristematic dome has been performed by Hamant et al. (2008) and Traas and Hamant (2009), first giving rise to the Pressurized Vessel model (PVm). The meristematic zone is modeled as a vessel according to thin-shell theory. The vessel "wall" corresponds to the outer wall of the L1 layer, which is thicker than the other walls and likely to bear much of the load due to the turgor pressure of inner cells. The modeled vessel wall is built of thin shell elements of infinitesimal dimensions ds and dr and of thickness t. Their material properties are considered to be homogeneous across the SAM (for discussion see Baluska et al., 2003). Hamant et al. (2008) proposed that the elements should be linear elastic, but this is not necessary as the material could equally well be viscoelastic. The only restriction is that the material element should not show pure plastic properties as this would induce loss of rheological homogeneity during loading. These shell elements are smoothly assembled (i.e., essentially they are virtually "glued" together along their sides) into a typical SAM structure, modeled geometrically by

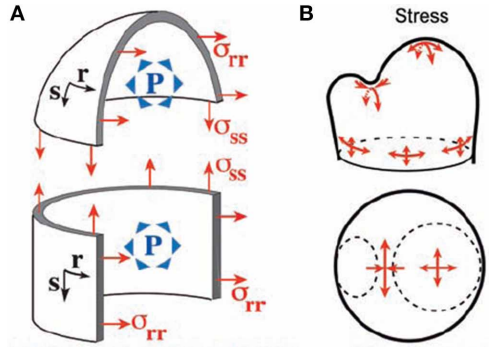

FIGURE 5 | The thin-walled pressurized vessel model of the shoot apical meristem. Integrative structural mechanics (ISM) model used to analyze the loading of the SAM by internal turgor pressure, using very thin shell theory (Hamant et al., 2008), reprinted with permission from AAAS. **(A)** The SAM modeled as a pressurized vessel. Each point has a coordinate in the orthoradial (*r*) and meridional (*s*) direction and P is pressure. **(B)** At the top of the apical dome, represented as a spherical dome, the stress is isotropic. If the flanks of the meristem are represented as a cylinder, the stress is greater in the circumferential (orthoradial) direction than along the meridian and strongly anisotropic stresses occurrs on the flanks of the meristem. Maximal stress anisotropy occurs at the saddle-shaped boundary between the primordium and the central dome.

combining three simple adjoining structures (**Figure 5**). (i) The apical dome is represented as a spherical dome of radius R. (ii) The flanks of the meristem are represented by a cylinder of radius R. (iii) Where relevant an incipient primordium is represented by a smaller lateral dome. Each point of the vessel "wall" is characterized by its coordinates in orthoradial (r) and meridional (s) directions (**Figure 5A**). The difference between a beam slice and a shell element is that each shell element can display curvatures in two directions (i.e., C_{rr} along an orthoradial line, C_{ss} along a meridian) and may also display a twist (C_{rs}). Note that in the central or primordial domes, C_{ss} and C_{rr} have the same sign, the concave surface faces into the meristem and $C_{rs} = 0$), whereas in the boundary, C_{ss} and C_{rr} have opposite signs. Importantly, this geometry is assumed to be under static equilibrium, so that the model only aims at calculating the stresses required to achieve this static equilibrium in the specified geometrical configuration and strains are unknown. The load is considered to be a uniform and constant inner pressure P. The effect of this internal load in the model can be described verbally as follows. Each shell element builds up stresses in three directions, and its stress state is thus represented by a stress tensor (σ_{ss}, σ_{rr}, σ_{rs}), with σ_{ss} and σ_{rr} being tensions in the meridional and orthoradial directions, and σ_{rs} is a shear stress within the vessel wall (a kind of internal friction stress). The values of each stress component can be fully estimated using the conditions of static equilibrium, and depends on the curvatures in each zone of the SAM. This was solved analytically at specific points of local symmetry.

In the central dome, equilibrium yields $\sigma_{ss} = \sigma_{rr} = \frac{PR}{2}$, $\sigma_{rs} = 0$ (Equation 7). The tensile stresses are isotropic as they have same value in the s and r directions. In the flanks of the meristem cylinder, $\sigma_{rr} = PR$, $\sigma_{ss} = \frac{PR}{2}$ (Equation 8), so the stress is highly anisotropic, being twice as high in the circumferential direction as in the longitudinal direction.

In the saddle-shaped boundary between the apex and a primordium, one may assume that the orthoradial curvature is approximately the curvature of the dome $Crr \approx \frac{1}{R}$ whereas the meridional curvature C_{ss} is much higher (in absolute terms). The stresses matching static equilibrium are therefore: $\sigma_{ss} \approx \frac{P}{2C_{ss}}$, $\sigma_{rr} \approx \frac{P}{2C_{rr}} \approx \frac{PR}{2}$, $|\sigma_{rr}| \succ\succ |\sigma_{ss}|$ (Equation 9). The outer wall of the SAM is under tension across the crease, but in compression along the crease. The amount of the stress depends on P and on one of the two curvatures C_{rr} and C_{ss}, with higher curvature inducing lower stresses for a given P. The absolute amount of stress is much higher across the crease, and the stress distribution is highly anisotropic.

This model of the SAM as a thin-walled pressurized vessel was very instructive. However, it did not provide detailed insights into how stress is distributed in the cell walls of a given SAM zone. It was therefore, complemented by a second "zoom-in" model at the scale of a small patch of tissue in the L1 and L2 layers (**Figure 6**). This model is a Finite Elements model (FEm) of two patches of the L1 + L2 tissues, one in the primordium-boundary zone and one at the top of the dome. Detailed specification of the geometry of the cell walls of this patch was achieved by experimental measurements. Elements were meshed piecewise to form plates of finite size. Just as for the PVm, the material was assumed to be homogeneous, but also linear elastic (with no plastic deformation or growth) and the load resulted from a uniform internal pressure putting the L1 layer into a curved configuration. No internal pressure within the cells of the L1 and L2 layers was considered as the effect of uniform pressure among the neighboring cells cancels out within a cell layer. The boundaries of the patch were given the proper saddle shape of the primordial boundary or the hemispherical shape of the dome. The mechanical equilibrium state was then computed numerically. This was done both for the intact patch, and for a patch in which one or two cells were ablated (i.e., their outer walls were deleted from the model). Making one hole in the patch redirects the orientation of the main stresses to surround the hole, and increases the magnitude of these stresses. When holes are made in two adjacent elements, highly anisotropic stresses are induced between the two holes, even if they are positioned at the tip of the dome where stresses are normally isotropic. Note that as the elastic rheology of the cell wall was specified, the FEm could be used to estimate not only the stress distribution within the cell walls, but also the elastic strains of the walls (this was not possible using the PVm).

MECHANOSENSING AND MECHANOTRANSDUCTION

Now that we have tracked the distribution of stresses and strains within the two types of organs and the two types of loads, we can study how the cells sense their local mechanical state. Models can be helpful tools at this stage too to define quantitative behaviors and to deduce which variable is sensed.

STRAIN-SENSING OR STRESS-SENSING? DOES IT MATTER?

Mechanobiologists have paid relatively little attention to the issue of whether plant cells sense stress or strain, implicitly assuming that mechanical "stress" is the variable of interest perhaps due

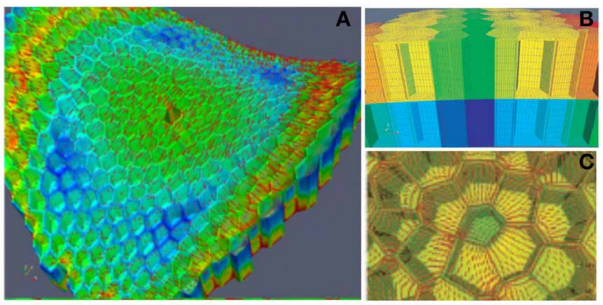

FIGURE 6 | Finite elements model (FEm) of a patch of the L1 + L2 layer of the SAM. ISM model for the numerical mechanical analysis of a small patch of the SAM with full cellular resolution. The example here displays the model (and the numerical simulation of its stress-field output) of a patch at the boundary between the primordium and the central dome, with the ablation of one L1 cell from Hamant et al. (2008), reprinted with permission from AAAS. **(A)** General view of the FEm of the patch in the primordium boundary zone from above indicating the simulated pattern of principal stress directions (red lines) on the outer surface of meristem tissue. Colors indicate relative values of stress (blue, low; green, medium; red, high). **(B)** Side view of the outermost cell layers L1 and L2. **(C)** Detail of the stress pattern around one hole due to cell ablation.

to semantic confusion with physiological "stress" (Moulia et al., 2011). However, it is important to remember that stresses and strains do not parallel in heterogeneous constitutive materials (e.g., stems) or in materials behaving in the plastic range (e.g., during growth). Thus, a strain-sensing mechanism would not give the same output as a stress-sensing mechanism. Recently a "stress-sensing vs. strain-sensing controversy" has been stirred up [see replies to Hamant et al. (2008) by Schopfer and Meyerowitz in science e-letters, and (Moulia et al., 2011) and (Hamant, 2013)]. Addressing this issue requires a further step in the modeling.

FROM CELLULAR MECHANISMS TO QUANTITATIVE LOCAL MECHANOSENSING

Local mechanosensing of external loads: the "strain-sensing model"

Among the mechanisms involved in mechanosensing, mechanosensitive ionic channels, often known as stretch-activated channels (SAC) have been the subject of detailed quantitative studies using the patch-voltage-pressure-clamp technique on protoplasts, cells enzymatically stripped of their walls (e.g., Ding and Pickard, 1993; Haswell et al., 2008). Altering the turgor pressure induces strains and tensional stresses in the plasma membrane and in the channel. The ionic current passing through the channels can be monitored after clamping the voltage, thus quantifying their mechanosensitive responses. The general shape of these response curves is sigmoidal, and can easily be linearized in the range of small strains (**Figure 7A**). Based on these results, we assumed that the local mechanosensitive function of a tissue element can be approximated through a linear function over a threshold (Coutand and Moulia, 2000; Moulia et al., 2011):

$$dS_i = k_s \cdot (\varepsilon - \varepsilon_0)\,.dV \;\text{ if }\; \varepsilon > \varepsilon_0, \text{ else } \mathrm{dS}_i = 0 \qquad (10)$$

where dS_i is the local signal in the cell (in **Figure 7A**, $\mathrm{dS}_i = \mathrm{dI}$, where I is the ionic current), k_s is a mechanosensitivity factor ($k_s = 0$ defines an insensitive tissue, while higher k_s values equate to greater sensitivity), ε is the local mechanical strain of the tissue element, ε_0 is a possible strain threshold or minimal effective strain ($\varepsilon_0 \geq 0$) (see Moulia et al., 2006 for a review), and dV is the volume of the tissue element.

Equation (10) assumes that only tensile strains are sensed ($\varepsilon > \varepsilon_0 \geq 0$), but it can be extended straightforwardly to the case where both tensile and compressive strains are sensed in proportion to their absolute value, as is observed in animal bone tissues (Schriefer et al., 2005).

Equation (10) was assessed experimentally in *Populus tremula* × *alba* (*Pta*) (Coutand et al., 2009) by measuring the expression of the primary mechanosensitive gene *ZFP2*. *ZFP2* codes for a zinc finger protein that is transiently over-expressed as early as 5 min after straining in the strained tissues, probably in a cell-autonomous manner (Leblanc-Fournier et al., 2008; Martin et al., 2009, 2010) The response of the cell mechanotransduction pathway—from the initial reaction in the cytoplasm to primary gene expression in the nucleus—could thus be assessed by measuring Q_r, the relative abundance of *ZFP2* transcripts in small slices of the stem using quantitative real-time PCR (Coutand et al., 2009). The bending stresses and strains are highly heterogeneous across a stem element. An integrative model was thus necessary to express the prediction of Equation (10) at the level of a stem segment and to assess it experimentally. Combining Equation (10) with the strain field equation in bending (Equation 4), it was possible to derive

$$Q_{rorgan} = \frac{k_s.k_{ds}}{C_0} \cdot \bar{\varepsilon} - \left(\frac{k_s.k_{ds}}{C_0} \cdot \bar{\varepsilon}_0 - 1\right) = k_r \cdot \bar{\varepsilon} - (k_r \cdot \bar{\varepsilon}_0 - 1) \qquad (11)$$

where Q_r is the ratio between the abundances of *Pta ZFP2* transcripts in the strained tissue elements and those in the unstrained control), k_{ds} is the sensitivity of the pathway downstream of the primary sensory reaction, C_0 is the baseline transcript concentration in the unstrained control, $\mathrm{k}_r = \mathrm{k}_s\,\mathrm{k}_{ds} / \mathrm{C}_0$ is the apparent sensitivity of relative gene expression, and $\bar{\varepsilon}$ is the volume-averaged tensile strain (see Moulia et al., 2011 for details).

Our local mechanosensing model (Equation 11) thus predicts a linear increase in the relative expression of *ZFP2* with an increase in the mean strain $\bar{\varepsilon}$, a prediction that can be tested experimentally. Indeed, the experimental relationship between measured Q_r and volume-averaged strain $\bar{\varepsilon}$ was found to be linear (**Figure 7B**), with Equation (11) explaining 77% of the 1:500 variation in Q_r. This validates the hypothetical strain-sensing model stated in Equation (10) and gives the first *in planta* measurement of the mechanosensitivity of the mechanotransduction pathway. Under the conditions of this experiment, a 1% strain induces a transient 200-fold increment in transcription of *Pta-ZFP2*. It was surprising that the strain range in which this linear mechanosensing model holds true goes up to at least 5%, i.e., well beyond the range of elastic strains in cell walls. Cell internal components are likely to undergo a much larger range of elastic deformation than the cell wall alone, explaining the proportional sensing of strain even when wall stresses eventually plateau (see Sato et al., 2005).

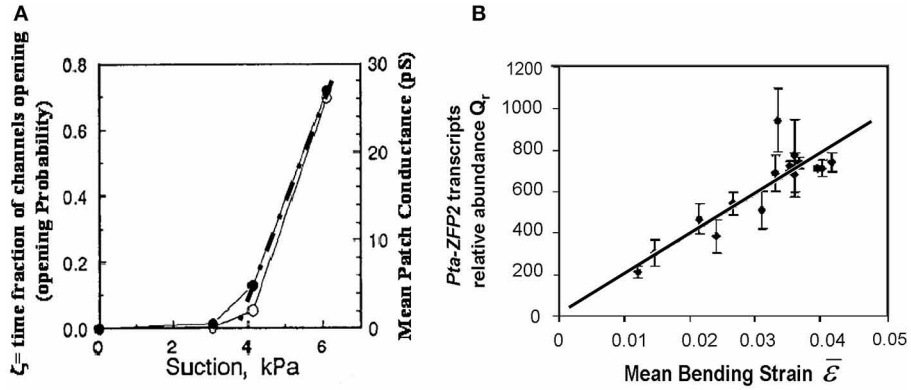

FIGURE 7 | Local mechanosensing of external loads. (A) Probability of mechanosensitive channel (MsC) opening and mean patch conductance as a function of patch depression (and hence membrane tension and MsC strain). Open and filled circles, two replicates. Dashed dotted line, linear fit. Modified from Ding and Pickard (1993), Copyright# 1993, The Plant Journal, John Wiley and Sons. **(B)** Relationship between the relative transcript abundance Qr of the primary mechanosensitive gene *Pta ZFP2* (measured by Q-RT-PCR) and predictions from the Strain-Sensing model through the volume-averaged strain in the bent stem segment $\bar{\varepsilon}$, (i.e., Sum of the Strain-Sensing normalized to the volume of the bent tissue; Coutand et al., 2009, Journal of Experimental Botany, by permission of the Society for Experimental Biology).

Local mechanosensing of internal loads: cellular stress-feedback model

The mechanisms underlying the responses to internal loads have been investigated much less than those involved in sensing external loads. Mechanical signals control (i) the amount and distribution of the active PIN1 auxin transporters, possibly though Ca^{2+} influx acting on PINOID proteins via TOUCH3 proteins (Heisler and Lam, 2010; Nakayama et al., 2012), and (ii) the alignments of cortical microtubules (CMT) and the orientation of cell division planes. The calculated stress pattern in the SAM outer L1 layer, and the CMT distribution determined experimentally (Hamant et al., 2008) were very similar (**Figure 8A**).

However, this observation is only correlative. A step forward was made when it was confirmed that the distribution of microtubules changed to match the redistribution of the wall stresses as predicted by the local FEm when the meristematic dome was compressed or when two holes were made in the L1 layer, (**Figures 8B,C**). However, this still did not provide a mechanistic link. A putative sensing mechanism may involve wall-associated protein complexes linking the cell wall to CMT that would then be directly subject to cell wall stresses, but there is no direct experimental evidence for this at the subcellular level (see Baluska et al., 2003; Landrein and Hamant, 2013 for discussion).

In order to assess this mechanism of microtubule alignment by wall stresses with respect to the data on SAM dynamics, a new model was needed. Microtubule reorientation takes 4–12 h, long enough for growth to occur. Thus, a model was required that included cell geometry, growth, mechanosensing of load distribution, and microtubule orientation. This model was called the Two-Dimensional Cellular Stress Feedback model (2D SFm, **Figure 9**; Supplemental Material SM2).

Mechanical structure. The material element of this model is a piece of cell wall, assumed to display linear elastic properties, i.e., its stresses are proportional to its strains. The coefficient of proportionality is the stiffness of the wall material E_w, its Young's modulus. Only one-dimensional (1D) stretching of the wall is considered. E_w is under biological control, modeled as depending on the auxin concentrations in adjoining cells on both sides of the wall (see Supplemental data), and on microtubule orientation in the same cells (θ_{c1} and θ_{c2}), according to:

$$E_w = E_{min} + E_{max}\left(\frac{\cos^2(\theta_1) + \cos^2(\theta_2)}{2}\right) \qquad (12)$$

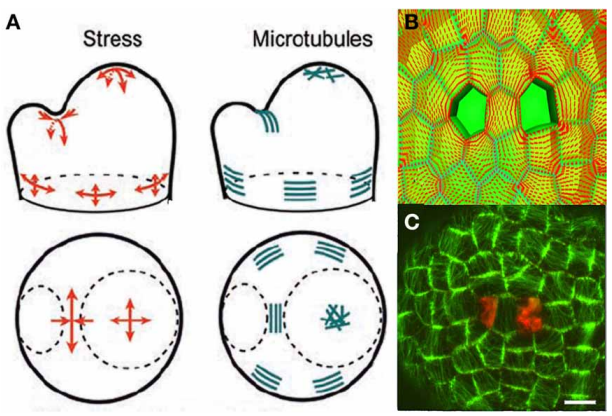

FIGURE 8 | Mechanosensing of internal loads in the SAM and microtubule re-orientation from Hamant et al. (2008), reprinted with permission from AAAS. (A) Schematic representation of stress directions and microtubule orientations in the different parts of an SAM bearing a cylindrical primordium. **(B)** Principal stress pattern at the outer surface of the meristem simulated in an FEm of a patch of SAM at the top of the dome with a two-cell ablation. The stress pattern is circumferential to each of the ablated regions and stress alignment is enhanced in the cell between the two ablated cells. **(C)** Cortical microtubule distribution in the L1 layer in the central zone after a two-cell ablation as visualized by the expression of a construct fusing the Green Fluorescent Protein and the Microtubule Binding Domain (GFP-MBD), Scalebar, 5 μm.

E_{min} is the elastic stiffness of the isotropic cell wall matrix, and $E_{max}\left(\frac{\cos^2(\theta_1)+\cos^2(\theta_2)}{2}\right)$ is a stiffening term related to the directional angle Θ of CMTs (and hence microfibrils) relative to the wall direction on both sides of the cell wall. This $\cos^2(\Theta)$ angular dependency simply specifies mathematically the idea that parallel and antiparallel orientations both lead to the maximal longitudinal stiffening, whereas perpendicular orientation leads to no stiffening.

Interphasic expansion growth of the walls of meristematic cells is modeled by increasing the resting length of walls l_{w0} at an absolute rate that is proportional to the amount of elastic strain of the wall above a yield threshold. Cell wall synthesis is assumed to follow wall extension (and cell division). The wall elements are assembled into a two-dimensional tissue model representing the cells of the L1 layer as hexagonal boxes, only considering the lateral walls of L1 cells. Each wall is considered to act as a 1D spring carrying a force F_w. The cell corners are assumed to behave like ball-joints in that there is no stiffness when the angle is changed. Finally, cell division is assumed to occur when cells reach a threshold size, and the new wall runs through the barycenter of the original cell and parallel to the direction of microtubules.

Load modeling mechanical equilibrium. Just as in the PVm, the load comes from the turgor pressure of the inner cells and is assumed to be homogeneous. This puts the L1 layer under 2D stress and the curved configuration allows local curvature to balance the inner force and the tensile reaction within the L1 wall.

Mechanosensing and feed-back mechanisms. The mechanosensitive reorientation of CMTs is modeled assuming that Θ_c, the CMT direction for a cell, is sensitive to wall stresses. The model does not address the stress distribution within the wall-associated proteins and the cytoskeleton though. It is only assumed that the mean CMT orientation somehow follows the orientation of the net force resulting from the tensions in all the side walls:

$$\theta_c = \theta_{\underset{\sum F_w}{\longrightarrow}} \tag{13}$$

This alignment response is not instantaneous but occurs at a constant rate. This is the only mechanosensitive step in the model.

The feedback mechanism then comes from the following assumptions. The current mean CMT orientation is supposed to alter the elastic stiffness of each cell wall by modifying the direction of the cellulose microfibrils in the wall and hence the anisotropy of cell wall stiffness. This modifies the amount of growth in the different cell walls and the direction in which the new cell wall is laid down when a cell divides.

The inputs of the model are the turgor pressure, the shape of the L1 cells, and possibly the distribution of auxin. It predicts the elastic stresses and strains in the walls, the expansion growth, the mean orientation of CMT, and the orientation of phragmoplasts. These outputs depend on seven parameters (E_{min}, E_{max}, plastic growth extensibility, yield strain threshold for growth, the two parameters of auxin sensitivity, and rate of mechanosensitive reorientation of CMT, see Supplemental material for more details).

An important feature of this model is that different rates of expansion originate from the applied forces (pressure and wall-wall interactions), and the dynamics of the cell wall elastic stiffness. Hence, there is no explicit relationship between maximal stress and maximal growth direction in the model. Depending on the stress patterns, the model can predict maximal growth along the maximal stress direction and perpendicular to it.

The validity of this model could not be assessed experimentally at the local level, but it was included in a model of the mechanosensitive behavior of the whole SAM (Section Whole-organ integration and experimental assessment).

WHOLE-ORGAN INTEGRATION AND EXPERIMENTAL ASSESSMENT

THE SUM OF STRAIN-SENSING MODEL, S^{3}M

Quantifying global thigmomorphogenetic responses

To properly lay out the problem of integrated mechanosensing at this point, we need to consider the global growth responses of the plant to external bending loads in more detail. This has been made possible by using a quantitatively-controlled bending device while continuously monitoring primary elongation or secondary thickening using linear voltage displacement transducers (Coutand et al., 2000). It was found that elastic bending at the base of the stem induced a thigmomorphogenetic response in the distal primary growth zone, implying that a long-range internal secondary signal $S_{i,1}$ traveled from the bent tissues to the responding primary tissues (Coutand et al., 2000; also Brenner et al., 2006). The propagation of this signal to the apex is much faster than the typical reaction time of growth responses, and there is no obvious damping over longer distances (Moulia et al., 2011). The nature of the carrier of this long-distance signal is currently being investigated. Given its velocity it could be either an electric signal in the phloem, or more likely a pressure pulse in the xylem (Lopez-Rodriguez et al., 2014; Tixier et al., 2014). In contrast, the secondary growth response seems local to the bent zone (Mattheck and Bethge, 1998; Coutand et al., 2009). For both primary and secondary growth responses, the initially growth stops for one to a few hours, then growth restarts and eventually the growth rate returns to that of unstimulated controls. For primary growth, the recovery time is highly dependent on the amount of bending strain applied, typically ranging from 100 to 1000 min. No compensatory growth is observed so at the end of the experiment bent plants are shorter than control plants (e.g., 2 mm shorter per bending stimulus in the experiment by Coutand et al., 2000). Secondary growth though shows clear and long-lasting growth stimulation after the initial inhibition, with growth rate increasing over 3 days then decreasing to the control rate over the next 3–4 days. The effect of this stimulation of secondary growth (+0.35 mm per bending stimulus) was approximately 30 times higher than the effect of the initial inhibition, resulting in an overall stimulation of radial growth. Unlike primary growth, the timing of the response was much less dependent on the amount of bending strain than on the peak (and total) increment in growth rate (Coutand et al., 2009, 2010).

Integrating local mechanotransduction into plant mechanosensing

Why do stems of different shape and structure respond differently to the same external load? We aimed to assess whether the strain-sensing hypothesis, combined with structural and geometrical effects on load distribution across the stem structure, can explain

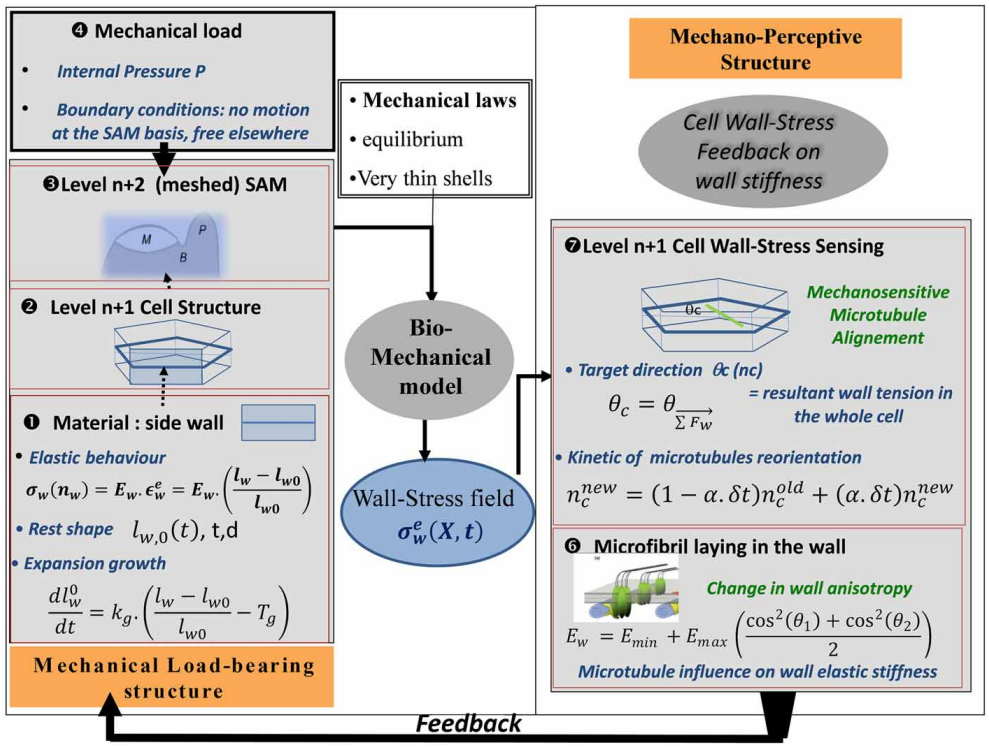

FIGURE 9 | Schematic representation of the SAM Stress Feedback model (SAM SFm). The SAM SFm (Hamant et al., 2008) incorporates an ISM biomechanical model of the mechanical load-bearing structure of the SAM, and a mechanobiological model of the responses to the mechanical state of a cell in terms of (i) cell-wall stress sensing by CMTs and (ii) the consequences on the longitudinal elastic stiffness of the cell wall due to the direction of the laying down of cellulose microfibrils with respect to the longitudinal direction of the cell wall. The elemental brick of the biomechanical model is a piece of cell wall ❶ (called the cell-wall element) which displays two rheological behaviors: (i) elastic straining and (ii) expansion growth changing the rest length $l_{w,0}$ of the element at a rate that is proportional to its elastic strain over a certain threshold. Cell wall growth is therefore analogous to visco-plastic creep. The transverse height (d) and thickness (t) of the wall element are assumed to be constant. Two levels of structure can then be assembled. At the first level, ❷ the side walls of a single hexagonal cell are assembled The model can be run at this level, giving rise to the cell-level formulation of the SFm. Otherwise the cells can be assembled to form a surface mesh with typical SAM geometry❸, in the SAM-level formulation of the SFm. The load is the turgor pressure of inner tissues considered to be fully borne by the L1 cell(s) ❹. This ISM biomechanical module outputs the (elastic) wall-stress field σ_w^e at every position X on the different cell-wall elements composing the mechanical structure, at a given time, as well as the changes in rest-lengths of all the cell-wall elements due to expansion growth. This updates the geometry of the cellular structure for the next step and the outputs are transmitted to the mechanobiological module. In the mechanobiological module of the SAM SFm, the mechanosensitive step occurs at the level of the cell ❼, as it is an intrinsic cellular process. The central hypothesis of the module is that CMTs are re-aligned to the current direction of the direction of the resulting stress θc, but this occurs at a constant pace with only some of the overall CMT population (n_{cnew}) being reoriented during each step (the rate is assumed to be independent of the mechanical state). The current mean orientations of CMTs in two cells sharing a given cell-wall (θ_1(t), θ_2(t)) determines the longitudinal elastic stiffness of the side cell wall E_w presumably through the orientation of the laying down of the new cellulose microfibrils with respect to the existing wall, changing the anisotropy of the cell wall elastic rigidity and hence its longitudinal stiffness (here assumed to be instantaneous) ❻ (note that (θ_1(t), θ_2(t)) may differ from the targeted orientations (θc_1, θc_2) specified by the stress-feedback as CMT reorientation takes time). The latter process occurs at the level of each cell-wall element so different walls of the same cell differ in the amount of elastic stiffening they undergo. The new value of wall elastic stiffness E_w is the output of the mechanosensitive module and is transferred to the mechanical module, in which the elastic stiffness is updated, immediately changing the constitutive law of the cell walls, and thus giving rise to a new mechanical equilibrium at the next step. This change in wall elastic rigidity is the way the current wall-stress state feeds back on the growth of the meristematic cells. Note that cell division may occur (not shown). A phragmoplast (new cell wall) is laid down parallel to the current CMT direction θ1 whenever the size of the stem passes a certain size threshold thereby changing the structure of the L1 cell wall "mesh."

the variability in plant responses (Coutand and Moulia, 2000; Coutand et al., 2000, 2009). For this, we set out to build a *minimal model* of mechanosensing integration, from the level of the strained tissue element up to the thigmomorphogenetic growth responses in the entire stem. This model has been called the Sum of Strain-Sensing model (S^3m). Its development involved several steps (Coutand and Moulia, 2000; Coutand et al., 2009) and it was only completely assembled a few years ago (Moulia et al., 2011). This model is designed to chart the effects on the global thigmomorphogenetic responses of both the mechanical and the mechanoperceptive structures of the organ. The model was made with the purpose of competitively assessing two possible candidate mechanisms for the mechanosensing of external loads, strain-sensing vs. stress-sensing. Building the model was analogous with the process of integrative modeling in structural mechanics as illustrated in **Figure 10** (presented in detail in the

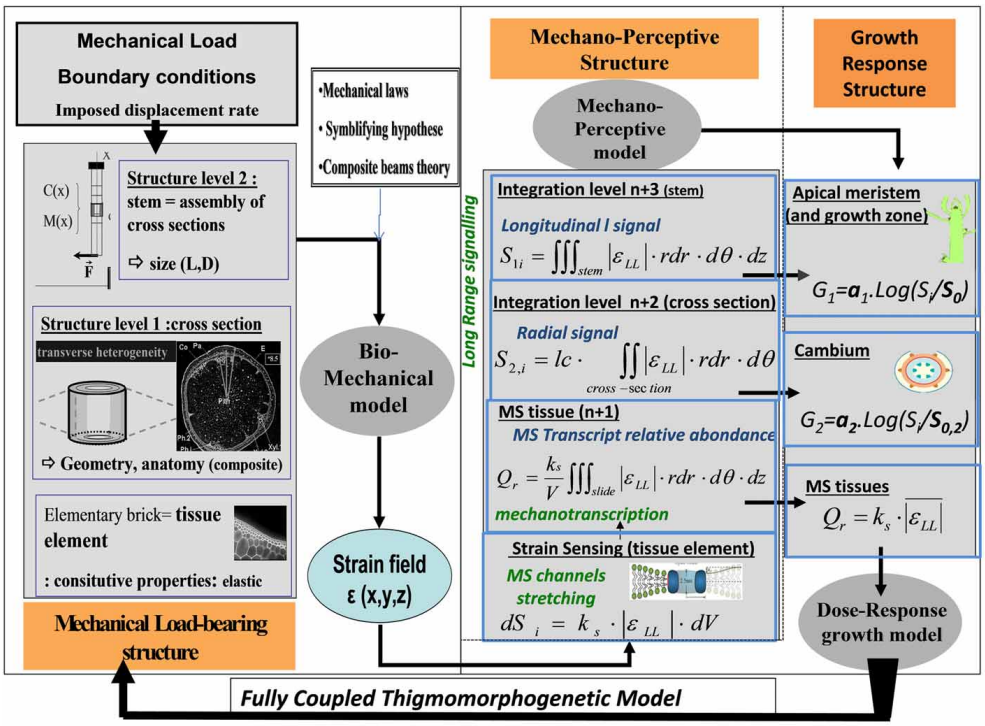

FIGURE 10 | Schematic representation of thigmomorphogenetic model including the ISM beam model and the S^{3}m. The ISM model of the mechanical load-bearing structure (left) is the CBmS designed by Coutand and Moulia (2000) to analyze stem bending experiments (see **Figure 3**). It is based on a validated composite-beam model of plant organ flexion (Moulia and Fournier, 1997). In its most simple configuration its inputs are the curvature field $C(\zeta)$ and the bending moment $M(\zeta)$ along the stem (measured as in Moulia et al., 1994). Its parameters are: (i) length, L, and diameters along the stem, $D(\zeta)$; (ii) estimates of tissue stiffness (longitudinal Young's moduli Coutand and Moulia, 2000); and (iii) the anatomical cross-sectional images processed using the model by Moulia and Fournier (1997). The elementary unit is a piece of tissue assumed to behave in the linear elastic range. Like all models based on beam-theory, this model defines two integration levels: the cross-section (which can be heterogeneous) and the stem. From the curvature field, it computes the strain field, $\varepsilon(x, y, \zeta, t)$ (and the stress field $\sigma(x, y, \zeta, t)$ if required) with ζ being the position along the stem and x,y the coordinates within the current cross-section of the stem, and t the time. The mechanosensitive model is the S^{3}m model (Moulia et al., 2011). Its inputs are the strain fields $\varepsilon(x, y, \zeta, t)$ in each stem, and the stem geometry factors L and $D(\zeta)$, (all these data are received from the ISM beam model). S^{3}m then generates the local sensing in a tissue element, and, if needed, the predicted amount of transcription Qr of a primary mechanosensitive gene. Then the integrated secondary signals $S_{i,1}$ and $S_{i,2}$ reaching the primary and secondary meristems, respectively, are computed. These signals are inputs of a module of thigmomorphogenetic growth responses (Coutand and Moulia, 2000; Coutand et al., 2009) outputting logarithmic dose-response modulations of primary and secondary growth. In a fully-coupled dynamic model of thigmomorphogenesis, the outputs of the thigmomorphogenetic growth response module can be used to update the size and geometry of the stem at the next step, so time integration can be simulated.

supplemental data), but extended it to include purely biological sensory responses.

The starting point was the local strain-sensing model (Equation 10) which states that the secondary signal output of each cell, dS_o, is proportional to the mechanotransduced signal in the mechanostimulated cell, and hence to dS_i (hypothesis H1).

The long-distance signal propagation was very fast compared with the growth response and was not damped down, so it could be neglected. The simplest model for the integration of the mechanical sensing is that the output signals, dS_o, of all the mechanosensitive cells simply sum up into a global secondary internal signal S_i (hypothesis H2). In short, for a given strain amplitude, the more cells that are strained, the higher the S_i is.

Subapical primary growth responds to distant sensing throughout the stem volume Vs. The internal signal propagated axially along the whole stem and controlling the response of primary growth $S_{i,1}$ can then be written as the sum total of all the local signal outputs from the strained cells across the stem volume Vs (Coutand and Moulia, 2000):

$$S_{i,1_{(\varepsilon)}} = \iiint_{V_s} k_{o_{(\varsigma,y,z)}} \cdot \left(\varepsilon_{(\varsigma,y,z)} - \varepsilon_0\right) .dV \qquad (14)$$

where ζ is the distance from the apex and (y, z) describes the position of the tissue elements across the cross-section of the stem and the triple sign means the sum along the three dimensions of the stem volume.

By analogy the thigmomorphogenetical signal controlling secondary growth $S_{i,2}$ can be computed as the sum of the elementary signals dS_o on a one-cell thick cross-section (see **Figure 10**).

As can be seen in Equation (14) the mechanosensitive structure of the plant (at a particular time) is given by the spatial distribution of mechanosensitivity $k_{o(\varsigma,y,z)}$ and threshold$\varepsilon_{o(\varsigma,y,z)}$. However, comparative tests of the S^{3}m have shown that the most

determinant factor was the geometry of the stem. For simplicity, more recent studies took mechanosensitivity to be homogeneous over all tissues (e.g., Coutand et al., 2009). If $k_{o(\varsigma,y,z)}$ and $\varepsilon_{o(\varsigma,y,z)}$ are constant, then they can be factorized in the spatial integrals, so that the model for the control of primary growth becomes

$$S_{i,1_{(\varepsilon)}} = k_o \left(\iiint_{V_s} \varepsilon_{(\varsigma,y,z)}.dV \right) - k_o \varepsilon_0 . V_s = k_o S_{1\text{strains}} - \Sigma_0 \quad (15)$$

where $S_{1\text{strains}}$ is the integrated stimulus summing all the strains of the cells and Σ_0 is the integrated minimal effective strain. The same expression can be used for secondary growth.

This model thus predicts that the integrated signals reaching the two meristems are linearly dependent on integrals of the strain field over the domains of mechanosensitive integration for primary and secondary growth ($S_{1\text{strains}}$ and $S_{2\text{strains}}$, respectively).

This prediction was tested quantitatively against the corresponding growth responses described earlier. Compared with what we studied for the local mechanosensitive gene expression (Equation 11 and **Figure 7B**),the prediction of S^{3}m is no longer that the growth response should be linear with $S_{i,\text{strains}}$ but that the growth responds in a dose-dependent manner to the sum of strains $S_{i,\text{strains}}$. Another way of thinking about this is that collecting more cells in the strained tissues for the analysis necessarily entails adding RNA to the sample (linearity), but the biological thigmomorphogenetic response of growing tissues to the supposed integrated signal S_i may not be additive.

As shown in **Figure 11A**, a tight logarithmic relation was found between the primary growth response (recovery time τ_r) and $S_{1\text{strains}}$ which explains 75% of the 1:10 variation in the response (Coutand and Moulia, 2000).

$$\tau_{recovery} = a_1 . \ln \left(\frac{S_{1\text{strains}}}{S_{0_{1\text{strains}}}} \right) \text{ for } S_{1\text{strains}} > S_{0_{1\text{strains}}} \quad (16)$$

where a_1 is the global thigmomorphogenetic sensitivity of a plant (including both the initial sensitivity of the mechanoperceptive structure of the plant $k_{o(\varsigma,y,z)}$ and the responsiveness of the meristem to a long distance signal $S_{i,1}$) and $S_{0_{1\text{strains}}}$ is the threshold over which meristematic cells perceive the global systemic signal reaching the growth zone. (Note that $S_{0_{1\text{strains}}}$ is not the same as the integrated minimal effective strain threshold Σ_0 presented earlier).

Similarly, a relationship was found between $S_{2\text{strains}}$and the radial growth response, which again explains 75% of the 1:5 variation generated by varying stem bending with different stem sizes (Coutand et al., 2009). An initial experiment on poplar suggested that a linear relationship between the radial growth response and $S_{2\text{strains}}$ was statistically slightly more significant than a logarithmic relationship. However, analysis of a set of dicot tree species (Coutand et al., 2010) showed that the logarithmic relationship is more generic (also see Telewski, 2006).

It should be noted that using S^{3}m the global thigmomorphogenetic sensitivity of a plant can be described quantitatively using just two parameters for the primary growth response (a_1, $S_{0_{1\text{strains}}}$) (Coutand and Moulia, 2000) and two for the secondary response (a_2, $S_{0_{2\text{strains}}}$) (Coutand et al., 2010). Varying the load and/or plant size and anatomy affects the $S_{1\text{strains}}$ value along the x-axis in **Figure 9**, and thus the value of the response, but the relationship expressed in Equation (16) (and the corresponding log response curve) are invariant. This relationship and the a_1 parameter in Equation (16) are thus independent of both load intensity and plant size/structure.

Equation (15) involves an explicit integration of the effect of the mechanical and perceptive structures of the plant through the S^{3}m model, a model that has been validated experimentally. This is not the same as a purely correlative dose-response curves with an "arbitrarily chosen" measure of the stimulus (e.g., force Jaffe, 1980a).

Finally, and very interestingly, we modified the local sensing equation so that local stress was the sensed variable instead of local strain. In this Sum of Stress-Sensing model, the 1:10 variation in the response was no longer explained, clearly disproving the stress-mechanosensing hypothesis for the control of growth by external mechanical loads (**Figure 11B**).

INTEGRATIVE STRESS-SENSING MODEL IN SAM SUBJECT TO INTERNAL LOADS

The SFm of a cell has been assembled into a cellular network encompassing a realistic SAM shape to simulate the entire dynamics of meristematic growth and morphogenesis, including primordial bulging, phyllotactic patterning, and distribution of CMT orientation. This integrative SAM Stress Feedback model (SAM SFm) was derived from an existing model relating auxin transport to phyllotactic dynamics (Jonsson et al., 2006). To account for a realistic distribution of growth rate across the meristem an *ad-hoc* dependency of the growth extensibility parameter k_g on distance to the center of the SAM was included (thereby introducing an 8th parameter, while artificially constraining the possible dynamics of the model).

The overall dynamics of the model was qualitatively satisfactory. Moreover, as shown in **Figure 12** the predicted CMT orientation was found to match experimental observation at the primordial boundaries, at the side of a growing primordium and at the stem-side base of the SAM. The robustness of the stabilization of CMT orientation during the formation of the primordial boundary and crease could be also assessed. Last but not least, an alternative Growth-Strain Feedback model (GSFm) for cellular mechanosensing was implemented and simulated within the same framework, and found to produce erroneous qualitative predictions (see replies to Hamant et al., 2008) by Schopfer and Meyerowitz in Science e-letters).

However, in these studies, the prediction by the SAM SFm could not be quantitatively assessed vs. the observed CMT reorientation. Growth-induced strains (and strain rates) were not measured concurrently, so the validity of the competing GSFm could not be really assessed. In other words, the GSFm might generate the wrong SAM dynamics not because its sensing hypothesis is wrong but because the modeling of growth and growth-induced auto-stresses is problematic. The elaborate task of testing the models was undertaken by Burian et al. (2013) who combined confocal measurement of CMT orientation dynamics with the sequential-cast (replica) technique, and careful comparative

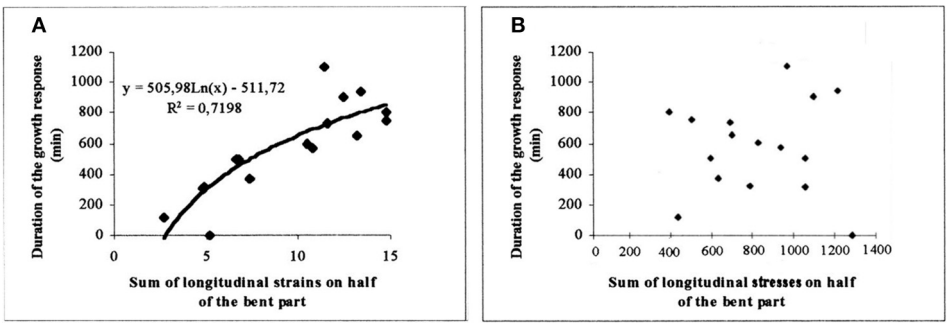

FIGURE 11 | Experimental assessment of the S^3m model. Dose-response curve of the recovery time of the primary growth response after bending plotted against the candidate internal signal ($S_{1,strains}$) predicted by the S^3m model (adapted from Coutand and Moulia, 2000 Journal of Experimental Botany, by permission of the Society for Experimental Biology). **(A)** A logarithmic relationship is obtained under the hypothesis that the mechanosensed variable is the strain and which explains 72% of the overall response. **(B)** No relationship is obtained under the hypothesis that the mechanosensed variable is the stress. —, log fit; ♦, experimental results.

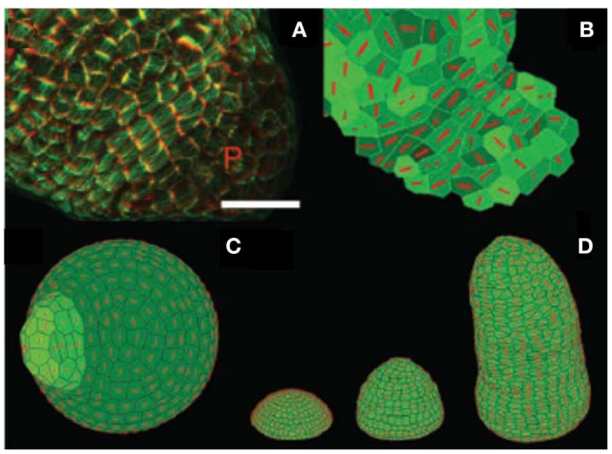

FIGURE 12 | Experimental assessment of the 2D Stress Feedback model (SFm) of the entire morphogenetic dynamics of the SAM from Hamant et al. (2008), reprinted with permission from AAAS. (A) marking cortical microtubules (green) and cell shape (red) at the surface of a meristem generating a young primordium (P). Cortical microtubule marking is obtained using the expression of a fusion protein involving the Green Fluorescent Protein and the Microtubule Binding Domain (GFP-MBD) under the control of the constitutive promoter 35S (*p35S::GFP-MBD*) Scale bar, 20 mm. **(B)** Microtubule orientation (red bars) in cells in the 2D SFm (extracted from confocal data). Note the alignment of the virtual microtubule orientations in the boundary zone and compare to **(A)**. **(C)** Simulation of an auxin-induced primordium. The 2D SFm results in orthoradial alignment of microtubules around the growing primordium. **(D)** Tip-growing simulation with the stress-feedback model generating a growing stem. Microtubules align mainly orthoradially in the stem, which has a regular shape.

mapping of CMT orientation statistics, local surface curvature and strain-rates. First Burian et al. (2013) clearly disproved the GSFm and its central hypothesis that CMTs are always oriented perpendicular to the maximal growth. However, the analysis of the relationship between wall stress pattern and CMT orientation proved more complex. A priori two models were available to test for inferred stresses: the simple PVm (**Figure 5**), and the more complex numerical SAM SFm (**Figures 9**, **12**). However, as seen before, using the numerical cellular SFm requires the estimation of eight parameters, as well as exact knowledge of the initial geometry of cells. This requires very complex, destructive and time-consuming measurements. Therefore, the authors relied on the much simpler PVm (Hamant et al., 2008) which only requires mapping of the curvatures of the L1 layer. This was achieved through the sequential replica method followed by three-dimensional (3D) reconstruction and differential geometry. Burian et al. (2013) found that the presumed geometry-derived stress distribution is not sufficient to predict CMT orientation throughout the SAM (i.e., other than at the primordium boundary), thereby rejecting the simple stress-feedback hypothesis. They argued that a better, qualitative match between estimated developmental changes in stress and CMT were found when mechanical auto-stresses derived from differential and heterogeneous growth were considered. However, a full assessment of this new hypothesis requires an extension of the numerical cellular SFm to include differences in pressure in the L1 layer, so that in-plane stressing between neighboring cells can be considered. The modeling of possible differential behavior of the inner and outer sides of the L1 layer may also be considered (as has been done in drosophila embryo models Supatto et al., 2005). This is likely to require substantial changes in the model such as a full coupling with water flows, and therefore many additional parameters entailing more experimental assessment of models.

MAJOR INSIGHTS FROM THE TWO EXAMPLES OF MODELING

These two sets of work on the mechanosensitive control of growth and morphogenesis by mechanical cues have a lot in common. In both cases it was necessary to combine integrative models with guided experiments and to progress iteratively in a model↔experiment loop. The role of the models was to allow for the predictions of mechanistic hypotheses to be assessed experimentally both at the cellular and whole-organ scales. In both cases, ISM integrative biomechanical models were coupled with a mechanobiological model to study the load distribution, the mechanosensing, and the building of the overall growth and morphogenetic responses. This has allowed the clear definition of the three "superimposed" structures of the plant: the mechanical

structure bearing and distributing the load, the mechanosensitive structure, and the responsive morphogenetic structure. The SAM could be considered a borderline case for this theoretical framework because there is very little visible tissue differentiation, so the three structures are merged (even though invisible dynamic patterning of cell fate is underway). On the contrary, the growing dicot stem offers a much clearer spatial and functional distinction between the three structures. The mechanical structure mostly involves the stiff tissues (although parenchyma does act as a filler and stabilizer, Gibson, 2013), the mechanosensitive structure is mostly parenchyma (and phloem), and the morphogenetic structures are the primary and secondary meristems. Therefore, changes in the geometry of the stem, and on the balance between the three structures may change the overall responsiveness of the plant to a given mechanical load (even if the intrinsic sensitivities of the mechanosensing cells and meristematic cells remain unchanged).

In all cases, the major insight is how the geometry of the organ influences both the load distribution and the amount of mechanosensing. Insightful dose-response curves cannot be obtained when only the overall mechanical load is considered (e.g., the force applied on the organ). In some experiments apparently good correlative dose-response curves with the overall load can be produced (e.g., Jaffe, 1980b), but this is because the three structures of the plant displayed very little variability, while there was a wide range of loads. Global dose-response curves risk causing confusion as they do not consider the mechanical and mechanobiological structures and processes involved in the interaction between the organ and its load and may be misleading when analyzing genetic variability of natural populations or mutant or stage variability.

The second insight brought by these two approaches is that the sensing is distributed, so that the relevant variable is the distributed change in mechanical state, i.e., stress or strain. It is now time to revisit briefly the strain-sensing vs. stress-sensing controversy (a more complete discussion can be found in Moulia et al., 2011). The conclusions of the two sets of studies outlined in this review are contradictory. However, these findings can be reconciled by postulating that different sensing pathways may be involved, each having a different mechanical relationship with the cell wall. Mechanosensing of external loads is thought to involve mechanosensitive ionic channels that sit in the soft cellular membranes and are gated by membrane tensional stresses (Haswell et al., 2008). They thus cannot sense wall stresses. But the membrane is more compliant than the cell wall by orders of magnitude and it is attached to and pressed against the cell wall, so it is forced to follow the straining of the wall. As a consequence the intrinsic stretch-activated-channels are stretched according to cell wall strains. On the contrary, cytoskeleton elements link to the cell wall at direct adhesion domains (Baluska et al., 2003). These linkers are partially embedded in the cell wall, so any cell wall stresses are directly transmitted to them. Moreover, unlike the surrounding polysaccharide wall, they are likely to behave elastically. So the change in their configuration, the strain, that ultimately modulates their biological activity (Monshausen and Haswell, 2013) is directly linked with elastic stresses within the surrounding wall. As these proteins are minute inclusions within the cell wall, their very local stress-strain pattern cannot be resolved from that of the surrounding cell wall, so the changes in their configuration are better predicted by the stresses they receive from the surrounding cell wall than by its global strain. This illustrates how important it is to precisely consider the cellular (and macromolecular) structures involved, and how strain and stress patterns propagate, not only through tissues and cells, but ultimately in the apoplasm and symplasm. This is a new domain in which modeling will proved a very valuable tool.

BIOMECHANICAL AND MECHANOBIOLOGICAL MODELS FOR PLANT MECHANOSENSING: FROM THE PLANT IN ITS ENVIRONMENT TO GENES AND BACK

BIOMECHANICAL MODELS AS A TOOL TO DESIGN AND ANALYZE EXPERIMENTS

We now review more systematically some of the many ways in which biomechanical and mechanobiological models have been used to gain insights into the mechanosensitivity of plants in their natural environments.

Mechanical models as state observers estimating stress and strain distributions

Mechanical models are almost indispensable tools for tracking how the mechanical loads are distributed throughout the organ or plant, scaling down to the mechanosensitive cells themselves. Indeed the load acts through the whole organ or plant structure, with possible mechanical focusing and amplification at specific places (related to lever arms, holes and curvatures). The stress distribution in the SAM (**Figure 5**) is primarily prescribed by the geometry of the dome and its connection with primordia, the saddle-shape of the crease having a huge effect. If one stem has a diameter that is twice that of another stem, when they are both submitted to the same bending moment M (**Figure 4**), the strains will be 8-fold higher in the more slender stem. If the two stems have same diameter the Young's modulus of one is twice that of the other, the strains in the stem with the lower Young's modulus will be only twice as high. Without a proper understanding of these effects a mechanobiologist can easily misinterpret experimental data. The case of stresses is particularly compelling and indeed, as already emphasized, stress is not an observable or measurable quantity. Engineers and mathematicians create models that act as "state observers" for the very purpose of inferring stresses in a structure (Villaverde and Banga, 2014). Interestingly though, a model to estimate stress distribution can be rather simple, as long as the equilibrium configuration of the organ and its mechanical load can be measured with sufficient accuracy and the organ is not rheologically too heterogeneous. In this case, the stress field can be calculated by applying the law of mechanical equilibrium. This was done in the PVm by Hamant et al. (2008). However, as soon as tissue patterns and/or growth-induced stresses among cells [also known as residual stresses or auto-equilibrated stresses, see (Moulia and Fournier, 2009; Moulia, 2013) for definitions] are involved, the picture becomes far more complex (Burian et al., 2013). Models then also need to consider strains and growth. Both elastic and growth-induced strains are observable quantities that can be measured even with non-contact techniques as long as the organ is accessible (e.g., Silk

and Erickson, 1980; Barbacci et al., 2013, 2014). However, only models can give insights into the full distribution of strains (and strain rates) across the tissues and their dependency on the structure of the plant and the load. These models acting as strain-state observers (such as the CBmS) are more advanced than stress-state observers, as they handle the changes in configuration of the organ structure under the load as well as the reference length of its constitutive elements, their changes through growth (e.g., Barbacci et al., 2013), and other visco-plastic effects.

A guide for experimental strategies

We have seen that stem geometry has a major influence on the strains resulting from bending One problem that biologists face is that plants are never uniform. When studying thigmomorphogenesis, the classic experimental approach has been to apply a range of forces to "standardized" sets of plants. However, we now know that force is not the perceived variable. Therefore, a more appropriate strategy is to apply a range of strains in a controlled manner. The natural heterogeneity of stem diameters is a natural source of continuous variation in applied strains. We can therefore, take advantage of the two sources of variation in the amount of strain, the load, and the size of the plant. This strategy was used to disentangle the "strain-sensing vs. force-sensing" issue (Coutand and Moulia, 2000; Coutand et al., 2000). It is important to use appropriate controls as the size variations may confer other biological properties that produce confounding effects.

This experimental strategy can even be extended to study plants growing in windy conditions outdoors. In natural conditions, wind cannot be controlled easily. If the aim is to study a range of strains due to wind, using standardized plants will make the experimental design completely dependent on wind velocity so it can take a long time to accumulate the data on the desired range of strains. However, if plants with different geometries are chosen, the natural variability in geometry will bring a range of vibration frequencies and a range of strains for any given wind velocity. To choose suitable plant geometries, a mechanical model is required (Rodriguez et al., 2008; Sellier et al., 2008). The model would also give insights into the strain field, so the positioning of detectors measuring growth responses can be optimized.

Finally the wind-plant interaction model can be coupled with S^3m (instead of the static bending mechanical model CBmS in **Figures 4**, **10**) to test thigmomorphogenetic hypotheses on plant development outdoors.

A TOOLBOX FOR MECHANISTIC SYSTEMS BIOLOGY

While mechanical and biomechanical models are instrumental in mechanobiology, hypothesis-driven plant mechanobiology can also benefit from well-based models.

A tool for handling scale changes in integrative biology

Throughout this review, we have emphasized that models are necessary tools whenever effects of changes in organizational levels and scales are involved. Considering that the cell is the structural unit of life, it is intuitive to ask whether the cell with its constitutive molecules should be the usual scale for modeling. A central insight from biomechanical and biological modeling is that there is no absolute need to burrow down to the macromolecular or even cellular scale, even when cellular mechanobiological responses are the object of the study (e.g., Hamant et al., 2008). This is certainly true for mechanical models. For example, both the CBmS and the PVm do not specify cells as finite elements, but they can still be used to understand the distribution of stress and strain in the apoplast, mechanosensitive cytoskeletal remodeling, and even gene expression. The SFm does not really consider the biological cell as the structural units as the inner mechanical structure of the cell, the cortical cytoskeleton, the transverse actin stress fibers, the vacuole, the nucleus or the endoplasmic reticulum are not considered. The stress and strain distribution through the cell ultrastructure is unknown. The model is simply a honeycomb-like apoplastic structure. Models of the inner structure of the cell are only necessary when the localization of the intracellular mechanosensitive responses are being studied, namely the precise molecular mechanism of mechanoreception (e.g., mechanosensitive channel opening or anisotropic cytoskeleton disassembly). The internal mechanical structure of the cell protoplast, and its links with the cell wall, is beginning to be revealed. Some models of animal cell ultrastructure have been built (Nick, 2011; Asnacios and Hamant, 2012), but they rely on simplified representation of the cellular structures (e.g., microtubule are modeled as cables). Detailed 3D molecular mechanical models are only feasible when studying the molecular dynamics of isolated macromolecules or oligomolecular complexes for which the crystallographic structure is known (e.g., a mechanosensitive channel in a patch of lipid bilayer, Sotomayor and Shulten, 2014). Another viewpoint is that plasmodesmata form a cytoplasmic continuum in tissues for mRNA trafficking between cells, so the cell is not the intuitive unit for mechanotransduction in plants. Finally, quantitative functional genomics has shown that master transcription factors may be less concentrated than their respective promoter sites in a given cell. In this context, transcriptional regulation at the single cell level may have a highly stochastic component that only becomes deterministic at the scale of a tissue element containing many interacting cells (Elowitz et al., 2002; Gandrillon et al., 2012).

A Tool for Genetic Dissection

Thigmomorphogenetic responses have been described in many plant species and it is interesting to compare responses between species. The responses may be different because (i) the level of applied strain is different, for example, due to the geometry of the different species, (ii) the species sensitivity to mechanical loading is different, or (iii) both. The sensitivity must be an intrinsic character of the species and it must be independent of plant size. From the S^3m model we know

$$\frac{dR}{dt_{\max}} = a_2 . \ln\left(\frac{S_{2\text{strains}}}{S0_{2\text{strains}}}\right) = a_2 . \ln\left(S_{2\text{strains}}\right) - a_2 . \ln\left(S0_{2\text{strains}}\right) \text{ for } S_{2\text{strains}} > S0_{2\text{strains}} \quad (17)$$

Therefore, by applying similar ranges of $S_{2\text{strains}}$ and measuring the daily increment in diameter of different species, we can plot the growth response against the logarithm of the applied $S_{2strains}$, and fit a regression line in which the slope (a_2) is the intrinsic mechanosensing sensitivity of the species and the intercept can be used to estimate the mechanical signal threshold ($S0_{2\text{strains}}$).

The values of parameters a_2 and S_{02} can be compared to see if there is any variability in mechanosensing between species. This conceptual framework has been used to study the mechanosensing variability between five sympatric tropical tree species (Coutand et al., 2010). No variability in mechanosensing sensitivity was found but differences in signal thresholds were found (**Figure 13**). Note that this conceptual framework could also be used to compare mechanosensing sensitivity between organs for example.

Enabling model-assisted phenotyping

The previous genetic study can be seen as an example of model-assisted phenotyping in which the S^3m combined with a fairly simple experiment was used to extract two intrinsic parameters describing the mechanosensitivity of a species. The same approach can be used to phenotype collections of mutants or varieties. Defining intrinsic characteristics and enabling model-assisted high-throughput phenotyping is becoming a major challenge of systems biology (Bastien et al., 2013).

Identifying rewarding molecular studies

Another interesting heuristic property of integrative models is that they can help to identify (i) which modules are more influential than others in the global mechanobiological response, and (ii) which are insufficiently understood. This can help to guide molecular studies of gene regulation, for example, so that the most rewarding projects are designed. Genes targeted in this way are likely to trigger particularly significant phenotypes, and identifying key regulators significantly would improve our understanding of the whole system response. An example is our recent study of thigmomorphogenesis in wind acclimation of plants, which clearly pinpointed a current deadlock in advancing our understanding of mechanosensitivity accommodation in response to successive bending (see Leblanc-Fournier et al., 2014).

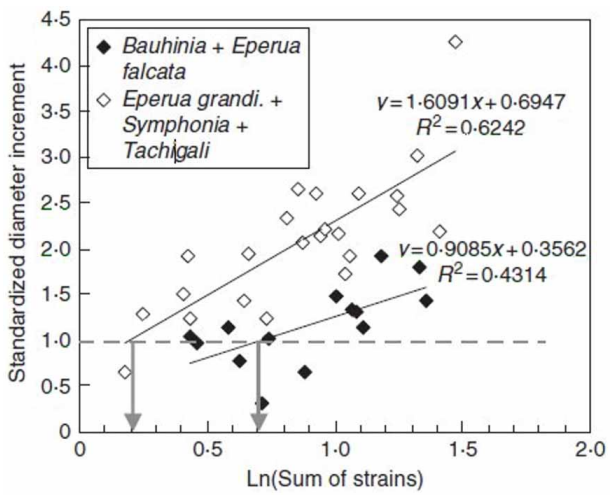

FIGURE 13 | S^3m-assisted dissection of natural genetic diversity in mechanosensing. Relationship between the standardized diametric growth responses of five neotropical forest species and the log of the candidate internal signal ($S_{2,strain}$) predicted by the S^3m model. $S_{2,strain}$ = sum of strains over the cross-section during the bending treatment from Coutand et al. (2010), Annals of Botany, by permission of Oxford University Press.

UNDERSTANDING PLANT RESPONSES TO MECHANICAL LOADS IN THEIR NATURAL ENVIRONMENT

Ideally the ultimate goal of systems mechanobiology would be to understand how plants acclimate in their natural environment. For example, for wind resistance, models are available to describe the mechanics of lodging, wind-throw and wind-break (see De Langre, 2008; Gardiner et al., 2008) for reviews), but existing growth models disregard thigmomorphogenesis so they do not deal with wind acclimation (Moulia et al., 2006). A major asset of the S^3m is that it can be coupled with mechanical models to analyze the effects of the static and dynamic strains produced by wind-induced vibrations in plants (e.g., Gardiner et al., 2008; Rodriguez et al., 2008; Sellier et al., 2008). On the other hand, as S^3m can also handle growth responses to wind, it can be coupled with structure-function growth models (see Moulia et al., 2006; Fourcaud et al., 2008 for general discussion). The overall wind resistance of plants due to genetic variation in intrinsic mechanosensitivity could be assessed in various (present, past or forecasted) climatic scenarii during *in silico* numerical experiments. There is obviously a lot of work to accomplish, but integrative mechanosensing models are surely a key breakthrough paving the way to a better understanding of the ecological and economic relevance of thigmomorphogenetic acclimation, for example, by exploring the consequences of global climate changes on stand growth and resistance to wind hazards.

CONCLUSION: THE CHALLENGES OF SYSTEMS MECHANOBIOLOGY

Plants respond to internal and external mechanical loads at many scales. The mechanical growth response can theoretically be broken down into four processes.

- Bearing the load, how the mechanical load is distributed by a plant structure.
- Sensing the effect of the load distribution by mechanosensing of local mechanical states.
- Transducing the signal through mechanoreceptor pathways to alter the expression of a specific set of transcription factors.
- Responding by the global retuning of growth rate and direction.
- However, none of these processes are disconnected from one another. The challenge of the integrative biology of mechanosensing is to operate across scales and processes and understand outputs in terms of the overall syndrome of mechanosensitive growth responses and their adaptive relevance.

As this loop involves several organizational levels and scales plus a host of interactions, it cannot be handled without models, placing this challenge within the realm of systems biology (Tardieu, 2003; Moulia and Fournier, 2009; Traas and Moneger, 2010). The bottom line here is that systems biology modeling and

cross-comparisons against data produced through suitable experimentation makes it possible to test hypotheses. If a combination of hypotheses cannot be worked out without calculus, modeling becomes an extension of the experimental method (Legay, 1997). Therefore, the mechanical models need to be adjusted whenever necessary, such as to cope with a different experimental set-up or to natural conditions.

These mechanistic models have to be evaluated on their outputs, on the performance of their component mechanistic modules (e.g., Coutand et al., 2009), and their capacity to reflect natural genetic variation (e.g., Sierra-De-Grado et al., 2008; Almeras et al., 2009; Coutand et al., 2010). To be useful however, models need to be kept simple and amenable enough to use. Multiplying the number of elements and degrees of freedom makes models more difficult to analyze and assess experimentally. This difficulty may be partly circumvented by implementing a clear modular design and explicitly setting up organizational levels. Additionally, the development of non-destructive bio-imaging and micromechanical techniques (see references in Milani et al., 2013; Moulia, 2013) are ways to gather more information to precisely assess the modules. But there are still some intrinsic limits to model complexity if the model is to be used to assess mechanobiological hypotheses and/or to capture very nonlinear behavior. Here mechanobiology diverges from standard mechanical engineering in which the model is mostly an attempt to assemble well-established physical laws into a given structure, not a way to assess a biological hypothesis. From this perspective, it is instructive that the SAM SFm with its eight parameters has yet to be assessed experimentally and that experimental progress has relied on the PVm. Hence, an effort to simplify models is called for (as is common in physics through dimensional analysis; see Rodriguez et al., 2008; Bastien et al., 2013, 2014) at the same time addressing them to specific hypotheses that can be experimentally falsified or upheld.

Overall, this strategy of combining heuristic models with experiments has provided many insights into the mechanosensitive control of growth. However, the complexity of the structural, dynamic, and regulatory aspects requires intense interdisciplinary work (Moulia, 2013). In particular, biologists need to become familiar with the key concepts of mechanics to collaborate productively with physicists and modelers in designing, criticizing, and experimentally assessing biomechanical and mechanobiological models. It is hoped that our review has convinced readers of the usefulness and reward of this interdisciplinary approach and made it more accessible. This interactive approach, including using modeling as a tool to extend the experimental method, contrasts with and complements alternative set-ups, for example, where experimentalists intensively collect data while bioinformaticians set up models and data mining programs.

The chosen examples considered in this review deal only with dicot growth, but the approach can be extended easily to monocots (with obvious adaptions to omit secondary growth responses), and even to most *Viridiplantae*. Again the examples all involved the shoot system, ranging from the cell to the organ level, but the methodology is in no way specific to these systems. Indeed there is a very active research making extensive use of integrative modeling to discover how root growth and morphogenesis is controlled by external and internal mechanical cues (see for example Ditengou et al., 2008; Bengough et al., 2011; Band et al., 2012; Jin et al., 2013). By the same token, works at the scale of the intracellular structures would be extremely useful. The way stresses and strains act inside the cell through the cell wall-membrane-cytoskeleton-nucleus continuum is yet to be fully grasped. The tensegrity model of the structural mechanics of the cytoskeleton has started to reveal unexpectedly how mechanical amplifications can take place through the cytoskeleton network (Nick, 2011), but the way it interacts dynamically with wall stressing and deformation remains to be elucidated (Hamant, 2013). Similarly, the responses of cell trafficking and plasma membrane straining and turnover upon cell stretching are very promising fields (Asnacios and Hamant, 2012; Nakayama et al., 2012). A more complete elucidation of the mechanosensitive gene networks controlling the cellular response is also a priority including how the cell division-cell elongation complex is modulated by mechanical cues. Finally this review has mostly focused on spatial integration, but the challenge of time integration is as important. When successive signals are applied to a living system, relative or absolute refractory periods of the mechanosensors and gene-regulated accommodation of the mechanosensitivity make it complicated to study the relationship between the signals and the system's responses (see Leblanc-Fournier et al., 2014). The analysis of the time aspect will also require two-way interaction between models and experiments.

The first successes of integrative mechanobiology of growth control have thus opened up a large set of questions for interdisciplinary research, which hopefully will elucidate many more aspects of the way plants have evolved to bear loads and remain stable when responding to internal and external mechanical challenges.

ACKNOWLEDGMENTS

This work was supported by the grant AN5-09-BLAN-0245-01 (ANR, France, project "Senzo").

SUPPLEMENTARY MATERIAL

The Supplementary Material for this article can be found online at: http://www.frontiersin.org/journal/10.3389/fpls.2015.00052/abstract

REFERENCES

Almeras, T., Derycke, M., Jaouen, G., Beauchene, J., and Fournier, M. (2009). Functional diversity in gravitropic reaction among tropical seedlings in relation to ecological and developmental traits. *J. Exp. Bot.* 60, 4397–4410. doi: 10.1093/jxb/erp276

Asnacios, A., and Hamant, O. (2012). The mechanics behind cell polarity. *Trends Cell Biol.* 22, 584–591. doi: 10.1016/j.tcb.2012.08.005

Baluska, F., Samaj, J., Wojtaszek, P., Volkmann, D., and Menzel, D. (2003). Cytoskeleton-plasma membrane-cell wall continuum in plants. Emerging links revisited. *Plant Physiol.* 133, 482–491. doi: 10.1104/pp.103.027250

Band, L. R., Fozard, J. A., Godin, C., Jensen, O. E., Pridmore, T., Bennett, M. J., et al. (2012). Multiscale systems analysis of root growth and development: modeling beyond the network and cellular scales. *Plant Cell* 24, 3892–3906. doi: 10.1105/tpc.112.101550

Barbacci, A., Diener, J., Hemon, P., Adam, B., Dones, N., Reveret, L., et al. (2014). A robust videogrametric method for the velocimetry of wind-induced motion in trees. *Agri. Forest Meteorol.* 184, 220–229. doi: 10.1016/j.agrformet.2013.10.003

Barbacci, A., Lahaye, M., and Magnenet, V. (2013). Another brick in the cell wall: biosynthesis dependent growth model. *PLoS ONE* 8:e74400. doi: 10.1371/journal.pone.0074400

Baskin, T. I., and Jensen, O. E. (2013). On the role of stress anisotropy in the growth of stems. *J. Exp. Bot.* 64, 4697–4707. doi: 10.1093/jxb/ert176

Bastien, R., Bohr, T., Moulia, B., and Douady, S. (2013). Unifying model of shoot gravitropism reveals proprioception as a central feature of posture control in plants. *Proc. Natl. Acad. Sci. U.S.A.* 110, 755–760. doi: 10.1073/pnas.1214301109

Bastien, R., Douady, S., and Moulia, B. (2014). A unifying modeling of plant shoot gravitropism with an explicit account of the effects of growth. *Front. Plant Sci.* 5:136. doi: 10.3389/Fpls.2014.00136

Bengough, A. G., Mckenzie, B. M., Hallett, P. D., and Valentine, T. A. (2011). Root elongation, water stress, and mechanical impedance: a review of limiting stresses and beneficial root tip traits. *J. Exp. Bot.* 62, 59–68. doi: 10.1093/jxb/erq350

Boudaoud, A. (2010). An introduction to the mechanics of morphogenesis for plant biologists. *Trends Plant Sci.* 15, 353–360. doi: 10.1016/j.tplants.2010.04.002

Braam, J. (2005). In touch: plant responses to mechanical stimuli. *N. Phytol.* 165, 373–389. doi: 10.1111/j.1469-8137.2004.01263.x

Brenner, E. D., Stahlberg, R., Mancuso, S., Vivanco, J., Baluska, F., and Van Volkenburgh, E. (2006). Plant neurobiology: an integrated view of plant signaling. *Trends Plant Sci.* 11, 413–419. doi: 10.1016/j.tplants.2006.06.009

Burian, A., Ludynia, M., Uyttewaal, M., Traas, J., Boudaoud, A., Hamant, O., et al. (2013). A correlative microscopy approach relates microtubule behaviour, local organ geometry, and cell growth at the *Arabidopsis* shoot apical meristem. *J. Exp. Bot.* 64, 5753–5767. doi: 10.1093/jxb/ert352

Coutand, C. (2010). Mechanosensing and thigmomorphogenesis, a physiological and biomechanical point of view. *Plant Sci.* 179, 168–182. doi: 10.1016/j.plantsci.2010.05.001

Coutand, C., and Moulia, B. (2000). Biomechanical study of the effect of a controlled bending on tomato stem elongation: local strain sensing and spatial integration of the signal. *J. Exp. Bot.* 51, 1825–1842. doi: 10.1093/jexbot/51.352.1825

Coutand, C., Chevolot, M., Lacointe, A., Rowe, N., and Scotti, I. (2010). Mechanosensing of stem bending and its interspecific variability in five neotropical rainforest species. *Ann. Bot.* 105, 341–347. doi: 10.1093/aob/mcp286

Coutand, C., Julien, J. L., Moulia, B., Mauget, J. C., and Guitard, D. (2000). Biomechanical study of the effect of a controlled bending on tomato stem elongation: global mechanical analysis. *J. Exp. Bot.* 51, 1813–1824. doi: 10.1093/jexbot/51.352.1813

Coutand, C., Martin, L., Leblanc-Fournier, N., Decourteix, M., Julien, J. L., and Moulia, B. (2009). Strain mechanosensing quantitatively controls diameter growth and PtaZFP2 gene expression in poplar. *Plant Physiol.* 151, 223–232. doi: 10.1104/pp.109.138164

Coutand, C., Mathias, J. D., Jeronimidis, G., and Destrebecq, J. F. (2011). TWIG: a model to simulate the gravitropic response of a tree axis in the frame of elasticity and viscoelasticity, at intra-annual time scale. *J. Theor. Biol.* 273, 115–129. doi: 10.1016/j.jtbi.2010.12.027

Couturier, E., Brunel, N., Douady, S., and Nakayama, N. (2012). Abaxial growth and steric constraints guide leaf folding and shape in acer pseudoplatanus. *Am. J. Bot.* 99, 1289–1299. doi: 10.3732/ajb.1100325

De Langre, E. (2008). Effects of wind on plants. *Annu. Rev. Fluid Mech.* 40, 141–168. doi: 10.1146/annurev.fluid.40.111406.102135

Der Loughian, C., Tadrist, L., Allain, J.-M., Diener, J., Moulia, B., and De Langre, E. (2014). Measuring local and global vibration modes in model plants. *C. R. Mécanique* 342, 1–7. doi: 10.1016/j.crme.2013.10.010

Ding, J. P., and Pickard, B. G. (1993). Modulation of mechanosensitive calcium-selective cation channels by temperature. *Plant J.* 3, 713–720. doi: 10.1111/j.1365-313X.1993.00713.x

Ditengou, F. A., Tealea, W. D., Kochersperger, P., Flittner, K. A., Kneuper, I., Van Der Graaff, E., et al. (2008). Mechanical induction of lateral root initiation in *Arabidopsis thaliana*. *Proc. Natl. Acad. Sci. U.S.A.* 105, 18818–18823. doi: 10.1073/pnas.0807814105

Dumais, J. (2013). Modes of deformation of walled cells. *J. Exp. Bot.* 64, 4681–4695. doi: 10.1093/jxb/ert268

Elowitz, M. B., Levine, A. J., Siggia, E. D., and Swain, P. S. (2002). Stochastic gene expression in a single cell. *Science* 297, 1183–1186. doi: 10.1126/science.1070919

Fourcaud, T., Zhang, X., Stokes, A., Lambers, H., and Korner, C. (2008). Plant growth modelling and applications: the increasing importance of plant architecture in growth models. *Ann. Bot.* 101, 1053–1063. doi: 10.1093/aob/mcn050

Fournier, M., Baillères, H., and Chanson, B. (1994). Tree biomechanics: growth, cumulative prestresses, and reorientations. *Biomimetics* 2, 229–251.

Gandrillon, O., Kolesnik-Antoine, D., Kupiec, J. J., and Beslon, G. (2012). Special Issue: chance at the heart of the cell. *Prog. Biophys. Mol. Biol.* 110, 1–4. doi: 10.1016/j.pbiomolbio.2012.05.006

Gardiner, B., Byrne, K., Hale, S., Kamimura, K., Mitchell, S. J., Peltola, H., et al. (2008). A review of mechanistic modelling of wind damage risk to forests. *Forestry* 81, 447–463. doi: 10.1093/forestry/cpn022

Gibson, L. J. (2013). The hierarchical sturcture and mechanics of plant materials. *J. R. Soc. Interface* 9, 2749–2766. doi: 10.1098/rsif.2012.0341

Gibson, L. J., Ashby, M. F., and Easterling, K. E. (1988). Structure and mechanics of the iris leaf. *J. Mater. Sci.* 23, 3041–3048. doi: 10.1007/BF00551271

Hamant, O. (2013). Widespread mechanosensing controls the structure behind the architecture in plants. *Curr. Opin. Plant Biol.* 16, 654–660. doi: 10.1016/j.pbi.2013.06.006

Hamant, O., Heisler, M. G., Jonsson, H., Krupinski, P., Uyttewaal, M., Bokov, P., et al. (2008). Developmental patterning by mechanical signals in *Arabidopsis*. *Science* 322, 1650–1655. doi: 10.1126/science.1165594

Haswell, E. S., Peyronnet, R., Barbier-Brygoo, H., Meyerowitz, E. M., and Frachisse, J. M. (2008). Two MscS homologs provide mechanosensitive channel activities in the *Arabidopsis* root. *Curr. Biol.* 18, 730–734. doi: 10.1016/j.cub.2008.04.039

Heisler, L. K., and Lam, D. D. (2010). 5-HT2C receptor ligands in the treatment of obesity and type 2 diabetes. *Eur. Neuropsychopharmacol.* 20, S182–S182. doi: 10.1016/S0924-977X(10)70171-1

Jaffe, M. J. (1980a). Morphogenetic responses of plants to mechanical stimuli or stress. *Bioscience* 30, 239–243.

Jaffe, M. J. (1980b). Morphogenetic responses of plants to mechanical stimuli or stress. *Bioscience* 30, 239–243. doi: 10.2307/1307878

Jin, K., Shen, J. B., Ashton, R. W., Dodd, I. C., Parry, M. A. J., and Whalley, W. R. (2013). How do roots elongate in a structured soil? *J. Exp. Bot.* 64, 4761–4777. doi: 10.1093/Jxb/Ert286

Jonsson, H., Heisler, M. G., Shapiro, B. E., Meyerowitz, E. M., and Mjolsness, E. (2006). An auxin-driven polarized transport model for phyllotaxis. *Proc. Natl. Acad. Sci. U.S.A.* 103, 1633–1638. doi: 10.1073/pnas.0509839103

Kwiatkowska, D. (2008). Flowering and apical meristem growth dynamics. *J. Exp. Bot.* 59, 187–201. doi: 10.1093/jxb/erm290

Landrein, B., and Hamant, O. (2013). How mechanical stress controls microtubule behavior and morphogenesis in plants: history, experiments and revisited theories. *Plant J.* 75, 324–338. doi: 10.1111/tpj.12188

Leblanc-Fournier, N., Coutand, C., Crouzet, J., Brunel, N., Lenne, C., Moulia, B., et al. (2008). Jr-ZFP2, encoding a Cys2/His2-type transcription factor, is involved in the early stages of the mechano-perception pathway and specifically expressed in mechanically stimulated tissues in woody plants. *Plant Cell Environ.* 31, 715–726. doi: 10.1111/j.1365-3040.2008.01785.x

Leblanc-Fournier, N., Martin, L., Lenne, C., and Decourteix, M. (2014). To respond or not to respond, the recurring question in plant mechanosensitivity. *Front. Plant Sci.* 5:401. doi: 10.3389/fpls.2014.00401

Legay, J. M. (1997). *L'expérience et Le Modèle, Un Dicours Sur La Méthode*. Paris: Quae Editions.

Lopez-Rodriguez, A. M., Venkataraman, G., and Holmgren, M. (2014). Shaker Kv Channel's sugar remotion in real-time. *Biophys. J.* 106, 537a. doi: 10.1016/j.bpj.2013.11.2996

Martin, L., Leblanc-Fournier, N., Azri, W., Lenne, C., Henry, C., Coutand, C., et al. (2009). Characterization and expression analysis under bending and other abiotic factors of PtaZFP2, a poplar gene encoding a Cys2/His2 zinc finger protein. *Tree Physiol.* 29, 125–136. doi: 10.1093/treephys/tpn011

Martin, L., Leblanc-Fournier, N., Julien, J. L., Moulia, B., and Coutand, C. (2010). Acclimation kinetics of physiological and molecular responses of plants to multiple mechanical loadings. *J. Exp. Bot.* 61, 2403–2412. doi: 10.1093/jxb/erq069

Mattheck, C., and Bethge, K. (1998). The mechanical survival strategy of trees. *Arboric. J.* 22, 369–386. doi: 10.1080/03071375.1998.9747222

Milani, P., Braybrook, S. A., and Boudaoud, A. (2013). Shrinking the hammer: micromechanical approaches to morphogenesis. *J. Exp. Bot.* 64, 4651–4662. doi: 10.1093/jxb/ert169

Monshausen, G. B., and Haswell, E. S. (2013). A force of nature: molecular mechanisms of mechanoperception in plants. *J. Exp. Bot.* 64, 4663–4680. doi: 10.1093/jxb/ert204

Moulia, B. (2000). Leaves as shell structures: double curvature, auto-stresses, and minimal mechanical energy constraints on leaf rolling in grasses. *J. Plant Growth Regul.* 19, 19–30. doi: 10.1007/s003440000004

Moulia, B. (2013). Plant biomechanics and mechanobiology are convergent paths to flourishing interdisciplinary research. *J. Exp. Bot.* 64, 4617–4633. doi: 10.1093/jxb/ert320

Moulia, B., Fournier, M., and Guitard, D. (1994). Mechanics and form of the maize leaf: *in vivo* qualification of flexural behavior. *J. Mater. Sci.* 29, 2359–2366. doi: 10.1007/Bf00363427

Moulia, B., and Fournier, M. (1997). Mechanics of the maize leaf: a composite beam model of the midrib. *J. Mater. Sci.* 32, 2771–2780. doi: 10.1023/A:1018604012754

Moulia, B., and Fournier, M. (2009). The power and control of gravitropic movements in plants: a biomechanical and systems biology view. *J. Exp. Bot.* 60, 461–486. doi: 10.1093/jxb/ern341

Moulia, B., Coutand, C., and Lenne, C. (2006). Posture control and skeletal mechanical acclimation in terrestrial plants: implications for mechanical modeling of plant architecture. *Am. J. Bot.* 93, 1477–1489. doi: 10.3732/ajb.93.10.1477

Moulia, B., Der Loughian, C., Bastien, R., Martin, L., Rodriguez, M., Gourcilleau, D., et al. (2011). "Integrative mechanobiology of growth and architectural development in changing mechanical environments," in *Mechanical Integrative of Plant Cells and Plants* ed P. Wojtaszek (Berlin: Springer-Verlag), 269–302.

Nakayama, N., Smith, R. S., Mandel, T., Robinson, S., Kimura, S., Boudaoud, A., et al. (2012). Mechanical regulation of auxin-mediated growth. *Curr. Biol.* 22, 1468–1476. doi: 10.1016/j.cub.2012.06.050editors

Nick, P. (2011). "Mechanics of the cytoskeleton," in *Mechanical Integration of Plant Cells and Plants*, ed P. Wojtaszek (Berlin; Heidelberg: Springer), 53–90.

Niklas, K. J., and Spatz, H. C. (2012). Mechanical properties of wood disproportionately increase with increasing density. *Am. J. Bot.* 99, 169–170. doi: 10.3732/ajb.1100567

Peaucelle, A., Braybrook, S. A., Le Guillou, L., Bron, E., Kuhlemeier, C., and Hofte, H. (2011). Pectin-induced changes in cell wall mechanics underlie organ initiation in *Arabidopsis*. *Curr. Biol.* 21, 1720–1726. doi: 10.1016/j.cub.2011.08.057

Pivato, D., Dupont, S., and Brunet, Y. (2014). A simple tree swaying model for forest motion in windstorm conditions. *Trees* 28, 281–293. doi: 10.1007/s00468-013-0948-z

Pot, G., Toussaint, E., Coutand, C., Le Cam, J. B., and Saudreau, M. (2014). A model to simulate the gravitropic response and internal stresses in trees, considering the progressive maturation of wood. *Trees* 28, 1235–1248. doi: 10.1007/s00468-014-1033-y

Robinson, S., Burian, A., Couturier, E., Landrein, B., Louveaux, M., Neumann, E. D., et al. (2013). Mechanical control of morphogenesis at the shoot apex. *J. Exp. Bot.* 64, 4729–4744. doi: 10.1093/jxb/ert199

Rodriguez, M., De Langre, E., and Moulia, B. (2008). A scaling law for the effects of architecture and allometry on tree vibration modes suggests a biological tuning to modal compartmentalization. *Am. J. Bot.* 95, 1523–1537. doi: 10.3732/ajb.0800161

Routier-Kierzkowska, A. L., Weber, A., Kochova, P., Felekis, D., Nelson, B. J., Kuhlemeier, C., et al. (2012). Cellular force microscopy for *in vivo* measurements of plant tissue mechanics. *Plant Physiol.* 158, 1514–1522. doi: 10.1104/pp.111.191460

Sato, K., Adachi, T., Matsuo, M., and Tomita, Y. (2005). Quantitative evaluation of threshold fiber strain that induces reorganization of cytoskeletal actin fiber structure in osteoblastic cells. *J. Biomech.* 38, 1895–1901. doi: 10.1016/j.jbiomech.2004.08.012

Schriefer, J., Warden, S., Saxon, L., Robling, A., and Turner, C. (2005). Cellular accomodation and the response of bone to mechanical loading. *J. Biomech.* 38, 1838–1845. doi: 10.1016/j.jbiomech.2004.08.017

Sellier, D., Brunet, Y., and Fourcaud, T. (2008). A numerical model of tree aerodynamic response to a turbulent airflow. *Forestry* 81, 279–297. doi: 10.1093/forestry/cpn024

Sierra-De-Grado, R., Pando, V., Martinez-Zurimendi, P., Penalvo, A., Bascones, E., and Moulia, B. (2008). Biomechanical differences in the stem straightening process among Pinus pinaster provenances. A new approach for early selection of stem straightness. *Tree Physiol.* 28, 835–846. doi: 10.1093/treephys/28.6.835

Silk, W. K., and Erickson, R. O. (1980). Local biosynthesis rates of cytoplasmic constituents in growing tissue. *J. Theor. Biol.* 83, 701–703. doi: 10.1016/0022-5193(80)90197-6

Sotomayor, M., and Shulten, K. (2014). Molecular dynamics study of gating in the mechanosensitive channel of small conductance MscS. *Biophys. J.* 87, 3050–3065. doi: 10.1529/biophysj.104.046045

Supatto, W., Debarre, D., Moulia, B., Brouzes, E., Martin, J. L., Farge, E., et al. (2005). *In vivo* modulation of morphogenetic movements in *Drosophila* embryos with femtosecond laser pulses. *Proc. Natl. Acad. Sci. U.S.A.* 102, 1047–1052. doi: 10.1073/pnas.0405316102

Tardieu, F. (2003). Virtual plants: modelling as a tool for the genomics of tolerance to water deficit. *Trends Plant Sci.* 8, 9–14. doi: 10.1016/S1360-1385(02)00008-0

Telewski, F. W. (2006). A unified hypothesis of mechanoperception in plants. *Am. J. Bot.* 93, 1466–1476. doi: 10.3732/ajb.93.10.1466

Telewski, F. W., and Pruyn, M. L. (1998). Thigmomorphogenesis: a dose response to flexing in Ulmus americana seedlings. *Tree Physiol.* 18, 65–68. doi: 10.1093/treephys/18.1.65

Tixier, A., Badel, E., Franchel, J., Lakhal, W., Leblanc-Fournier, N., Moulia, B., et al. (2014). Growth and molecular responses to long-distance stimuli in poplars: bending vs flame wounding. *Physiol. Plant.* 150, 225–237. doi: 10.1111/ppl.12089

Traas, J., and Hamant, O. (2009). From genes to shape: understanding the control of morphogenesis at the shoot meristem in higher plants using systems biology. *C. R. Biol.* 332, 974–985. doi: 10.1016/j.crvi.2009.09.008

Traas, J., and Moneger, F. (2010). Systems biology of organ initiation at the shoot apex. *Plant Physiol.* 152, 420–427. doi: 10.1104/pp.109.150409

Villaverde, A. F., and Banga, J. R. (2014). Reverse engineering and identification in systems biology: strategies, perspectives and challenges. *J. R. Soc. Interface* 11:20130505. doi: 10.1098/Rsif.2013.0505

Conflict of Interest Statement: The authors declare that the research was conducted in the absence of any commercial or financial relationships that could be construed as a potential conflict of interest.

Received: 14 August 2014; accepted: 20 January 2015; published online: 23 February 2015.

*Citation: Moulia B, Coutand C and Julien J-L (2015) Mechanosensitive control of plant growth: bearing the load, sensing, transducing, and responding. Front. Plant Sci. **6**:52. doi: 10.3389/fpls.2015.00052*

This article was submitted to Plant Physiology, a section of the journal Frontiers in Plant Science.

frontiers in
PLANT SCIENCE

MINI REVIEW ARTICLE
published: 14 August 2014
doi: 10.3389/fpls.2014.00401

To respond or not to respond, the recurring question in plant mechanosensitivity

Nathalie Leblanc-Fournier[1,2] *, Ludovic Martin[3], Catherine Lenne[1,2] and Mélanie Decourteix[1,2]

[1] Clermont Université – Université Blaise Pascal, UMR547 PIAF, Clermont-Ferrand, France
[2] INRA, UMR547 PIAF, Clermont-Ferrand, France
[3] Laboratoire de Biologie du Développement des Plantes, UMR 7265, Centre National de la Recherche Scientifique/Commissariat à l'Energie Atomique/Aix-Marseille Université, Saint-Paul-lez-Durance, France

Edited by:
Sara Puijalon, Université Lyon 1, France

Reviewed by:
Janet Braam, Rice University, USA
Vasileios Fotopoulos, Cyprus University of Technology, Cyprus
Frank W. Telewski, Michigan State University, USA

***Correspondence:**
Nathalie Leblanc-Fournier, Clermont Université – Université Blaise Pascal, UMR547 PIAF, BP 10448, F-63000 Clermont-Ferrand, France
e-mail: nathalie.leblanc@univ-bpclermont.fr

In nature, terrestrial plants experience many kinds of external mechanical stimulation and respond by triggering a network of signaling events to acclimate their growth and development. Some environmental cues, especially wind, recur on time scales varying from seconds to days. Plants thus have to adapt their sensitivity to such stimulations to avoid constitutive activation of stress responses. The study of plant mechanosensing has been attracting more interest in the last two decades, but plant responses to repetitive mechanical stimulation have yet to be described in detail. In this mini review, alongside classic experiments we survey recent descriptions of the kinetics of plant responses to recurrent stimulation. The ability of plants to modulate their responses to recurrent stimulation at the molecular, cellular, or organ scale is also relevant to other abiotic stimuli. It is possible that plants reduce their responsiveness to environmental signals as a function of their recurrence, recovering full sensitivity several days later. Finally, putative mechanisms underlying mechanosensing regulation are discussed.

Keywords: mechanosensitivity, accommodation, mechanical stimulus, abiotic stress, wind, acclimation to stress

INTRODUCTION

Mechanosensing is an important factor regulating plant growth and development (Hamant, 2013). Mechanical cues may be internal signals produced during tissue or cellular expansion (Ingber, 2005; Hamant et al., 2008) or external signals from the environment, mainly from wind (Moulia et al., 2011). To understand the influence of wind on plant development, different methods have been used in the laboratory to simulate the mechanical effect of wind, like bending, touching, shaking, or brushing the aboveground parts of plants. These mechanical stimulations result in a thigmomorphogenetic syndrome generally characterized by reduction in stem height, modification of the mechanical properties of the stem, increase in root biomass and local increases in stem radial growth depending on the species (Telewski, 2006).

These physiological responses that alter the growth trajectory and form of the plants are thought to be involved in a long-term process of acclimation, tending to reduce the impact of subsequent mechanical stimulation (Moulia et al., 2006; Telewski, 2006). However, less is known about how plants respond to rapid recurrent mechanical stimulations. Wind typically induces repeated flexing of plant organs at different frequencies (De Langre, 2008). Plant stems may oscillate at frequencies in the range of 1–5 Hz in wind, corresponding to 60–300 bends per minute (Rodriguez et al., 2008; Der Loughian et al., 2014). In temperate climates, windy and calm days alternate on a time scale of several days (Stull, 1988). If every response to each mechanical stimulus was of the same magnitude, plants would invest greatly in withstanding mechanical perturbation to the detriment of growth. Plants thus need to permanently fine-tune their response to mechanical stimulation in order to avoid the cost of a constitutive protection system. This holds especially true for trees because of their long-term growth period and their high stature. There is some experimental evidence that plants reduce their responsiveness to mechanical signals as a function of their mechanical history. This acclimation of mechanosensitivity has been named accommodation (Moulia et al., 2011) in reference to the cellular accommodation that bones undergo in response to external mechanical loading (Schriefer et al., 2005). Here we summarize and discuss experimental observations of plants responding to recurrent mechanical simulation. Regulation of plant responsiveness to recurrent cold and drought stress is compared to mechanosensitivity accommodation. Finally, preliminary evidence and speculation about the molecular mechanisms involved in such processes are discussed.

SATURATION AND DESENSITIZATION, WAYS TO DEAL WITH SUCCESSIVE MECHANICAL STIMULATION

When studying variation in plant responsiveness to successive mechanical stimulations, two parameters need to be taken into account. (i) The intensity of the mechanical stimulation should be quantified so it can be reproducibly and repeatedly applied. (ii) The kinetics of plant responses to single and successive stimulations should be characterized.

Formerly, a first approach to investigate plant mechanosensitivity was to quantify and compare the effect of different magnitudes or numbers of mechanical stimulations. When *Phaseolus vulgaris* internodes are rubbed repeatedly (following a standardized method), the amount of mechanical stimulation correlates positively with the extent of internode elongation, but the sensory function becomes saturated even with small amounts of rubbing

(Jaffe et al., 1980). To mimic the effect of wind, mechanical experiments on tree species are usually done by bending the stem for a few seconds then releasing it. This transitory stimulus (which will be here called bending) has the added advantage of allowing the experimenter to control how much strain is applied, so the physical stimulus perceived by plant cells is known (Coutand and Moulia, 2000; Coutand et al., 2009). In such experiments on *Ulmus americana*, no increment in the secondary growth response was detected after three weeks when stimulation frequency was increased from 5–80 bends a day (Telewski and Pruyn, 1998). In another set of observations on *Prunus persica,* stems were bent in a controlled manner eight times a day. Over the 6 weeks of the experiment, the stimulus of repeated bending affected growth less, even when the actual strains applied were increased slightly over time to compensate for stem radial growth (Coutand et al., 2008). Altogether, these results suggest that saturation of either the mechanosensory or the response systems was reached. However, because the responses were measured at the end of several weeks of treatment, it was not possible to exclude the possibility that plant sensitivity was adjusted with each successive bend and that only some of the first mechanical treatments were responsible for the observed responses. In poplar, controlled stem flexing at a sub-saturation level was coupled with kinetics analyses of the responses to each successive bending. The result was a rapid reduction in responsiveness of both radial growth and gene expression (Martin et al., 2010). In particular, these experiments showed that the second bending, 24 h after the first, was markedly weaker in inducing four early mechanoresponsive genes encoding, respectively, two calmodulins, a C2H2 transcription factor (**Figure 1A**) and a xyloglucan endotransglycosylase. As the abundance of these genes transcripts returned to basal levels before 24 h (Martin et al., 2009), the expression levels observed could only have been due to the second bending and not due to response saturation. These data demonstrated that a single bending is sufficient to initiate a change in plant responsiveness, in this case a down-regulation or desensitization, to subsequent bending. In *Arabidopsis*, an even faster desensitization occurred after unquantified successive touch stimulation (Arteca and Arteca, 1999). As soon as 1 h after the first stimulation, a second touch was less effective in inducing *ACS6* expression, a gene encoding 1-aminocyclopropane-1-carboxylic acid (ACC) synthase enzyme (**Figure 1A**). In the conditions described above

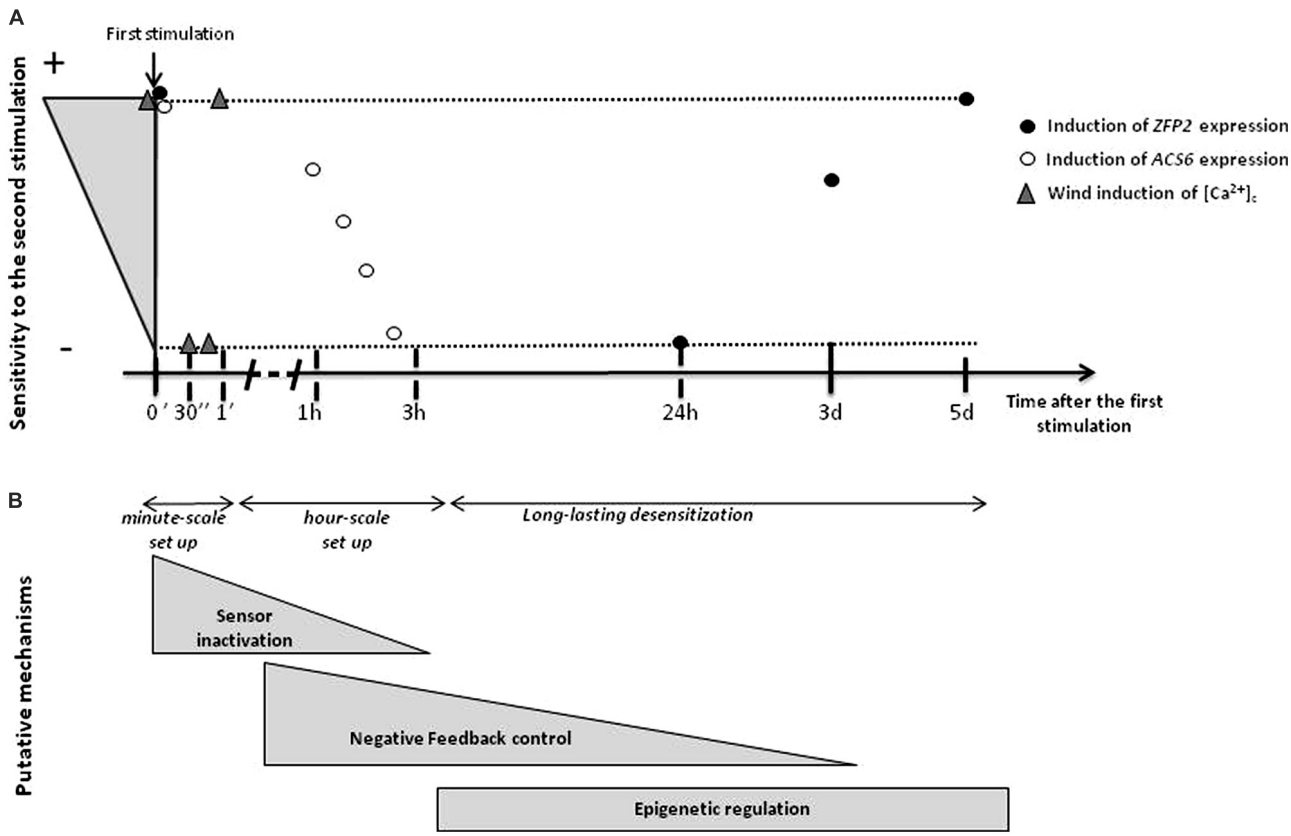

FIGURE 1 | (A) Desensitization kinetics set up in response to recurrent mechanical stimulations applied at high frequency in case of wind induced Ca^{2+}cytosolic concentration in *Nicotiana tabacum* (Knight et al., 1992) or at low frequency in case of touch-induced *ACS6* expression in *Arabidopsis* (Arteca and Arteca, 1999) and bending-induced *ZFP2* expression in *Populus tremula x P. alba* (Martin et al., 2010). **(B)** Hypothetical mechanisms for the short-term or long-lasting desensitization: (i) alterations of perception through sensor turnover, modification or in activation, (ii) negative feedback from long-term accumulation of signaling molecules or transcription factors and (iii) information storage through epigenetic regulation.

after the second bending of the poplar stem, about seven days without any bending stimulus were necessary to recover the full capacity for induction of gene expression (**Figure 1A**, Martin et al., 2010), suggesting that this state of desensitization to mechanical loads lasts for several days. Such desenzitisation was also observed in case of the typical defensive leaf-folding reflex of Mimosa plants (Gagliano et al., 2014). However, in this case, the resenzitisation was assessed with a mechanical disturbance different from the one responsible of the desenzitisation.

The above kinetics could be said to more closely mimic the alternation between windy and calm days in nature rather than oscillations in the wind at frequencies between 1 and 5 Hz (Rodriguez et al., 2008). The effects of mechanical treatments that recur at short intervals were investigated by analyzing rapid cellular events. Knight et al. (1992) showed that wind-induced mechanical stimulations of *Nicotiana* seedlings generate peaks of elevated cytosolic calcium concentrations. The amplitudes of calcium peaks diminished when stimulations were repeated every 5 s until cells became refractory to further stimulation. Full desensitization was attained after about 6–7 stimulations (about 30 s of intermittent stimulation) and full responsiveness was recovered less than 60 s later when stimulation was decreased (**Figure 1A**). However, attenuation of this type of calcium response was not detected in *Arabidopsis* roots when the two touch stimuli were separated by 20 s (Monshausen et al., 2009).

Intuitively we would expect down-regulation of sensitivity upon prolonged mechanical or recurrent stimulation to be a key component of any biological sensory process. However, kinetics and mechanistic data are still lacking to fully describe desensitization. Moreover, the link between the decrease in responsiveness of mechanoresponsive genes and the regulation of mechanoperception is yet to be elucidated.

FINE-TUNING SENSITIVITY, A RECURRING THEME

Modifying plant responsiveness is not restricted to recurrent mechanical stimuli as other abiotic stimuli act in a similar way. However, a plethora of terminologies have been used to describe these different stress situations which may mask some of the similarities. Generally, altered physiological responses to recurrent abiotic stress that allow a plant to maintain its performances despite the stress, is referred to as "acclimation" or "hardening." For biotic stress, the term "priming" is usually preferred, and is defined as "the phenomenon whereby previous exposure makes a plant more resistant to future exposure" (Bruce et al., 2007). When the response to a stimulus is modified at the cellular or molecular level, authors predominantly use terms to describe the state of sensitivity of the cells. For example, to describe how peaks of cytosolic free calcium concentration decrease with repeated stimulation/stress, the terms "attenuation" or "desensitization" are used (Knight et al., 1992; Plieth et al., 1999). Bruce et al. (2007) suggested the general term of "stress imprint" to designate "a genetic or biochemical modification of a plant that occurs after stress exposure that causes future responses to future stresses to be different." This is less anthropomorphic than the concept of "memory" or "training," but many authors are using "plant stress memory" to encapsulate the idea that plants store information related to a first stress exposure, leading to increased or decreased responses to subsequent exposures (Galis et al., 2009; Stork et al., 2009; Ding et al., 2013).

The time-courses of desensitization–resensitization phenomena have barely been investigated. The kinetics of the generation of peaks in intracellular calcium concentration in response to cold were studied in *Arabidopsis* roots with regimes of recurrent cold stimulation at a range of intervals on the time-scale of several minutes. As in wind-stimulated *Nicotiana* seedlings (Knight et al., 1992), attenuation of the height of calcium peaks was observed and desensitization started minutes after the first stimulation and lasted for a minimum of 30 min before re-sensitization occurred (Plieth et al., 1999). However, this desensitization was overridden if the intensity of the subsequent stimulus was increased (i.e., with a decrease in the temperature). These phases of desensitization or attenuation at the calcium level could avoid an over-mobilization of internal and external stores of calcium which would hamper any further response.

Exposing *Arabidopsis* plants to cold temperatures (+4°C) also triggers rapid modifications in gene expression. One example is the up-regulation of genes encoding members of the AP2/EREBP family of DNA-binding proteins, the cold binding factors (CBFs; Gilmour et al., 1998). Using the accumulation of CBF transcripts as a marker, Zarka et al. (2003) found that the cold-sensing mechanism can be desensitized within a few hours of exposure to a low temperature. In the case of desensitization to +4°C, resensitization (i.e., recovery of *CBF* induction at this same temperature), took between 8 and 24 h of re-exposure to warm temperatures. As for the calcium response, the desensitized state could be overridden by a further decrease in temperature.

In the phenomena described above, desensitization is a way for plants to avoid over-responding, using excess signaling molecules (e.g., calcium) or saturating the sensing machinery. However, in the case of plant defense (Galis et al., 2009; Conrath, 2011) or dehydration (Ding et al., 2012), adjustments in plant sensitivity can also make plants more responsive to subsequent exposures, in what we could call hypersensitization. For example, *Arabidopsis* plants trained by a first exposure to a dehydration stress wilt more slowly than untrained plants when they are exposed a second time. When the plants are subjected to cycles of 2 h of dehydration and 22 h of rehydration, "trainable" genes (e.g., *RD29B*, *RAB18*) produced higher transcript levels in response to subsequent stresses than to the initial stress, whereas "non-trainable" genes expressed similar transcript levels for each stress events (e.g., *RD29A* and *COR15A*). This "transcriptional memory" persisted for at least 5 days and was lost after 7 days (Ding et al., 2012). More recently, a large-scale transcriptional analysis revealed there are 1963 such "memory" genes in the *Arabidopsis* transcriptional network triggered by dehydration stress (Ding et al., 2013).

To conclude, different plant species modify their sensitivity to abiotic stresses at the physiological, cellular and molecular levels with very different kinetics. However, it should be noted that the different mechanisms have some features in common despite the very different environmental cues. For example, at the level of the molecular response, desensitization is usually rapid and lasts for several days.

HOW TO CONTROL DESENSITIZATION

If desensitization occurs in response to a variety of recurring biotic and abiotic cues, how have the common features of responsiveness regulation emerged in these different signaling pathways? What are the underlying mechanisms? Three potential mechanisms could be proposed depending on the kinetics of their occurrence (**Figure 1B**).

ALTERATIONS OF PERCEPTION THROUGH SENSOR TURNOVER, MODIFICATION OR INACTIVATION

The natures of potentially numerous touch, cold, and osmotic sensors are still to be fully elucidated. As discussed by Telewski (2006), abiotic stimuli cause membrane deformation by modifying turgor pressure or membrane fluidity, and some are also sensed as mechanical stimuli by living cells. Two classes of putative mechanosensors are currently under investigation, stretch-activated channels and transmembrane proteins inserted into the cell wall/plasma membrane/cytoskeleton (CWPMC) network (Monshausen and Gilroy, 2009; Haswell and Monshausen, 2013).

Two types of stretch-activated channels have been identified so far. Mid1-complementing activity (MCA) proteins are calcium channels (Nakagawa et al., 2007; Yamanaka et al., 2010) and MscS-like (MSL) family members are non-selective channels identified based on homology to bacterial MscS (Kung, 2005; Haswell et al., 2008). Is the rapid desensitization of calcium influx after repeated cold and mechanical sensing linked to the gating kinetics of these channels? In bacteria, results of patch-clamp experiments have indeed shown that MscS channels are inactivated after prolonged exposure to membrane tension (Koprowski and Kubalski, 1998; Levina et al., 1999). In plants, the only gating kinetics obtained for a stretch-activated channel was for the *Arabidopsis* MSL10 channel, but no inactivation of the channel was detected (Maksaev and Haswell, 2012).

The initial sensor of mechanical stress could also be a component of the CWPMC network like receptor-like kinase (RLK) transmembrane proteins (Monshausen and Gilroy, 2009; Haswell and Monshausen, 2013). Whereas a direct link between membrane protein kinases and mechanosensing has not been established, several reports suggest that the cytoskeleton, through its tethering with transmembrane proteins, could be involved. In the *Arabidopsis* meristem, cortical microtubules re-oriented rapidly (within 6 h) in the presence of a mechanical stress (Hamant et al., 2008). A more recent study demonstrated that katanin, a microtubule-severing protein, is required for cell responsiveness to the mechanical stresses generated by growth in *Arabidopsis* meristem cells (Uyttewaal et al., 2012). This provides the outline for a model in which microtubule dynamics allow the cell to respond efficiently to mechanical forces (Nick, 2013).

NEGATIVE FEEDBACK FROM LONG-TERM ACCUMULATION OF SIGNALING MOLECULES OR TRANSCRIPTION FACTORS

Peaks of cytosolic calcium accumulation are a common feature in many stress signaling pathways. As this calcium response is attenuated by repetitive stimulation, Ca^{2+} influx and efflux transporters regulating calcium homeostasis could be considered as components of a "mechanical memory." Cyclic nucleotide-gated channels (CNGCs) can mediate fluxes of Ca^{2+} ions, and binding of Ca^{2+}/calmodulin inactivates CNGCs (Hua et al., 2003; Ali et al., 2006). Thus, the negative action of calmodulin or calmodulin-like proteins on CNGC activity could diminish plant responsiveness through a direct feedback pathway restricting Ca^{2+} influx into plant cells. Genes encoding calmodulin or calmodulin-like proteins are up-regulated early after touch or stem bending (Depège et al., 1997; Lee et al., 2005; Martin et al., 2009), but the involvement of CNGC channels has not been directly addressed in relation to mechanical loading. Glutamate receptors are nonselective cation channels activated by glutamate and glycine (Qi et al., 2006; Stephens et al., 2008) that mediate an increase in cytosolic Ca^{2+} upon cold stress and touch (Meyerhoff et al., 2005). When a second glutamate treatment was applied after the first stimulus, no additional Ca^{2+} response was observed, suggesting that these receptors remain in a putative desensitized state for 1 h (Meyerhoff et al., 2005). Again, the potential role of such glutamate receptors in the mechanotransduction pathway needs to be established.

The desensitization process could also involve transcription factors exerting a negative feedback control on the first stages of the mechanotransduction pathway. In poplar, *PtaZFP2*, a gene encoding a C2H2 transcription factor, is rapidly up-regulated after stem bending (Martin et al., 2009). In *PtaZFP2*-overexpressing poplars, the up-regulation of several mechanoresponsive genes was much weaker after stem bending than in wild-type plants (Martin et al., 2014). Thus, PtaZFP2 negatively modulates poplar responsiveness to mechanical stimulation. Among the genes downstream of PtaZFP2, *CML42*, a calmodulin-like encoding gene, and *WRKY53* and *WRKY40*, transcription factor encoding genes are up-regulated. The *Arabidopsis* homologs of these poplar genes have been described as negative regulators of plant defense responses (Xu et al., 2006; Vadassery et al., 2012). Thus, in concert with these molecular suppressors, PtaZFP2 could reduce the reactivation of the mechanical signaling pathway when stems are bent again.

INFORMATION STORAGE THROUGH EPIGENETIC REGULATION

One intriguing result is that desensitization of the expression of mechanosensitive genes to mechanical stimuli lasts at least three days (Martin et al., 2010). Bruce et al. (2007) suggested epigenetic changes could be a mechanism for long-term information storage after various abiotic stresses. Chromatin remodeling during drought and cold stresses, which alters accessibility of genes to proteins regulating transcription, has received more attention recently (Kim et al., 2008, 2010; Chinnusamy and Zhu, 2009; To and Kim, 2014). For example, the dynamics of the chromatin status of four stress-responsive candidate genes were analyzed during recovery (i.e., rehydration) of *Arabidopsis* from drought stress (Kim et al., 2012). These studies focused on changes in acetylation (ac) and methylation (me) of lysine (K) residues of histone H3 N-terminal tails. While the proportion of H3K9ac was reduced rapidly during rehydration, H3K4me3 decreased more gradually and was maintained at low levels on the drought-inducible genes even up to 5 h after rehydration. As H3K4me3 is correlated with

positive gene responsiveness, the authors suggested that this epigenetic mark of stress memory might help plants respond more effectively to subsequent stresses (Kim et al., 2012; To and Kim, 2014). Indeed, in the *Arabidopsis* H3K4 methyltransferase mutant *atx1*, which is defective in methylating H3K4, the responsiveness of drought-stress inducible genes during the second stress exposure does not increase as much as in wild-type (Ding et al., 2011, 2012).

In an example of cold sensing, the *hos15 Arabidopsis* mutant showed modifications in both histone deacetylation and cold tolerance (Zhu et al., 2008). HOS15 is a WD-40 protein similar to human transducin-beta like protein, a component of repressor complexes involved in histone deacetylation. Apart from an analysis of DNA methylation in *Bryonia* internodes stimulated by rubbing (Galaud et al., 1993), information about epigenetic regulation during plant responses to mechanical loads is scarce. However, some structural features of the aforementioned poplar transcription factor PtaZFP2 indicate that it could be involved in histone modification. The PtaZFP2 protein contains a DLN-box (Gourcilleau et al., 2011), also known as an ERF-associated amphiphilic repression motif (Ohta et al., 2001; Kazan, 2006). Recently, transcription factors containing this motif were reported to exhibit repression activity via histone deacetylation and stimulation of heterochromatin formation in *Arabidopsis* (Causier et al., 2012), so this is preliminary evidence on which to base wider study of epigenetic regulation of responsiveness to mechanical stimuli.

CONCLUSION

The regulation of plant mechanosensing could be an important part of acclimation to wind by modulating the magnitude and duration of the response and preventing costly investment in reducing or redirecting growth. Modulation of responsiveness could also occur in response to internal mechanical signals produced during tissue or cellular expansion or maturation as part of morphogenesis. The mechanisms underlying this phenomenon are largely unknown essentially because there is so little data on the nature of the presumed mechanosensors or the timing of the regulation. Although some mechanisms are beginning to be identified for other abiotic stresses, they remain largely hypothetical in the case of mechanical stimulation such as bending caused by wind. More high-resolution description of the timing of plant responses at the tissue and cellular level would help to demonstrate the importance of mechanosensing regulation for plant acclimation.

ACKNOWLEDGMENTS

This work has received support from the French Agence Nationale de la Recherche, grant ANR-09-BLAN-0245-01. We thank Emendo (Boston, UK) for editing the English.

REFERENCES

Ali, R., Zielinski, R. E., and Berkowitz, G. A. (2006). Expression of plant cyclic nucleotide-gated cation channels in yeast. *J. Exp. Bot.* 57, 125–138. doi: 10.1093/jxb/erj012

Arteca, J. M., and Arteca, R. N. (1999). A multi-responsive gene encoding 1-aminocyclopropane-1-carboxylate synthase (ACS6) in mature *Arabidopsis* leaves. *Plant Mol. Biol.* 39, 209–219. doi: 10.1023/A:1006177902093

Bruce, T. J. A., Matthes, M. C., Napier, J. A., and Pickett, J. A. (2007). Stressful 'memories' of plants: evidence and possible mechanisms. *Plant Sci.* 173, 603–608. doi: 10.1016/j.plantsci.2007.09.002

Causier, B., Ashworth, M., Guo, W., and Davies, B. (2012). The TOPLESS interactome: a framework for gene repression in *Arabidopsis*. *Plant Physiol.* 158, 423–438. doi: 10.1104/pp.111.186999

Chinnusamy, V., and Zhu, J. K. (2009). Epigenetic regulation of stress responses in plants. *Curr. Opin. Plant Biol.* 12, 133–139. doi: 10.1016/j.pbi.2008.12.006

Conrath, U. (2011). Molecular aspects of defence priming. *Trends Plant Sci.* 16, 524–531. doi: 10.1016/j.tplants.2011.06.004

Coutand, C., Dupraz, C., Jaouen, G., Ploquin, S., and Adam, B. (2008). Mechanical stimuli regulate the allocation of biomass in trees: demonstration with young *Prunus avium* trees. *Ann. Bot.* 101, 1421–1432. doi: 10.1093/aob/mcn054

Coutand, C., Martin, L., Leblanc-Fournier, N., Decourteix, M., Julien, J. L., and Moulia, B. (2009). Strain mechanosensing quantitatively controls diameter growth and the level of expression of the PtaZFP2 mechanosensitive gene in poplar. *Plant Physiol.* 151, 223–232. doi: 10.1104/pp.109.138164

Coutand, C., and Moulia, B. (2000). Biomechanical study of the effect of a controlled bending on tomato stem elongation: local strain sensing and spatial integration of the signal. *J. Exp. Bot.* 51, 1825–1842. doi: 10.1093/jexbot/51.352.1825

De Langre, E. (2008). Effects of wind on plants. *Annu. Rev. Fluid Mech.* 40, 141–168. doi: 10.1146/annurev.fluid.40.111406.102135

Depège, N., Thonat, C., Coutand, C., Julien, J. L., and Boyer, N. (1997). Morphological responses and molecular modifications in tomato plants after mechanical stimulation. *Plant Cell Physiol.* 38, 1127–1134. doi: 10.1093/oxfordjournals.pcp.a029097

Der Loughian, C., Tadrist, L., Allain, J. M., Diener, J., Moulia, B., and de Langre, E. (2014). Measuring local and global vibration modes in model plants. *C. R. Méc.* 342, 1–7. doi: 10.1016/j.crme.2013.10.010

Ding, Y., Avramova, Z., and Fromm, M. (2011). Two distinct roles of *ARABIDOPSIS* HOMOLOG OF TRITHORAX1 (ATX1) at promoters and within transcribed regions of ATX1-regulated genes. *Plant Cell* 23, 350–363. doi: 10.1105/tpc.110.080150

Ding, Y., Fromm, M., and Avramova, Z. (2012). Multiple exposures to drought 'train' transcriptional responses in *Arabidopsis*. *Nat. Commun.* 3, 740. doi: 10.1038/ncomms1732

Ding, Y., Liu, N., Virlouvet, L., Riethoven, J. J., Fromm, M., and Avramova, Z. (2013). Four distinct types of dehydration stress memory genes in *Arabidopsis thaliana*. *BMC Plant Biol.* 13:229. doi: 10.1186/1471-2229-13-229

Gagliano, M., Renton, M., Depczynski, M., and Mancuso, S. (2014). Experience teaches plants to learn faster and forget slower in environments where it matters. *Oecologia* 175, 63–72. doi: 10.1007/s00442-013-2873-7

Galaud, J. P., Gaspar, T., and Boyer, N. (1993). Inhibition of internode growth due to mechanical stress in *Bryonia dioica*: relationship between changes in DNA methylation and ethylene metabolism. *Physiol. Plant.* 87, 25–30. doi: 10.1111/j.1399-3054.1993.tb08786.x

Galis, I., Gaquerel, E., Pandey, S., and Baldwin, I. T. (2009). Molecular mechanisms underlying plant memory in JA-mediated defence responses. *Plant Cell Environ.* 32, 617–627. doi: 10.1111/j.1365-3040.2008.01862.x

Gilmour, S. J., Zarka, D. G., Stockinger, E. J., Salazar, M. P., Houghton, J. M., and Thomashow, M. F. (1998). Low temperature regulation of the *Arabidopsis* CBF family of AP2 transcriptional activators as an early step in cold-induced COR gene expression. *Plant J.* 16, 433–442. doi: 10.1046/j.1365-313x.1998.00310.x

Gourcilleau, D., Lenne, C., Armenise, C., Moulia, B., Julien, J. L., Bronner, G., et al. (2011). Phylogenetic study of plant Q-type C2H2 zinc finger proteins and expression analysis of poplar genes in response to osmotic, cold and mechanical stresses. *DNA Res.* 18, 77–92. doi: 10.1093/dnares/dsr001

Hamant, O. (2013). Widespread mechanosensing controls the structure behind the architecture in plants. *Curr. Opin. Plant Biol.* 16, 654–660. doi: 10.1016/j.pbi.2013.06.006

Hamant, O., Heisler, M. G., Jonsson, H., Krupinski, P., Uyttewaal, M., Bokov, P., et al. (2008). Developmental patterning by mechanical signals in *Arabidopsis*. *Science* 322, 1650–1655. doi: 10.1126/science.1165594

Haswell, E. S., and Monshausen, G. B. (2013). A force of nature: molecular mechanisms of mechanoperception in plants. *J. Exp. Bot.* 64, 4663–4680. doi: 10.1093/jxb/ert204

Haswell, E. S., Peyronnet, R., Barbier-Brygoo, H., Meyerowits, E. M., and Frachisse, J. M. (2008). Two MscS homologs provide mechanosensitive channel activities in the *Arabidopsis* root. *Curr. Biol.* 18, 730–734. doi: 10.1016/j.cub.2008.04.039

Hua, B. G., Mercier, R. W., Zielinski, R. E., and Berkowitz, G. A. (2003). Functional interaction of calmodulin with a plant cyclic nucleotide gated cation channel. *Plant Physiol. Biochem.* 41, 945–954. doi: 10.1016/j.plaphy.2003.07.006

Ingber, D. E. (2005). Mechanical control of tissue growth: function follows form. *Proc. Natl. Acad. Sci. U.S.A.* 102, 11571–11572. doi: 10.1073/pnas.0505939102

Jaffe, M. J., Biro, R., and Bridle, K. (1980). Thigmomorphogenesis: calibration of the parameters of the sensory function in beans. *Physiol. Plant.* 49, 410–416. doi: 10.1111/j.1399-3054.1980.tb03326.x

Kazan, K. (2006). Negative regulation of defense and stress genes by EAR motif containing repressors. *Trends Plant Sci.* 11, 109–112. doi: 10.1016/j.tplants.2006.01.004

Kim, J. M., To, T. K., Ishida, J., Matsui, A., Kimura, H., and Seki, M. (2012). Transition of chromatin ctatus during the process of recovery from drought stress in *Arabidopsis thaliana. Plant Cell Physiol.* 53, 847–856. doi: 10.1093/pcp/pcs053

Kim, J. M., To, T. K., Ishida, J., Morosawa, T., Kawashima, M., Matsui, A., et al. (2008). Alterations of lysine modifications on the histone H3 N-tail under drought stress conditions in *Arabidopsis thaliana. Plant Cell Physiol.* 49, 1580–1588. doi: 10.1093/pcp/pcn133

Kim, J. M., To, T. K., Nishioka, T., and Seki, M. (2010). Chromatin regulation functions in plant abiotic stress responses. *Plant Cell Environ.* 33, 604–611. doi: 10.1111/j.1365-3040.2009.02076.x

Knight, M. R., Smith, S. M., and Trewavas, A. J. (1992). Wind-induced plant motion immediately increases cytosolic calcium. *Proc. Natl. Acad. Sci. U.S.A.* 89, 4967–4971. doi: 10.1073/pnas.89.11.4967

Koprowski, P., and Kubalski, A. (1998). Voltage-independent adaptation of mechanosensitive channels in *Escherichia coli* protoplasts. *J. Membr. Biol.* 164, 253–262. doi: 10.1007/s002329900410

Kung, C. (2005). A possible unifying principle for mechanosensation. *Nature* 436, 647–654. doi: 10.1038/nature03896

Lee, D., Polisensky, D. H., and Braam, J. (2005). Genome-wide identification of touch- and darkness-regulated Arabidopsis genes: a focus on calmoduline-like and XTH genes. *New Phytol.* 165, 429–444. doi: 10.1111/j.1469-8137.2004.01238.x

Levina, N., Totemeyer, S., Stokes, N. R., Louis, P., Jones, M. A., and Booth, I. R. (1999). Protection of *Escherichia coli* cells against extreme turgor by activation of MscS and MscL mechanosensitive channels: identification of genes required for MscS activity. *EMBO J.* 18, 1730–1737. doi: 10.1093/emboj/18.7.1730

Maksaev, G., and Haswell, E. S. (2012). MscS-Like10 is a stretch-activated ion channel from *Arabidopsis thaliana* with a preference for anions. *Proc. Natl. Acad. Sci. U.S.A.* 109, 19015–19020. doi: 10.1073/pnas.1213931109

Martin, L., Decourteix, M., Badel, E., Huguet, S., Moulia, B., Julien, J. L., et al. (2014). The zinc finger protein PtaZFP2 negatively controls stem growth and gene expression responsiveness to external mechanical loads in poplar. *New Phytol.* 203, 168–181. doi: 10.1111/nph.12781

Martin, L., Leblanc-Fournier, N., Azri, W., Lenne, C., Henry, C., Coutand, C., et al. (2009). Characterization and expression analysis under bending and other abiotic factors of PtaZFP2, a poplar gene encoding a Cys2/His2 zinc finger protein. *Tree Physiol.* 29, 125–136. doi: 10.1093/treephys/tpn011

Martin, L., Leblanc-Fournier, N., Julien, J. L., Moulia, B., and Coutand, C. (2010). Acclimation kinetics of physiological and molecular responses of plants to multiple mechanical loadings. *J. Exp. Bot.* 61, 2403–2412. doi: 10.1093/jxb/erq069

Meyerhoff, O., Müller, K., Roelfsema, M. R., Latz, A., Lacombe, B., Hedrich, R., et al. (2005). AtGLR3.4, a glutamate receptor channel-like gene is sensitive to touch and cold. *Planta* 222, 418–427. doi: 10.1007/s00425-005-1551-3

Monshausen, G. B., Bibikova, T. N., Weisenseel, M. H., and Gilroy, S. (2009). Ca^{2+} regulates reactive oxygen species production and pH during mechanosensing in *Arabidopsis* roots. *Plant Cell* 21, 2341–2356. doi: 10.1105/tpc.109.068395

Monshausen, G. B., and Gilroy, S. (2009). Feeling green: mechanosensing in plants. *Trends Cell Biol.* 19, 228–235. doi: 10.1016/j.tcb.2009.02.005

Moulia, B., Coutand, C., and Lenne, C. (2006). Posture control and skeletal mechanical acclimation in terrestrial plants: implications for mechanical modeling of plant architecture. *Am. J. Bot.* 93, 1477–1489. doi: 10.3732/ajb.93.10.1477

Moulia, B., Der Loughian, C., Bastien, R., Martin, L., Rodríguez, M., Gourcilleau, D., et al. (2011). "Integrative mechanobiology of growth and architectural development in changing mechanical environments," in *Mechanical Integration of Plant Cells and Plants Springer, Series: Signalling and Communication in Plants*, ed. P. Wojtaszek (Berlin: Springer-Verlag), 269–302.

Nakagawa, Y., Katagiri, T., Shinozaki, K., Qi, Z., Tatsumi, H., Furuichi, T., et al. (2007). *Arabidopsis* plasma membrane protein crucial for Ca^{2+} influx and touch sensing in roots. *Proc. Natl. Acad. Sci. U.S.A.* 104, 3639–3644. doi: 10.1073/pnas.0607703104

Nick, P. (2013). Microtubules, signalling and abiotic stress. *Plant J.* 75, 309–323. doi: 10.1111/tpj.12102

Ohta, M., Matsui, K., Hiratsu, K., Shinshi, H., and Ohme Takagi, M. (2001). Repression domains of class II ERF transcriptional repressors share an essential motif for active repression. *Plant Cell* 13, 1959–1968. doi: 10.1105/tpc.13.8.1959

Plieth, C., Hansen, U., Knight, H., and Marc, R. K. (1999). Temperature sensing by plants: the primary characteristics of signal perception and calcium response. *Plant J.* 18, 491–497. doi: 10.1046/j.1365-313X.1999.00471.x

Qi, Z., Stephens, N. R., and Spalding, E. P. (2006). Calcium entry mediated by GLR3.3, an *Arabidopsis* glutamate receptor with a broad agonist profile. *Plant Physiol.* 142, 963–971. doi: 10.1104/pp.106.088989

Rodriguez, M., De Langre, E., and Moulia, B. (2008). A scaling law for the effects of architecture and allometry on tree vibration modes suggests a biological tuning to modal compartmentalization. *Am. J. Bot.* 95, 1523–1537. doi: 10.3732/ajb.0800161

Schriefer, J. L., Warden, S. J., Saxon, L. K., Robling, A. G., and Turner, C. H. (2005). Cellular accommodation and the response of bone to mechanical loading. *J. Biomech.* 38, 1838–1845. doi: 10.1016/j.jbiomech.2004.08.017

Stephens, N. R., Qi, Z., and Spalding, E. P. (2008). Glutamate receptors subtypes evidenced by differences in desensitization and dependance on the GLR 3.3 and GLR3.4 genes. *Plant Physiol.* 146, 529–538. doi: 10.1104/pp.107.108134

Stork, W., Diezel, C., Halitschke, R., Galis, I., and Baldwin, I. T. (2009). An ecological analysis of the herbivory-elicited JA burst and its metabolism: plant memory processes and predictions of the moving target model. *PLoS ONE* 4:e4697. doi: 10.1371/journal.pone.0004697

Stull, R. B. (1988). *An Introduction To Boundary Layer Meteorology*. London: Kluwer Academic Publishers. doi: 10.1007/978-94-009-3027-8

Telewski, F. W. (2006). A unified hypothesis of mechanoperception in plants. *Am. J. Bot.* 93, 1466–1476. doi: 10.3732/ajb.93.10.1466

Telewski, F. W., and Pruyn, M. (1998). Thigmomorphogenesis: a dose response to flexing in *Ulmus americana* seedlings. *Tree Physiol.* 18, 65–68. doi: 10.1093/treephys/18.1.65

To, T. K., and Kim, J. M. (2014). Epigenetic regulation of gene responsiveness in *Arabidopsis. Front. Plant Sci.* 4:548. doi: 10.3389/fpls.2013.00548

Uyttewaal, M., Burian, A., Alim, K., Landrein, B., Borowska-Wykret, D., Dedieu, A., et al. (2012). Mechanical stress acts via katanin to amplify differences in growth rate between adjacent cells in *Arabidopsis. Cell* 149, 439–451. doi: 10.1016/j.cell.2012.02.048

Vadassery, J., Reichelt, M., Hause, B., Gershenzon, J., Boland, W., and Mithöfer, A. (2012). CML42-mediated calcium signaling coordinates responses to spodoptera herbivory and abiotic stresses in *Arabidopsis. Plant Physiol.* 159, 1159–1175. doi: 10.1104/pp.112.198150

Xu, X., Chen, C., Fan, B., and Chen, Z. (2006). Physical and functional interactions between pathogen-induced *Arabidopsis* WRKY18, WRKY40, and WRKY60 transcription factors. *Plant Cell* 18, 1310–1326. doi: 10.1105/tpc.105.037523

Yamanaka, T., Nakagawa, Y., Mori, K., Nakano, M., Imamura, T., Kataoka, H., et al. (2010). MCA1 and MCA2 that mediate Ca^{2+} uptake have distinct and overlapping roles in *Arabidopsis. Plant Physiol.* 152, 1284–1296. doi: 10.1104/pp.109.147371

Zarka, D. G., Vogel, J. T., Cook, D., and Thomashow, M. F. (2003). Cold induction of *Arabidopsis* CBF genes involves multiple ICE (inducer of CBF expression) promoter elements and a cold-regulatory circuit that is desensitized by low temperature. *Plant Physiol.* 133, 910–918. doi: 10.1104/pp.103.027169

Zhu, J., Jeong, J., Zhu, Y., Sokolchik, I., Miyazaki, S., Zhu, J. K., et al. (2008). Involvement of *Arabidopsis* HOS15 in histone deacetylation and cold tolerance. *Proc. Natl. Acad. Sci. U.S.A.* 105, 4945–4950. doi: 10.1073/pnas.0801029105

Conflict of Interest Statement: The authors declare that the research was conducted in the absence of any commercial or financial relationships that could be construed as a potential conflict of interest.

Received: 27 May 2014; accepted: 28 July 2014; published online: 14 August 2014.
*Citation: Leblanc-Fournier N, Martin L, Lenne C and Decourteix M (2014) To respond or not to respond, the recurring question in plant mechanosensitivity. Front. Plant Sci. **5**:401. doi: 10.3389/fpls.2014.00401*
This article was submitted to Plant Physiology, a section of the journal Frontiers in Plant Science.

frontiers in
PLANT SCIENCE

ORIGINAL RESEARCH ARTICLE
published: 21 October 2014
doi: 10.3389/fpls.2014.00533

A chromatin modifying enzyme, SDG8, is involved in morphological, gene expression, and epigenetic responses to mechanical stimulation

Christopher I. Cazzonelli[1,2]*, Nazia Nisar[2], Andrea C. Roberts[2], Kevin D. Murray[2], Justin O. Borevitz[2] and Barry J. Pogson[2]

[1] Hawkesbury Institute for the Environment, University of Western Sydney, Penrith, NSW, Australia
[2] Australian Research Council Centre of Excellence in Plant Energy Biology, Research School of Biology, College of Medicine, Biology and Environment, The Australian National University, Canberra, ACT, Australia

Edited by:
Catherine Coutand, Institut Nationale de la Recherche Agronomique, France

Reviewed by:
Christoph Peterhaensel, Lebniz University Hannover, Germany
Bin YU, University of Nebraska, USA

***Correspondence:**
Christopher I. Cazzonelli, Environmental Epigenetics Laboratory, Hawkesbury Institute for the Environment, University of Western Sydney, Hawkesbury Campus, Bourke Street, Richmond, NSW 2753, Australia
e-mail: c.cazzonelli@uws.edu.au

Thigmomorphogenesis is viewed as being a response process of acclimation to short repetitive bursts of mechanical stimulation or touch. The underlying molecular mechanisms that coordinate changes in how touch signals lead to long-term morphological changes are enigmatic. Touch responsive gene expression is rapid and transient, and no transcription factor or DNA regulatory motif has been reported that could confer a genome wide mechanical stimulus. We report here on a chromatin modifying enzyme, SDG8/ASHH2, which can regulate the expression of many touch responsive genes identified in Arabidopsis. SDG8 is required for the permissive expression of touch induced genes; and the loss of function of *sdg8* perturbs the maximum levels of induction on selected touch gene targets. SDG8 is required to maintain permissive H3K4 trimethylation marks surrounding the Arabidopsis touch-inducible gene TOUCH 3 (TCH3), which encodes a calmodulin-like protein (CML12). The gene neighboring was also slightly down regulated, revealing a new target for SDG8 mediated chromatin modification. Finally, *sdg8* mutants show perturbed morphological response to wind-agitated mechanical stimuli, implicating an epigenetic memory-forming process in the acclimation response of thigmomorphogenesis.

Keywords: acclimation, Arabidopsis, histone, touch, transcription, thigmomorphogenesis, mechanical, regulation

INTRODUCTION

Mechanical forces imposed by environment stimuli such as touch, strong winds, rubbing, tree strangling, insect feeding, passing animals, weight of climbing plants, heavy rain and even the navigation of roots around obstacles in the soil, can be perceived by plants (Braam, 2005; Monshausen and Haswell, 2013). When plants are grown in the wind-protected whole tree chambers, greenhouses, or growth chambers, it is possible to separate out the long term effects of mechanical stimulation from other natural environmental and seasonal climatic transitions that shape plant development. Repeated touching of plant organs for short periods of time eventually alters growth leading to phenotypic changes, which is a phenomenon referred to as thigmomorphogenesis (Jaffe, 1973; Chehab et al., 2009). The sensitivity of plants to repeated mechanical stress alters the degree of carbon allocation and the shoot-root biomass balance. Plants physiologically and morphologically acclimate to these mechanical wind forces that threaten reproduction and survival (Biddington, 1986; Mitchell, 1996; Coutand et al., 2008).

Although thigmomorphogenesis is perceived as a slow response to mechanical perturbation, there are very fast physiological changes associated with mechanical stress. These rapid responses can affect photosynthesis and respiration by impacting the resistance to movement of carbon dioxide into leaves and altering stomatal aperture (Jaffe and Forbes, 1993; Smith and Ennos, 2003). Long term morphological changes can include internode compression, pithiness, decreased rate of stem and petiole elongation, lateral or radial enlargement (i.e., swelling) of stems, inhibition of leaf expansion. Developmental changes include enhanced senescence, delayed flowering, and stronger roots (Jaffe and Forbes, 1993; Braam, 2005; Chehab et al., 2009). Other responses include enhanced pest resistance and decreased susceptibility to various stresses as well as alterations in chlorophyll content and hormone levels (Biddington, 1986; Tretner et al., 2008; Chehab et al., 2012; Monshausen and Haswell, 2013).

Various signaling pathways and molecules function interdependently to mediate mechanical stimulation of physiological and morphological responses to touch. Characteristic early signaling events of touch-induced responses involve secondary messenger molecules (calcium, nitric oxide and reactive oxygen

Abbreviations: ccr, carotenoid and chloroplast regulation; sdg8, set domain group eight; efs, early flowering under short days; ashh2, ASH homolog2; H3K4, histone-3 lysine-4 methylation; H3K36, histone-3 lysine-36 methylation; H3K9, histone-3 lysine-9 methylation; H3K27, histone-3 lysine-27 methylation; HKM, histone lysine methylation; HKMTs, histone lysine methytransferases; SET, Su(var)3-9, E(Z), trithorax; DAG, days after germination.

species) and protein phosphorylation (Braam and Davis, 1990; Hofmann, 2009; Monshausen et al., 2009; Kurusu et al., 2012a,b). Touch-induced genes identified encode calmodulin (TCH1), calmodulin-like-proteins (TCH2 and TCH3) and a xyloglucan endotransglucosylase/ hydrolase (TCH4), all known to play a central role in touch signal transduction (Chehab et al., 2009). In addition, more recent progress has identified various putative mechanoreceptors including mechano-sensitive ion channel-like proteins and receptor-like kinases, which has paved further exploration toward understanding mechanical signal transduction (Kurusu et al., 2013; Monshausen and Haswell, 2013). Later signaling events involve hormones (jasmonates, ethylene, abscisic acid, auxin, brassinosteroids) that can confer the external environmental stimulus to the nucleus and promote morphological adaptation (Chehab et al., 2009). The phytohomones auxin and jasmonic acid (JA), play key roles in promoting thigmomorphogenesis. In particular, jasmonates have been shown to be required for, and promote, the salient characteristics of thigmomorphogenesis in *Arabidopsis*, including a touch induced delay in flowering and rosette diameter reduction (Chehab et al., 2012).

The physiological and morphological changes resulting from mechanical stimulation require alterations in gene expression and the production of new proteins. *TCH* gene expression can be observed at sites of potential mechanical strain and/or increased growth, such as the shoot branching points, root–shoot junction, elongating hypocotyls and roots, as well as developing trichomes (Sistrunk et al., 1994; Antosiewicz et al., 1995; Xu et al., 1995). A genome-wide differential expression analysis of mechanical stimulated leaves revealed that over 2.5% of *Arabidopsis* genes were up-regulated by at least 2-fold in response to touch stimulation (Lee et al., 2005). The vast majority of *TCH* regulated genes in Arabidopsis encode protein kinases, transcription factors and putative disease resistance proteins. They function in various cellular processes including calcium sensing/binding, cell wall modifications, and defense (Lee et al., 2005). Consistent with these findings, the molecular basis of the touch response has been implicated with multiple biotic and abiotic stimuli, including hormones, darkness, salt, and temperature (Braam, 2005). Large upstream promoter regions from the TCH4/XTH22 (xyloglucan endotransglucosylase/ hydrolase), CBF2/DREB1c (ERF/AP2 transcription factor), and TCH2/CML24 (Calmodulin-like/calcium binding protein) genes have been shown to be touch responsive (Iliev et al., 2002; Zarka et al., 2003; Braam, 2005). A transcriptional regulator known as Jr-ZFP2, encodes a Cys2/His2-type two-zinc-fingered protein and mRNA expression was shown to be associated with an acclimation response to mechanical bending (Leblanc-Fournier et al., 2008; Coutand et al., 2009; Martin et al., 2009). However, despite all these findings, not a single well characterized touch-inducible *cis*-acting element has been identified to date. Perhaps a more complex regulatory layer is involved whereby multiple signals converge to stimulate touch induced expression of select gene targets.

Coordinating a large number of TCH-inducible gene changes may require a degree of chromatin modification. Touch gene expression needs to be precisely timed and coordinated during all developmental stages as well as in the response to other environmental changes. Plant tissues that are mechanically perturbed by wind, rain or touch show a rapid and transient change in gene expression, usually within 5–30 min, that in some cases can be undetectable at basal levels in untouched tissues (Botella et al., 1992; Cazzonelli et al., 2005; Chehab et al., 2009). One of the central regulators of gene transcription is conferred through the organization of the genome into chromatin (Cazzonelli et al., 2009b). Histone proteins are key components of chromatin, forming the basic nucleosome packaging structure. Posttranslational modifications, such as the methylation of lysine residues on the tails of histone proteins can activate (e.g., H3K4, H3K36) or repress (e.g., H3K9, H3K9) gene expression depending upon changes in the environment (e.g., drought, cold and high-salinity stress) or developmental cues (Cazzonelli et al., 2009b; Kim et al., 2010; Berr et al., 2011b; Song et al., 2013). Histone modifications can be read, written, and edited, which highlights their plasticity to tune regulatory processes (Justin et al., 2010). In particular, histone lysine methylation (HKM) can promote strong and inducible target gene expression within a very short period of time of receiving a stress stimulus (Lim et al., 2009; Kim et al., 2010). Such characteristics of an epigenetic mark could be envisioned as important for conferring a nuclear wide response to a mechanical stimulus.

In order to address the molecular nature behind the phenomenon of thigmomorphogenesis, we have investigated if chromatin regulatory mechanisms. This includes the well-studied permissive modification of trimethylation of H3K4, which can enhance the expression of mechanical-induced genes. We provide evidence to show that many gene targets regulated by the chromatin modifying gene, SET DOMAIN GROUP 8 (SDG8) are also responsive to mechanical stimulation in *Arabidopsis* (Cazzonelli et al., 2009a, 2010). The loss of function of *sdg8* altered morphological responses to long-term mechanical stimulation revealing a potential new layer in the regulation of thigmormorphogenesis, and provides a basis for further understanding the molecular regulation of this enigmatic phenomenon.

METHODS AND MATERIALS

PLANT GROWTH CONDITIONS AND GERMPLASM

Soil grown plants were incubated at 4°C for 2–3 days in the dark before transferring to 12 h of illumination (100–150 μE) and temperature maintained at 21°C. All germplasm are in the Arabidopsis thaliana ecotype Columbia (Col-0) background and mutants used in this study include *chloroplast carotenoid regulation 1-1* (*ccr1-1*; referred to as *sdg8-1*) and *ccr1.4* (referred to as *sdg8-4*), which have a null lesion in SDG8/ASHH2, a histone lysine methyltransferase; AT1G77300 (Cazzonelli et al., 2009a).

MECHANICAL STIMULATION OF TCH GENE EXPRESSION AND THIGMOMORPHOGENESIS

A mechanical force was applied by lightly bending mature Arabidopsis (29 DAG) leaves 30 times for 30 s with four repeats and harvesting tissues 30 min following stimulation. To promote thigmomorphogenesis, a treatment of constant mechanical force was applied to unstimulated plants (20 DAG; 6–13 true leaves; no sign of floral bolt) growing in separate trays using stationary fans (twice a day for 15 min). The stimulation was visible

as leaf vibration. Three additional trays of control plants were shielded from the mechanical stimulation using cardboard boxing. A constant temperature of 21°C was maintained for both the wind-stimulated and control plants. After 7 days fan-forced mechanical stimulation was stopped and photos taken 2 days later for further analysis of morphological traits (e.g., leaf blade length and width, and petiole length). Experimental set up involved growing 8–15 plants for each wild type and *sdg8* mutant in separate trays. Plant level measures were taken as the average of 5 fully expanded rosette leaves calibrated to the standard pot size using image processing software ImageJ2 (Schneider et al., 2012).

REAL TIME QUANTITATIVE PCR

Total RNA was extracted using the SIGMA-aldrich Spectrum kit and included an on-column DNase treatment step following the manufacturer's instructions. First strand cDNA synthesis was performed using Oligo dT primer and SuperScript® III Reverse Transcriptase (Invitrogen) according to manufacturer's instructions. The relative transcript abundance was quantified using Light Cycler 480 SYBR Green I Master and three technical replicates for each of one to three biological replicates were performed using the Light Cycler 480 (ROCHE, Australia). The take-off point was determined using relative quantification [Target Eff Ct(Wt-target) / Reference Eff Ct(Wt-target)] and fit point analysis (Pfaffl, 2001). *Cyclophilin* (At2g29960) and *Protein Phosphatase 2A* (At1g13320) were included as house-keeper reference control genes (Czechowski et al., 2005). Primer sequences are listed in **Supplemental Table 1**.

BIOINFORMATICS ANALYSIS OF MICROARRAY DATA AND GENE ONTOLOGY ANLYSIS

Analysis of *sdg8* microarray data was obtained from the following sources: mature leaves (Cazzonelli et al., 2009a), 6 DAG seedling leaves (Xu et al., 2008) and inflorescences (Grini et al., 2009), as well as wild type touch induced leaves (Lee et al., 2005). Gene ontology analysis was performed using the agriGO -GO Analysis Toolkit and Database for Agricultural Community (Du et al., 2010).

CHROMATIN IMMUNOPRECIPITATION

Chromatin immunoprecipitation (ChIP) assays were performed using a pool of 3-week-old leaf tissue as previously described (Cazzonelli et al., 2009a). There were three biological replicates for each of the two genotypes analyzed. The chromatin/DNA extracted from leaf pools was divided into three aliquots, two of which were used for different antibodies and the third used as a control to which no antibody was added. Antibodies recognizing H3K4me3 (Millipore Cat#04-745) and H3K4me2 (Millipore Cat#07-030) were purchased from Upstate Biotechnology (Charlottesville, VI, USA). The no antibody control was included to verify that H3K4 antibodies were able to enrich ChIP DNA by at least 10-fold. ChIP DNA was tested in triplicate by PCR for enriched regions of DNA and normalized to the housekeeping gene S-Adenosyl Methionine Synthase, (SAM; At4g01850) (Finnegan et al., 2004). qRT-PCR primers used for ChIP analysis are given in **Supplemental Table 2**.

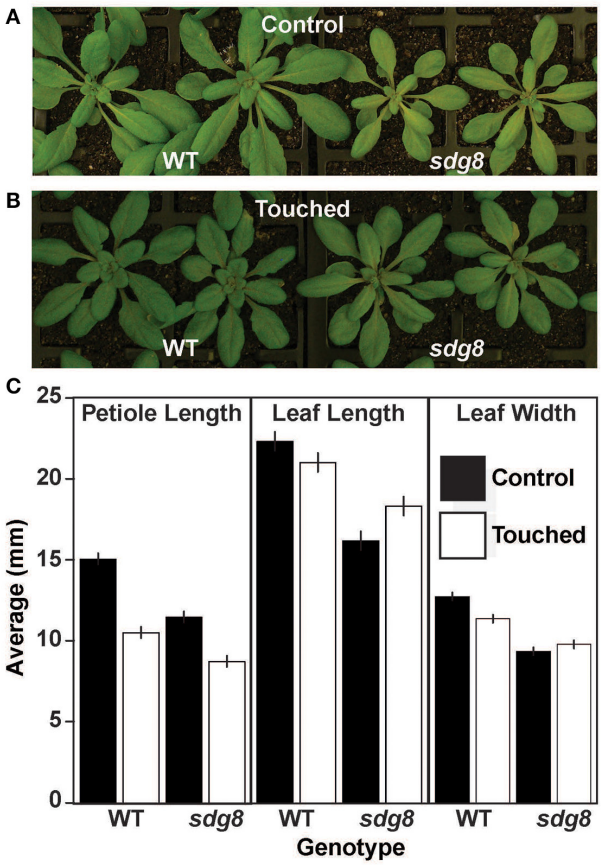

FIGURE 1 | Thigmomorphogenic responses of the *sdg8* mutant to mechanical stress. Wild type (WT) and *sdg8* mutant Arabidopsis plants were grown under controlled conditions **(A)** or subject to 1 week of short, repetitive bursts of wind-agitated mechanical stimulation **(B)**. **(C)** Morphological traits (petiole length, leaf blade length and leaf blade width) were measured for WT and *sdg8*, with and without mechanical treatment. $N = 449$ plants. Error bars are displayed (+/− twice the standard error).

DATA ANALYSIS

Data analyses were performed in R using the nlme package. 449 plants from six trays each with WT and *sdg8* were analyzed. Three trays were treated with fans to provide mechanical stress from wind. A mixed effect model was used to estimate the fixed effects of genotype, treatment, and genotype by treatment interaction and the random effect of Tray, as lme(TraitValue ∼ geno*Treatment, random = ∼1|Tray). The fitted values from each of the genotype and treatment classes are shown in **Figure 1C**.

ACCESSION NUMBERS

Arabidopsis Genome Initiative locus identifiers for the genes mentioned in this article are as follows: At1g77300 (*SDG8; SET DOMAIN GROUP 8*), At1g06810 (*CYCLO*; *CYCLOPHILIN*), At1g13320 (*PP2A*; *PROTEIN PHOSPHATASE 2A*), AT4g34270 (TIP41; TIP41-LIKE FAMILY PROTEIN), At4g01850 (*SAM; S-ADENOSYL METHIONINE TRANSFERASE*), AT2G41100 (*TCH3; CALMODULIN-LIKE PROTEIN*), AT2G47060 (*STPK*;

SERINE/THREONINE PROTEIN KINASE); AT4G23810 (*WRKY; DNA-BINDING PROTEIN 53*), At1g06820 (*CRTISO; CAROTENOID ISOMERASE*).

RESULTS

MICROARRAY ANALYSIS REVEALS SDG8 REGULATES TOUCH RESPONSIVE GENE EXPRESSION

Active chromatin modifications are required for inducible gene expression. SDG8 is a well characterized chromatin-modifying enzyme that catalyzes the trimethylation of active marks of histone-3-lysine-4 (H3K4) and histone-3-lysine-36 (H3K36) at selected permissive gene loci involved in carotenogenesis, flowering, and defense responses (Kim et al., 2005; Cazzonelli et al., 2009a; Berr et al., 2010). Previously published microarray analyses of mature leaf tissues from the *sdg8* mutant revealed misregulation of a mechanical responsive *TOUCH3* (*TCH3*) gene, which encodes a calmodulin-like protein (CML12) (Sistrunk et al., 1994; Antosiewicz et al., 1995) (**Supplemental Table 1**) (Cazzonelli et al., 2009a). The genes neighboring *TCH3* were also slightly down-regulated ($p < 0.05$; data not shown) and consistent with previous reports demonstrating that active chromatin marks can spread to surrounding gene loci (Cazzonelli et al., 2009a). These findings paved the way for a more thorough bioinformatics analysis to determine if SDG8 plays a more prominent role in the regulation of touch induced gene expression.

We next analyzed four separate genome-wide transcript studies of different tissues (mature leaves, whole seedlings and inflorescences) from different *sdg8* mutant alleles (**Supplemental Table 1**). These studies identified the majority of differentially expressed genes to be down-regulated (65–75%; **Table 1**) and consistent with the function of SDG8 in actively promoting gene expression (Cazzonelli et al., 2009a). Further analysis revealed many differentially expressed genes in *sdg8* were also touch responsive in leaves (8.7%), seedlings (16–40%) and to some small extent inflorescences (3.3%; **Table 1**). The genes that were down-regulated in *sdg8* were largely inducible by mechanical stimulation (50–85%) and consistent with the function of SDG8 in promoting a more permissive chromatin structure that activates gene expression (**Table 1**).

Comparison of touch inducible genes regulated by *sdg8* identified 65 differentially co-expressed genes (8.6%) of which the majority were down-regulated in the *sdg8* mutant and touch inducible (>88%; **Table 1** and **Supplemental Table 1**). Gene ontology analysis of the 65 differentially expressed genes showed significant (FDR < 0.00005) enrichment in transcripts involved in response to abiotic stress (cold temperature and oxidative damage), defense (chitin, fungus, and immune system), chemicals (carbohydrates and organic substances), wounding and other external stimuli (**Table 2**). These gene classes have often been implicated in the activation of touch responsive genes (Braam, 2005). Furthermore, these results mirrored the gene ontology analysis of 760 touch responsive genes identified in Arabidopsis (**Supplemental Table 1**). In summary, there were many genes down-regulated in the *sdg8* mutant that were also inducible by mechanical stimulation.

THIGMOMORPHOGENIC RESPONSES ARE PERTURBED IN THE *sdg8* MUTANT

Mechanical stimulation of Arabidopsis plants by wind-forced agitation promoted a large thigmomorphogenic response in wild type (**Figures 1A,B**) that was consistent with previous reports (Braam and Davis, 1990; Braam, 2005). The morphological traits altered included a shortening of petiole length and a reduction in leaf blade length and width (**Figure 1C**). In contrast, the *sdg8* mutant had perturbed responses to stimulation ($p < 0.01$ differential sensitivity for all traits) displaying a minor reduction in petiole length, an increase in leaf blade length and no response in leaf width. Overall, the *sdg8* mutants were less sensitive to mechanical stress (**Data Analysis S1** in Supplementary Material).

TCH GENE EXPRESSION LEVELS ARE REDUCED IN *sdg8* MUTANT TISSUES

Next we decided to validate the relative transcript levels of three touch inducible genes (*WRKY53*, *STPK* and *TCH3*), which were identified as significantly down-regulated in *sdg8* and inducible by mechanical stimulation (*ccr1.1*; **Supplemental Table 1**). These genes were chosen for the following reasons; (1) *WRKY53* (DNA-binding protein transcription factor) showed the highest level of touch induction (>11 fold) with a 2.5 fold down-regulation of expression in *sdg8*, (2) *STPK* (putative serine/threonine protein kinase) was down-regulated in three independent microarray studies (2–4 fold) and up-regulated 4.2 fold by touch simulation, and (3) *TCH3* (calcium signaling protein whose gene expression has been well characterized as touch inducible) was down regulated 3.7 fold in *sdg8* and up-regulated by 2.4 fold following mechanical stimulation.

The relative levels of *WRKY53*, *STPK* and *TCH3* mRNA expression were quantified in rosette leaves, shoot apices, and floral tissues of *sdg8* (**Figures 2A–C**). The transcript levels of *WRKY* and *STPK* were significantly reduced in the shoot apex, as well as

Table 1 | Differentially expressed genes regulated by SDG8 and mechanical stimulation.

Microarray publication	Cazzonelli et al., 2009a	Xu et al., 2008		Grini et al., 2009	Lee et al., 2005
Genotype and/or treatment	*ccr1.1*	*sdg8-1*	*sdg8-2*	*ashh2-1*	Touch (TCH)
Tissue	Leaves	Seedlings	Seedlings	Inflorescence	Leaves
Differentially expressed genes	113	83	142	448	760
Genes down-regulated	85 (75%)	123 (67%)	93 (65%)	298 (67%)	171 (22%)
Genes up-regulated	28 (25%)	40 (33%)	49 (35%)	150 (33%)	589 (78%)
TCH responsive genes in *sdg8*	13 (8.7%)	33 (40%)	22 (16%)	15 (3.3%)	65 (8.6%)
TCH inducible and down-regulated in *sdg8*	11 (85%)	29 (88%)	11 (50%)	0	57 (88%)

Table 2 | Gene ontology analysis of touch inducible genes regulated by mechanical stimulation in the sdg8 mutant.

GO term	Ontology process	Description	Co-reg. Genes	Ref. genes	FDR
GO:0010200	P	Response to chitin	11	151	1.30E-12
GO:0050896	P	Response to stimulus	31	4057	1.10E-11
GO:0009743	P	Response to carbohydrate stimulus	11	240	5.30E-11
GO:0042221	P	Response to chemical stimulus	22	2085	1.90E-10
GO:0006950	P	Response to stress	22	2320	1.20E-09
GO:0010033	P	Response to organic substance	17	1342	4.20E-09
GO:0006952	P	Defense response	13	766	2.60E-08
GO:0009605	P	Response to external stimulus	8	429	2.90E-05
GO:0009611	P	Response to wounding	6	197	4.30E-05
GO:0006955	P	Immune response	7	367	9.40E-05
GO:0002376	P	Immune system process	7	368	9.40E-05
GO:0051704	P	Multi-organism process	9	776	1.80E-04
GO:0051707	P	Response to other organism	8	599	1.90E-04
GO:0009620	P	Response to fungus	5	158	1.90E-04
GO:0009607	P	Response to biotic stimulus	8	638	2.70E-04
GO:0009266	P	Response to temperature stimulus	6	485	3.30E-03
GO:0009628	P	Response to abiotic stimulus	10	1471	3.30E-03
GO:0009409	P	Response to cold	5	328	4.20E-03
GO:0006979	P	Response to oxidative stress	5	332	4.20E-03
GO:0045087	P	Innate immune response	5	347	4.90E-03
GO:0050794	P	Regulation of cellular process	14	3375	2.10E-02
GO:0009416	P	Response to light stimulus	5	596	4.50E-02
GO:0050789	P	Regulation of biological process	14	3697	4.50E-02
GO:0009314	P	Response to radiation	5	613	4.70E-02
GO:0010556	P	Regulation of macromolecule biosynthetic process	9	1843	4.70E-02
GO:0031326	P	Regulation of cellular biosynthetic process	9	1881	5.00E-02
GO:0009889	P	Regulation of biosynthetic process	9	1881	5.00E-02

The agriGO – gene ontology analysis toolkit was used to determine responses in 65 genes regulated by SDG8 and mechanical stimulation.

flowers and leaves, respectively. *TCH3* mRNA levels were also significantly reduced (40–60%) in these *sdg8* mutant tissues as well as during seedling development (>50%) (**Figure 2D**).

Mechanical stimulation of leaf tissues by bending for 30 s (tissue harvested 30 min after touch stimulus) significantly enhanced the relative transcript levels of *WRKY53*, *STPK*, and *TCH3* in wild type (∼2–5 fold above unstimulated control leaves), and to a lesser degree in the *sdg8* mutant (**Figure 2E**). The interaction between mutant and touch treatment was significantly compromised for *WRKY* ($p < 0.01$). Transcript levels in *sdg8* were similar to wild type and the induction of *WRKY* mRNA levels following touch stimulation was less in *sdg8* when compared to wild type (**Figure 2E**). The transcript levels of *STPK* and *TCH3* in *sdg8* was significantly lower in both untreated and touched leaf tissues when compared to wild type (**Figure 2E**), however the fold change in touch induction of *TCH3* and *STPK* gene expression in *sdg8* mutants (3- and 4-fold respectively) was similar to WT plants (2- and 4-fold, respectively). It should be noted that our experiments addressed a single time point of 30 min to keep consistent with previous TCH microarray data (Lee et al., 2005). In summary, SDG8 is required to promote high levels of *TCH* gene expression following mechanical stimulation, but does not appear to be necessary for activating the induction of *TCH* gene expression.

CHROMATIN SURROUNDING TCH3 GENE LOCUS SHOWS REDUCED H3 LYSINE 4 TRIMETHYLATION

Next we established if *TCH3* was a target of SDG8 mediated chromatin modification. Chromatin immunoprecipitation of DNA from Arabidopsis leaf tissues using antibodies against H3 trimethylK4 (H3K4me3) and histone H3 dimethylK4 (H3K4me2) was followed by quantification using real-time PCR. One upstream (promoter) and two downstream (exon 1 and exon 4) regions flanking the *TCH3* translation start site (**Figure 3A**) were used to monitor the effect of SDG8 mutation on permissive histone marks surrounding *TCH3*. Genomic regions flanking *SAM* and *CRTISO* were also quantified as housekeeper and positive controls of histone methylation, respectively (Finnegan et al., 2004; Cazzonelli et al., 2009a). Analysis of the no antibody control samples revealed over 64-fold enrichment (>6 qPCR cycles) of ChiP precipitated DNA enriched in H3K4me3 and H3K4me2 marks.

Chromatin immunoprecipitation assays using antibodies recognizing H3K4 di- and tri-methylation (H3K4m3 and H3K4m2, respectively) showed that SDG8 activity perturbed permissive chromatin marks surrounding the *TCH3* promoter and two exon loci (**Figure 3**). In both *sdg8* mutant alleles (*sdg8-1 and sdg8-4*), there was an approximate 30–60% reduction in H3K4 trimethylation (**Figure 3B**), accompanied by an expected subtle

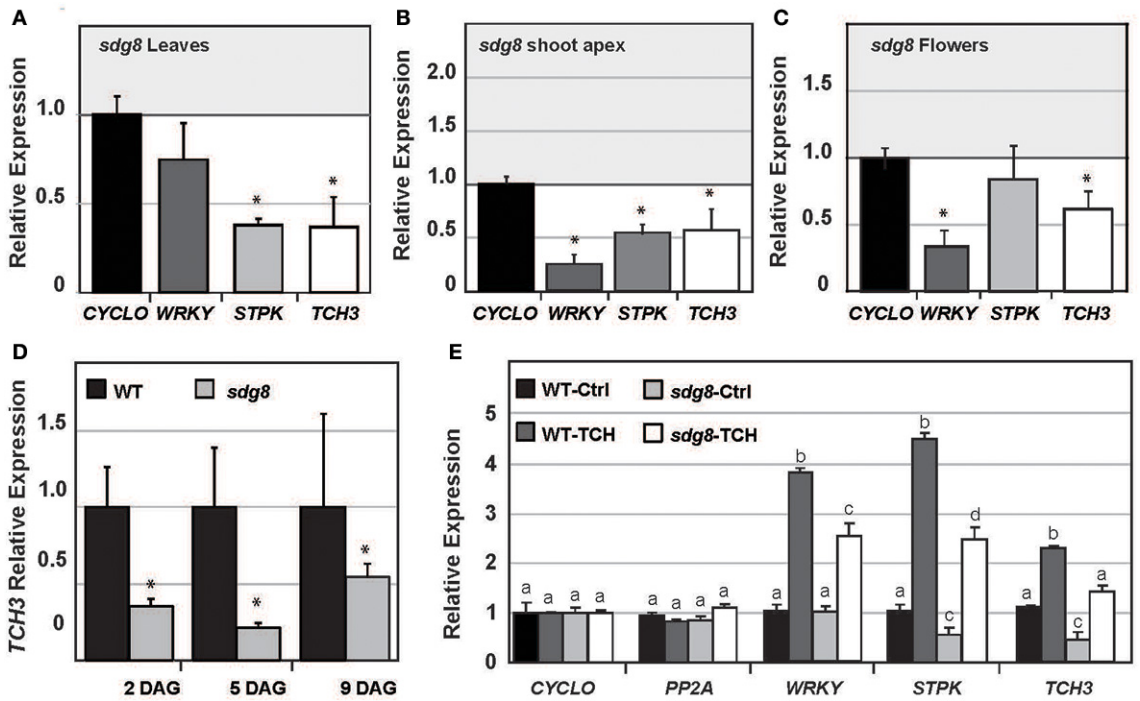

FIGURE 2 | Relative transcript levels of touch-responsive genes in *sdg8* mutant tissues. Leaf and floral tissues were pooled from independent plants and qRT-PCR used to quantify gene expression levels from three biological replicates in mutant *sdg8* lines and normalized to wild type. **(A–C)** Relative gene expression levels of *WRKY53, STPK* and *TCH3* in *sdg8* mutant rosette leaves (21 DAG), shoot apical meristem (21 DAG) or floral tissues (35 DAG), respectively. **(D)** *TCH3* transcript levels in wild type and *sdg8* mutant whole seedlings tissues. **(E)** Relative expression levels of *WRKY53*, *STPK* and *TCH3* in mechanically stimulated mature rosette leaves. Values above the bar sets represent an ANOVA *p*-value (<0.05 signifies more than 95% confidence) considering the interaction of genotype by touch treatment. Relative expression levels represent ratios normalized to wild type and using house keeper reference genes (*CYCLO*, *PP2A*, or *TIP41*). Standard error bars represent 2–3 biological repeats and up to 2 experimental repeats ($n = 2$–6). *Denotes $p < 0.05$ (unpaired Welch's *T*-Test). Primer sequences are given in **Supplemental Table 2**. Unless otherwise specified, plants were grown in controlled environments without any mechanical stimulation.

increase in H3K4 dimethylation (**Figure 3C**). A similar reduction in the H3K4m3 and higher increase in the H3K4m2 marks were observed surrounding the *CRTISO* gene locus, which is consistent with previous findings (Cazzonelli et al., 2009a). Collectively, these data show that chromatin surrounding different regions spanning the *TCH3* locus have altered H3K4 methylation in *sdg8* alleles relative to wild-type plants, consistent with the decrease in *TCH3* transcript abundance.

The distribution of H3K4 methylation marks (mono, di and tri) as well as the nucleosome density of *TCH3, WRKY* and *STPK* was assessed using the UCSC Genome Browser (http://epigenomics.mcdb.ucla.edu/) (Zhang et al., 2009). Experimental derivations of marks surrounding the SAM reference gene showed no enrichment of H3K4m2, while H3K4m3 was restricted to the first intron (**Figure S1A**). Chromatin surrounding *WRKY53* and *TCH3* showed an enrichment in H3K4m2 and H3K4m3 extended throughout the gene locus (**Figures S1B–D**). The *WRKY* and *STPK* gene loci also showed an enrichment of H3K4m2 at the 5′ and 3′ untranslated mRNA leader regions (**Figure S1B,C**). All three touch inducible genes showed relatively no H3K4m1, which operates as an epigenetic mark for repressed euchromatin (**Figure S1**) (Van Dijk et al., 2005). The abundance of H3k4m2/m3 active marks of methylation surrounding the three touch inducible genes are consistent with transcriptional initiation (Cazzonelli et al., 2009b) and in good agreement with our findings showing a reduction in H3K4m3 marks surrounding the *TCH3* loci in *sdg8* mutant leaves (**Figure S1**).

DISCUSSION

Despite a widespread understanding of the signaling events leading to thigmomorphogenesis, the molecular nature that underpins plant mechanostimulus-induced gene expression remains largely unknown and open for discovery. Plants have evolved a very elaborate and sophisticated mechanical responsive regulatory network and this is illustrated by the fact that over 2.5% of Arabidopsis transcripts are responsive to touch stimulation (Lee et al., 2005). Yet, it is intriguing that not a single investigation has identified a *cis*-acting DNA regulatory element that can transcriptionally transmit the external touch stimulus to such a large array of mechanical responsive genes. Indeed, the characterization of a few upstream promoters from mechanical inducible genes have identified touch-responsive sequence domains (e.g., TCH2/TCH4; Chehab et al., 2009) as well as aberrant promoters that become deregulated and strongly constitutive rather than inducible (e.g., VRACS-1; Cazzonelli et al., 2005; Wever et al., 2010). Perhaps there are multiple signaling pathways required to

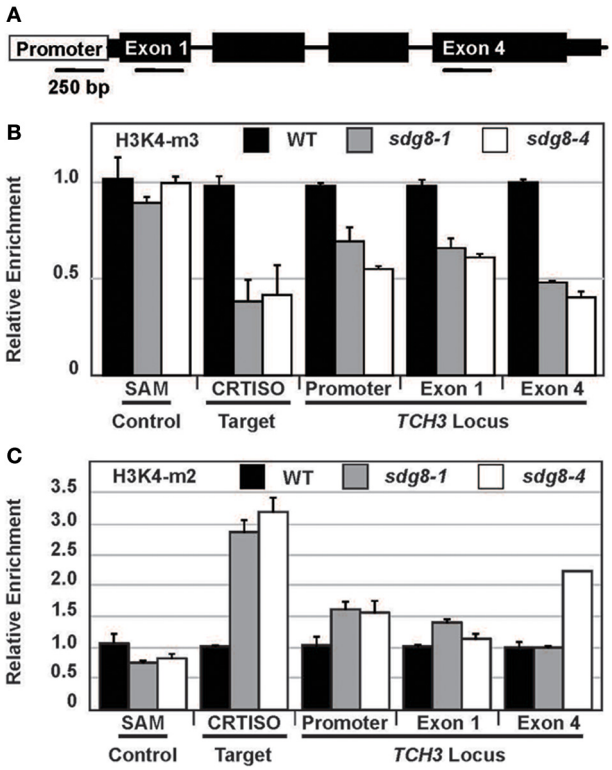

FIGURE 3 | Relative enrichment of histone 3 lysine 4 methylation of chromatin surrounding the *TCH3* locus in the *sdg8* mutants. (A) The position of PCR amplicons used to quantify H3K4 methylation associated with the TCH3 locus is schematically represented. Primer sequences are presented in **Supplemental Table 2** online. **(B,C)** The level of H3K4me3 **(B)** and H3K4me2 **(C)** surrounding TCH3 chromatin is presented as a ratio mutant/wild type, following normalization using a region of the house-keeping gene, S-ADENOSYL METHIONINE SYNTHASE (SAM). CRTISO was included as a positive control for H3K4 di- or tri-methylation activity. For most amplicons two biological and 3 technical repeats were performed, except for TCH3-exon2 where only a single biological repeat was successful. In all experiments there was an enrichment of at least 10 fold above the no antibody background.

activate gene expression following touch stimulation, rather than just relying upon a single universal mechanism.

Our discovery that SDG8 regulates 8.7% (65 out of 760 genes reported) of touch-responsive gene targets comprising calmodulins, kinases, disease resistance proteins and transcription factors supports a multitude of signaling events and highlights the importance of chromatin modifications in regulating a cascade of touch responsive transcriptional events. Furthermore, gene ontology analysis revealed similar responses (abiotic stress, defense, chemicals, wounding and other external stimuli) between the TCH:*sdg8* set of 65 genes and the complete 760 genes identified as being touch responsive. It is interesting to note that SDG8 plays a crucial role in plant defense against fungal pathogens by regulating a subset of genes within the jasmonic acid (JA) signaling pathway (Berr et al., 2010). Jasmonates have also been shown to mediate mechanostimulus-induced plant developmental responses by promoting the salient characteristics of thigmomorphogenesis in Arabidopsis, including a touch-induced delay in flowering and rosette diameter reduction (Chehab et al., 2012). Indeed our touch experiments confirm that *sdg8* mutants show perturbed leaf development, however they flower early making it difficult to infer any effect of mechanical stimulation upon flowering time in *sdg8*. A similar link was found between SDG8 mediated control of brassinosteroid regulated gene expression in Arabidopsis (Dong and Li, 2013) and 24-epibrassinolide mediates induction of TCH4/XTH22 expression (Iliev et al., 2002; Chehab et al., 2009). Overall, there is substantial evidence to implicate SDG8 mediated chromatin modifications in conferring mechano-sensing signals through an array of hormone and other signaling networks that promote thigmomorphogenesis.

The fact that the permissive chromatin-modifying enzyme SDG8 is necessary to promote full expression of such a large array of *TCH* genes partly implies that mechanical stimulation of target gene expression could be regulated by a universal regulator. Our finding that 88% of the 65 touch responsive genes regulated by SDG8 are also down-regulated, support a genuine need for chromatin modifications in the mechanical response. Plants mechanically perturbed by wind, rain, or touch induce the expression of *TCH* genes within 10–30 min post-stimulation. Our investigations showed that SDG8 was not necessary for the induction process of *TCH* gene expression; however it was clearly required for promoting maximum levels of *TCH* expression. A more comprehensive study examining a range of time points would enable identification of genes, which require SDG8 for the rapid induction of transcription rates. Chromatin modifications are well known for priming the regulatory apparatus in order to promote rapid inducible transcriptional activation of gene expression in response to environmental stresses (Kim et al., 2010; Berr et al., 2011b). The RNA polymerase would need to be docked or primed, ready to perceive a signal and rapidly activate gene expression. Nucleosome spacing would also need to be correctly configured to allow an efficient transcriptional process and these are areas worthy of future investigation. In any case, the reduced levels of *TCH* gene expression following touch stimulation in *sdg8* would affect protein levels and therefore influence downstream physiological and morphological acclimation.

Our repetitive touch experiments confirmed that several thigmomorphogenic responses were perturbed in the *sdg8* mutant. The morphological responses were varied suggesting the action of multiple signaling pathways. SDG8 mediated chromatin modifications can play a role in the acclimation of rosette development to repetitive mechanical stimulation.

Epigenetics can be viewed as a sophisticated tuner that relays environmental and developmental signals through structural adjustment of chromosomal regions so as to register, signal, or perpetuate altered activity states (Bird, 2007). Epigenetic modifications can be inherited through cell division or mitosis (e.g., chromatin modifications and DNA methylation) and in rare instances through meiosis into subsequent generations (e.g., DNA methylation) (Saze, 2008). Histone modifications can be reversible and serve to provide an additional regulatory layer to control programmed differentiation of a cell to activate or deactivate gene expression (Justin et al., 2010; Berr et al., 2011a). Our analysis of *TCH* gene expression revealed some tissue specific affects, although the expression of all three genes was significantly

reduced in the shoot apex of *sdg8* mutants. The shoot apex consists of undifferentiated stem cells that can become epigenetic programmed in order to facilitate acclimation to the surrounding environment.

Given that thigomomorphogenesis is a process of cellular signal transduction and morphological acclimation it is conceivable that mechanical-induced growth responses involve some level of epigenetic memory formation. Indeed SDG8 is involved in memory forming events leading to changes in flower development (Zhao et al., 2005; Dong et al., 2008; Xu et al., 2008; Cazzonelli et al., 2009a; Grini et al., 2009; Berr et al., 2010; Tang et al., 2012; Dong and Li, 2013) and can be viewed as a combined "reader" and "writer" of the histone code possessing intrinsic H3K4 and H3K36 methyltransferase activities (Ko et al., 2010; Hoppmann et al., 2011). There is solid evidence to show that SDG8 affects both H3K4 and H3K36 tri-methylation of chromatin surrounding select gene targets and there appears to be a degree of combinatorial functions that exist between the diversity of histone methylation enzymes that exist (Kim et al., 2005; Cazzonelli et al., 2009a; Feng and Shen, 2014; Shafiq et al., 2014).

Our chromatin immunoprecipitation experiments confirmed that the *TCH3* locus requires SDG8 activity to maintain H3K4m3 marks and a permissive chromatin structure that enhances gene expression. Our bioinformatic meta-analysis of published transcriptome studies revealed that three rapidly inducible TCH gene targets (*WRKY53*, *STPK*, and *TCH3*) were enriched in the active marks of di- and tri-methylation of H3K4, yet lack the more repressive H3K4m1 modification. We showed that SDG8 is required to enhance *TCH* gene expression. Furthermore, the expression of genes neighboring *TCH3* were slightly reduced perhaps due to spreading of a less permissive chromatin state in the absence of *sdg8* (Kim et al., 2005; Cazzonelli et al., 2009a). While the induction of *TCH3*, *WRKY53* and *STPK* expression was not perturbed in the *sdg8* mutant, the level of expression following touch stimulation was clearly reduced. The fact that *TCH3* transcript levels were not so different to wild type plants following touch stimulation highlights the importance of chromatin in enhancing induced gene expression. This would imply that regulation of SDG8 could control the relative level of certain *TCH* genes following mechanical stimulation and perhaps perturb acclimation to mechanical stimulation.

Our discovery that gene expression of the potential Ca2+ sensor, CML12, first identified as TCH3 (Braam and Davis, 1990; Braam, 1992; Sistrunk et al., 1994; Antosiewicz et al., 1995) is potentially a key target of SDG8 activity is another step forward toward understanding calcium and touch mediated signaling events. *TCH3* gene expression is inducible within minutes of multiple stimuli, including touch, darkness and temperature as well as being important in mediating auxin transport and hence plant morphology. For example, TCH3 interacts with and regulates the activity of pinoid (PID), a serine/threonine protein kinase that potentially acts as a switch in regulating the activity of the PIN family of auxin regulators (Benjamins et al., 2003; Friml et al., 2004; Wisniewska et al., 2006). More recently, TCH3 was identified as having an important role in the regulation of the mechanical properties of the cell wall via an upstream signaling network dependent on Ca2+ and reactive oxygen species (ROS) (Kurusu et al., 2013). Interestingly, the expression of *TCH3* was up-regulated by overexpressors of Ca2+-permeable mechanosensitive channels (MCAs), suggesting that MCA1 stimulates the expression and activity of TCH3 through Ca2 influx (Nakagawa et al., 2007; Kurusu et al., 2012b, 2013). These channel proteins are localized in the plasma membrane and appear to be required for sensing touch, and gravity as well as osmotic shock through ROS production (Kurusu et al., 2013). Therefore regulatory proteins like MCAs and SDG8 are shedding light on how to keep genes like *TCH3* permissibly active and inducible to external stimuli. The relationship between calcium signaling, auxin transport, ROS signaling and now chromatin modifications paves the way forward to uncover the enigmatic nature behind mechanical inducible gene expression and signaling events leading to thigmomorphogenesis.

In summary, we provide new insights into the molecular nature by which a chromatin modifying enzyme SDG8, can coordinate permissive chromatin structure and enhance gene expression of mechanically responsive *TCH* genes. We reveal evidence that the active mark of H3K4m3 is required to promote the full expression of a mechanically responsive *TCH3* gene, whose protein is involved in calcium signaling events that convey the touch message. The specific role of SDG8 in thigmomorphogenesis appears to be somewhat more general when compared to carotenogenesis or flowering time, where SDG8 controls single gene loci (Cazzonelli et al., 2009a). An SDG8 mediated enrichment of H3K4 trimethylation surrounding many *TCH* gene loci could insure the rapid signaling of multiple pathways in response to a mechanical stimulus. The nature of the inducing signal(s) still remains enigmatic. How epigenetic modifications regulate transcription activation of *TCH* genes and promote memory formation in response to repetitive touch stimulation, are new areas of exciting research that will ultimately link physiological responses and morphological acclimation underlying thigmomophogenesis.

AUTHOR CONTRIBUTIONS

Christopher I. Cazzonelli conceived idea, designed research, and wrote the paper. Christopher I. Cazzonelli, Andrea C. Roberts, and Nazia Nisar performed research, analyzed data and prepared figures. Statistical analysis by Kevin D. Murray and supervised by Justin O. Borevitz. Christopher I. Cazzonelli and Barry J. Pogson supervised Andrea C. Roberts. All authors read and commented on manuscript.

ACKNOWLEDGMENTS

This work was supported by Grant CE140100008 of the Australian Research Council Centre of Excellence in Plant Energy Biology (to Barry J. Pogson).

SUPPLEMENTARY MATERIAL

The Supplementary Material for this article can be found online at: http://www.frontiersin.org/journal/10.3389/fpls.2014.00533/abstract

Figure S1 | Experimental derived H3K4 methylation patterns surrounding selected touch inducible gene loci. The UCSC Genome Browser (http://epigenomics.mcdb.ucla.edu/) was used to create tracts of mono-, di- and

tri-methylation patterns surrounding **(A)** house keeper reference gene target SAM, **(B)** WRKY53, **(C)** STPK, and **(D)** TCH3.

Supplemental Table 1 | Bioinformatic analysis comparing genes regulated by SDG8 and responsive to mechanical stimulation.

Supplemental Table 2 | PCR Primers used to quantify mRNA levels and chromatin modifications.

Data Analysis S1 | Statistical analyses of morphological data using R code and nlme package.

REFERENCES

Antosiewicz, D. M., Polisensky, D. H., and Braam, J. (1995). Cellular localization of the Ca2+ binding TCH3 protein of Arabidopsis. *Plant J.* 8, 623–636. doi: 10.1046/j.1365-313X.1995.08050623.x

Benjamins, R., Ampudia, C. S., Hooykaas, P. J., and Offringa, R. (2003). PINOID-mediated signaling involves calcium-binding proteins. *Plant Physiol.* 132, 1623–1630. doi: 10.1104/pp.103.019943

Berr, A., McCallum, E. J., Alioua, A., Heintz, D., Heitz, T., and Shen, W. H. (2010). Arabidopsis histone methyltransferase SET DOMAIN GROUP8 mediates induction of the jasmonate/ethylene pathway genes in plant defense response to necrotrophic fungi. *Plant Physiol.* 154, 1403–1414. doi: 10.1104/pp.110.161497

Berr, A., Shafiq, S., and Shen, W. H. (2011b). Histone modifications in transcriptional activation during plant development. *Biochim. Biophys. Acta* 1809, 567–576. doi: 10.1016/j.bbagrm.2011.07.001

Berr, A., Shafiq, S., and Shen, W.-H. (2011a). Histone modifications in transcriptional activation during plant development. *Biochim. Biophys. Acta* 1809, 567–576. doi: 10.1016/j.bbagrm.2011.07.001

Biddington, N. (1986). The effects of mechanically-induced stress in plants. *Plant Growth Regul.* 4, 103–123. doi: 10.1007/BF00025193

Bird, A. (2007). Perceptions of epigenetics. *Nature* 447, 396–398. doi: 10.1038/nature05913

Botella, J. R., Arteca, J. M., Schlagnhaufer, C. D., Arteca, R. N., and Phillips, A. T. (1992). Identification and characterization of a full-length cDNA encoding for an auxin-induced 1-aminocyclopropane-1-carboxylate synthase from etiolated mung bean hypocotyl segments and expression of its mRNA in response to indole-3-acetic acid. *Plant Mol. Biol.* 20, 425–436. doi: 10.1007/BF00040602

Braam, J. (1992). Regulated expression of the calmodulin-related TCH genes in cultured Arabidopsis cells: induction by calcium and heat shock. *Proc. Natl. Acad. Sci. U.S.A.* 89, 3213–3216. doi: 10.1073/pnas.89.8.3213

Braam, J. (2005). In touch: plant responses to mechanical stimuli. *New Phytol.* 165, 373–389. doi: 10.1111/j.1469-8137.2004.01263.x

Braam, J., and Davis, R. W. (1990). Rain-, wind-, and touch-induced expression of calmodulin and calmodulin-related genes in Arabidopsis. *Cell* 60, 357–364. doi: 10.1016/0092-8674(90)90587-5

Cazzonelli, C. I., Cuttriss, A. J., Cossetto, S. B., Pye, W., Crisp, P., Whelan, J., et al. (2009a). Regulation of carotenoid composition and shoot branching in *Arabidopsis* by a chromatin modifying histone methyltransferase, SDG8. *Plant Cell* 21, 39–53. doi: 10.1105/tpc.108.063131

Cazzonelli, C. I., McCallum, E. J., Lee, R., and Botella, J. R. (2005). Characterization of a strong, constitutive mung bean (*Vigna radiata L.*) promoter with a complex mode of regulation in planta. *Transgenic Res.* 14, 941–967. doi: 10.1007/s11248-005-2539-2

Cazzonelli, C. I., Millar, T., Finnegan, E. J., and Pogson, B. J. (2009b). Promoting gene expression in plants by permissive histone lysine methylation. *Plant Signal. Behav.* 4, 484–488. doi: 10.4161/psb.4.6.8316

Cazzonelli, C. I., Roberts, A. C., Carmody, M. E., and Pogson, B. J. (2010). Transcriptional control of SET DOMAIN GROUP8 and CAROTENOID ISOMERASE during Arabidopsis development. *Mol. Plant* 3, 174–191. doi: 10.1093/mp/ssp092

Chehab, E. W., Eich, E., and Braam, J. (2009). Thigmomorphogenesis: a complex plant response to mechano-stimulation. *J. Exp. Bot.* 60, 43–56. doi: 10.1093/jxb/ern315

Chehab, E. W., Yao, C., Henderson, Z., Kim, S., and Braam, J. (2012). Arabidopsis touch-induced morphogenesis is jasmonate mediated and protects against pests. *Curr. Biol.* 22, 701–706. doi: 10.1016/j.cub.2012.02.061

Coutand, C., Dupraz, C., Jaouen, G., Ploquin, S., and Adam, B. (2008). Mechanical stimuli regulate the allocation of biomass in trees: demonstration with young Prunus avium trees. *Ann. Bot.* 101, 1421–1432. doi: 10.1093/aob/mcn054

Coutand, C., Martin, L., Leblanc-Fournier, N., Decourteix, M., Julien, J. L., and Moulia, B. (2009). Strain mechanosensing quantitatively controls diameter growth and PtaZFP2 gene expression in poplar. *Plant Physiol.* 151, 223–232. doi: 10.1104/pp.109.138164

Czechowski, T., Stitt, M., Altmann, T., Udvardi, M. K., and Scheible, W. R. (2005). Genome-wide identification and testing of superior reference genes for transcript normalization in Arabidopsis. *Plant Physiol.* 139, 5–17. doi: 10.1104/pp.105.063743

Dong, G., and Li, J. (2013). MicroRNAs profiling reveals a potential link between the SDG8 methyltransferase and brassinosteroid-regulated gene expression in Arabidopsis. *Data Mining Genomics Proteomics* 4:e110. doi: 10.4172/2153-0602.1000e110

Dong, G., Ma, D. P., and Li, J. (2008). The histone methyltransferase SDG8 regulates shoot branching in Arabidopsis. *Biochem. Biophys. Res. Commun.* 373, 659–664. doi: 10.1016/j.bbrc.2008.06.096

Du, Z., Zhou, X., Ling, Y., Zhang, Z., and Su, Z. (2010). agriGO: a GO analysis toolkit for the agricultural community. *Nucleic Acids Res.* 38, W64–W70. doi: 10.1093/nar/gkq310

Feng, J., and Shen, W.-H. (2014). Dynamic regulation and function of histone monoubiquitination in plants. *Front. Plant Sci.* 5:83. doi: 10.3389/fpls.2014.00083

Finnegan, E. J., Sheldon, C. C., Jardinaud, F., Peacock, W. J., and Dennis, E. S. (2004). A cluster of Arabidopsis genes with a coordinate response to an environmental stimulus. *Curr. Biol.* 14, 911–916. doi: 10.1016/j.cub.2004.04.045

Friml, J., Yang, X., Michniewicz, M., Weijers, D., Quint, A., Tietz, O., et al. (2004). A PINOID-dependent binary switch in apical-basal PIN polar targeting directs auxin efflux. *Science* 306, 862–865. doi: 10.1126/science.1100618

Grini, P. E., Thorstensen, T., Alm, V., Vizcay-Barrena, G., Windju, S. S., Jorstad, T. S., et al. (2009). The ASH1 HOMOLOG 2 (ASHH2) histone H3 methyltransferase is required for ovule and anther development in Arabidopsis. *PLoS ONE* 4:e7817. doi: 10.1371/journal.pone.0007817

Hofmann, N. R. (2009). Early signaling events in mechanosensing. *Plant Cell* 21, 2191. doi: 10.1105/tpc.109.210810

Hoppmann, V., Thorstensen, T., Kristiansen, P. E., Veiseth, S. V., Rahman, M. A., Finne, K., et al. (2011). The CW domain, a new histone recognition module in chromatin proteins. *EMBO J.* 30, 1939–1952. doi: 10.1038/emboj.2011.108

Iliev, E. A., Xu, W., Polisensky, D. H., Oh, M. H., Torisky, R. S., Clouse, S. D., et al. (2002). Transcriptional and posttranscriptional regulation of Arabidopsis TCH4 expression by diverse stimuli. Roles of cis regions and brassinosteroids. *Plant Physiol.* 130, 770–783. doi: 10.1104/pp.008680

Jaffe, M. J. (1973). Thigmomorphogenesis: the response of plant growth and development to mechanical stimulation: with special reference to *Bryonia dioica*. *Planta* 114, 143–157. doi: 10.1007/BF00387472

Jaffe, M. J., and Forbes, S. (1993). Thigmomorphogenesis: the effect of mechanical perturbation on plants. *Plant Growth Regul.* 12, 313–324. doi: 10.1007/BF00027213

Justin, N., De Marco, V., Aasland, R., and Gamblin, S. J. (2010). Reading, writing and editing methylated lysines on histone tails: new insights from recent structural studies. *Curr. Opin. Struct. Biol.* 20, 730–738. doi: 10.1016/j.sbi.2010.09.012

Kim, J. M., To, T. K., Nishioka, T., and Seki, M. (2010). Chromatin regulation functions in plant abiotic stress responses. *Plant Cell Environ.* 33, 604–611. doi: 10.1111/j.1365-3040.2009.02076.x

Kim, S. Y., He, Y., Jacob, Y., Noh, Y. S., Michaels, S., and Amasino, R. (2005). Establishment of the vernalization-responsive, winter-annual habit in Arabidopsis requires a putative histone H3 methyl transferase. *Plant Cell* 17, 3301–3310. doi: 10.1105/tpc.105.034645

Ko, J. H., Mitina, I., Tamada, Y., Hyun, Y., Choi, Y., Amasino, R. M., et al. (2010). Growth habit determination by the balance of histone methylation activities in Arabidopsis. *EMBO J.* 29, 3208–3215. doi: 10.1038/emboj.2010.198

Kurusu, T., Iida, H., and Kuchitsu, K. (2012a). Roles of a putative mechanosensitive plasma membrane Ca2+-permeable channel OsMCA1 in generation of reactive oxygen species and hypo-osmotic signaling in rice. *Plant Signal. Behav.* 7, 796–798. doi: 10.4161/psb.20521

Kurusu, T., Kuchitsu, K., Nakano, M., Nakayama, Y., and Iida, H. (2013). Plant mechanosensing and Ca2+ transport. *Trends Plant Sci.* 18, 227–233. doi: 10.1016/j.tplants.2012.12.002

Kurusu, T., Nishikawa, D., Yamazaki, Y., Gotoh, M., Nakano, M., Hamada, H., et al. (2012b). Plasma membrane protein OsMCA1 is involved in regulation of hypo-osmotic shock-induced Ca2+ influx and modulates generation of reactive oxygen species in cultured rice cells. *BMC Plant Biol.* 12:11. doi: 10.1186/1471-2229-12-11

Leblanc-Fournier, N., Coutand, C., Crouzet, J., Brunel, N., Lenne, C., Moulia, B., et al. (2008). Jr-ZFP2, encoding a Cys2/His2-type transcription factor, is involved in the early stages of the mechano-perception pathway and specifically expressed in mechanically stimulated tissues in woody plants. *Plant Cell Environ.* 31, 715–726. doi: 10.1111/j.1365-3040.2008.01785.x

Lee, D., Polisensky, D. H., and Braam, J. (2005). Genome-wide identification of touch- and darkness-regulated Arabidopsis genes: a focus on calmodulin-like and XTH genes. *New Phytol.* 165, 429–444. doi: 10.1111/j.1469-8137.2004.01238.x

Lim, P. S., Hardy, K., Bunting, K. L., Ma, L., Peng, K., Chen, X., et al. (2009). Defining the chromatin signature of inducible genes in T cells. *Genome Biol.* 10, R107. doi: 10.1186/gb-2009-10-10-r107

Martin, L., Leblanc-Fournier, N., Azri, W., Lenne, C., Henry, C., Coutand, C., et al. (2009). Characterization and expression analysis under bending and other abiotic factors of PtaZFP2, a poplar gene encoding a Cys2/His2 zinc finger protein. *Tree Physiol.* 29, 125–136. doi: 10.1093/treephys/tpn011

Mitchell, C. A. (1996). Recent Advances in plant response to mechanical stress: theory and application. *Hortscience* 31, 31–35.

Monshausen, G. B., Bibikova, T. N., Weisenseel, M. H., and Gilroy, S. (2009). Ca2+ regulates reactive oxygen species production and pH during mechanosensing in Arabidopsis roots. *Plant Cell* 21, 2341–2356. doi: 10.1105/tpc.109.068395

Monshausen, G. B., and Haswell, E. S. (2013). A force of nature: molecular mechanisms of mechanoperception in plants. *J. Exp. Bot.* 64, 4663–4680. doi: 10.1093/jxb/ert204

Nakagawa, Y., Katagiri, T., Shinozaki, K., Qi, Z., Tatsumi, H., Furuichi, T., et al. (2007). Arabidopsis plasma membrane protein crucial for Ca2+ influx and touch sensing in roots. *Proc. Natl. Acad. Sci. U.S.A.* 104, 3639–3644. doi: 10.1073/pnas.0607703104

Pfaffl, M. (2001). A new mathematical model for relative quantification in real-time RT-PCR. *Nucleic Acids Res.* 29, 2002–2007. doi: 10.1093/nar/29.9.e45

Saze, H. (2008). Epigenetic memory transmission through mitosis and meiosis in plants. *Semin. Cell Dev. Biol.* 19, 527–536. doi: 10.1016/j.semcdb.2008.07.017

Schneider, C. A., Rasband, W. S., and Eliceiri, K. W. (2012). NIH Image to ImageJ: 25 years of image analysis. *Nat. Methods* 9, 671–675. doi: 10.1038/nmeth.2089

Shafiq, S., Berr, A., and Shen, W.-H. (2014). Combinatorial functions of diverse histone methylations in *Arabidopsis thaliana* flowering time regulation. *New Phytol.* 201, 312–322. doi: 10.1111/nph.12493

Sistrunk, M. L., Antosiewicz, D. M., Purugganan, M. M., and Braam, J. (1994). Arabidopsis TCH3 encodes a novel Ca2+ binding protein and shows environmentally induced and tissue-specific regulation. *Plant Cell* 6, 1553–1565.

Smith, V. C., and Ennos, A. R. (2003). The effects of air flow and stem flexure on the mechanical and hydraulic properties of the stems of sunflowers *Helianthus annuus* L. *J. Exp. Bot.* 54, 845–849. doi: 10.1093/jxb/erg068

Song, J., Irwin, J., and Dean, C. (2013). Remembering the prolonged cold of winter. *Curr. Biol.* 23, R807–R811. doi: 10.1016/j.cub.2013.07.027

Tang, X., Lim, M. H., Pelletier, J., Tang, M., Nguyen, V., Keller, W. A., et al. (2012). Synergistic repression of the embryonic programme by SET DOMAIN GROUP 8 and EMBRYONIC FLOWER 2 in Arabidopsis seedlings. *J. Exp. Bot.* 63, 1391–1404. doi: 10.1093/jxb/err383

Tretner, C., Huth, U., and Hause, B. (2008). Mechanostimulation of *Medicago truncatula* leads to enhanced levels of jasmonic acid. *J. Exp. Bot.* 59, 2847–2856. doi: 10.1093/jxb/ern145

Van Dijk, K., Marley, K. E., Jeong, B. R., Xu, J., Hesson, J., Cerny, R. L., et al. (2005). Monomethyl histone H3 lysine 4 as an epigenetic mark for silenced euchromatin in Chlamydomonas. *Plant Cell* 17, 2439–2453. doi: 10.1105/tpc.105.034165

Wever, W., McCallum, E. J., Chakravorty, D., Cazzonelli, C. I., and Botella, J. R. (2010). The 5′ untranslated region of the VR-ACS1 mRNA acts as a strong translational enhancer in plants. *Transgenic Res.* 19, 667–674. doi: 10.1007/s11248-009-9332-6

Wisniewska, J., Xu, J., Seifertova, D., Brewer, P. B., Ruzicka, K., Blilou, I., et al. (2006). Polar PIN localization directs auxin flow in plants. *Science* 312, 883. doi: 10.1126/science.1121356

Xu, L., Zhao, Z., Dong, A., Soubigou-Taconnat, L., Renou, J. P., Steinmetz, A., et al. (2008). Di- and tri- but not monomethylation on histone H3 lysine 36 marks active transcription of genes involved in flowering time regulation and other processes in *Arabidopsis thaliana*. *Mol. Cell. Biol.* 28, 1348–1360. doi: 10.1128/MCB.01607-07

Xu, W., Purugganan, M. M., Polisensky, D. H., Antosiewicz, D. M., Fry, S. C., and Braam, J. (1995). Arabidopsis TCH4, regulated by hormones and the environment, encodes a xyloglucan endotransglycosylase. *Plant Cell* 7, 1555–1567. doi: 10.1105/tpc.7.10.1555

Zarka, D. G., Vogel, J. T., Cook, D., and Thomashow, M. F. (2003). Cold induction of Arabidopsis CBF genes involves multiple ICE (inducer of CBF expression) promoter elements and a cold-regulatory circuit that is desensitized by low temperature. *Plant Physiol.* 133, 910–918. doi: 10.1104/pp.103.027169

Zhang, X., Bernatavichute, Y. V., Cokus, S., Pellegrini, M., and Jacobsen, S. E. (2009). Genome-wide analysis of mono-, di- and trimethylation of histone H3 lysine 4 in *Arabidopsis thaliana*. *Genome Biol.* 10:R62. doi: 10.1186/gb-2009-10-6-r62

Zhao, Z., Yu, Y., Meyer, D., Wu, C., and Shen, W. H. (2005). Prevention of early flowering by expression of FLOWERING LOCUS C requires methylation of histone H3 K36. *Nat. Cell Biol.* 7, 1256–1260. doi: 10.1038/ncb1329

Conflict of Interest Statement: The authors declare that the research was conducted in the absence of any commercial or financial relationships that could be construed as a potential conflict of interest.

Received: 05 June 2014; accepted: 19 September 2014; published online: 21 October 2014.

Citation: Cazzonelli CI, Nisar N, Roberts AC, Murray KD, Borevitz JO and Pogson BJ (2014) A chromatin modifying enzyme, SDG8, is involved in morphological, gene expression, and epigenetic responses to mechanical stimulation. Front. Plant Sci. ***5****:533. doi: 10.3389/fpls.2014.00533*

This article was submitted to Plant Physiology, a section of the journal Frontiers in Plant Science.

frontiers in Plant Science

REVIEW
published: 22 April 2015
doi: 10.3389/fpls.2015.00266

Acclimation of mechanical and hydraulic functions in trees: impact of the thigmomorphogenetic process

Eric Badel[1,2], Frank W. Ewers[3], Hervé Cochard[1,2] and Frank W. Telewski[4]*

[1] INRA, UMR 547 PIAF, Clermont-Ferrand, France, [2] Clermont Université–Université Blaise-Pascal, UMR 547 PIAF, Clermont-Ferrand, France, [3] Department of Biological Sciences, California State Polytechnic University, Pomona, CA, USA, [4] Department of Plant Biology, Michigan State University, East Lansing, MI, USA

The secondary xylem (wood) of trees mediates several functions including water transport and storage, mechanical support and storage of photosynthates. The optimal structures for each of these functions will most likely differ. The complex structure and function of xylem could lead to trade-offs between conductive efficiency, resistance to embolism, and mechanical strength needed to count for mechanical loading due to gravity and wind. This has been referred to as the trade-off triangle, with the different optimal solutions to the structure/function problems depending on the environmental constraints as well as taxonomic histories. Thus, the optimisation of each function will lead to drastically different anatomical structures. Trees are able to acclimate the internal structure of their trunk and branches according to the stress they experience. These acclimations lead to specific structures that favor the efficiency or the safety of one function but can be antagonistic with other functions. Currently, there are no means to predict the way a tree will acclimate or optimize its internal structure in support of its various functions under differing environmental conditions. In this review, we will focus on the acclimation of xylem anatomy and its resulting mechanical and hydraulic functions to recurrent mechanical strain that usually result from wind-induced thigmomorphogenesis with a special focus on the construction cost and the possible trade-off between wood functions.

Keywords: trees, wood, trade-off, thigmomorphogenesis, mechanics, hydraulics, wood anatomy, acclimation to stress

OPEN ACCESS

Edited by:
Stephen Jarvis Mitchell, University of British Columbia, Canada

Reviewed by:
Serge Delrot, University of Bordeaux, France
Roland Ennos, University of Hull, UK

****Correspondence:***
Eric Badel, INRA, UMR 547 PIAF, 63100 Clermont-Ferrand, France; Clermont Université–Université Blaise-Pascal, UMR 547 PIAF, 63000 Clermont-Ferrand, France
eric.badel@clermont.inra.fr

Specialty section:
This article was submitted to Plant Physiology, a section of the journal Frontiers in Plant Science

Received: *07 October 2014*
Accepted: *03 April 2015*
Published: *22 April 2015*

Citation:
Badel E, Ewers FW, Cochard H and Telewski FW (2015) Acclimation of mechanical and hydraulic functions in trees: impact of the thigmomorphogenetic process. Front. Plant Sci. 6:266. doi: 10.3389/fpls.2015.00266

Introduction

Secondary xylem (wood) arises as a result of cell divisions of the vascular cambium and is referred to as a type of secondary growth. After division, these cells go through phases of differentiation, enlargement, and maturation. During this process, the cell wall develops, most significantly, the secondary cell wall composed of organized layers of (crystalline) cellulose microfibrils and lignin. Lignin deposition also occurs in the middle lamella region between cells. At the end of the maturation process, the conducting cells (tracheids in conifers, vessels in angiosperms) die through a process of autolysis, the living components (cytoplasm and organelles) are reabsorbed by the tree, and the water-filled cell lumen becomes physiologically functional providing hydraulic conductivity. The resulting structure is a complex porous network of interconnected cells that fulfills several functions that are required for the continued life of the tree in a variable environment. In both

dicotyledonous trees and in conifers the vascular cambium can continue to produce new layers of wood throughout the life of the stem or root and so the response to environmental cues is ongoing.

The xylem of the stem mainly provides three types of functions: (i) the xylem is the hydraulic pathway for the transport of water from the soil to the transpiring leaves, providing hydration to all living cells along the way; (ii) the stem mechanically supports the heavy structure of the tree; (iii) the xylem is a place where many biochemical components that are required for the tree in order to withstand external stresses (like freezing, insect attacks, etc.) are stored as well as the storage of photosynthate (carbohydrates, lipids, and proteins) over the winter for future growth in the subsequent spring (Telewski et al., 1996). Water storage, both on a seasonal and diurnal basis, can also be a crucial function of the xylem (Pratt et al., 2007; Meinzer et al., 2009). The optimal structures for each of these functions will most likely differ. Selection, either natural, via breeding programs or via genetic engineering, to optimize for one function could lead to sub-optimal performance, or even complete failure of another function (Lachenbruch and McCulloh, 2014). For instance, xylem that is highly efficient in water conduction might be so mechanically weak that it could not withstand wind, snow, or ice loading resulting in failure of the stem or branches. In this paper, we will focus on the first two functions of xylem namely hydraulic transport and mechanical support.

As a result of an acclimation process, plants modify their growth when they experience mechanical loading: plants are able to perceive external mechanical stresses that generate the strain of the living tissues (Moulia et al., 2015). These living cells generate signals that engender local or remote molecular responses that modify the wood formation by the way of modifying the cambial activity and the differentiation process (Jaffe et al., 2002; Telewski, 2006; Chehab et al., 2009; Coutand, 2010). The response of plants to mechanically induced flexing, including the brushing or movement of animals against plants, or the flexing of the above ground portions of a plant by wind, ice, or snow loading was defined as thigmomorphogenesis by Jaffe (1973). However, the influence of wind on plants, and specifically trees, was first identified in a study by Knight (1803). Over the course of the ensuing 170 years between Knight's (1803) and Jaffe's (1973) publications and subsequently, many studies have been published on the effect of wind on tree growth and morphology (for reviews see Grace, 1977; Jaffe, 1985; Biddington, 1986; Vogel, 1994; Telewski, 1995, 2006, 2012; Mitchell, 1996, 2013; Jaffe et al., 2002; Braam, 2005; Moulia et al., 2006; de Langre, 2008). The most consistent thigmomorphogenetic effects are a reduction in shoot elongation and an increase in radial growth in response to a flexing stimulus resulting in a plant of shorter stature and thicker, stiffer stem. This change in growth results in a change in plant allometry which reduces the effective canopy profile to wind and reduces drag (Telewski and Jaffe, 1986a,b; Rudnicki et al., 2004; Vollsinger et al., 2005; Telewski, 2012).

At the anatomical level, Telewski (1989) described a thigmomorphogenetic acclimation of xylem formation, leading to particular wood structure termed flexure wood. However, the anatomical characterization of flexure wood is still poorly documented. In the same way, very little is known about the direct consequences of the acclimation of the material structure on the mechanical and hydraulic functions of wood formed under mechanical stimuli. Especially, the growth modifications appear to potentially compromise conductive efficiency resulting in a trade-off between the mechanical and hydraulic functions of xylem. Due to the complexity of the interactions between anatomy, hydraulic conductivity, and mechanical strength of wood, there have been few studies addressing all three variables and their corresponding construction cost; especially in the case of acclimation processes like thigmomorphogenesis.

The Xylem Anatomical Structure

Gymnosperm wood is mainly composed of non-living tracheids with a small portion of living ray parenchyma and when resin ducts are present, living epithelial cells lining the ducts. The earlywood portion of gymnosperms is characterized as large diameter cells with thin cell walls, whereas the latewood is composed of smaller diameter cells with thicker cell walls (**Figure 1A**). The tracheid performs both the conductive and supportive functions within the secondary xylem. The ray parenchyma cells are aligned radially and are usually small compared to angiosperms. On the contrary, the annual ring of angiosperms is composed of more specialized cell types. In addition to ray parenchyma, angiosperms can have axial parenchyma, fibers, fiber tracheids, and vessels depending on the species of tree (**Figures 1B,C**).

Wood density is often used as a key functional trait correlated with other ecophysiological behavior including growth rate, hydraulic conductivity, and mechanical strength (Poorter, 2008; Stegen et al., 2009; Swenson and Weiser, 2010; Swenson et al., 2011; Liu et al., 2012, 2013; Iida et al., 2014). Typically, low density wood results from greater porosities (due to larger diameter, thinner walled cells) that increase the efficiency of water transport, while the material rigidity may be compromised. However, the wood density is an integrative parameter that mainly results from the fiber cell wall thickness and lumen diameter was well as vessel density and size (for angiosperms). It is obvious that for the same mean porosity, different anatomical patterns provide different functional properties.

Reaction Wood

Trees show a great ability to modify the orientation of their main organs, stem, and branches. They do it in a way that improves their architecture via phototropism or gravitropism, in response to neighbor shading, displacement by the wind, or other mechanical perturbations (avalanches, landslides, slope slippage, ice, and snow, etc.,; for review, see Wilson and Archer, 1977; Timell, 1986a,b,c; Du and Yamamoto, 2007). The dynamic reorientation of these organs involves the formation of a particular type of wood called reaction wood. Usually produced on one side of the organ, the physical and mechanical properties of reaction wood and opposite wood (see for example, Clair et al., 2006) are such as to generate a large difference in growth strains between the sides which can result in a change of curvature of the organ.

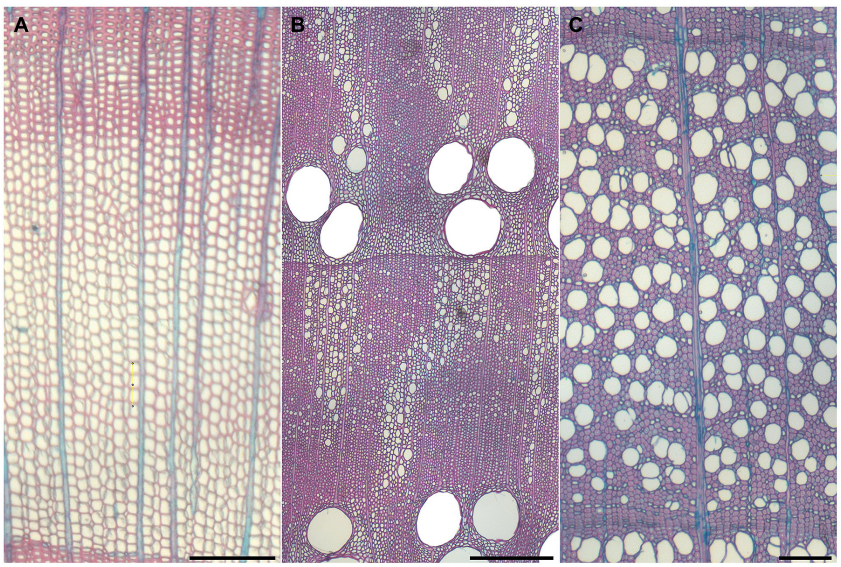

FIGURE 1 | Typical anatomical cross sections of annual rings in trees. Gymnosperms show mainly longitudinal tracheids that perform both mechanical and hydraulical functions **(A)**. Angiosperms show heterogeneous **(B)** or homogeneous **(C)** structures that include large vessels that fulfill only the water conduction function, while mechanical support of the tree is provided by fibers. **(A)** *Larix decidua*, **(B)** *Quercus robur*, and **(C)** *Fagus sylvatica*. Scale bar represents 200 μm.

This wood shows specific anatomical patterns that differ between gymnosperms and angiosperms.

In gymnosperms, the reaction wood is called compression wood (**Figures 2A,B**), which occurs on the lower side of non-vertical branches. Compression wood tracheids are shorter than normal wood tracheids. In the transversal direction, they are more rounded and show intercellular spaces at would have been cell corners that do not appear in normal wood. At the cell wall level, the compression wood cells usually possess an S3 layer that is not common for normal wood and the thicker S2 layer has a higher microfibril angle (MFA) than normal wood (Evans, 1998).

In porous wood angiosperms, the reaction wood is termed tension wood. The hardwood fibers of tension wood can produce a gelatinous cell wall layer (**Figures 2C,D**), called the G-layer. This G-layer exhibits very particular physical property that generate the differential mechanical states on opposite sides of the organ thus forcing it to modify its curvature via contraction of the tension wood fibers upon maturation. The G-layer is mainly made of cellulose and hemicellulose, has a very small MFA and high degree of crystallinity (Yamamoto et al., 2010).

When trees experience transient wind loadings, the cambium produces a specific wood called "flexure wood" (Telewski, 1989). The anatomy and specific functions of flexure wood are poorly understood. A few observations have been carried out at the tissue level for *Pinus* (Telewski and Jaffe, 1986b) and *Abies* (Telewski, 1989) and by Kern et al. (2005) for poplar. In the conifer *Abies fraseri* the increase in radial growth results from an increase

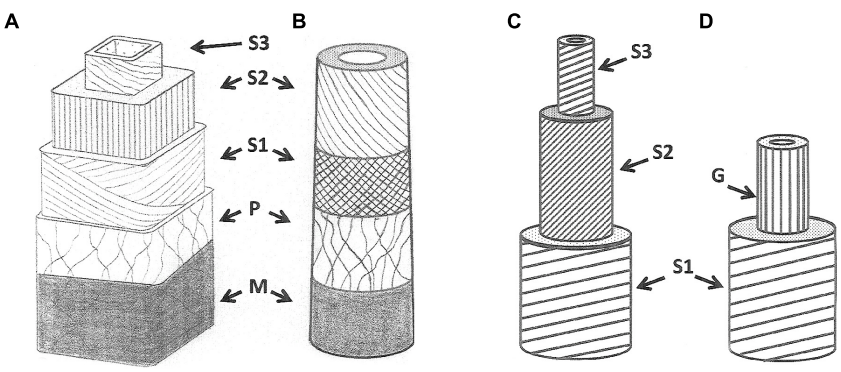

FIGURE 2 | Normal and reaction wood cell wall structures in gymnosperms (A,B) and angiosperms (C,D). (A) tracheid in normal wood, **(B)** tracheid in compression wood, **(C)** fiber in normal wood, **(D)** fiber in tension wood. G refers to the gelatinous layer.

in cell divisions from the vascular cambium, but the tracheid lumens were smaller in size (Telewski, 1989). The angiosperm *Liquidambar styraciflua* exposed to shaking for 30 s once per day exhibited smaller vessel elements in both diameter and length, and fibers were shorter compared to untreated trees (Neel and Harris, 1971). For poplar clones, Kern et al. (2005) reported a significant reduction in vessel lumen area, vessel diameter, and vessel frequency with flexure treatment. Moreover, they observed many similarities between flexure wood and reaction wood. Butterfield and Li (2000) showed that tied trees of *Pinus radiata* produced compression wood and tracheids with lower MFA than non-tied trees. Also at the cell wall level, it has been observed on *P. radiata* that juvenile wood show large MFA in trees growing in open plantations (Cave and Walker, 1994). On the contrary, this MFA is low in established forests, suggesting that wind loadings have a great role in the structure of the S2 layer. In angiosperms, flexing increased the amount of syringyl monolignols over guaiacyl monolignols within the lignin polymer (Koehler and Telewski, 2006). With regard to a functional role for flexure wood, Telewski and Jaffe (1986a) pointed out that flexure wood needs to function in both compression and tension due to alternating sway, and that wood is weaker under compressive loading than tensional loading. Therefore, they suggested that cells with a functional structure more suited to deal with compression would be advantageous to a tree growing in a windy environment. However, the lack of data on flexure wood anatomy, especially at the cell wall level, does not permit a rigorous comparison with reaction wood. More detailed characterizations need to be done before claiming that flexure and reaction woods are structurally the same wood provided by different external mechanical loadings.

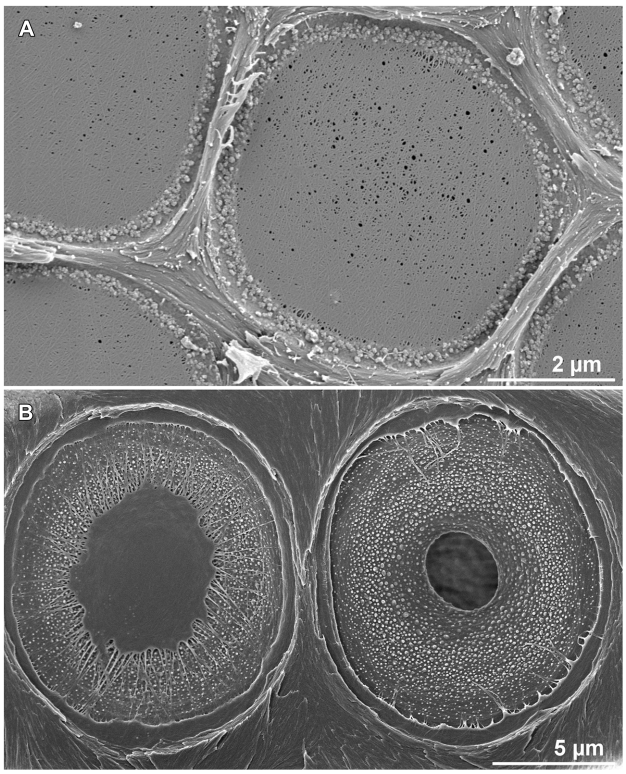

FIGURE 3 | Structure of pits in angiosperms (A) and gymnosperms (B). The inter-vessel pit in angiosperms is composed of a pit chamber and a thin continuous membrane made of primary wall. Inter-tracheids pits in gymnosperms are made of a pit chamber that includes a thick torus connected to the cell wall by cellulose microfibrils. (photos credit: S. Jansen).

Interconduit Connections

Pits in the double cell wall are the main pathways for water to be transported from one cell to its adjacent cell, connecting two softwood tracheids or hardwood vessels. A hydraulic conduit is connected to multiple other adjacent conduits, providing redundancy in multiple pathways for water movement in case of embolism of one conduit element.

In angiosperms, pits are made of a pit chamber that occurs in the double cell wall and is connected to the cell lumens by the way of holes called apertures (**Figure 3A**). This chamber is separated into two parts by a thin and flexible continuous membrane resulting from the remaining primary wall. In gymnosperms, the membrane is not continuous: the central structure, the torus, is reduced to a central plate; which is physically linked to the cell wall by the margo made of thin threads of cellulose microfibrils (**Figure 3B**).

Wood Mechanical Behavior

The mechanical functions include: self-support against the pull of gravity in the form of axial compression upon the trunk (McMahon, 1973; Wainwright et al., 1976; Niklas, 1992, 1994), a degree of stiffness or flexibility to bending under windy conditions or under conditions of loading due to ice, snow, or fruit loading (Telewski, 1995, 2006; Valinger et al., 1995; Alméras et al., 2004; Vaast et al., 2005; Mayr et al., 2006) and the ability to generate internal growth strains in developing xylem to produce corrective growth in stems displaced with respect to gravity with the formation of reaction wood. The mechanical parameters that most inform us about significant functional roles in the xylem include the elastic modulus (or Young's modulus) E_L, the modulus of rupture (MOR), and the second moment of cross sectional area I, which varies with the fourth power of stem diameter D (Eq. 1). The ecologically important parameter of stem strength is the flexural stiffness $E_L I$ that drives the ability of an elongated organ to deform when it experiences bending loads.

$$I = \pi \frac{D^4}{64} \quad (1)$$

The longitudinal Young's modulus E_L of wood refers to the stiffness of the wood vertically. Since wood is a porous material with longitudinally oriented cells, E_L is mainly linked to porosity (i.e., the cell wall fraction). Thus, in a first approximation, E_L can be estimated as proportional to the wood density (Fournier et al., 2006).

The intrinsic mechanical properties of the cell wall are functions of the cell wall structure (mainly MFA; Cave and Hutt, 1969) and chemical composition (lignin, cellulose, and hemicellulose). For few species (eucalyptus for example) the knowledge of wood density and MFA can explain almost completely the wood Young's modulus (Evans and Elic, 2001).

Thigmomorphogenesis greatly affects the mechanical behavior of the stem. On the one hand, thigmomorphogenesis modifies the cell differentiation. It results in anatomical changes that decrease E_L of the wood material (Telewski and Jaffe, 1986a,b; Telewski, 1989; Telewski and Pruyn, 1998; Pruyn et al., 2000; Anten et al., 2005; Koehler and Telewski, 2006; Martin et al., 2010). The reduction in E_L is likely a result of increased MFA and not an increase in the syringyl content of the xylem of angiosperms since increasing the syringyl content in transgenic poplar trees increased E_L (Koehler and Telewski, 2006).

The stems of flexed *P. taeda* have a higher MOR compared to non-flexed control trees (Telewski and Jaffe, 1986b), whereas flexing was reported to decrease the MOR of hybrid poplar stems (Kern et al., 2005). This decrease of mechanical behavior cannot be directly explained at the tissue level because the wood density of flexure wood does not decrease (Telewski, 1989). Thus, the physical parameter should be found at the cell wall level and probably involves the MFA in the S2 layer. Telewski (1989) suggested that the reported increase in the MFA of the secondary cell wall of tracheids in *Abies* as part of the thigmomorphogenetic response was responsible for decreasing Young's modulus.

On the other hand, all the works that dealt with responses to mechanical stimulation of trees reported a large increase in radial growth that increases the second moment of cross sectional area I (Jacobs, 1954; Telewski and Jaffe, 1986a,b; Telewski and Pruyn, 1998; Pruyn et al., 2000; Anten et al., 2005; Martin et al., 2010). This is a consistent response across species and even within half-sib or clonal lines (Telewski and Jaffe, 1986b; Telewski, 1995; Pruyn et al., 2000; Kern et al., 2005). In most cases, the increase in I overrides the decrease in E_L resulting in an increase in stem rigidity or flexural stiffness ($E_L I$). The end result is an overall stiffer stem composed of more pliable xylem capable of absorbing more mechanical energy in response to wind loading (Telewski, 1989, 1995, 2012; Pruyn et al., 2000). Moreover, when a circular stem is bent, the maximum longitudinal strain ϵ_{max} is proportional to the ratio $D/E_L I$ (Eq. 2) and the maximum strain σ_{max} the stem experiences is proportional to the ratio D/I (Eq. 3).

$$\varepsilon_{max} = M_b \frac{D}{2\, E_L I} \tag{2}$$

$$\sigma_{max} = M_b \frac{D}{2\, I} \tag{3}$$

Where M_b is the bending moment applied on the stem (by wind for example). Thus thigmomorphogenesis tends to reduce the strain and stress the stem experiences, making it less likely to fail under mechanical loading.

Hydraulic Behavior

Conduction

Trees have developed efficient hydraulic networks to transport water from the roots into the leaves (Sperry, 2003). This process involves small pores (around 20 nm) that generate menisci having a very small radius of curvature, resulting in a surface tension that causes a negative pressure that pulls up the water column from the roots into the leaves, helped by water molecule cohesion.

Xylem is the main long distance transport pathway for water and soluble mineral nutrients from roots to the leaves. One of its main functions is to provide a low resistance pathway for water transport. Transport is provided by vessel elements (angiosperms) or tracheids (gymnosperms). This water transport does not involve energy consumption by the hydraulic network that act as passive conduits. Conduction efficiency is driven by the Hagen–Poiseuille equation that indicates that hydraulic conductivity Ks varies with the fourth power (Eq. 4) of the conduit diameter (Zimmermann, 1983). Thus, the optimization of an efficient hydraulic conduction function leads to the construction of a wood structure made of long and very large diameter cells (**Figure 4**).

$$K_S \propto \sum_{xylem} d_h^4 \tag{4}$$

However, comparing gymnosperm and angiosperm structure, Sperry et al. (2006) clarified the role of the end-wall connections that represented more than 50% of the total resistance of the hydraulic network. They concluded that the conduit length limits the conducting efficiency.

High positive correlations have been observed between water conduction efficiency of the xylem and the growth rate (Tyree et al., 1998; Poorter et al., 2010). This is in accordance with the simple idea that species with fast growth rates usually produce low-density wood that is more porous, with large conduits that are more efficient in transporting water (Eq. 4). Following this correlation, and assuming that thigmomorphogenesis typically generates an increase of the stem diameter growth rate, the flexure wood should show improved hydraulic efficiency. An increase

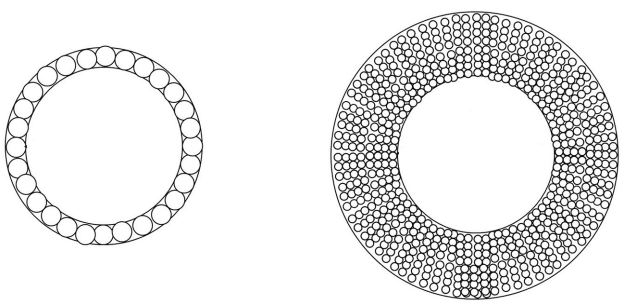

FIGURE 4 | One ring of large cells are compared with many ½ times smaller cells that provide the same hydraulic conductivity. The mass allocation for the cell wall construction is eight times higher for small cells. (computed from Tyree and Zimmermann, 2002 and Awad et al., 2012).

in hydraulic conductivity (reported as sapwood permeability) in free swaying seedlings of *P. elliottii* compared to staked seedlings was reported by Dean (1991). Liu et al. (2002) reported a decrease in specific conductivity despite an increase in radial growth in a thinned stand of *P. contorta* exposed to more wind sway. They concluded the reduction in conductivity was due to sway induced functional damage to sapwood. Kern et al. (2005) reported systematic lower specific conductivity in the stem of different hybrid poplars when they were bent. This local property was mainly due to the formation of smaller vessels as a result of thigmomorphogenesis. However, they reported that the total conductivity of the stem was not affected, suggesting that the increase of wood cross-sectional area due to the thigmomorphogenetic response compensates for the lower local transport efficiency of the xylem.

Cavitation Resistance

According to the cohesion–tension theory (Dixon, 1914) water ascent in plants takes place in a metastable state under tension. Then, the hydraulic conduction is subjected to transport dysfunctions; drought, and frost stresses can induce very large negative pressure in the water columns that break. This leads to embolism of the conduits that makes it non-operational (Tyree and Zimmermann, 2002). Cavitation is triggered by air entry in hydraulic conduits (Sperry and Tyree, 1988; Cochard et al., 1992). It occurs when the pressure difference between adjacent air- and water-filled xylem conduits becomes large enough to pull the air-water meniscus through inter-conduit pores toward the water filled conduit (Zimmermann, 1983). The required pressure difference ΔP is inversely proportional to the diameter of the pores, d, according to the Jurin's law:

$$\Delta P = \frac{4\ \tau\ \cos\theta}{d} \tag{5}$$

where τ is the liquid surface tension, θ is the contact angle of the liquid with the pore walls. Thus, the plant structural parameter that determines the vulnerability to drought-induced xylem embolism is the diameter of the largest inter-vessel pore (Eq. 5).

The main sites of air seeding to the xylem pathway are inter-vessel or inter-tracheids pits. What is the physical role of the pits during the cavitation process? Many anatomical measurements have been performed on gymnosperm and angiosperm pits. There are statistical correlations between anatomical parameters like pit membrane thickness, aperture diameter, torus diameter, etc., with the cavitation sensitivity. The mechanical behavior of the pit membrane was investigated by the way of modeling (Sperry and Hacke, 2004; Tixier et al., 2014). They showed that the pit aperture diameter together with the diameter and the thickness of the pit membrane plays a great role in its mechanical behavior; which was highly correlated with cavitation sensitivity at the inter-specific level. However, no clear mechanism has been described and no anatomical parameter can be clearly said to be the key point. Again, the pit is probably the most relevant level of observation of air-seeding and there is no evidence of relationship with the conduit diameter or length (Dalla-Salda et al., 2014). However, the "rare pit" hypothesis (also named "pit area" hypothesis; Hacke et al., 2001; Wheeler et al., 2005; Pittermann et al., 2006) suggests that the bigger the conduit, the larger its surface and the more pits are located in its wall, thus the greater probability of a defective, wide, or less efficient pit, that could be the air-seeding starting point. Following this hypothesis, cavitation sensitivity may be lower for flexure wood that shows smaller conduit diameters. For gymnosperms, one of the most relevant anatomical parameters that may drive the cavitation resistance is the overlap between the torus and the pit border (torus diameter/aperture diameter). This is consistent with the seal-capillary seeding hypothesis (Bouche et al., 2014). Finally, the xylem anatomy determines how much water can be transported and at the same time, the plant's vulnerability to transport dysfunctions (the formation and propagation of embolism) associated to water stress.

Despite the cavitation mechanism not being clearly elucidated, several correlations were investigated in order to focus on the relevant anatomical parameters. At the macroscopic scale, the wood density is often investigated and species that show denser wood usually show higher cavitation resistance (Sperry et al., 2006). This is coherent with previous observations that suspected that wider conduits are more vulnerable to cavitation (Carlquist, 1975; Baas, 1986; Cochard and Tyree, 1990; Tyree et al., 1994). However, this interspecific correlation hides a large variability and finally, the relationships between diameter conduits and their vulnerability is probably an indirect and non-causal correlation when it comes to water stress induced embolism. However, freezing induced embolism appears to be fairly well understood and is closely related to the size of the conduit (Sperry et al., 1994; Davis et al., 1999; Pittermann and Sperry, 2003; Mayr et al., 2006). According to these correlations, wood formed under thigmomorphogenetic process should be less prone to freezing induced embolism since the conduits may be reduced in size. However, no work has reported experimental data on the cavitation resistance of flexure wood, suggesting that hydraulic properties need to be investigated in order to confirm these hypotheses.

Trade-offs

Considering trees need to continuously manage all their vital hydraulic and vital mechanical functions, it is suspected that trade-offs could exist. Possible trade-offs between mechanical and hydraulic properties are inherently complex since both are subject to fourth power relationships. As noted above, axial stiffness ($E_L I$) is proportional to stem diameter to the fourth power due to the second moment of area calculation, and conductive efficiency is proportional to vessel or tracheid diameter to the fourth power, following the Hagen–Poiseuille law. To increase the hydraulic conductivity the obvious solution is to increase vessel or tracheid diameter, but those solutions could weaken the wood. Is there a necessary trade-off between strength and hydraulic conductivity, and what are the other ramifications of this trade-off? (**Figure 5**). If so, what are the consequences for cavitation and implosion resistance? What is the effect on hydraulic capacitance?

A number of studies have investigated the interrelations between conductive efficiency and mechanical stress

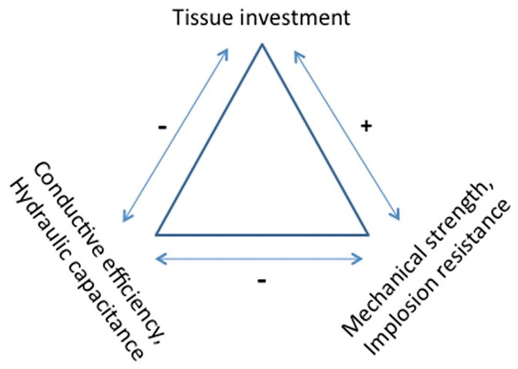

FIGURE 5 | Functions vs. cost trade-off in wood tissues.

acclimation, with inconsistent results. Several studies have found a trade-off between hydraulic conductivity and mechanical strength (Gartner, 1991a,b,c; Wagner et al., 1998; Jagels et al., 2003; Smith and Ennos, 2003; Christensen-Dalsgaard et al., 2007). Others have failed to find any trade-off (Woodrum et al., 2003; Pratt et al., 2007; Rosner et al., 2007, 2008; Utsumi et al., 2010). They suggest that several anatomical variables may confound the influence of the number and diameter of conduits. These variables include pith diameter, ray width, and fiber cell wall thickness, to name a few. Additionally, cell wall structure such as MFA and chemical composition (ratio of lignin to cellulose and lignin monomer composition) are also variables that will influence the mechanical strength of xylem. Inferences can be made based on previous studies. For example, reductions in both tracheid length and vessel element length combined with smaller lumen diameters should increase resistance to conductive flow as well as reduce the volume of water conducted on a per conductive element basis. This may be compensated for by an increase in the number of conductive elements, as is the case in conifers, but may be less likely in angiosperms as the total number of vessels also appears to be reduced in thigmomorphogenetic response to wind sway or flexing. Woodrum et al. (2003) investigated the interspecific relationship between anatomy, mechanical properties and water transport of *Acer* but they observed no trade-off between K_s max and MOE or MOR across the genus. Although compression wood has narrower tracheids and lower conductivity (Spicer and Gartner, 1998) and lower cavitation resistance (Mayr and Cochard, 2003) than opposite wood, in angiosperms tension wood may be similar in conductivity and cavitation resistance as opposite wood (Gartner et al., 2003). Unfortunately there is no published data for cavitation resistance in flexure wood except Kern et al. (2005) who reported that mechanical flexure increased stem rigidity, reduced the number and diameter of vessels, and significantly reduced K_S. However, the treatment did not significantly impact whole-stem K_h or the percent loss of conductivity due to embolism, suggesting the lack of hydraulic-mechanical trade-off during mechanical acclimation.

Although the existence of a trade-off between conductive efficiency and resistance to cavitation or implosion (efficiency versus safety) has not been consistently reported in the literature (Cochard, 1992; Sperry et al., 1994), available evidence suggests at least a weak negative correlation (Tyree et al., 1994). The hydraulic efficiency versus safety trade-off was reported by many authors (Martinez-Vilalta et al., 2002; Choat et al., 2005). Martinez-Vilalta et al. (2002) reported for nine co-occuring species that the relationship between specific hydraulic conductivity (K_s) and resistance to cavitation followed a power function with exponent ≈ -2, consistent with the existence of a trade-off between conductivity and security in the xylem. However, they suggested that this relationship was consistent with a linear relationship between vessel diameter and the size of inter-vessel pores, which has never been demonstrated. For instance, Choat et al. (2003, 2005) reported trade-offs between conductive efficiency and resistance to cavitation in seasonally dry rainforest trees, but they found no evidence of differences in pit membrane porosities in those species (Choat et al., 2003). Therefore the inverse relationship between water-stress embolism and conductive efficiency is probably indirect (see pit area hypothesis above) whereas the inverse relationship with freezing-induced embolism appears to be direct, as the size of the conduit is directly related to freeze-thaw embolism.

Xylem safety (resistance to cavitation or conduit implosion) and mechanical strength have been found to be positively correlated (Jacobsen et al., 2005; Pratt et al., 2007; Rosner et al., 2008; Utsumi et al., 2010; Bouche et al., 2014). Hacke et al. (2001) defined a mechanical safety factor that evaluates the resistance of a theoretical 2D regular cellular structure to bulk in the transverse direction when submitted to negative pressure. It involves the lumen diameter (b) and the cell wall thickness (t). The higher the thickness to span ratio $(t/b)^2$, the greater the resistant to implosion. This safety factor was then used for evaluating the implosion resistance of vessels. All these works suggest that wood density, which is highly correlated with conduit size and cell wall thickness, may impact the both functions in the same way, with thicker cell walls that make the tissues stiffer and more mechanically resistant (Hacke et al., 2001). However, smaller lumens impair the hydraulic conduction. According to Pratt et al. (2007), the stem mechanical strength appears to be important in maintaining xylem transport under negative pressure and this could be a strategy both to prevent vessel collapse and to withstand mechanical stresses caused by gravity or wind. However, Bouche et al. (2014) recently argued for angiosperms that the implosion process is unrealistic since most of the species do not experience the pressure level that should be involved. Note that for angiosperms, the implosion resistance is usually computed using the vessel wall thickness and the vessel diameter, since implosion resistance of an isolated vessel probably depends essentially on the transversal rigidity of the surrounding tissues.

Jacobsen et al. (2005) suggested the hypothesis that fibers may be essential for enabling the vessels to achieve great sizes: larger cell wall thickness of surrounding fiber tissues probably provides better implosion resistance with a cost of carbon allocation that is observed in the wood density data (Sperry et al., 2006). Following this consideration, the angiosperm species are probably able to adjust the fiber formation around the vessel in order to avoid

vessel implosion (Jacobsen et al., 2005). But perhaps that would be more expensive than putting more cellulose and lignin into the vessel cell wall. Turner and Somerville (1997) showed vessel implosion in an *Arabidopsis* mutant deficient in the deposition of secondary cell wall cellulose. Jones et al. (2001) reported that a 50% reduction in lignin content also resulted in collapsing vessels in *Arabidopsis*. Genetically modified hybrid poplar trees (*Populus alba* × *Populus grandidentata*) with reduced cell wall lignin have also shown collapsed xylem (Coleman et al., 2008). In a global study of 3005 angiosperm species, vessel diameter was strongly linked to conductive efficiency, but not linked to overall xylem density. The fiber tissues are extremely variable and may compensate for weaknesses that large vessel lumen areas can present (Zanne et al., 2010).

A significant but less studied relationship is the positive correlation between conductive efficiency and hydraulic capacitance of the sapwood. This relationship has been found in a wide range of conifers and angiosperms (Choat et al., 2005; Domec et al., 2006; Pratt et al., 2007; Meinzer et al., 2009). At least in the Rhamnaceae, hydraulic capacitance was not related to the sapwood parenchyma area (Pratt et al., 2007) Species with high conductive efficiency apparently have greater stores of apoplastic water in fibers as well as in tracheids and vessel lumens. In one model it is shown that embolism of vessels could contribute significantly to hydraulic capacitance on a daily or seasonal basis (Hölttä et al., 2009). Here again, because of a dramatic lack of experimental data, the impact of thigmomorphogenetic response on the balance between hydraulic and mechanical functions is a virgin field of research that needs to be investigated in order to evaluate the possible impact of deformation due to windy conditions on the hydraulic efficiency and safety.

Function vs. Tissue Investment

Where are the costs needed in order to improve the functional properties? As seen previously, there are two ways to increase the flexural rigidity $E_L I$ of the stem: increasing the elastic modulus of wood or increasing the stem diameter. At the cell level, increasing the module of elasticity usually involves a carbon allocation cost in order to increase the cell wall thickness and to reduce the material porosity (Larjavaara, 2010). Another mechanism to increase the Young's modulus is to decrease the MFA in the S2 layer of the cell way. Modifying the MFA probably does not involve an energetic cost, but it could impact the dimension of the strengthening. While a low MFA increases Young's modulus, it might also decrease hoop strength and cause a conduit to become more prone to implosion. The formation of cellulosic G-layer in angiosperm, provides an higher stiffness to the cell but again involves a large amount of cellulose and definitely an additional construction cost in term of carbon allocation.

At the trunk level, increasing the organ size is an efficient option too. Awad et al. (2012) stated that for the same amount of cell wall, it is more efficient in terms of stem flexural rigidity $E_L I$ to add large cells with thin cell walls than adding small cells with thick cell walls. The lower elastic modulus of the wood material is clearly counterbalanced by the large increase in the second moment of cross sectional area I of the trunk (**Figure 6C**). This can be easily demonstrated assuming that the Young's modulus is proportional to the wood density ρ (Fournier et al., 2006; **Figure 6A**)

$$E_L = \alpha\ \rho \tag{6}$$

When a beam experiences a bending moment Mb, the Eq. 2 tell us that the maximum strain varies as the inverse of D^3.

$$\varepsilon_{max} = M_b \frac{D}{2\ E_L I} = M_b \frac{32}{\pi\ E_L\ D^3} \tag{7}$$

Assuming the allocated biomass m can be estimated as (**Figure 6B**)

$$m = \rho\ D^2 \tag{8}$$

Merging Eqs 6, 7, and 8, we can write that the strain varies as the square root of the density and the maximum strain varies according to $\rho^{3/2}$ (**Figures 6D,E**):

$$\varepsilon_{max} = M_b \frac{32\ \sqrt{\rho}}{\alpha\ \pi\ m^{3/2}} \tag{9}$$

$$\sigma_{max} = M_b \frac{32\ \rho^{3/2}}{\pi\ m^{3/2}} \tag{10}$$

These Eqs 9 and 10 demonstrate that, for the same biomass allocation m, the mechanical strain and stress increase with the wood density and put the trunk at risk. This conclusion is still available even if we consider that the critical stress increases in a proportional way to the wood density (Chave et al., 2009). Finally, from a pure mechanical point of view, the formation of annual rings made of large cells with thin cell walls is probably a better strategy than the building of small annual rings made of small cells showing thick cell wall, even if locally the mechanical property E_L is higher in this last case (**Figure 5**).

As seen previously, the optimization of conduction properties and biomass allocation leads to large cells with thin cell walls. Thus, finally, low density wood that includes large lumens would be the best way to manage both mechanical and conduction properties. But what is the cost for building cavitation resistant xylem tissue? The pit is probably the very relevant level of observation. This suggests that building resistant pits has a cost and should take account in maintaining the conduction efficiency. And what is the relative importance of resistant pit members to prevent air seeding, versus mechanical support by walls of tracheids or fibers, to prevent implosion? If both parameters are relevant, and have co-evolved, this could explain some contradictions in the literature. The existence or otherwise of functional trade-offs in wood structure is still unclear and has been debated for the past several years. The anatomical parameters that drive the mechanical properties are now well identified and most of the drivers of the conduction efficiency are identified too. But the way the trees build wood that is resistant to cavitation is still a key question that needs to be elucidated in the next years.

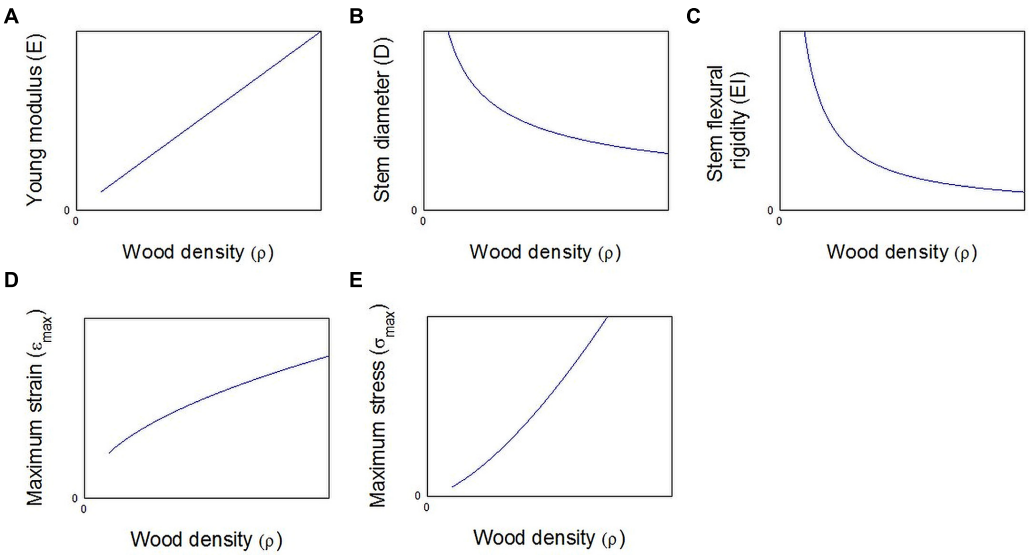

FIGURE 6 | Mechanical parameters as functions of wood density for a constant biomass *m* in the stem cross section. (A) The Young modulus is computed according to the Eq. 6. **(B)** The stem diameter is computed according to Eq. 8 and **(C)** the stem flexural rigidity is computed according to Eqs 1, 6, and 8. **(D)** Maximum strain and **(E)** maximum stress are computed for the same fixed external load, respectively, according to Eqs 9 and 10.

Conclusion

Trees have many ways, at the cell wall level or at the organ level, to acclimate their xylem structure to recurrent mechanical stimuli (**Table 1**). The acclimation process differs between angiosperms and gymnosperms and the consequences on the hydraulic and mechanical properties of wood are highly variable. Because of the lack of experimental data, there is a crucial need for new investigations in order to characterize the mechanical and hydraulic properties of flexure wood. Moreover, in many windy regions, wind is often directional. Hence, bending occurs in a non-symmetric way, with the leeward part of the stem experiencing more compression stress and the windward portion experience more tension stress. Thus, what is really flexure wood? We suggest to the need to investigate separately the thigmomorphogenetic response of wood formation of both elementary stress (compression or tension) to better understand the acclimation process. On the one hand, there is a real need to investigate the relationships between the mechanical stimuli and the modifications of the anatomical structure and its associated construction cost. For this task, there is a real need to investigate the wood formation process, including at the level of cell division and the cell differentiation. This also requires new studies regarding the molecular mechanisms that link mechanical perception to the mechanical stress induced wood formation.

On the other hand, we need to characterize the consequences of the thigmomorphogenetic process on the mechanical properties that help the trees to be better acclimated to further mechanical stimuli without drastic compromises to the other hydraulic functions. Research involving controlled mechanical stimuli and using transgenic trees with modified cell wall structure (e.g., altered lignin or cellulose), may be a promising mean of elucidating mechanisms of xylem construction that may be constrained by the functional trade-offs.

TABLE 1 | Comparison of flexure wood features with normal wood in conifers and angiosperms.

Flexure wood anatomy and functions	Angiosperms	Gymnosperms
Radial increment	+	+
Wood density	0	+
Vessels density (nb vessel/mm^2)	−	NA
Vessel diameter	−	NA
Fiber length	−	NA
Tracheid diameter	NA	−
Tracheid length	NA	−
Microfibril angle (MFA)	+	+
Module of elasticity (E_L)	−	−
Modulus of rupture (MOR)	−	+
Second moment of cross sectional area (I)	+	+
Flexural rigidity ($E_L I$)	+	+
Specific conductivity (Ks)	+	−
Total conductivity (K)	0	0
Cavitation resistance	NA	NA

"+" indicates the increase, "−" indicates the decrease, and "0" indicates no change. "NA" refers to non-available data.

Acknowledgment

This project has been supported by ANR-12-AGRO-0007-04 project "ForWind." We thank Steven Jansen for the images of the **Figure 3**.

References

Alméras, T., Costes, E., and Salles, J.-C. (2004). Identification of biomechanical factors involved in stem shape variability between apricot tree varieties. *Ann. Bot.* 93, 455–468. doi: 10.1093/aob/mch054

Anten, N. P. R., Casado-Garcia, R., and Nagashima, H. (2005). Effects of mechanical stress and plant density on mechanical properties, growth, and lifetime reproduction of Tobacco plants. *Am. Nat.* 166, 650–660. doi: 10.1086/497442

Awad, H., Herbette, H., Brunel, N., Tixier, A., Pilate, G., Cochard, H., et al. (2012). No trade-off between hydraulic and mechanical properties in several transgenic poplars modified for lignins metabolism. *Environ. Exp. Bot.* 77, 185–195. doi: 10.1016/j.envexpbot.2011.11.023

Baas, P. (1986). "Ecological patterns of xylem anatomy," in *On the Economy of Plant form and Function*, ed. T. J. Givnish (Cambridge: Cambridge University Press), 327–351.

Biddington, N. L. (1986). The effects of mechanically-induced stress in plants- a review. *Plant Growth Regul.* 4, 103–123. doi: 10.1007/BF00025193

Bouche, P. S., Larter, M., Domec, J. C., Burlett, R., Gasson, P., Jansen, S., et al. (2014). A broad survey of hydraulic and mechanical safety in the xylem of conifers. *J. Exp. Bot.* 65, 4419–4431. doi: 10.1093/jxb/eru218

Braam, J. (2005). In touch: plant responses to mechanical stimuli. *New Phytol.* 165, 373–389. doi: 10.1111/j.1469-8137.2004.01263.x

Butterfield, B. G., and Li, G. (2000). *Wood Properties of Glass House Grown Clonal Radiata Plantlets.* Report to the multiclient seedling group, University of Canterbery, 12.

Carlquist, S. (1975). *Ecological Strategies of Xylem Evolution*. Berkeley, CA: University of California Press.

Cave, I. D., and Hutt, L. (1969). The longitudinal Young's modulus of *Pinus Radiata*. *Wood Sci. Technol.* 3, 40–48. doi: 10.1007/BF00349983

Cave, I. D., and Walker, J. C. F. (1994). Stiffness of wood in fast-grown plantation softwoods: the influence of microfibril angle. *Forest Prod. J.* 44, 43–48.

Chave, J., Coomes, D., Jansen, S., Lewis, S. L., Swenson, N. G., and Zanne, A. E. (2009). Towards a worldwide wood economics spectrum. *Ecol. Lett.* 12, 351–366. doi: 10.1111/j.1461-0248.2009.01285.x

Chehab, E. W., Eich, E., and Braam, J. (2009). Thigmomorphogenesis: a complex plant response to mechano-stimulation. *J. Exp. Bot.* 60, 43–56. doi: 10.1093/jxb/ern315

Choat, B., Ball, M., Luly, J., and Holtum, J. (2003). Pit membrane porosity and water stress-induced cavitation in four co-existing dry rainforest tree species. *Plant Physiol.* 131, 41–48. doi: 10.1104/pp.014100

Choat, B., Ball, M. C., Luly, J. G., and Holtum, J. A. M. (2005). Hydraulic architecture of deciduous and evergreen dry rainforest tree species from north-eastern Australia. *Trees* 19, 305–311. doi: 10.1007/s00468-004-0392-1

Christensen-Dalsgaard, K. K., Fournier, M., Ennos, A. R., and Barfod, A. S. (2007). Changes in vessel anatomy in response to mechanical loading in six species of tropical trees. *New Phytol.* 176, 610–622. doi: 10.1111/j.1469-8137.2007.02227.x

Clair, B., Almeras, T., and Sugiyama, J. (2006). Compression stress in opposite wood of angiosperms: observations in chestnut, mani and poplar. *Ann. For. Sci.* 63, 507–510. doi: 10.1051/forest:2006032

Cochard, H. (1992). Vulnerability of several conifers to air embolism. *Tree Physiol.* 11, 73–83. doi: 10.1093/treephys/11.1.73

Cochard, H., Cruiziat, P., and Tyree, M. T. (1992). Use of positive pressures to establish vulnerability curves. Further support for the air-seeding hypothesis and implications for pressure-volume analysis. *Plant Physiol.* 100, 205–209. doi: 10.1104/pp.100.1.205

Cochard, H., and Tyree, M. T. (1990). Xylem dysfunction in *Quercus*: vessel sizes, tyloses, cavitation and seasonal changes in embolism. *Tree Physiol.* 6, 393–408. doi: 10.1093/treephys/6.4.393

Coleman, H. D., Samuels, A. L., Guy, R. D., and Mansfield, S. D. (2008). Perturbed lignification impacts tree growth in hybrid poplar-A function of sink strength, vascular integrity, and photosynthetic assimilation. *Plant Physiol.* 148, 1229–1237. doi: 10.1104/pp.108.125500

Coutand, C. (2010). Mechanosensing and thigmomorphogenesis, a physiological and biomechanical point of view. *Plant Sci.* 179, 168–182. doi: 10.1016/j.plantsci.2010.05.001

Dalla-Salda, G., Fernández, M. E., Sergent, A. S., Rozenberg, P., Badel, E., and Martinez-Meier, A. (2014). Dynamics of cavitation in a Douglas-fir tree-ring: transition-wood, the lord of the ring? *J. Plant Hydraulics* 1:e-0005.

Davis, S. D., Sperry, J. S., and Hacke, U. G. (1999). The relationship between xylem conduit diameter and cavitation caused by freezing. *Am. J. Bot.* 86, 1367–1372. doi: 10.2307/2656919

Dean, T. J. (1991). Effects of growth rate and wind sway on the relationship between mechanical and water-flow properties in slash pine seedlings. *Can. J. For. Res.* 21, 1501–1506. doi: 10.1139/x91-210

de Langre, E. (2008). Effects of wind on plants. *Ann. Rev. Fluid Mech.* 40, 141–168. doi: 10.1146/annurev.fluid.40.111406.102135

Dixon, H. (1914). *Transpiration and the Ascent of Sap in Plants*. London: Macmillian, 216. doi: 10.5962/bhl.title.1943

Domec, J. C., Scholz, F. G., Bucci, S. J., Meinzer, F. C., Goldstein, G., and Villalobos-Vega, R. (2006). Diurnal and seasonal variation in root xylem embolism in neotropical savanna woody species: impact on stomatal control of plant water status. *Plant Cell Environ.* 29, 26–35. doi: 10.1111/j.1365-3040.2005.01397.x

Du, S., and Yamamoto, F. (2007). An overview of the biology of reaction wood formation. *J. Integr. Plant Biol.* 49, 131–143. doi: 10.1111/j.1744-7909.2007.00427.x

Evans, R. (1998). "Rapid scanning of microfibril angles in increments cores by X-ray diffraction," in *Microfibril Angle in Wood*, ed. B. G. Butterfield (Christchurch: University of Canterbury), 116–139.

Evans, R., and Elic, J. (2001). Rapid prediction of wood stiffness from microfibril angle and density. *Forest Prod. J.* 51, 53.

Fournier, M., Stokes, A., Coutand, C., Fourcaud, T., and Moulia, B. (2006). "Tree biomechanics and growth strategies in the context of forest functional ecology," in *Ecology and Biomechanics: A Mechanical Approach to the Ecology of Animals and Plants*, eds A. Herrel, T. Speck, and N. Rowe (Boca Raton, FL: CRC Press), 1–34. doi: 10.2307/2389490

Gartner, B. L. (1991a). Is the climbing habit of poison oak ecotypic? *Funct. Ecol.* 5, 696–704. doi: 10.2307/2389490

Gartner, B. L. (1991b). Stem hydraulic-properties of vines vs. shrubs of western poison oak *Toxicodendron diversilobum*. *Oecologia* 87, 180–189. doi: 10.1007/BF00325255

Gartner, B. L. (1991c). Structural stability and architecture of vines vs. shrubs of poison oak *Toxicodendron diversilobum*. *Oecologia* 72, 2005–2015. doi: 10.2307/1941555

Gartner, B. L., Roy, J., and Huc, R. (2003). Effects of tension wood on specific conductivity and vulnerability to embolism of *Quercus ilex* seedlings grown at two atmospheric CO_2 concentrations. *Tree Physiol.* 23, 387–395. doi: 10.1093/treephys/23.6.387

Grace, J. (1977). *Plant Response to Wind*. London: Academic Press.

Hacke, U. G., Sperry, J. S., Pockman, W. T., Davis, S. D., and McCulloh, K. A. (2001). Trends in wood density and structure are linked to prevention of xylem implosion by negative pressure. *Oecologia* 126, 457–461. doi: 10.1007/s004420100628

Hölttä, T., Cochard, H., Nikinmaa, E., and Mencuccini, M. (2009). Capacitive effect of cavitation in xylem conduits: results from a dynamic model. *Plant Cell Environ.* 32, 10–21. doi: 10.1111/j.1365-3040.2008.01894.x

Iida, Y., Kohyama, T. S., Swenson, N. G., Su, S. H., Chen, C. T., Chiang, J. M., et al. (2014). Linking functional traits and demographic rates in a subtropical tree community: the importance of size dependency. *J. Ecol.* 102, 641–650. doi: 10.1111/1365-2745.12221

Jacobs, M. R. (1954). The effect of wind sway on the formand development of *Pinus radiate* D. Don. *Aust. J. Bot.* 2, 35–51. doi: 10.1071/BT9540035

Jacobsen, A. L., Ewers, F. W., Pratt, R. B., Paddock, W. A., and Davis, S. D. (2005). Do xylem fibers affect xylem cavitation resistance? *Plant Physiol.* 139, 546–556. doi: 10.1104/pp.104.058404

Jaffe, M. J. (1973). Thigmomorphogenesis: the response of plant growth and development to mechanical stimulation. *Planta* 114, 143–157. doi: 10.1007/BF00387472

Jaffe, M. J. (1985). "Wind and other mechanical effects in the development and behaviour of plants, with special emphasis on the role of hormones," in *Hormonal Regulation of Development*, Vol. 11, *III Role of Environmental Factors*, *Encyclopedia of Plant Physiology*, *NS*, eds R. P. Pharis and D. M. Reid (Berlin: Springer), 444–483.

Jaffe, M. J., Leopold, A. C., and Staples, R. A. (2002). Thigmo responses in plants and fungi. *Am. J. Bot.* 89, 375–382. doi: 10.3732/ajb.89.3.375

Jagels, R., Visscher, G. E., Lucas, J., and Goodell, B. (2003). Paleo-adaptive properties of the xylem of *Metasequoia*: mechanical/hydraulic compromises. *Ann. Bot.* 92, 79–88. doi: 10.1093/aob/mcg117

Jones, L., Ennos, A. R., and Turner, S. R. (2001). Cloning and characterization of irregular xylem4 (irx4): a severely lignin-deficient mutant of *Arabidopsis*. *Plant J.* 2, 205–216. doi: 10.1046/j.1365-313x.2001.01021.x

Kern, K. A., Ewers, F. W., Telewski, F. W., and Koehler, L. (2005). Mechanical perturbation affects conductivity, mechanical properties and aboveground biomass of hybrid poplars. *Tree Physiol.* 25, 1243–1251. doi: 10.1093/treephys/25.10.1243

Knight, T. A. (1803). Account of some experiments on the decent of sap in trees. *Philos. Trans. R. Soc.* 96, 277–289. doi: 10.1098/rstl.1803.0011

Koehler, L., and Telewski, F. W. (2006). Biomechanics and transgenic wood. *Am. J. Bot.* 93, 1433–1438. doi: 10.3732/ajb.93.10.1433

Lachenbruch, B., and McCulloh, K. A. (2014). Traits, properties, and performance: how woody plants combine hydraulic and mechanical functions in a cell, tissue, or whole plant. *New Phytologist.* 204, 747–764. doi: 10.1111/nph.13035

Larjavaara, M. (2010). Maintenance cost, toppling risk and size of trees in a self-thinning stand. *J. Theor. Biol.* 265, 63–67. doi: 10.1016/j.jtbi.2010.04.021

Liu, X., Silins, U., Lieffers, V. J., and Man, R. (2002). Stem hydraulic properties and growth in lodgepole pine stands following thinning and sway treatment. *Can. J. For. Res.* 33, 1295–1303. doi: 10.1139/x03-061

Liu, X., Swenson, N. G., Wright, S. J., Zhang, L., Song, K., Du, Y., et al. (2012). Covariation in plant functional traits and soil fertility within two species-rich forests. *PLoS ONE* 7:e34767. doi: 10.1371/journal.pone.0034767

Liu, X.,Swenson, N. G., Zhang, J., and Ma, K. (2013). The environment and space, not phylogeny, determine trait dispersion in a subtropical forest. *Funct. Ecol.* 27, 264–272. doi: 10.1111/1365-2435.12018

Martin, L., Leblanc-Fournier, N., Julien, J. L., Moulia, B., and Coutand, C. (2010). Acclimation kinetics of physiological and molecular responses of plants to multiple mechanical loadings. *J. Exp. Bot.* 61, 2403–2412. doi: 10.1093/jxb/erq069

Martinez-Vilalta, J., Prat, E., Oliveras, I., and Pinol, J. (2002). Xylem hydraulic properties of roots and stems of nine Mediterranean woody species. *Oecologia* 133, 19–29. doi: 10.1007/s00442-002-1009-2

Mayr, S., and Cochard, H. (2003). A new method for vulnerability analysis of small xylem areas reveals that compression wood of Norway spruce has lower hydraulic safety than opposite wood. *Plant Cell Environ.* 26, 1365–1371. doi: 10.1046/j.0016-8025.2003.01060.x

Mayr, S., Hacke, U. G., Schmid, P., Schwienbacher, F., and Gruber, A. (2006). Frost drought in conifers at the alpine timberline: xylem dysfunction and adaptations. *Ecology* 87, 3175–3185. doi: 10.1890/0012-9658(2006)87[3175:FDICAT]2.0.CO;2

McMahon, T. A. (1973). Size and shape in biology. *Science* 179, 1201–1204. doi: 10.1126/science.179.4079.1201

Meinzer, F. C., Johnson, D. M., Lachenbruch, B., McCulloh, K. A., and Woodruff, D. R. (2009). Xylem hydraulic safety margins in woody plants: coordination of stomatal control of xylem tension with hydraulic capacitance. *Funct. Ecol.* 23, 922–930. doi: 10.1111/j.1365-2435.2009.01577.x

Mitchell, C. A. (1996). Recent advances in plant responses to mechanical stress: theory and application. *Hort Science* 31, 31–35.

Mitchell, S. J. (2013). Wind as a natural disturbance agent in forests: a synthesis. *Forestry* 86, 147–157. doi: 10.1093/forestry/cps058

Moulia, B., Coutand, C., and Julien, J. L. (2015). Mechanosensitive control of plant growth: bearing the load, sensing, transducing, and responding. *Front. Plant Sci.* 6:52. doi: 10.3389/fpls.2015.00052

Moulia, B., Coutand, C., and Lenne, C. (2006). Posture control and skeletal mechanical acclimation in terrestrial plants: implications for mechanical modeling of plant architecture. *Am. J. Bot.* 93, 1477–1489. doi: 10.3732/ajb.93.10.1477

Neel, P. L., and Harris, R. W. (1971). Motion-induced inhibition of elongation and induction of dormancy in *Liquidambar*. *Science* 173, 58–59. doi: 10.1126/science.173.3991.58

Niklas, K. J. (1992). *Plant Biomechanics: An Engineering Approach to Plant form and Function*. Chicago: University of Chicago Press.

Niklas, K. J. (1994). Interspecific allometries of critical buckling height and actual plant height. *Am. J. Bot.* 81, 1275–1279. doi: 10.2307/2445403

Pittermann, J., and Sperry, J. (2003). Tracheid diameter is the key trait determining the extent of freezing-induced embolism in conifers. *Tree Physiol.* 23, 907–914. doi: 10.1093/treephys/23.13.907

Pittermann, J., Sperry, J. S., Wheeler, J. K., Hacke, U. G., and Sikkema, E. H. (2006). Mechanical reinforcement of tracheids compromises the hydraulic efficiency of conifer xylem. *Plant Cell Environ.* 29, 1618–1628. doi: 10.1111/j.1365-3040.2006.01539.x

Poorter, L. (2008). The relationships of wood-, gas- and water fractions of tree stems to performance and life history variation in tropical trees. *Ann. Bot.* 102, 367–375. doi: 10.1093/aob/mcn103

Poorter, L., McDonald, I., Alarcón, A., Fichtler, E., Licona, J. C., Peña-Claros, M., et al. (2010). The importance of wood traits and hydraulic conductance for the performance and life history strategies of 42 rainforest tree species. *New Phytol.* 185, 481–492. doi: 10.1111/j.1469-8137.2009.03092.x

Pratt, R. B., Jacobsen, A. L., Ewers, F. W., and Davis, S. D. (2007). Relationships among xylem transport, biomechanical and storage in stems and roots of nine Rhamnaceae species of the California chaparral. *New Phytol.* 174, 787–798. doi: 10.1111/j.1469-8137.2007.02061.x

Pruyn, M., Ewers, B. J., and Telewski, F. W. (2000). Thigmomorphogenesis: change in the morphology and mechanical properties of two *Populus* hybrids in response to mechanical perturbation. *Tree Physiol.* 20, 535–540. doi: 10.1093/treephys/20.8.535

Rosner, S., Klein, A., Muller, U., and Karlsson, B. (2007). Hydraulic and mechanical properties of young Norway spruce clones related to growth and wood structure. *Tree Physiol.* 27, 1165–1178. doi: 10.1093/treephys/27.8.1165

Rosner, S., Klein, A., Muller, U., and Karlsson, B. (2008). Tradeoffs between hydraulic and mechanical stress responses of mature Norway spruce trunk wood. *Tree Physiol.* 28, 1179–1188. doi: 10.1093/treephys/28.8.1179

Rudnicki, M., Mitchell, S. J., and Novak, M. D. (2004). Wind tunnel measurements of crown streamlining and drag relationships for three conifer species. *Can. J. For. Res.* 34, 666–676. doi: 10.1139/x03-233

Smith, V. C., and Ennos, A. R. (2003). The effects of air flow and stem flexure on the mechanical and hydraulic properties of the stems of sunflowers *Helianthus annuus* L. *J. Exp. Bot.* 54, 845–849. doi: 10.1093/jxb/erg068

Sperry, J. S. (2003). Evolution of water transport and xylem structure. *Int. J. Plant Sci.* 164, 115–127. doi: 10.1086/368398

Sperry, J. S., and Hacke, U. G. (2004). Analysis of circular bordered pit function. I. Angiosperm vessels with homogenous pit membranes. *Am. J. Bot.* 91, 369–385. doi: 10.3732/ajb.91.3.369

Sperry, J., Hacke, U. G., and Pittermann, J. (2006). Size and function in conifer tracheids and and angiosperm vessels. *Am. J. Bot.* 93, 1490–1500. doi: 10.3732/ajb.93.10.1490

Sperry, J. S., Nichols, K. L., Sullivan, J. E. M., and Eastlack, S. E. (1994). Xylem embolism in ring-porous, diffuse-porous, and coniferous trees of Northern Utah and Interior Alaska. *Ecology* 75, 1736–1752. doi: 10.2307/1939633

Sperry, J. S., and Tyree, M. T. (1988). Mechanism of water stress-induced xylem embolism. *Plant Physiol.* 88, 581–587. doi: 10.1104/pp.88.3.581

Spicer, R., and Gartner, B. L. (1998). Hydraulic properties of douglas-fir (*Pseudotsuga menziesii*) branches and branch halves with reference to compression wood. *Tree Physiol.* 18, 777–784. doi: 10.1093/treephys/18.11.777

Stegen, J. C., Swenson, N. G., Valencia, R., Enquist, B. J., and Thompson, J. (2009). Above-ground forest biomass is not consistently related to wood density in tropical forests. *Global Ecol. Biogeogr.* 18, 617–625. doi: 10.1111/j.1466-8238.2009.00471.x

Swenson, N. G., Anglada-Cordero, P., and Barone, J. A. (2011). Deterministic tropical tree community turnover: evidence from patterns of functional beta diversity along an elevational gradient. *Proc. R. Soc. B Biol. Sci.* 278, 877–884. doi: 10.1098/rspb.2010.1369

Swenson, N. G., and Weiser, M. D. (2010). Plant geography upon the basis of functional traits: an example from eastern North American trees. *Ecology* 91, 2234–2241. doi: 10.1890/09-1743.1

Telewski, F. W. (1989). Structure and function of flexure wood in *Abies fraseri*. *Tree Physiol.* 5, 113–121. doi: 10.1093/treephys/5.1.113

Telewski, F. W. (1995). "Wind induced physiological and developmental responses in trees," in *Wind and Trees*, eds M. P. Coutts and J. Grace (Cambridge: Cambridge University Press), 237–263.

Telewski, F. W. (2006). A unified hypothesis of mechanoperception in plants. *Am. J. Bot.* 93, 1306–1316. doi: 10.3732/ajb.93.10.1466

Telewski, F. W. (2012). Is windswept tree growth negative Thigmotropism? *Plant Sci.* 184, 20–28. doi: 10.1016/j.plantsci.2011.12.001

Telewski, F. W., Aloni, R., and Sauter, J. (1996). "Physiology of Secondary Tissues of Populus," in *Biology of Populus and its Implications for Management and Conservation*, *Part II. Physiology of Growth, Productivity and Stress Responses*,

eds R. F. Stettler, H. D. Jr. Bradshaw, P. E. Heilman, and T. M. Hinckley (Ottawa: NCR Research Press), 301–329. doi: 10.1111/j.1399-3054.1986.tb02411.x

Telewski, F. W., and Jaffe, M. J. (1986a). Thigmomorphogenesis: field and laboratory studies of *Abies fraseri* in response to wind or mechanical perturbation. *Physiol. Plant.* 66, 211–218. doi: 10.1111/j.1399-3054.1986.tb02411.x

Telewski, F. W., and Jaffe, M. J. (1986b). Thigmomorphogenesis: anatomical, morphological and mechanical analysis of genetically different sibs of *Pinus taeda* L. in response to mechanical perturbation. *Physiol. Plant.* 66, 219–226. doi: 10.1111/j.1399-3054.1986.tb02412.x

Telewski, F. W., and Pruyn, M. (1998). Thigmomorphogenesis: a dose response to flexing in *Ulmus americana* seedlings. *Tree Physiol.* 18, 65–68. doi: 10.1093/treephys/18.1.65

Timell, T. E. (1986a). *Compression Wood in Gymnosperms*, Vol. 1. Berlin: Springer-Verlag.

Timell, T. E. (1986b). *Compression Wood in Gymnosperms*, Vol. 2. Berlin: Springer-Verlag.

Timell, T. E. (1986c). *Compression Wood in Gymnosperms*, Vol. 3. Berlin: Springer-Verlag.

Tixier, A., Herbette, S., Jansen, S., Capron, M., Tordjeman, P., Cochard, H., et al. (2014). Modelling the mechanical behaviour of pit membranes in bordered pits with respect to cavitation resistance in angiosperms. *Ann. Bot.* 114, 325–334. doi: 10.1093/aob/mcu109

Turner, S. R., and Somerville, C. R. (1997). Collapsed xylem phenotype of *Arabidopsis* identifies mutants deficient in cellulose deposition in the secondary cell wall. *Plant Cell* 9, 689–701. doi: 10.1105/tpc.9.5.689

Tyree, M. T., Davis, S. D., and Cochard, H. (1994). Biophysical perspectives of xylem evolution: is there a trade-off of hydraulic efficiency for vulnerability to dysfunction? *IAWA J.* 15, 335–360. doi: 10.1163/22941932-90001369

Tyree, M. T., Velez, V., and Dalling, J. W. (1998). Growth dynamics of root and shoot hydraulic conductance in seedlings of five neotropical tree species. Scaling to show possible adaptation to differing light regimes. *Oecologia* 114, 293–298. doi: 10.1007/s004420050450

Tyree, M. T., and Zimmermann, M. H. (2002). *Xylem Structure and the Ascent of Sap*, 2nd Edn. Berlin: Springer. doi: 10.1007/978-3-662-04931-0

Utsumi, Y., Bobich, E. G., and Ewers, F. W. (2010). Photosynthetic, hydraulic and biome-chanical responses of *Juglans californica* shoots to wildfire. *Oecologia* 164, 331–338. doi: 10.1007/s00442-010-1653-x

Vaast, P., Angrand, J., Ffranck, N., Dauzat, J., and Génard, M. (2005). Fruit load and branch ring-barking affect carbon allocation and photosynthesis of leaf and fruit of *Coffea arabica* in the field. *Tree Physiol.* 25, 753–760. doi: 10.1093/treephys/25.6.753

Valinger, E., Lundquist, L., and Sundberg, B. (1995). Mechanical bending stress applied during dormancy and (or) growth stimulates stem diameter growth of scots pine-seedlings. *Can. J. For. Res.* 25, 886–890. doi: 10.1139/x95-097

Vogel, S. (1994). *Life in Moving Fluids: The Physical Biology of Flow*. 2nd Edn. Princeton, NJ: Princeton University Press.

Vollsinger, S., Mitchell, S. J., Byrne, K. E., Novak, M. D., and Rudnicki, M. (2005). Wind tunnel measurements of crown streamlining and drag relationships for several hardwood species. *Can. J. For. Res.* 35, 1238–1249. doi: 10.1139/x05-051

Wagner, K. R., Ewers, F. W., and Davis, S. D. (1998). Tradeoffs between hydraulic efficiency and mechanical strength in the stems of four co-occurring species of chaparral shrubs. *Oecologia* 117, 53–62. doi: 10.1007/s004420050631

Wainwright, S. A., Briggs, W. D., Currey, J. D., and Gosline, J. M. (1976). *Mechanical Design in Organisms*. New York, NY: John Wiley and Sons.

Wheeler, J. K., Sperry, J. S., Hacke, U. G., and Hoang, N. (2005). Inter-vessel pitting and cavitation in woody Rosaceae and other vesselled plants: a basis for a safety versus efficiency trade-off in xylem transport. *Plant Cell Environ.* 28, 800–813. doi: 10.1111/j.1365-3040.2005.01330.x

Wilson, B. F., and Archer, R. R. (1977). Reaction wood: inducvtion and mechanical action. *Ann. Rev. Plant Physiol.* 28, 23–43. doi: 10.1146/annurev.pp.28.060177.000323

Woodrum, C. L., Ewers, F. W., and Telewski, F. W. (2003). Hydraulic, biomechanical, and anatomical interactions of xylem from five species of Acer (Aceraceae). *Am. J. Bot.* 90, 693–699. doi: 10.3732/ajb.90.5.693

Yamamoto, H., Ruelle, J., Arakawa, Y., Yoshida, M., Clair, B., and Gril, J. (2010). Origin of the characteristic hygro-mechanical properties of the gelatinous layer in tension wood from Kunugi oak (*Quercus acutissima*), *Wood Sci. Technol.* 44, 149–163. doi: 10.1007/s00226-009-0262-5

Zanne, A. E., Westoby, M., Falster, D. S., Ackerly, D. D., Loarie, S. R., Arnold, S. E., et al. (2010). Angiosperm wood structure: global patterns in vessel anatomy and their relation to wood density and potential conductivity. *Am. J. Bot.* 97, 207–215. doi: 10.3732/ajb.0900178

Zimmermann, M. H. (1983). *Xylem Structure, and the Ascent of Sap*. Berlin: Springer-Verlag. doi: 10.1007/978-3-662-22627-8

Conflict of Interest Statement: The authors declare that the research was conducted in the absence of any commercial or financial relationships that could be construed as a potential conflict of interest.

frontiers in
PLANT SCIENCE

MINI REVIEW ARTICLE
published: 05 November 2014
doi: 10.3389/fpls.2014.00610

Gravity sensing, a largely misunderstood trigger of plant orientated growth

David Lopez[1,2†], Kévin Tocquard[1,2†], Jean-Stéphane Venisse[1,2], Valerie Legué[1,2*] and Patricia Roeckel-Drevet[1,2*]

[1] Clermont Université – Université Blaise Pascal, UMR 547 PIAF, Aubière, France
[2] INRA, UMR 547 PIAF, Clermont-Ferrand, France

Edited by:
Sara Puijalon, Université Lyon 1, France

Reviewed by:
Uener Kolukisaoglu, University of Tübingen, Germany
Miyo Terao Morita, Nagoya University, Japan

***Correspondence:**
Valerie Legué and Patricia Roeckel-Drevet, Clermont Université – Université Blaise Pascal, UMR 547 PIAF, BP 10448, F-63171 Aubière, France
e-mail: valerie.legue@univ-boclermont.fr; patricia.drevet@univ-bpclermont.fr

[†] David Lopez and Kévin Tocquard have contributed equally to this work.

Gravity is a crucial environmental factor regulating plant growth and development. Plants have the ability to sense a change in the direction of gravity, which leads to the re-orientation of their growth direction, so-called gravitropism. In general, plant stems grow upward (negative gravitropism), whereas roots grow downward (positive gravitropism). Models describing the gravitropic response following the tilting of plants are presented and highlight that gravitropic curvature involves both gravisensing and mechanosensing, thus allowing to revisit experimental data. We also discuss the challenge to set up experimental designs for discriminating between gravisensing and mechanosensing. We then present the cellular events and the molecular actors known to be specifically involved in gravity sensing.

Keywords: amyloplast, gravisensing, membrane receptor, reaction wood, root growth, stem growth

INTRODUCTION

Among the factors that influence the growth orientation in plants (e.g., light, gravity, water availability, and touch), gravity represents one of the most important environmental signals. This biological process known as gravitropism, starts from seed germination through the upright growth of shoots, ensuring the photosynthesis and the reproduction as well as the dispersion of seeds, and the downright growth of roots, supplying the plant in water and nutrients. When a plant organ is tilted, it adjusts its growth orientation relative to gravity direction, which is achieved by a curvature of the organ. Growth reorientation is the result of a differential cell elongation rate between the two sides of organs undergoing primary growth (Barlow and Rathfelder, 1985; Tomos et al., 1989). In trees and perennial plants, the active cambium initiated in organs undergoing secondary growth contributes to the reorientation of the shoot through the differentiation and shrinkage of reaction wood (RW – i.e., tension wood or compression wood in eudicotyledonous and conifers respectively; IAWA, 1964; Archer, 1986). Gravitropism is therefore essential in the control of the posture and the form of land plants (Coutand et al., 2007; Moulia et al., 2011).

MODELS DESCRIBE THE GRAVITROPIC MOVEMENTS IN PLANTS

Mathematic and kinematic tools have been extensively used for describing and quantifying the gravitropic movements in plants, and have been recently supplemented by integrative models. Even if gravity sensing events are not yet completely deciphered, these tools provide essential information to address the complex molecular and cellular mechanisms involved in gravitropism.

The time course of gravitropic curvature investigated in hypocotyl, stem, as well as in the trunk and branches illustrate the following steps in several species: the upward curving of the organs is observed after a latency phase and progressively followed by a "decurving" which starts at the tip and propagates downward. This latest has been described as autotropic (Firn and Digby, 1979) and may occur before the tip reaches the vertical (Firn and Digby, 1979; Stankovic et al., 1998).

Curvature time course in growing organs was initially calculated using the inclination angle of the organ's tip relative to the vertical, and revealed that the gravitropic curvature obeys the so-called sine law (Sachs, 1882; review, Moulia and Fournier, 2009). The sine law represents the size of the gravitropic stimulus (S_{gravi}) as equal to g sin γ, where g is the gravitational acceleration and γ the inclination angle. In other words this law predicts that the amplitude of gravitropism depends of the sinus of inclination angle. Even if this sine law has been confirmed in several species both in stems and roots, it is valid only in a limited range of inclination angles, ranging from 0 to 90° (see introduction in Göttig and Galland, 2014) and therefore, it does not characterize gravitropic movements of the whole organ over-time (reviewed in Moulia and Fournier, 2009). Later on, a curvature angle which is the change in tip inclination angle over time was proposed (Galland, 2002; Perbal et al., 2002; Hoshino et al., 2007). This parameter again is not satisfactory especially because it was not measured using the same reference from one experiment to another (horizontal, vertical, initial position of the tilted stem). Starting from the observation that the gravitropic

responses of aerial organs showed general curving followed by basipetal straightening (Pickard, 1985), Bastien et al. (2013) proposed a model that takes into account the sensing of the local inclination angle but also of the local curvature, which progressively takes place. The sensing of the local inclination reflects the gravisensing mechanisms while the sensing of the local curvature could be referred as mechanosensing which has been described as graviproprioceptive. The authors defined a measurable ratio B that is a ratio between graviceptive and proprioceptive sensitivities. B was shown to control crucial aspects of the dynamics of the gravitropic response. The curving and decurving phases initially described as sequential, are in fact concomitant and linked to the initial degrees of inclination and curvature (Bastien et al., 2013). Recently, Bastien et al. (2014) extended this model by taking into account the growth effects, considered as the motor of movement, i.e., expansion of the curved zone and immobilization of the curvature state at elongation zone boundary (Selker and Sievers, 1987; Ishikawa and Evans, 1993). This model highlights that stems in primary growth rapidly straightened as to escape the growth destabilizing effects. To our mind, these findings precised the notion of autotropism as a reorientation of the axis controlled by internal cues such as the organ curvature. The consequence of the autotropic decurving is that RW and/or increased cell elongation occur alternatively from one side of the stem to the other.

Despite the fact that proprioceptive sensitivity has not been integrated in models of root gravitropism, it seems that the autotropic decurving has been observed during the last step of the gravitropic response in stems and as well in roots. Curiously, the analysis of the position of the lentil root tip and the root curvature as a function of time in microgravity revealed that the embryonic root curved strongly away from the cotyledons and then straightened out slowly following hydration (Perbal and Driss-Ecole, 2003; Driss-Ecole et al., 2008), suggesting an autotropic decurving in the absence of gravity signal. It is not clear if this decurving could occur in soil which structure can sometimes greatly restrict root growth and where the root system is mediated by a wide variety of processes including nutrient and water uptake, anchoring and mechanical support.

Another parameter that has been explored for elucidating the gravisensing mechanisms is the measurement of thresholds. Detailed kinetics of gravitropic curvature in horizontally stimulated roots have been reported in several studies and revealed for example that maize roots oriented at $<40°$ from the vertical, overshot the vertical and then oscillated around this axis (Barlow et al., 1993). The angle of 10° seemed to be the minimum angle to induce a gravitropic response. On the contrary, when roots were tilted at more than 60°, verticality was hardly achieved. It is interesting to note that comparable thresholds occurred in root and stem. When coleoptiles were tilted at an angle of $<10°$ from the vertical, the gravitropic response did not happen (Iiono et al., 1996). The first models of differential root growth leading to curvature took into account the presentation time (minimal duration of stimulation in the gravitational field; Larsen, 1957), in which the response was the function of the logarithm of the stimulus. Later, Perbal et al. (2002) observed that the hyperbolic model (H), related to a ligand-receptor system response, fitted better the experimental data. Other models took into account the differential growth among opposite cell lineages (Zieschang et al., 1997). Another interesting parameter used for approaching gravisensing mechanisms is the estimation of threshold acceleration perceived by organs. Lentil seedlings were grown in microgravity and subjected to low accelerations for several hours (Driss-Ecole et al., 2008). In these conditions, threshold acceleration perceived was inferior to 2.0×10^{-3} *g*.

MOST EXPERIMENTAL DESIGNS DO NOT ALLOW TO DISCRIMINATE BETWEEN GRAVISENSING AND MECHANOSENSING

As demonstrated above through mathematical models of stem gravitropic movements (Bastien et al., 2013, 2014), both gravisensing and mechanosensing lead to the reorientation of the plant. It is not clear whether gravisensing and mechanosensing act through the same mechanisms, and to what extent one can differentiate these stimuli. Trewavas and Knight (1994) considered that gravisensing is derived from an ancestral touch perception apparatus.

Mechanosensing occurs when plants are touched. Jaffe (1973) used the term of thigmomorphogenesis when describing the growth response of plants over time following repeated touching. In the literature numerous studies referring to mechanical stimulation concerned the response induced by external loading (Chehab et al., 2008) demonstrating that mechanical cues from the environment are sensed by the plant. Mechanical stresses are also intrinsic to plants and an increasing number of studies illustrate the occurrence of mechanosensing in cells and organs and its importance for the shape determination (Mirabet et al., 2011; Hamant, 2013). For example, it has been demonstrated that cells in *Arabidopsis* shoot apical meristem respond to local mechanical stresses by reorienting their growth, thereby guiding morphogenesis (Uyttewaal et al., 2012).

A gravistimulation as such should induce neither organ deformation nor touch. In several gravitropism studies, the plant or the organ have been tilted without being staked before (Azri et al., 2009; Tocquard et al., 2014b). Although such conditions allowed gravitropic movements, they also allowed organ bending under its own weight. This deformation of the organ can be considered as a thigmomorphogenetic stimulus (Coutand, 2010). In this context, both mechanosensing and gravisensing occur. Alternatively, staking of plants just before tilting might induce touch gene expression that could also interfere with graviresponse pathways. It remains a challenge to find an experimental design, which could allow discriminating between gravi and mechanosensing mechanisms.

IDENTIFICATION OF CELLULAR AND MOLECULAR ACTORS IN GRAVISENSING MECHANISMS

THE GRAVI-SENSING SITES

The most challenging research question is the identification of the tissues and/or cells able to sense and then perceive changes in the gravity vector.

Much insight on plant response to gravity is obtained by the study of organs exhibiting primary growth. The root columella located inside the root cap, which comprises polarized cells, is considered to be the key site of gravity sensing and perception.

Columella cells contain starch-filled amyloplasts able to move under a change of gravity direction. The singularity of these organs is the spatial separation of the perception site from the responsive zone. Conversely, gravity sensing and response occur in the same region of young stems. The endoderm, located between the epiderm and the phloem, is considered as the gravi-sensing site. This tissue contains amyloplasts in young stems of herbaceous and ligneous species such as poplar (**Figures 1A,C**; Azri et al., 2013).

What happens in organs showing secondary growth? It is not possible to identify the endoderm in tree shoots since most bark cells are filled with starch (**Figures 1B,D**). Hence, the gravisensing cells are not identified yet neither are the gravisensing mechanisms (Tocquard et al., 2014b) leading to RW formation. RW can be induced by inclining a staked tree (Coutand et al., 2014) which suggests the modulation of cambial activity by gravistimulation *per se*, that occurs without the influence of mechanical deformation of the stem. Even if the gravisensing site for root undergoing a secondary growth in root is not yet identified, one could question if the cambium could be considered as an additional gravi-sensing site in roots.

PROPOSED CONCEPTS AND MOLECULAR ACTORS

Despite, or maybe because of, the lack of indisputable protocol for the study of gravisensing in plants, various (opposite or complementary?) concepts are proposed related to the perception-transduction of the gravitropic stimulus. The starch-statolith hypothesis (Sack, 1997) explains that the direction of gravity is perceived by the plant through the sedimentation of starch-filled amyloplasts, named statolith, within specialized cells. The gravitational pressure hypothesis (Staves, 1997) suggests that mechanical deformation of the protoplast, cytoskeleton and cell wall components is the starting event of gravitropism. Another concept called "the tensegrity concept" (Ingber, 1997) assumes that the membrane is outstretched on the cytoskeleton backbone and that this system is in a state of equilibrium, between tensile and compressive forces. This concept is very suitable for explaining the perception of mechanical stress at the cell surface and the transmission to the intracellular compartment. The common idea that gravity-induced effects are initiated within the cells (Trewavas and Knight, 1994), is compatible with the tensegrity model which proposes that gravistimulation may unbalance the tensegrity forces and trigger

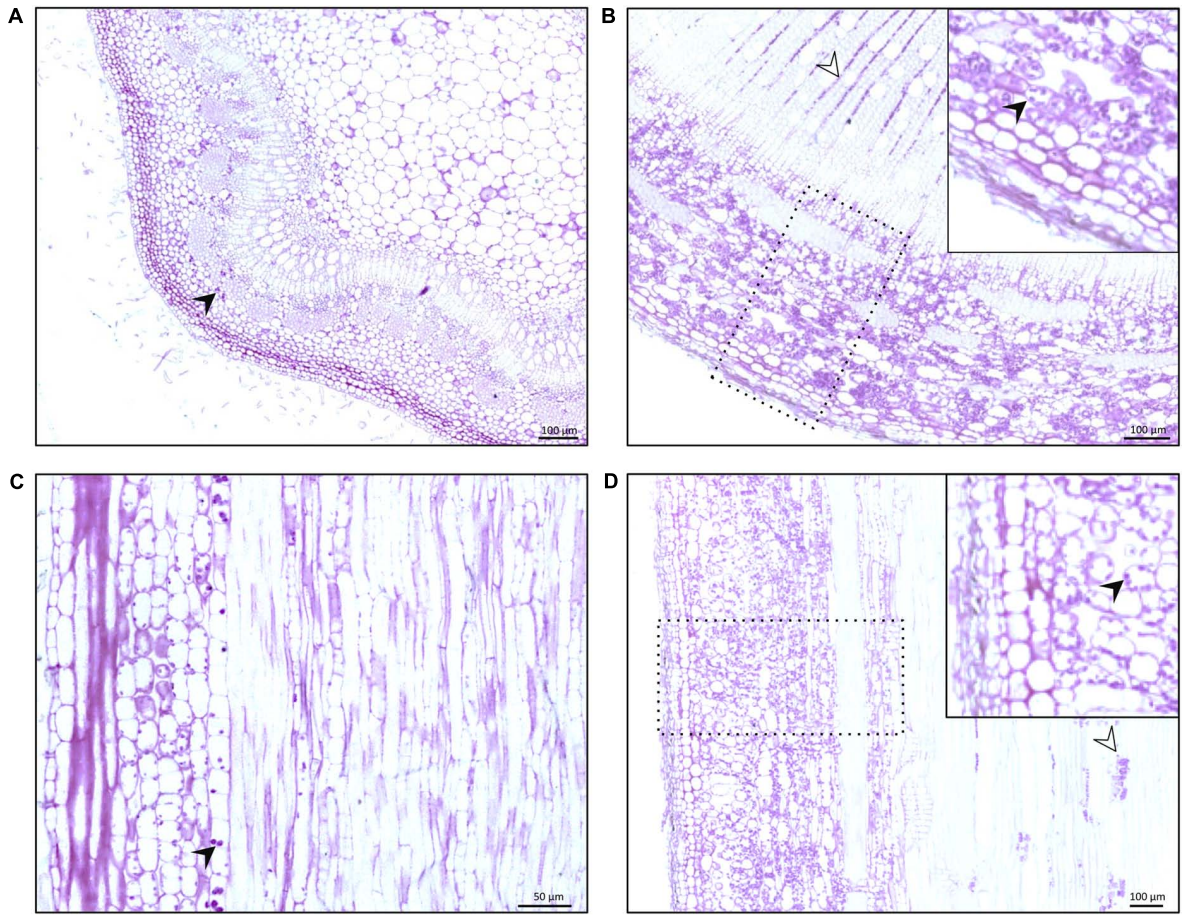

FIGURE 1 | Transversal (A,B) and longitudinal (C,D) stem sections of poplar tree, *Populus tremula* × *alba*, stained with Periodic Acid-Schiff (PAS). This stain reveals the presence of starch and polysaccharides in dark purple. **(A,C)** Arrows indicate the presence of starch rich-amyloplasts in the endoderm of the primary growth-stem, at 3 cm from the stem apex. **(B,D)** Arrows and rectangles indicate wood rays and bark of secondary growth stem, respectively. Both tissues contain starch rich-granules.

cellular responses via membrane kinase proteins (Volkmann and Baluška, 2006). A complementary concept proposes that plant cells could sense gravity using the cytoskeleton-plasma membrane-cell wall continuum (CPMCW; Pickard and Ding, 1993; Baluška et al., 2003). Baluška and Volkmann (2011) discussed these different theories. Whichever theory is applied, the role of the amyloplasts and of the CPMCW with possible protein linkers seems realistic.

In the literature, some arguments corroborate parts of these hypothetic mechanisms. In roots, it has been suggested that the gravity-induced movements of amyloplasts could activate mechanosensing ion channels either in the amyloplast envelope or in reticulum endoplasmic and/or plasma membrane (Boonsirichai et al., 2002; Perbal and Driss-Ecole, 2003). These mechanosensing channels could be considered as gravi-receptors in inducing calcium dependent-signaling pathways. More recently it has been shown that plastids participate to root gravitropism not only through their sedimentation but also they likely play a role in the signal transduction pathway through the Translocon of the Outer envelope of the Chloroplast (TOC; Strohm et al., 2014). These findings implicate the functional interaction between plastids and actin cytoskeleton possibly via functions of TOC. In the same way, the investigation of plastid behavior in stem clearly demonstrates their role in gravi-perception (Morita and Nakamura, 2012). The plastid movements in stem are affected by the large and central vacuole of the endodermal cells. Moreover, genetic screening for *Arabidopsis* mutants with modified shoot gravitropism indicated that the vacuole is important for gravity perception (Morita, 2010).

More generally, within a putative perceptive cell, several molecular candidates could play a role in gravisensing. Two types of receptors could be involved including mechanosensitive ion channels and receptor like kinases (RLK). RLK are transmembrane proteins, composed of one or more extracellular domains, a single transmembrane domain and an intracellular kinase domain (Lehti-Shiu et al., 2009; Gish and Clark, 2011). RLK could act as sensors of the cell wall and restore its status to the cell wall by phosphorylation of the kinase domain. Among RLK, wall associated kinase (WAK) and *Catharanthus roseus* RLK1-like subfamilies are proposed to be cell wall status sensors (Gish and Clark, 2011; Engelsdorf and Hamann, 2014; Tocquard et al., 2014a). They could be involved in gravisensing by perceiving the deformation between the cell wall and the plasma membrane. Gens et al. (2000) hypothesized the existence of an architectural organization involving WAK, arabinogalactan proteins (AGP) at the interface between cytoplasm and cell wall. Several studies also showed the upregulation of AGP in response to gravistimulation (Lafarguette et al., 2004; Azri et al., 2014). This "plasmalemmal reticulum" could play a critical role in mechanosensing and possibly gravisensing (Gens et al., 2000). More recently, it has been shown that mechanosensitive channels including MCA2 could be also involved in gravisensing (Monshausen and Haswell, 2013; Iida et al., 2014).

The plant cytoskeleton is considered as a major receiver as well as transducer of mechanical signals. Nick (2011) presented the cytoskeleton as a tensegrity sensor. In this model, microfilaments (MF) are considered as the contractile and tensile elements while the microtubules (MT) are more rigid and resistant to compression. Bancaflor (2013) highlighted the apparent inconsistencies about the effects of actin inhibitory compounds on root gravitropism, and proposed models for how MF might regulate negatively gravitropism. The full understanding of the MF involvement in gravitropism has also to take into account the differences in actin organization between the root columella and the shoot endodermis cells, the former having first fine and short MF while the latter contain distinct F-actin bundles (Morita, 2010; Bancaflor, 2013). Several authors have suggested that gravitropic bending can trigger altered MT organization (Ikushima and Shimmen, 2005; Jacques et al., 2013; Toyota and Gilroy, 2013). In addition, gravitropism can be inhibited by antimicrotubular drugs or mutations affecting the dynamics of MT (Nick, 2012). On the contrary, tropic bending occurred in roots pretreated with microtubule depolymerizing agents (Bisgrove, 2008). These observations and others (Bisgrove, 2008) do not allow to discriminate the involvement of MT in gravisensing versus graviresponse, i.e., gravitropic bending. The difficulty to univocally show that the cytoskeleton is a tensegrity sensor may come from the fact that most studies examined either the involvement of MF or MT (Nick, 2013; Tatsumi et al., 2014) in gravitropism, although the cytoskeleton is far more complex. Indeed, evidence was brought that functional and structural interactions occurred between MT and actin, and that numerous proteins interacted with the cytoskeleton (Collings et al., 1998; Kotzer and Wasteneys, 2006).

HOW TO GO FURTHER TO GRASP GRAVISENSING?

As just highlighted above, it is crucial to reliably discriminate gravisensing from mechanosensing, and the same goes for sensing from the signal transduction and early responsive elements. According to Nick (2011) clear concepts of the sensing mechanisms have to be elaborated in order to design unequivocal experimental approaches. Incidentally, the effect of the direction of light as well as the light quality have also to be taken into account in designing an experiment that wish to focus on gravisensing and graviresponse as multiple light signaling pathways interact with gravitropism (Mullen and Kiss, 2008). Importantly, to our mind the gravistimulation should not cause bending that could lead to organ and tissue deformation. Consequently, the study of gravisensing has to be done before any curving response occurred. Another way is the utilization of microgravity conditions through space experiments (Ruyters and Braun, 2014).

Furthermore, there is a general consensus on the identity of the gravisensing cells in primary shoot and root while these cells remained to be localized in organs driven by secondary growth. Further insights on this subject are impaired by the compulsory use of ligneous species models. For instance, in the ligneous model *Populus trichocarpa*, very few mutants are available compared to *Arabidopsis thaliana*, which was used in most studies. One can even ask if the tissues in secondary growth are able to perceive gravity or if they respond to a signal coming from the apexes.

Another challenge is to identify the gravity receptors in roots and in stems. Approaches such as transcriptomics and proteomics

combined with the study of mutants could lead to the inference of a network of genes involved in gravisensing. In addition, it will be interesting to investigate the functional interaction between the cytoskeleton and gravi-sensors. In parallel, modelization of the mechanical deformation of the cytoskeleton could help to understand the function of the cytoskeleton network in gravitropism.

ACKNOWLEDGMENTS

This work was supported by the Ministère de l'Enseignement Supérieur et de la Recherche and by the French National Research Agency (ANR, "TROPIC" project 11-BSV7-0012). The authors thank the French Space Agency, the Centre National d'Etudes Spatiales (CNES) for financial support.

REFERENCES

Archer, R. R. (1986). *Growth Stresses and Strains in Trees*. Berlin: Springer-Verlag.

Azri, W., Brunel, N., Franchel, J., Ben Rejeb, I., Jacquot, J.-P., Julien, J.-L., et al. (2013). Putative involvement of thioredoxin H in early response to gravitropic stimulation of poplar stems. *J. Plant Physiol.* 170, 707–711. doi: 10.1016/j.jplph.2012.12.017

Azri, W., Chambon, C., Herbette, S., Brunel, N., Coutand, C., Leplé, J. C., et al. (2009). Proteome analysis of apical and basal regions of poplar stems under gravitropic stimulation. *Physiol. Plant.* 136, 193–208. doi: 10.1111/j.1399-3054.2009.01230.x

Azri, W., Ennajah, A., Nasr, Z., Woo, S.-Y., and Khaldi, A. (2014). Transcriptome profiling the basal region of poplar stems during the early gravitropic response. *Biol. Plant.* 58, 55–63. doi: 10.1007/s10535-013-0364-7

Baluška, F., Šamaj, J., Wojtaszek, P., Volkmann, D., and Menzel, D. (2003). Cytoskeleton – plasma membrane – cell wall continuum in plants: emerging links revisited. *Plant Physiol.* 133, 482–491. doi: 10.1104/pp.103.027250

Baluška, F., and Volkmann, D. (2011). "Mechanical aspects of gravity-controlled growth, development and morphogenesis," in *Mechanical Integration of Plant Cells and Plants, Signaling and Communication in Plants*, ed. P. Wojtaszek (Heidelberg: Springer), 195–223.

Bancaflor, E. B. (2013). Regulation of plant gravity sensing and signaling by the actin cytoskeleton. *Am. J. Bot.* 100, 143–152. doi: 10.3732/ajb.1200283

Barlow, P. W., Parker, J. S., Butler, R., and Brain, P. (1993). Gravitropism of primary roots of *Zea mays* L. at different displacement angles. *Ann. Bot.* 71, 383–388. doi: 10.1006/anbo.1993.1048

Barlow, P. W., and Rathfelder, E. L. (1985). Distribution and redistribution of extension growth along vertical and horizontal gravireacting maize roots. *Planta* 165, 134–141. doi: 10.1007/BF00392222

Bastien, R., Bohr, T., Moulia, B., and Douady, S. (2013). Unifying model of shoot gravitropism reveals proprioception as a central feature of posture control in plants. *Proc. Natl. Acad. Sci. U.S.A.* 110, 755–760. doi: 10.1073/pnas.1214301109

Bastien, R., Douady, S., and Moulia, B. (2014). A unifying modeling of plant shoot gravitropism with an explicit account of the effects of growth. *Front. Plant Sci.* 5:136. doi: 10.3389/fpls.2014.00136

Bisgrove, S. R. (2008). The roles of microtubules in tropisms. *Plant Sci.* 175, 74. doi: 10.1016/j.plantsci.2008.08.009

Boonsirichai, K., Guan, C., Chen, R., and Masson, P. H. (2002). Root gravitropism: an experimental tool to investigate basic cellular and molecular processes underlying mechanosensing and signal transmission in plants. *Ann. Rev. Plant Biol.* 53, 421–447. doi: 10.1146/annurev.arplant.53.100301.135158

Chehab, W., Eich, E., and Braam, J. (2008). Thigmomorphogenesis: a complex plant response to mechano-stimulation. *J. Exp. Bot.* 60, 43–56. doi: 10.1093/jxb/ern315

Collings, D. A., Asada, T., Allen, N. S., and Shibaoka, H. (1998). Plasma membrane-associated actin in bright yellow 2 tobacco cells – evidence for interaction with microtubules. *Plant Physiol.* 118, 917–928. doi: 10.1104/pp.118.3.917

Coutand, C. (2010). Mechanosensing and thigmomorphogenesis, a physiological and biomechanical point of view. *Plant Sci.* 179, 168–182. doi: 10.1016/j.plantsci.2010.05.001

Coutand, C., Fournier, M., and Moulia, B. (2007). The gravitropic response of poplar trunks: key roles of prestressed wood regulation and the relative kinetics of cambial growth versus wood maturation. *Plant Physiol.* 144, 1166–1180. doi: 10.1104/pp.106.088153

Coutand, C., Pot, G., and Badel, E. (2014). Mechanosensing is involved in the regulation of autostress levels in tension wood. *Trees* 28, 687–697. doi: 10.1007/s00468-014-0981-6

Driss-Ecole, D., Driss-Ecole, D., Legué, V., Carnero-Diaz, E., and Perbal, G. (2008). Gravisensitivity and automorphogenesis of lentil seedling roots grown on board the International Space Station. *Physiol. Plant.* 134, 191–201. doi: 10.1111/j.1399-3054.2008.01121.x

Engelsdorf, T., and Hamann, T. (2014). An update on receptor-like kinase involvement in the maintenance of plant cell wall integrity. *Ann. Bot.* 114, 1339–1347. doi: 10.1093/aob/mcu043

Firn, R. D., and Digby, J. (1979). A study of the autotropic straightening reaction of a shoot previously curved during geotropism. *Plant Cell Environ.* 2, 149–154. doi: 10.1111/j.1365-3040.1979.tb00786.x

Galland, P. (2002). Tropisms of Avena coleoptiles: sine law for gravitropism, exponential law for photogravitropic equilibrium. *Planta* 215, 779–784. doi: 10.1007/s00425-002-0813-6

Gens, J. G., Fujiki, M., and Pickard, B. G. (2000). Arabinogalactan protein and wall-associated kinase in a plasmalemmal reticulum with specialized vertices. *Protoplasma* 212, 115–134. doi: 10.1007/BF01279353

Gish, L. A., and Clark, S. E. (2011). The RLK/Pelle family of kinases. *Plant J.* 66, 117–127. doi: 10.1111/j.1365-313X.2011.04518.x

Göttig, M., and Galland, P. (2014). Gravitropism in Phycomyces: violation of the so-called resultant law – evidence for two response components. *Plant Biol.* 16, 158–166. doi: 10.1111/plb.12112

Hamant, O. (2013). Widespread mechanosensing controls the structure behind the architecture in plants. *Curr. Opin. Plant Biol.* 16, 654–660. doi: 10.1016/j.pbi.2013.06.006

Hoshino, T., Miyamoto, K., and Ueda, J. (2007). Gravity controlled asymmetrical transport of auxin regulates a gravitropic response in the early growth stage of etiolated pea (*Pisum sativum*) epicotyls: studies using stimulated microgravity conditions on a three-dimensional clinostat and using an agravitropic mutant, ageotropum. *J. Plant Res.* 120, 619–628. doi: 10.1007/s10265-007-0103-2

IAWA. (1964). Multilingual glossary of terms used in wood anatomy. International Association of Wood Anatomists, Committee on Nomenclature Vergsanstalt Buchdruckerei Konkordia, Winterthur, 186.

Iida, H., Furuichi, T., Nakano, M., Toyota, M., Sokabe, M., and Tatsumi, H. (2014). New candidates for mechano-sensitive channels potentially involved in gravity sensing in *Arabidopsis thaliana*. *Plant Biol.* 16, 39–42. doi: 10.1111/plb.12044

Iiono, M., Tarui, Y., and Uematsu, C. (1996). Gravitropism of maize and rice coleoptiles: dependence on the stimulation angle. *Plant Cell Environ.* 19, 1160–1168. doi: 10.1111/j.1365-3040.1996.tb00431.x

Ikushima, T., and Shimmen, T. (2005). Mechano-sensitive orientation of cortical microtubules during gravitropism in azuki bean epicotyls. *J. Plant Res.* 118, 19–26. doi: 10.1007/s10265-004-0189-8

Ingber, D. E. (1997). Tensegrity: the architectural basis of cellular mechanotransduction. *Annu. Rev. Physiol.* 59, 575–599. doi: 10.1146/annurev.physiol.59.1.575

Ishikawa, H., and Evans, M. L. (1993). The role of the distal elongation zone in the response of maize rots to auxin and gravity. *Plant Physiol.* 102, 1203–1210. doi: 10.1104/pp.102.4.1203

Jacques, E., Buytaert, J., Wells, D. M., Lewandowski, M., Bennett, M. J., Dirckx, J., et al. (2013). Microfilament analyzer, an image analysis tool for quantifying fibrillar orientation, reveals changes in microtubule organization during gravitropism. *Plant J.* 74, 1045–1058. doi: 10.1111/tpj.12174

Jaffe, M. J. (1973). Thigmomorphogenesis: the response of plant growth and development to mechanical stimulation. *Planta* 114, 143–157. doi: 10.1007/BF00387472

Kotzer, A. M., and Wasteneys, G. O. (2006). Mechanisms behind the puzzle: microtubule-microfilament cross-talk in pavement cell formation. *Can. J. Bot.* 84, 594–603. doi: 10.1139/b06-023

Lafarguette, F., Leple, J. C., Dejardin, A., Laurans, F., Costa, G., Lesage-Descauses, M. C., et al. (2004). Poplar genes encoding fasciclin-like arabinogalactan proteins are highly expressed in tension wood. *New Phytol.* 164, 107–121. doi: 10.1111/j.1469-8137.2004.01175.x

Larsen, P. (1957). The development of geotropic and spontaneous curvatures in roots. *Physiol. Plant.* 10, 12–163. doi: 10.1111/j.1399-3054.1957.tb07617.x

Lehti-Shiu, M. D., Zou, C., Hanada, K., and Shiu, S. H. (2009). Evolutionary history and stress regulation of plant receptor-like kinase/pelle genes. *Plant Physiol.* 150, 12–26. doi: 10.1104/pp.108.134353

Mirabet, V., Das, P., Boudaoud, A., and Hamant, O. (2011). The role of mechanical forces in plant morphogenesis. *Annu. Rev. Plant Biol.* 62, 365–385. doi: 10.1146/annurev-arplant-042110-103852

Monshausen, G. B., and Haswell, E. S. (2013). A force of nature: molecular mechanisms of mechanoperception in plants. *J. Exp. Bot.* 64, 4663–4680. doi: 10.1093/jxb/ert204

Morita, M. T. (2010). Directional gravity sensing in gravitropism. *Annu. Rev. Plant Biol.* 61, 705–720. doi: 10.1146/annurev.arplant.043008.092042

Morita, M. T., and Nakamura, M. (2012). Dynamic behavior of plastids related to environmental response. *Curr. Opin. Plant Biol.* 15, 722–728. doi: 10.1016/j.pbi.2012.08.003

Moulia, B., Der Loughian, C., Bastien, R., Martin, L., Rodriguez, M., Gourcilleau, D., et al. (2011). "Integrative mechanobiology of growth and architectural development in changing mechanical environments," in *Mechanical Integration of Plant Cells and Plants, Signaling and Communication in Plants,* ed. P. Wojtaszek (Heidelberg: Springer), 269–302.

Moulia, B., and Fournier, M. (2009). The power and control of gravitropic movements in plants: a biochemical and systems view. *J. Exp. Bot.* 60, 461–486. doi: 10.1093/jxb/ern341

Mullen, J. L., and Kiss, J. Z. (2008). "Phototropism and its relationship to gravitropism," in *Plant Tropisms* eds S. Gilroy and P. Masson (Ames: Blackwell Publishing), 79–90.

Nick, P. (2011). "Mechanics of the cytoskeleton," in *Mechanical Integration of Plant Cells and Plants, Signaling and Communication in Plants*, ed. P. Wojtaszek (Heidelberg: Springer), 53–90. doi: 10.1007/978-3-642-19091-9_3

Nick, P. (2012). Microtubules and the tax payer. *Protoplasma* 249(Suppl. 2), S81–S94. doi: 10.1007/s00709-011-0339-5

Nick, P. (2013). A glorious half-century of microtubules–microtubules, signaling and abiotic stress. *Plant J.* 75, 309–323. doi: 10.1111/tpj.12102

Perbal, D., and Driss-Ecole, D. (2003). Mechanotransduction in gravisensing cells. *Trends Plant Sci.* 8, 498–504. doi: 10.1016/j.tplants.2003.09.005

Perbal, G., Jeune, B., Lefranc, A., Carnero-Diaz, E., and Driss-Ecole, D. (2002). The dose-response curve of the gravitropic reaction: a re-analysis. *Physiol. Plant.* 114, 336–342. doi: 10.1034/j.1399-3054.2002.1140302.x

Pickard, B. G. (1985). "Roles of hormones, protons and calcium in geotropism," in *Encyclopedia of Plant Physiology*, Vol. 3, eds R. P. Phais and D. M. Reid (Berlin: Springer), 193–281.

Pickard, B. G., and Ding, J. P. (1993). The mechanosensory calcium-selective ion channel: key component of a plasmalemmal control centre? *Aust. J. Plant Physiol.* 20, 439–459. doi: 10.1071/PP9930439

Ruyters, G., and Braun, M. (2014). Plant biology in space: recent accomplishments and recommendations for future research. *Plant Biol.* 16(Suppl. 1), 4–11. doi: 10.1111/plb.12127

Sachs, J. (1882). "Uber Ausschlieβung der geotropischen und heliotropischen Krümmungen während des Waschsens," in *Arbeiten des Botanischen Instituts in Würzburg* , Vol. 2 (Leipzig: Verlag Von Wilhelm Engelmann), 209–225.

Sack, F. D. (1997). Plastids and gravitropic sensing. *Planta* 203, S63–S68. doi: 10.1007/PL00008116

Selker, J. M. L., and Sievers, A. (1987). Analysis of extension and curvature during the graviresponse in Lepidium roots. *Am. J. Bot.* 74, 1863–1871. doi: 10.2307/2443968

Stankovic, B., Volkmann, D., and Sack, F. D. (1998). Autotropism, automorphogenesis and gravity. *Physiol. Plant.* 102, 328–335. doi: 10.1034/j.1399-3054.1998.1020222.x

Staves, M. P. (1997). Cytoplasmic streaming and gravity sensing in Chara internodal cells. *Planta* 203, S79–S84. doi: 10.1007/PL00008119

Strohm, A. K., Barrett-Wilt, G. A., and Masson, P. H. (2014). A functional TOC complex contributes to gravity signal transduction in *Arabidopsis. Front. Plant Sci.* 5:148. doi: 10.3389/fpls.2014.00148

Tatsumi, H., Furuichi, T., Nakano, M., Toyota, M., Hayakawa, K., Sokabe, M., et al. (2014). Mechanosensitive channels are activated by stress in the actin stress fibres, and could be involved in gravity sensing in plants. *Plant Biol.* 16, 18–22. doi: 10.1111/plb.12095

Tocquard, K., Lafon-Placette, C., Auguin, D., Muries, B., Bronner, G., Lopez, D., et al. (2014a). In silico study of wall-associated kinase family reveals large-scale expansion potentially connected with functional diversification in *Populus. Tree Genet. Genomes* 10, 1135–1147. doi: 10.1007/s11295-014-0748-7

Tocquard, K., Lopez, D., Decourteix, M., Thibaut, B., Julien, J. L., Label, P., et al. (2014b). "The molecular mechanisms of reaction wood induction," in *The Biology of Reaction Wood*, eds B. Gardiner, J. Barnett, P. Saranpää, and J. Gril (Heidelberg: Springer), 107–138.

Tomos, A. D., Malone, M., and Pritchard, J. (1989). The biophysics of differential growth. *Environ. Exp. Bot.* 29, 7–23. doi: 10.1016/0098-8472(89)90035-X

Toyota, M., and Gilroy, S. (2013). Gravitropism and mechanical signaling in plants. *Am. J. Bot.* 100, 111–125. doi: 10.3732/ajb.1200408

Trewavas, A., and Knight, M. (1994). Mechanical signaling, calcium and plant form. *Plant Mol. Biol.* 26, 1329–1341. doi: 10.1007/BF00016478

Uyttewaal, M., Burian, A., Alim, K., Landrein, B., Borowska-Wykret, D., Dedieu, A., et al. (2012). Mechanical stress acts via katanin to amplify differences in growth rate between adjacent cells in *Arabidopsis. Cell* 149, 439–451. doi: 10.1016/j.cell.2012.02.048

Volkmann, D., and Baluška, F. (2006). Gravity: one of the driving forces for evolution. *Protoplasma* 229, 143–148. doi: 10.1007/s00709-006-0200-4

Zieschang, H. E., Brain, P., and Barlow, P. W. (1997). Modelling of root growth and bending in two dimensions. *J. Theor. Biol.* 184, 237–246. doi: 10.1006/jtbi.1996.0259

Conflict of Interest Statement: The authors declare that the research was conducted in the absence of any commercial or financial relationships that could be construed as a potential conflict of interest.

Received: 02 June 2014; accepted: 20 October 2014; published online: 05 November 2014.

Citation: Lopez D, Tocquard K, Venisse J-S, Legué V and Roeckel-Drevet P (2014) Gravity sensing, a largely misunderstood trigger of plant orientated growth. Front. Plant Sci. 5:610. doi: 10.3389/fpls.2014.00610

This article was submitted to Plant Physiology, a section of the journal Frontiers in Plant Science.

Advantages of publishing in Frontiers

OPEN ACCESS
Articles are free to read, for greatest visibility

COLLABORATIVE PEER-REVIEW
Designed to be rigorous – yet also collaborative, fair and constructive

FAST PUBLICATION
Average 85 days from submission to publication (across all journals)

COPYRIGHT TO AUTHORS
No limit to article distribution and re-use

TRANSPARENT
Editors and reviewers acknowledged by name on published articles

SUPPORT
By our Swiss-based editorial team

IMPACT METRICS
Advanced metrics track your article's impact

GLOBAL SPREAD
5'100'000+ monthly article views and downloads

LOOP RESEARCH NETWORK
Our network increases readership for your article

Frontiers
EPFL Innovation Park, Building I • 1015 Lausanne • Switzerland
Tel +41 21 510 17 00 • Fax +41 21 510 17 01 • info@frontiersin.org
www.frontiersin.org

Find us on